CONTROL OF THE LONGITUDINAL DYNAMICS OF VEHICLE SYSTEMS USING FAST-SAMPLING TECHNIQUES

BY

JOHN ASTLEY CALDERBANK

A THESIS SUBMITTED FOR THE DEGREE OF

DOCTOR OF PHILOSOPHY

OF THE

UNIVERSITY OF SALFORD

DEPARTMENT OF AERONAUTICAL AND MECHANICAL ENGINEERING

1981

CONTENTS

Contents continued

Contents continued | Page

TABLES

Figures

ACKNOWLEDGEMENTS

I wish to express many thanks to my wife for her patience and help during the period of my research. I also express my sincere thanks to Doctor Alan Bradshaw for his friendship, guidance and encouragement and for his most helpful comments on the text of this thesis. I am grateful to the Science and Engineering Research Council and to G.E.C. Traction Limited for their financial support. My thanks are due to my parents for making it financially possible to produce this thesis, and to Mrs Scott for typing the script so efficiently.

SUMMARY

In this thesis singular perturbation methods of analysis have been applied to the design of algorithms that will produce effective, robust and high integrity fast-sampling control of the longitudinal motions of two types of vehicle systems. Both centralized and decentralized control of vehicle cascades is considered and the expected differences in the responses of the closed-loop systems identified by the use of asymptotic transfer function matrices. Furthermore the terms used by other authors are explained by use of the analytical asymptotic expressions. It is also explained how the fast-sampling controllers are able to entrain vehicles in cascades without requiring excessive control actions or loss of accuracy. The results of computer simulations of a ten vehicle cascade undergoing a constant speed entrainment manoeuvre with both centralized and decentralized controllers are presented to emphasize the results of the study.
The dynamical properties of trains of vehicles are presented and fast-sampling controllers are designed for the control of the speed of trains having single leading locomotives both without and with another locomotive in the train. The transmission zeros of such systems are identified and their physical meaning used to

explain why the fast-sampling control algorithms are able to cope with trains of differing lengths and configurations and still produce good disturbance-rejection and tracking properties. Finally, the theory is illustrated by the presentation of the results of a digital computer simulation study of the passage of a very long train over a vertical reverse curve.

CHAPTER 1

INTRODUCTION

1.1 Introduction

In this thesis recent developments in multivariable control system theory are extended and applied to the problem of the longitudinal control of vehicle systems. Two types of vehicle systems are considered. Firstly, vehicle cascades [1] , [2] , [3] are considered as these reflect the control problems arising from the operation of rapid transit systems and, secondly, connected vehicles [4], [5] [6] are considered as these reflect the control problems arising from the operation of very long freight trains over undulating terrain.

The control theory presented in chapter two, for the analysis of these vehicle systems and the design of suitable controllers, includes and extends the work carried out by Porter and Bradshaw [7] , [8] on fast-sampling error-actuated control of time-invariant linear multivariable continuous-time systems. Fast-sampling techniques incorporate fundamental concepts of modern control knowledge and as a direct result can be readily applied to the above class of systems, which includes vehicle systems, to produce robust and economical controllers.

It is the primary objective of this thesis to utilize the afore mentioned control theory to investigate the properties of fast-sampling controllers for vehicle systems. The design and analysis of closed-loop vehicle systems will indicate the problems arising from the choice of particular structures of control algorithms.

1.2 Outline of the Thesis

The two vehicle systems to be considered are introduced in chapter one together with the primary objective of the thesis. A review of the work on singularly perturbed systems is made, although it must be emphasized that open-loop singularly perturbed systems are not considered in this thesis. Fast-sampling control techniques are introduced and the two classes of systems considered in chapter two are described.

Porter and Shenton's [9] treatment of the open-loop transfer function matrices is summarized in chapter two, and is then used in the analysis of the closed-loop transfer function matrices of systems controlled with fast-sampling error-actuated controllers.

The synthesis of fast-sampling controllers is considered in chapter three, together with the implications of employing different structures of controllers . Transmission zeros are defined since they play an important role in the analysis of systems and are particularly relevant to the control of trains, considered in chapters six and seven.

In chapter four a mathematical model of a vehicle cascade is developed and a review of the relevant literature is made. The control theory developed in sections (2.3) and (3.2) is utilized to produce both centralized and decentralized controllers. These two closed-loop systems are then studied using the general expressions for the transfer function matrices derived in chapter two and the results related to the work of other authors. The transfer function matrices also indicate how to formulate the command inputs in a sensible way in order to avoid undesirable effects. A ten vehicle cascade is considered and the results of digital computer simulations are presented in order to emphasize the findings of the study.

Early attempts to understand the dynamics of trains are summarized in chapter five. This includes a review of Dudley's [10] work using a lumped parameter model and Wikander's [11] findings using an elastic bar model.

In chapter six single locomotive powered trains are considered and a mathematical model is developed. The theory developed in sections (2.4), (2.5) and (3.2) is then used to develop a fast-sampling speed controller for the train model and to predict the affects of implementing such a controller. The fast-sampling speed controller is simple and effective and is also independent of the train length. The performance of the controller is illustrated by presenting the results of digital computer simulations of three trains of different lengths running over a single gradient change. The results are related to the position of the open-loop poles and transmission zeros.

Trains with two locomotives are considered in chapter eight. Again tight speed control is achieved by using the theory developed in sections (2.4), (2.5) and (3.2). The independence of train length is again illustrated by presenting the results of digital computer simulations, which are also related to the position of the open-loop poles and transmission zeros. A review of the relevant literature on the problems and control of extra-long freight trains is then made. The results of a digital computer simulation of the fast-sampling control of a one hundred vehicle train travelling over undulating terrain are presented and related to the previous results in chapter seven and also to those presented in chapter six.

Finally chapter eight summarizes the results and suggests further areas of research.

1.3 Singularly Perturbed Systems

A system of n+m first order linear differential equations in which m of the derivatives are multiplied by a small parameter, ε , can be expressed in the matrix form

$$\begin{bmatrix} In & 0 \\ 0 & \varepsilon Im \end{bmatrix} \begin{bmatrix} \dot{x} \\ \dot{z} \end{bmatrix} = \begin{bmatrix} A_1 & A_2 \\ A_3 & A_4 \end{bmatrix} \begin{bmatrix} x \\ z \end{bmatrix} + \begin{bmatrix} B_1 \\ B_2 \end{bmatrix} u \qquad (1.1)$$

where $x \varepsilon R^n$, $z \varepsilon R^m$, $u \varepsilon R^{\ell}$, $A_1 \varepsilon R^{nxn}$, $A_2 \varepsilon R^{nxm}$, $A_3 \varepsilon R^{mxn}$, $A_4 \varepsilon R^{mxm}$, $B_1 \varepsilon R^{nx\ell}$, $B_2 \varepsilon R^{mx\ell}$ and it is assumed that A_4 is an invertible matrix. These systems are usually referred to as singularly perturbed since when $\varepsilon = 0$ the matrix

$$\begin{bmatrix} In & 0 \\ 0 & \varepsilon Im \end{bmatrix}$$

is singular. It follows directly from (1.1) that when $\varepsilon = 0$ the number of differential equations is reduced to n because m of the equations have become purely algebraic since (1.1) assumes the reduced form

$$\begin{bmatrix} \dot{\bar{x}} \\ 0 \end{bmatrix} = \begin{bmatrix} A_1 & A_2 \\ A_3 & A_4 \end{bmatrix} \begin{bmatrix} \bar{x} \\ \bar{z} \end{bmatrix} + \begin{bmatrix} B_1 \\ B_2 \end{bmatrix} \bar{u} \qquad (1.2)$$

or, equivalently,

$$\dot{\bar{x}} = (A_1 - A_2 A_4{}^{-1} A_3)\bar{x} + (B_1 - A_2 A_4{}^{-1} B_2)\bar{u} \qquad (1.3)$$

and

$$\bar{z} = -A_4{}^{-1} (A_3 \bar{x} + B_2 \bar{u}) \qquad (1.4)$$

where $\bar{x} \in R^n$, $\bar{z} \in R^m$, $\bar{u} \in R^\ell$ and the bars are used to differentiate between the full system governed by (1.1) and the reduced system governed by (1.2). As $\varepsilon \to 0$ it follows from (1.3)that the eigenvalues representing the slow modes in (1.1) approach the eigenvalues of the matrix $(A_1 - A_2 A_4{}^{-1} A_3)$. As $\varepsilon \to 0$, it follows from (1.1) that the eigenvalues representing the fast modes in (1.1) approach the eigenvalues of the matrix $({}^1/\varepsilon .\ A_4)$ and are clearly infinite for the case $\varepsilon = 0$. The fast modes represent high rates of change inside the system (1.1) and these occur in a short interval of time following the instant $t = 0$, known as the boundary layer. Following this boundary layer the solutions $x(t)$, $z(t)$ rapidly converge onto the solutions $\bar{x}(t)$, $\bar{z}(t)$ as $\varepsilon \to 0$. Thus singularly perturbed systems are characterized by high rates of change inside the boundary layer and by low rates of change away from the boundary layer.

A fundamental exposition of the singular perturbation theory of differential equations is due to Tihonov [12], [13], [14] who considered the dependence of the solutions of systems of autonomous non-linear differential equations of the form

$$\dot{x} = f(x,z) \qquad (1.5)$$

and

$$\varepsilon\dot{z} = g(x,z) \qquad (1.6)$$

on the perturbation parameter ε. It was shown that all trajectories from the set of initial conditions x(0), z(0) giving a stable response for the system

$$\varepsilon\dot{z} = g(x,z) \qquad (1.7)$$

for sufficiently small ε and for continuous f and g, converge rapidly onto the trajectories of the reduced system

$$\dot{\bar{x}} = f(x,z) \qquad (1.8)$$

$$0 = g(x,z). \qquad (1.9)$$

In 1961 Klimushev and Krasovskii [15] showed that certain systems are asymptotically stable by utilizing singular perturbation techniques together with a Liapunov function. The application of singular perturbation techniques to optimal controller design (see, for instance, Sannuti and Kokotovic [16]) simplifies the design problem by reducing the plant size. Porter [17] proved that the common practice of neglecting parasitic elements in the design of certain feedback systems was justified by showing that the asymptotic stability was unaffected by the introduction of small parameters. Shenton [18] and Sangolola [19] also obtained notable results concerning the structural and dynamical characteristics of time invariant singularly perturbed multi-input linear systems. A very important result (see section (2.2)) was obtained by Porter and Shenton [9] who showed that as the parasitic elements of a system approach zero then the open-loop transfer function matrix can be expressed as the sum of a 'fast' transfer function matrix and a 'slow' transfer function matrix. Equally important, the digital computer simulation of singularly perturbed dynamical systems has been greatly facilitated by the contributions of Gear [20] and Lapidus and Aitken [21], among others, who have developed efficient algorithms for the effective and automatic integration of stiff systems of differential equations. However Merson's method (see, for instance, Spencer et al [22]) of integrating a set of differential equations has been utilized in this thesis since the nature of the closed loop systems considered is such that the necessary computer processing times were far from excessive.

In chapter two Porter and Shentons' [9] analysis of the open loop transfer function matrix is used to analyse the transfer function matrices of closed-loop control systems incorporating fast-sampling controllers.

1.4 Fast-Sampling Control Techniques

The two main questions facing control engineers when designing sampled-data controllers for linear multi-variable continuous time plants are the choice of sampling frequency and the choice of the feedback gains. Problems can arise if these are considered independently but are obviated if the control law is expressed as an appropriate function of the sampling frequency and the controller gain matrices, and if the controller gain matrices are designed in accordance with the continuous-time high-gain techniques of Porter and Bradshaw [23] . The design of sampled-data controllers then becomes a root-locus problem in the discrete-time domain where, as the sampling frequency is increased, the roots either tend to the origin (fast modes) or to the inside edge of the unit disc (slow modes). Porter and Bradshaw [7] ,[8] used this approach for a class of systems that satisfy two criteria. The first of these criteria requires that the matrix equal to the product of the output and input matrices respectively , of the state-space representation of the system, has rank equal to the number of outputs and the second requires that all the transmission zeros (see Popov [24]) lie in the left half plane. If these criteria are satisfied then fast-sampling error-actuated output feedback controllers can readily be designed so that as the sampling frequency is increased the outputs are

(i) increasingly characterized by the fast modes in the system,

(ii) increasingly non-interacting

and

(iii) increasingly insensitive to plant parameter variations.

This substantial advance in the analysis and design of sampled-data systems was only possible because Porter and Bradshaw [7], [8] expressed the characteristic roots in the discrete-time domain in terms of the characteristic roots in the continuous-time domain.

If the criteria expressed above are not satisfied then a fast-sampling error-actuated controller can only be employed if extra-measurements are included with the outputs in the feedback loops. Such a fast-sampling controller will be robust if designed in accordance with the techniques presented in sections (2.3) and (3.2). It follows directly from sections (2.3) and (3.2) that such a fast-sampling controller can be designed so that the outputs are increasingly insensitive to plant parameter variations.

In this thesis it is the above techniques that will be utilized in order to design controllers for the two vehicle systems mentioned in section (1.1), and to illustrate their properties with relation to the possible controller structures.

CHAPTER 2

THEORY

2.1 Introduction

In this chapter the fast-sampling control theory used to synthesize the vehicle system controllers in chapters four, six and seven is presented in the form of singular perturbation analyses of the closed-loop transfer function matrices. The singular perturbation analyses are carried out by applying Porter and Shentons' [9] treatment of the transfer function matrices of open-loop singularly perturbed systems, summarized in section (2.2). The analysis of closed-loop systems having fast-sampling error-actuated controllers incorporating extra-measurements is considered in section (2.3). The analysis of closed-loop systems having fast-sampling error-actuated controllers is considered in section (2.4), summarizing Porter and Bradshaws' [7] , [8] results. Finally, in section (2.5) the rejection of disturbances from closed-loop systems having fast-sampling error-actuated controllers is considered.

2.2 Singular Perturbation Analysis of the Transfer Function Matrix

A singularly-perturbed linear time-invariant system is a multivariable dynamical system whose behaviour can be described by state and output equations of the respective forms

$$\begin{bmatrix} \dot{x} \\ \dot{z} \end{bmatrix} = \begin{bmatrix} A_1 & A_2 \\ A_3/\varepsilon & A_4/\varepsilon \end{bmatrix} \begin{bmatrix} x \\ z \end{bmatrix} + \begin{bmatrix} B_1 \\ B_2/\varepsilon \end{bmatrix} u \tag{2.1}$$

and

$$y = \begin{bmatrix} C_1 & C_2 \end{bmatrix} \begin{bmatrix} x \\ z \end{bmatrix}, \tag{2.2}$$

where ε is a small positive parameter, $x \in R^n$, $z \in R^m$, $u \in R^m$, $y \in R^\ell$, $A_1 \in R^{nxn}$, $A_2 \in R^{nxm}$, $A_3 \in R^{mxn}$, $A_4 \in R^{mxm}$, $B_1 \in R^{nxm}$, $B_2 \in R^{mxm}$, $C_1 \in R^{\ell xn}$ and $C_2 \in R^{\ell xm}$.

The corresponding transfer function matrices of the open-loop singularly perturbed systems governed by (2.1) and (2.2) assume the form

$$G(\lambda,\varepsilon) = \begin{bmatrix} C_1' \\ C_2' \end{bmatrix}' \begin{bmatrix} \lambda I_n - A_1 & -A_2 \\ -A_3/\varepsilon & \lambda I_m - A_4/\varepsilon \end{bmatrix}^{-1} \begin{bmatrix} B_1 \\ B_2/\varepsilon \end{bmatrix} \in R^{\ell xm}. \tag{2.3}$$

Porter and Shenton [9] showed that as $\varepsilon \to 0$ the transfer function matrices given by (2.3) approach the asymptotic form

$$\Gamma(\lambda) = \bar{\Gamma}(\lambda) + \hat{\Gamma}(\lambda) \in R^{\ell x m} \quad (2.4)$$

where

$$\bar{\Gamma}(\lambda) = C_o (\lambda I_n - A_o)^{-1} B_o \quad (2.5)$$

and

$$\hat{\Gamma}(\lambda) = C_2 (\varepsilon\lambda I_m - A_4)^{-1} B_2 \quad (2.6)$$

are respectively the slow and fast parts of the asymptotic transfer function matrices. In (2.5) and (2.6)

$$A_o = A_1 - A_2 A_4^{-1} A_3 \in R^{nxn} , \quad (2.7)$$

$$B_o = B_1 - A_2 A_4^{-1} B_2 \in R^{nxm}, \quad (2.8)$$

$$C_o = C_1 - C_2 A_4^{-1} A_3 \in R^{\ell xn} \quad (2.9)$$

and it is assumed that A_4 is non-singular.

2.3 Fast-Sampling Error-Actuated Controllers with Extra Measurements

Digital control of continuous-time plants requires that any measurements used for control are available in a discrete time form. Similarly since the plant exists in the time continuum it is clear that any control actions have to be in either a continuous-time or piecewise continuous-time form. Figure (2.1) shows the type of digital control used in this thesis and illustrates the typical interconnections in the control system. The samplers convert the continuous-time output signals y(t), the extra-measurement signals r(t), and the command input signals v(t) into discrete-time form. The discrete-time error signals, e(kT), are processed by the digital controller to produce the discrete-time control actions u(kT). The control actions are converted into piecewise continuous form u(t) by the 'zero order hold' that maintains u(t) at u(kT) for T seconds.

The theory presented in section (2.2) can be used to investigate the structure of the closed-loop transfer function matrices of the class of tracking systems incorporating controllable and observable linear multivariable plants and fast-sampling error-actuated controllers. The plants of such discrete-time tracking systems are governed on the continuous-time set $\tau = [0, +\infty)$ by state, output and extra-measurement equations of the respective forms

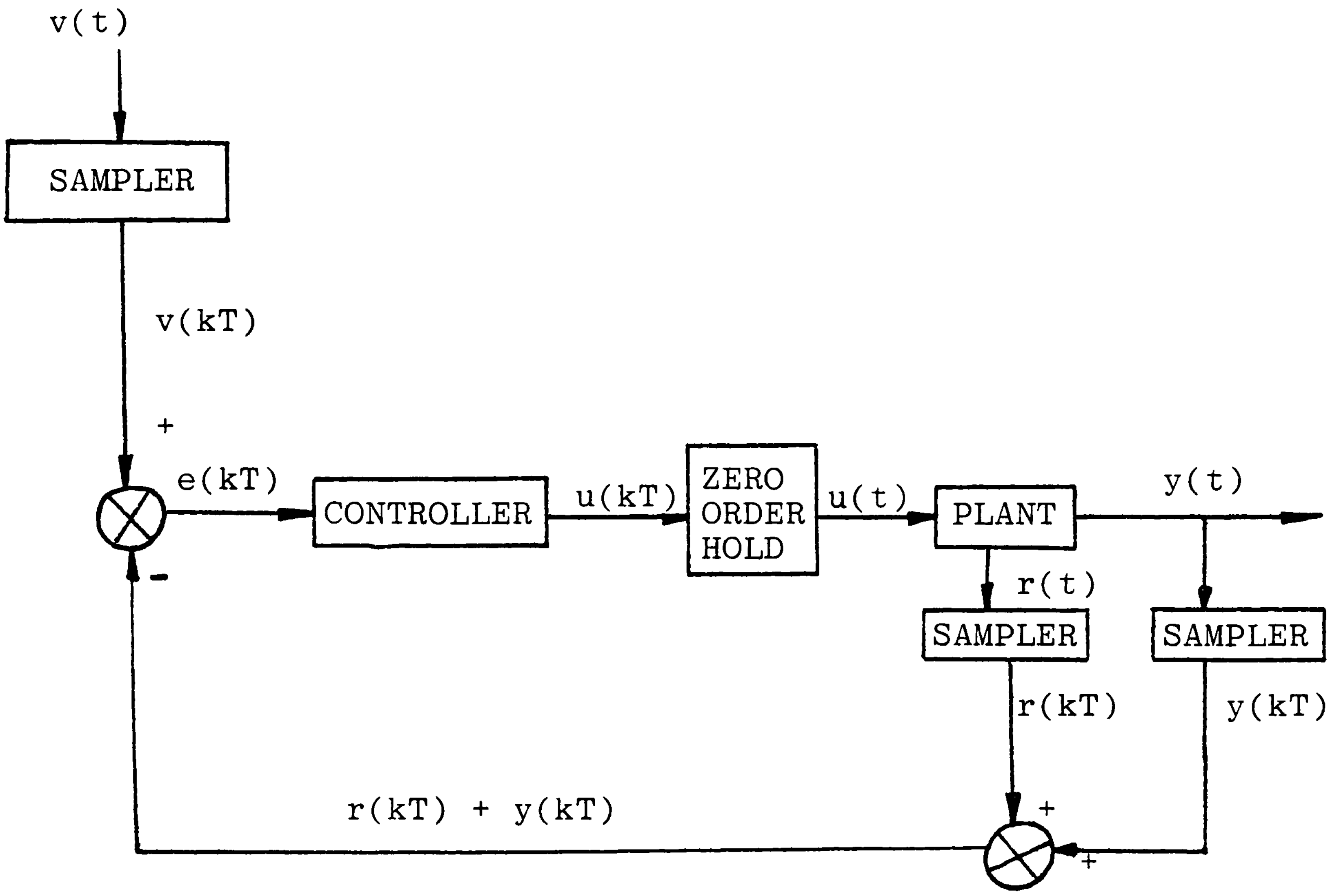

DIGITAL CONTROL WITH EXTRA-MEASUREMENTS

Figure 2.1

$$\begin{bmatrix} \dot{x}_1(t) \\ \dot{x}_2(t) \end{bmatrix} = \begin{bmatrix} A_{11} & A_{12} \\ A_{21} & A_{22} \end{bmatrix} \begin{bmatrix} x_1(t) \\ x_2(t) \end{bmatrix} + \begin{bmatrix} O \\ B \end{bmatrix} u(t), \qquad (2.10)$$

$$y(t) = \begin{bmatrix} C_1 & C_2 \end{bmatrix} \begin{bmatrix} x_1(t) \\ x_2(t) \end{bmatrix} \qquad (2.11)$$

and

$$r(t) = \begin{bmatrix} R_1 & R_2 \end{bmatrix} \begin{bmatrix} x_1(t) \\ x_2(t) \end{bmatrix}. \qquad (2.12)$$

The fast-sampling error-actuated digital controller employed is governed on the discrete-time set $\tau_T = \{ 0, T, 2T, --, \}$ by a control law equation of the form

$$u(KT) = f\{ K_o\, e(KT) + K_1 z(KT) \} \qquad (2.13)$$

where

$$e(KT) = v(KT) - y(KT) - r(KT) \qquad (2.14)$$

$$z\{(K+1)T\} = z(KT) + T\, e\,(KT) \qquad (2.15)$$

and v(KT) is the command input vector. It is assumed that K_o , K_1 and f are such that the controlled system is stable and hence (see Porter and Bradshaw [8])

$$\lim_{K\to\infty} e(KT) = \lim_{K\to\infty} v(KT) - y(KT) - r(KT)$$

$$= 0 \qquad (2.16)$$

for arbitrary initial conditions. It follows directly from (2.10) that, in any steady state,

$$\lim_{t\to\infty} \begin{bmatrix} A_{11} & A_{12} \end{bmatrix} \begin{bmatrix} x_1(t) \\ x_2(t) \end{bmatrix} = 0 \qquad (2.17)$$

and hence the vector

$$r(t) = \begin{bmatrix} MA_{11} & MA_{12} \end{bmatrix} \begin{bmatrix} x_1(t) \\ x_2(t) \end{bmatrix} \qquad (2.18)$$

of extra measurements is such that

$$\lim_{K\to\infty} r(KT) = 0 \qquad (2.19)$$

for any $M \in R^{\ell x(n-\ell)}$. In view of (2.16) and (2.19) it is clear that the control input vector $u(t) = u(KT)$, $t \in \left[KT, (K+1)T \right]$, $KT \in \tau_T$, will cause the output vector $y(t)$ to track any constant command input vector $v(t)$ on τ_T in the sense that

$$\lim_{K\to\infty} \{ v(KT) - y(KT) \} = 0 . \qquad (2.20)$$

In (2.11) to (2.21), $x_1(t) \varepsilon R^{n-\ell}$, $x_2(t) \varepsilon R^{\ell}$, $u(t) \varepsilon R^{\ell}$, $y(t) \varepsilon R^{\ell}$, $r(t) \varepsilon R^{\ell}$, $A_{11} \varepsilon R^{(n-\ell)x(n-\ell)}$, A_{12} $R^{(n-\ell)x\ell}$, $A_{21} \varepsilon R^{\ell x(n-\ell)}$, $A_{22} \varepsilon R^{\ell x\ell}$, $B \varepsilon R^{\ell x\ell}$, $C_1 \varepsilon R^{\ell xn-\ell}$, $C_2 \varepsilon R^{\ell x\ell}$, $R_1 \varepsilon R^{\ell x(n-\ell)}$, $R_2 \varepsilon R^{\ell x\ell}$, $e(t) \varepsilon R^{\ell}$, $v(t) \varepsilon R^{\ell}$, $z(KT) \varepsilon R^{\ell}$, $K_o \varepsilon R^{\ell x\ell}$, $K_1 \varepsilon R^{\ell x\ell}$, the sampling frequency $f = {}^1/T \varepsilon R^+$,

$$\text{rank} \quad \{ C_2B \} \quad < \quad \ell \quad , \tag{2.21}$$

$$\text{rank} \quad \{(C_2+R_2)B\} \quad = \quad \ell \tag{2.22}$$

and

$$\begin{bmatrix} R_1 & R_2 \end{bmatrix} = \begin{bmatrix} M\ A_{11} & M\ A_{12} \end{bmatrix} . \tag{2.23}$$

Furthermore condition (2.22) requires that C_2 and A_{12} are such that M can be chosen so that

$$\text{rank } (C_2+R_2) = \text{ rank } (C_2+MA_{12}) = \ell . \tag{2.24}$$

It is evident from (2.10) to (2.13) that such discrete time systems are governed on τ_T by state, output and extra-measurement equations of the respective forms

$$\begin{bmatrix} z\{(K+1)T\} \\ x_1\{(K+1)T\} \\ x_2\{(K+1)T\} \end{bmatrix} = \begin{bmatrix} I_\ell & -TF_1 & -TF_2 \\ f\psi_1K_1 & \Phi_{11}-f\psi_1K_oF_1 & \Phi_{12}-f\psi_1K_oF_2 \\ f\psi_2K_1 & \Phi_{21}-f\psi_2K_oF_1 & \Phi_{22}-f\psi_2K_oF_2 \end{bmatrix} \begin{bmatrix} z(KT) \\ x_1(KT) \\ x_2(KT) \end{bmatrix} + \begin{bmatrix} T\ \ I_\ell \\ f\psi_1K_o \\ f\psi_2K_o \end{bmatrix} v(KT) , \tag{2.25}$$

$$y(KT) = \begin{bmatrix} 0 & C_1 & C_2 \end{bmatrix} \begin{bmatrix} z(KT) \\ x_1(KT) \\ x_2(KT) \end{bmatrix} \qquad (2.26)$$

and

$$r(KT) = \begin{bmatrix} 0 & R_1 & R_2 \end{bmatrix} \begin{bmatrix} z(KT) \\ x_1(KT) \\ x_2(KT) \end{bmatrix} \qquad (2.27)$$

where

$$F_1 = \begin{bmatrix} R_1 + C_1 \end{bmatrix} \varepsilon \; R^{\ell x(n-\ell)}, \qquad (2.28)$$

$$F_2 = \begin{bmatrix} R_2 + C_2 \end{bmatrix} \varepsilon \; R^{\ell x \ell}, \qquad (2.29)$$

$$\begin{bmatrix} \Phi_{11} & \Phi_{12} \\ \Phi_{21} & \Phi_{22} \end{bmatrix} = \exp\left\{ \begin{bmatrix} A_{11} & A_{12} \\ A_{21} & A_{22} \end{bmatrix} T \right\} \qquad (2.30)$$

and

$$\begin{bmatrix} \psi_1 \\ \psi_2 \end{bmatrix} = \int_0^T \exp\left\{ \begin{bmatrix} A_{11} & A_{12} \\ A_{21} & A_{22} \end{bmatrix} t \right\} \begin{bmatrix} 0 \\ B \end{bmatrix} dt. \qquad (2.31)$$

The transfer function matrices relating the plant output vector and the extra-measurements vector to the command input vector of the discrete-time tracking systems governed by (2.25) to (2.27) are respectively

$$G_y(\lambda) =$$

$$\begin{bmatrix} 0 \\ C_1' \\ C_2' \end{bmatrix}' \begin{bmatrix} \lambda I_\ell - I_\ell & TF_1 & TF_2 \\ -f\psi_1 K_1 & \lambda I_{n-\ell} - \Phi_{11} + f\psi_1 K_o F_1 & -\Phi_{12} + f\psi_1 K_o F_2 \\ -f\psi_2 K_1 & -\Phi_{21} + f\psi_2 K_o F_1 & \lambda I_\ell - \Phi_{22} + f\psi_2 K_o F_2 \end{bmatrix}^{-1} \begin{bmatrix} T\ I_\ell \\ f\psi_1 K_o \\ f\psi_2 K_o \end{bmatrix}$$

(2.32)

and

$G_r(\lambda) =$

$$\begin{bmatrix} 0 \\ R_1' \\ R_2' \end{bmatrix}' \begin{bmatrix} \lambda I_\ell - I_\ell & TF_1 & TF_2 \\ -f\psi_1 K_1 & \lambda I_{n-\ell} - \Phi_{11} + f\psi_1 K_o F_1 & -\Phi_{12} + f\psi_1 K_o F_2 \\ -f\psi_2 K_1 & -\Phi_{21} + f\psi_2 K_o F_1 & \lambda I_\ell - \Phi_{22} + f\psi_2 K_o F_2 \end{bmatrix}^{-1} \begin{bmatrix} T\ I_\ell \\ f\psi_1 K_o \\ f\psi_2 K_o \end{bmatrix}$$

(2.33)

and the fast-sampling tracking characteristics can be elucidated by using the results of Porter and Shenton [9] summarized in section (2.2). In view of (2.30) and (2.31) it is clear that

$$\lim_{f\to\infty} f \begin{bmatrix} \Phi_{11} - I_{n-\ell} & \Phi_{12} \\ \Phi_{21} & \Phi_{22} - I_\ell \end{bmatrix} = \begin{bmatrix} A_{11} & A_{12} \\ A_{21} & A_{22} \end{bmatrix} \qquad (2.34)$$

and

$$\lim_{f\to\infty} f \begin{bmatrix} \psi_1 \\ \psi_2 \end{bmatrix} = \begin{bmatrix} 0 \\ B \end{bmatrix} \qquad (2.35)$$

and hence it follows that as $f \to \infty$ the transfer function matrices $G_y(\lambda)$ and $G_r(\lambda)$ assume the asymptotic forms

$$\Gamma_y(\lambda) = \bar{\Gamma}_y(\lambda) + \hat{\Gamma}_y(\lambda) \tag{2.36}$$

and

$$\Gamma_r(\lambda) = \bar{\Gamma}_r(\lambda) + \hat{\Gamma}_r(\lambda) \tag{2.37}$$

where

$$\bar{\Gamma}_y(\lambda) = C_{o_y} \{\lambda I_n - I_n - TA_o\}^{-1} T\, B_o, \tag{2.38}$$

$$\hat{\Gamma}_y(\lambda) = C_2 \{\lambda I_\ell - I_\ell - A_4\}^{-1} B\, K_o, \tag{2.39}$$

$$\bar{\Gamma}_r(\lambda) = C_{o_r} \{\lambda I_n - I_n - TA_o\}^{-1} T\, B_o, \tag{2.40}$$

$$\hat{\Gamma}_r(\lambda) = R_2 \{\lambda I_\ell - I_\ell - A_4\}^{-1} B\, K_o, \tag{2.41}$$

$$A_o = \begin{bmatrix} -K_o^{-1}K_1 & 0 \\ A_{12}F_2^{-1}K_o^{-1}K_1 & A_{11} - A_{12}F_2^{-1}F_1 \end{bmatrix}, \tag{2.42}$$

$$B_o = \begin{bmatrix} 0 \\ A_{12}F_2^{-1} \end{bmatrix}, \tag{2.43}$$

$$C_{o_y} = \begin{bmatrix} C_2F_2^{-1}K_o^{-1}K_1 & C_1 - C_2F_2^{-1}F_1 \end{bmatrix}, \tag{2.44}$$

$$C_{o_r} = \begin{bmatrix} R_2F_2^{-1}K_o^{-1}K_1 & R_1 - R_2F_2^{-1}F_1 \end{bmatrix} \tag{2.45}$$

and

$$A_4 = -BK_oF_2 \,. \tag{2.46}$$

It follows from (2.36), (2.38) and (2.42) that the set of 'slow' modes Z_s of the tracking system correspond as $f \to \infty$ to the set of poles $Z_1 \cup Z_2$ of $\bar{\Gamma}_r(\lambda)$ and $\bar{\Gamma}_y(\lambda)$,

where

$$Z_1 = \{\lambda \in \mathbb{C} : |\lambda I_\ell - I_\ell + TK_o^{-1}K_1| = 0 \} \quad (2.47)$$

and

$$Z_2 = \{\lambda \in \mathbb{C} : |\lambda I_{n-\ell} - I_{n-\ell} - TA_{11} + TA_{12}F_2^{-1}F_1| = 0 \} \quad (2.48)$$

and from (2.18) , (2.39), (2.41), (2.52) and (2.53) that the set of 'fast' modes Z_f of the tracking system correspond as $f \to \infty$ to the set of poles Z_3 of $\hat{\Gamma}_r(\lambda)$ and $\hat{\Gamma}_y(\lambda)$, where

$$Z_3 = \{\lambda \in \mathbb{C} : |\lambda I_\ell - I_\ell + F_2BK_o| = 0 \} . \quad (2.49)$$

Furthermore it follows from (2.23), (2.38) , (2.40) and (2.42) to (2.45) that the 'slow' output and extra-measurement transfer function matrices assume the respective forms

$\bar{\Gamma}_y(\lambda)$

$$= (C_1-C_2F_2^{-1}F_1)(\lambda I_{n-\ell}-I_{n-\ell}-TA_{11}+TA_{12}F_2^{-1}F_1)^{-1}TA_{12}F_2^{-1} \quad (2.50)$$

and

$\bar{\Gamma}_r(\lambda)$

$$= M(A_{11}-A_{12}F_2^{-1}F_1)(\lambda I_{n-\ell}-I_{n-\ell}-TA_{11}+TA_{12}F_2^{-1}F_1)^{-1}TA_{12}F_2^{-1} \quad (2.51)$$

and from (2.23), (2.39), (2.41) and (2.46) that the corresponding 'fast' parts assume the respective forms

$$\hat{\Gamma}_y(\lambda) = C_2F_2^{-1}(\lambda I_\ell-I_\ell+F_2BK_o)^{-1}F_2BK_o \quad (2.52)$$

and

$$\hat{\Gamma}_r(\lambda) = MA_{12}F_2^{-1}(\lambda I_\ell-I_\ell+F_2BK_o)^{-1}F_2BK_o \; . \quad (2.53)$$

Hence in view of (2.50) to (2.53) it is evident from (2.36) and (2.37) that as $f\to\infty$ the output and extra-measurement transfer function matrices $G_y(\lambda)$ and $G_r(\lambda)$ of the discrete-time tracking systems assume the respective asymptotic forms

$$\Gamma_y(\lambda) = (C_1-C_2F_2^{-1}F_1)(\lambda I_{n-\ell}-I_{n-\ell}-TA_{11}+TA_{12}F_2^{-1}F_1)^{-1}TA_{12}F_2^{-1} + C_2F_2^{-1}(\lambda I_\ell-I_\ell+F_2BK_o)^{-1}F_2BK_o \quad (2.54)$$

and

$$\Gamma_r(\lambda) = M(A_{11}-A_{12}F_2^{-1}F_1)(\lambda I_{n-\ell}-I_{n-\ell}-TA_{11}+TA_{12}F_2^{-1}F_1)^{-1}TA_{12}F_2^{-1}$$

$$+ MA_{12}F_2^{-1}(\lambda I_\ell-I_\ell+F_2BK_o)^{-1}F_2BK_o \qquad (2.55)$$

in consonance with the facts that both the set of 'slow' modes corresponding to the set of poles Z_2 and the set of 'fast' modes corresponding to the set of poles Z_3 possibly remain both controllable and observable as $f\to\infty$. However the 'slow' output and extra-measurement transfer function matrices reduce to the form expressed by (2.50) and (2.51) precisely because the set of 'slow' modes corresponding to the set of poles Z_1 definitely become asymptotically uncontrollable as $f\to\infty$ in view of the block structure of the matrices A_o and B_o given by (2.42) and (2.43).

2.4 Fast-Sampling Error-Actuated Controllers

The closed-loop transfer function matrices developed in section (2.3) can now be utilized to illustrate the results reported by Porter and Bradshaw [7], [8], who considered a class of tracking systems incorporating plants governed by state and output equations of the forms given by (2.10) and (2.11). Extra-measurements were not needed since Porter and Bradshaw [7], [8] guaranteed stable fast-sampling control by assuming that

$$\text{rank } (C_2 B) = \ell \tag{2.56}$$

and

$$\nu_j \subset \mathcal{C}^- \quad (j=1,--,n-\ell) \tag{2.57}$$

where the ν_j $(j=1,..,n-\ell)$ are the transmission zeros (see Popov [24]) of the triple

$$\left\{ \begin{bmatrix} A_{11} & A_{12} \\ A_{21} & A_{22} \end{bmatrix}, \begin{bmatrix} O \\ B \end{bmatrix}, \begin{bmatrix} C_1 & C_2 \end{bmatrix} \right\}.$$

In order to utilize the theory developed in section (2.3) the error-actuated control law given by (2.13) is employed, where it is assumed that

$$M = O \tag{2.58}$$

since no extra-measurements are needed, so that in view of (2.23), (2.28) and (2.29)

$$\begin{bmatrix} F_1 & F_2 \end{bmatrix} = \begin{bmatrix} C_1 & C_2 \end{bmatrix} . \tag{2.59}$$

It follows from (2.14), (2.16), (2.18) and (2.58) that the fast-sampling control law equation given by (2.13) will now cause the output vector y(t) to track any constant command input vector v(t) on τ_T in the sense that

$$\lim_{K\to\infty} \{v(KT) - y(KT)\} = 0 \tag{2.60}$$

as a consequence of the fact that the error vector

$$e(t) = v(t) - y(t) \tag{2.61}$$

still assumes the steady-state value

$$\lim_{K\to\infty} e(KT) = 0 . \tag{2.62}$$

It further follows from (2.59) and (2.32) that the transfer function matrix relating the plant output vector to the command input vector of the discrete-time tracking system governed by (2.25), (2.26) and (2.59) is

$G(\lambda) =$

$$\begin{bmatrix} 0 \\ C_1' \\ C_2' \end{bmatrix}' \begin{bmatrix} \lambda I_\ell - I_\ell & -TC_1 & -TC_2 \\ -f\psi_1 K_1 & \lambda I_{n-\ell} - \Phi_{11} + f\psi_1 K_o C_1 & -\Phi_{12} + f\psi_1 K_o C_2 \\ -f\psi_2 K_1 & -\Phi_{21} + f\psi_2 K_o C_1 & \lambda I_\ell - \Phi_{22} + f\psi_2 K_o C_2 \end{bmatrix}^{-1} \begin{bmatrix} TI_\ell \\ f\psi_1 K_o \\ f\psi_2 K_o \end{bmatrix} . \quad (2.63)$$

It finally follows from (2.36), (2.38), (2.39) and the simplification of (2.42), (2.43), (2.44) and (2.46) by using (2.59), that as $f\to\infty$ the output transfer function matrix assumes the asymptotic form

$$\Gamma(\lambda) = \bar{\Gamma}(\lambda) + \hat{\Gamma}(\lambda) \quad (2.64)$$

where

$$\bar{\Gamma}(\lambda) = C_o(\lambda I_n - I_n - TA_o)^{-1} TB_o \quad (2.65)$$

$$\hat{\Gamma}(\lambda) = C_2(\lambda I_n - I_\ell - A_4)^{-1} BK_o \quad (2.66)$$

$$A_o = \begin{bmatrix} -K_o^{-1}K_1 & 0 \\ A_{12}C_2^{-1}K_o^{-1}K_1 & A_{11} - A_{12}C_2^{-1}C_1 \end{bmatrix}, \quad (2.67)$$

$$B_o = \begin{bmatrix} 0 \\ A_{12}C_2^{-1} \end{bmatrix}, \quad (2.68)$$

$$C_o = \begin{bmatrix} K_o^{-1}K_1 & 0 \end{bmatrix} \quad (2.69)$$

and

$$A_4 = - BK_oC_2 \quad . \tag{2.70}$$

It is evident from (2.64), (2.65) and (2.67) that the set of 'slow' modes Z_s of the tracking systems correspond as $f \to \infty$ to the set of poles $Z_1 \cup Z_2$ of $\bar{\Gamma}(\lambda)$ where

$$Z_1 = \{\lambda \varepsilon C : |\lambda I_\ell - I_\ell + TK_o^{-1}K_1| = 0\} \tag{2.71}$$

and

$$Z_2 = \{\lambda \varepsilon C : |\lambda I_{n-\ell} - I_{n-\ell} - TA_{11} + TA_{12}C_2^{-1}C_1| = 0\} \tag{2.72}$$

and from (2.66), (2.70) and (2.75) that the 'fast' modes Z_f of the tracking systems correspond as $f \to \infty$ to the set of poles Z_3 of $\hat{\Gamma}(\lambda)$ where

$$Z_3 = \{\lambda \varepsilon C : |\lambda I_\ell - I_\ell + C_2BK_o| = 0\} \quad . \tag{2.73}$$

Furthermore it follows from (2.64) and (2.66) to (2.68) that the 'slow' transfer function matrix

$$\bar{\Gamma}(\lambda) = 0 \tag{2.74}$$

and from (2.66) and (2.70) that the 'fast' transfer function matrix assumes the form

$$\hat{\Gamma}(\lambda) = (\lambda I_\ell - I_\ell + C_2BK_o)^{-1}C_2BK_o \quad . \tag{2.75}$$

In view of (2.74) and (2.75) it is clear from (2.64) that

$$\lim_{f\to\infty} G(\lambda) = \Gamma(\lambda) = \hat{\Gamma}(\lambda) \tag{2.76}$$

in consonance with the fact that the 'fast' modes corresponding to the set of poles Z_3 remain controllable and observable as $f\to\infty$. However the 'slow' transfer function matrix $\bar{\Gamma}(\lambda)$ is null because the 'slow' modes corresponding to the sets of poles $Z_1 \cup Z_2$ respectively become uncontrollable and unobservable as $f\to\infty$ in view of the block structure of A_o, B_o and C_o given by (2.67) to (2.69).

2.5 Fast-Sampling Error-Actuated Controllers and Disturbance Rejection

The disturbance rejection properties of the tracking systems developed in section (2.4) are now considered. It will be shown that the outputs are increasingly unaffected by disturbances as $f \to \infty$. This will be achieved by considering the plants of the class of discrete-time tracking systems that are governed on the continuous time set $\tau = [0, +\infty)$ by the state equation

$$\begin{bmatrix} \dot{x}_1(t) \\ \dot{x}_2(t) \end{bmatrix} = \begin{bmatrix} A_{11} & A_{12} \\ A_{21} & A_{22} \end{bmatrix} \begin{bmatrix} x_1(t) \\ x_2(t) \end{bmatrix} + \begin{bmatrix} 0 \\ B \end{bmatrix} u(t) + \begin{bmatrix} D_1 \\ D_2 \end{bmatrix} d(t) \tag{2.77}$$

and by an output equation of the form given by (2.11). In order to utilize the theory presented in section (2.4) it is further assumed that d(t) is a constant unmeasureable disturbance so that the control law equation given by (2.13) can achieve complete rejection. It follows from (2.13), (2.15), (2.26), (2.30), (2.31), (2.59), (2.61) and (2.77) that such discrete-time disturbance rejection systems are governed on τ_T by state and output equations of the respective forms

$$\begin{bmatrix} z\{(K+1)T\} \\ x_1\{(K+1)T\} \\ x_2\{(K+1)T\} \end{bmatrix} = \begin{bmatrix} I_\ell & -TC_1 & -TC_2 \\ f\psi_1 K_1 & \Phi_{11} - f\psi_1 K_o C_1 & \Phi_{12} - f\psi_1 K_o C_2 \\ f\psi_1 K_1 & \Phi_{21} - f\psi_2 K_o C_1 & \Phi_{22} - f\psi_2 K_o C_2 \end{bmatrix} \begin{bmatrix} z(KT) \\ x_1(KT) \\ x_2(KT) \end{bmatrix}$$

$$+ \begin{bmatrix} T\ I_\ell \\ f\psi_1 K_o \\ f\psi_2 K_o \end{bmatrix} v(KT) + \begin{bmatrix} 0 \\ \Delta_1 \\ \Delta_2 \end{bmatrix} d(KT) \qquad (2.78)$$

and

$$y(KT) = \begin{bmatrix} 0 & C_1 & C_2 \end{bmatrix} \begin{bmatrix} z(KT) \\ x_1(KT) \\ x_2(KT) \end{bmatrix} \qquad (2.79)$$

where it has been assumed that d(t) is of such a form that

$$\begin{bmatrix} \Delta_1 \\ \Delta_2 \end{bmatrix} \triangleq \int_0^T \exp\left\{ \begin{bmatrix} A_{11} & A_{12} \\ A_{21} & A_{22} \end{bmatrix} t \right\} dt \begin{bmatrix} D_1 \\ D_2 \end{bmatrix} . \qquad (2.80)$$

The transfer function matrix relating the plant output vector to the disturbance vector is

$$G_D(\lambda) =$$

$$\begin{bmatrix} 0 \\ C_1' \\ C_2' \end{bmatrix}' \begin{bmatrix} \lambda I_\ell - I_\ell & TC_1 & TC_2 \\ -f\psi_1 K_1 & \lambda I_{n-\ell} - \Phi_{11} + f\psi_1 K_o C_1 & -\Phi_{12} + f\psi_1 K_o C_2 \\ -f\psi_2 K_1 & -\Phi_{21} + f\psi_2 K_o C_1 & \lambda I_\ell - \Phi_{22} + f\psi_2 K_o C_2 \end{bmatrix}^{-1} \begin{bmatrix} 0 \\ \Delta_1 \\ \Delta_2 \end{bmatrix} \quad (2.81)$$

and the fast-sampling characteristics will again be elucidated by using the results of Porter and Shenton [9] . It follows from (2.80) that

$$\lim_{f\to\infty} f \begin{bmatrix} \Delta_1 \\ \Delta_2 \end{bmatrix} = \begin{bmatrix} D_1 \\ D_2 \end{bmatrix} \quad (2.82)$$

which together with (2.34) and (2.35) indicates that, as $f\to\infty$, $G_D(\lambda)$ assumes the asymptotic form

$$\Gamma_D(\lambda) = \bar{\Gamma}_D(\lambda) + \hat{\Gamma}_D(\lambda) \quad (2.83)$$

where

$$\bar{\Gamma}_D(\lambda) = \begin{bmatrix} K_o^{-1}K_1 & 0 \end{bmatrix} \begin{bmatrix} \lambda I_{n-\ell} - I_{n-\ell} - A_o \end{bmatrix}^{-1} \begin{bmatrix} 0 \\ D_1 \end{bmatrix} \quad (2.84)$$

$$\hat{\Gamma}_D(\lambda) = C_2 \left[\lambda I_\ell - I_\ell - A_4\right]^{-1} O \equiv O \tag{2.85}$$

A_o is given by (2.67) and A_4 by (2.70). It follows from (2.84) and the structure of A_o that

$$\bar{\Gamma}_D(\lambda) = O \tag{2.86}$$

and hence

$$\lim_{f\to\infty} G_D(\lambda) = \Gamma_D(\lambda) = O . \tag{2.87}$$

It is therefore clear that as $f \to \infty$ the class of tracking systems developed in section (2.4) is increasingly unaffected by disturbances.

CHAPTER 3

CONTROLLER SYNTHESIS AND STRUCTURE

3.1 Introduction

The extreme example of a 'centralized' controller is a controller that simultaneously adjusts all the inputs with a change in any one, or more , errors. Similarly the extreme example of a decentralized controller is a controller that simultaneously adjusts only one input with a change in the corresponding error. Clearly a whole range of controllers exists between these two extremes. It follows from the theory developed in sections (2.3) and (2.4) that it may be possible to vary the structure of fast-sampling controllers between two such extremes, and these extremes are considered in sections (3.3) and (3.4).

Finally in section (3.5) a definition of transmission zeros is given in the light of the work initiated by Popov [24] .

3.2 Synthesis of Fast-Sampling Controllers

For the closed-loop systems developed in sections (2.3) and (2.4) it is clear that tracking will occur in the sense of (2.16) and (2.60) provided that

$$Z_s \cup Z_f \subset D^- \tag{3.1}$$

where D^- is the open unit disc. In view of (2.47) to (2.49) and (2.71) to (2.73) the 'slow' and 'fast' modes will satisfy the tracking requirement (3.1) for sufficiently small sampling periods if the controller matrices K_o, K_1, and, where applicable, M are chosen so that

$$Z_1 \subset D^- \tag{3.2}$$

$$Z_2 \subset D^- \tag{3.3}$$

and

$$Z_3 \subset D^- \tag{3.4}$$

where it has been assumed that M can be chosen so as to satisfy the measurement condition (2.24) when extra-measurements are needed, or that (2.56) and (2.57) are satisfied when extra-measurements are not utilized.

It follows from (2.49) and (2.73) that the set of closed-loop poles $Z_3(=1-\sigma_i, i=1,..,\ell)$ are assigned by a suitable choice of the eigenvalues $\sigma_i(i=1,..,\ell)$ of the matrix Σ, where either

$$\Sigma = F_2 B K_o \tag{3.5}$$

for the closed-loop systems utilizing extra-measurements in the controller as in section (2.3), or

$$\Sigma = C_2 B K_o \tag{3.6}$$

when output feedback alone is used as in section (2.4). Hence it is clear that the respective controllers are given either by

$$K_o = (F_2B)^{-1} \Sigma \tag{3.7}$$

or by

$$K_o = (C_2 B)^{-1} \Sigma \tag{3.8}$$

and that (3.4) will be satisifed if

$$\sigma_i = 1 \quad (i=1,..,\ell) \tag{3.9}$$

which will cause the corresponding closed-loop poles to approach the origin as $f \to \infty$. The structure of Σ or K_o may be chosen within the limits imposed by either F_2B or C_2B, and is further discussed in the next two sections.

It follows from (2.47) and (2.71) that the set of closed-loop poles Z_1 $(=1-\rho_i T,\ i=1,..,\ell)$ are assigned by a suitable choice of the eigenvalues ρ_i $(i=1,..,\ell)$ of the matrix

$$R_A = K_o^{-1} K_1 \,. \tag{3.10}$$

Hence the controller required to achieve the assignment is designed by setting

$$K_1 = K_o R_A \tag{3.11}$$

where a typical choice for R_A is

$$R_A = \text{diag}\,\{\rho_1, ..., \rho_\ell\} \tag{3.12}$$

and (3.2) will be satisfied if

$$\rho_i > 0 \qquad (i=1,..,\ell) . \tag{3.13}$$

Such an assignment will cause the corresponding closed-loop poles to approach the edge of the unit disc from the inside as $f\to\infty$.

The final part of the synthesis is concerned with satisfying condition (3.3) and the closed-loop systems developed in sections (2.3) and (2.4) are now considered separately.

For controllers utilizing extra-measurements, as in section (2.3), it follows from (2.48) that the set of closed-loop poles Z_2 $(=1-\eta_j T,\ j=1,..,n-\ell)$ are assigned by a suitable choice of the matrix M, since the η_j $(j=1,..,n-\ell)$ are the eigenvalues of the matrix

$$R_o = A_{12}(C_2+MA_{12})^{-1}\ (C_1-MA_{11})-A_{11} . \tag{3.14}$$

Clearly (3.3) will be satisfied provided that

$$\eta_j > 0, \quad (j=1,..,n-\ell). \tag{3.15}$$

Such an assignment will cause the corresponding closed-loop poles to approach the edge of the unit disc from the inside as $f\to\infty$.

For the closed-loop systems considered in section (2.4) it follows from (2.72) that the set of closed-loop poles Z_2 $(=1+\nu_j T,\ j=1,..,n-\ell)$ are not assignable since the $\nu_j (j=1,..,n-\ell)$ are the transmission zeros which are assumed to satisfy

$$\nu_j \subset C^- \ (j=1,..,n-\ell) \tag{3.16}$$

and, for the systems considered in sections (2.4) and (2.5),are the eigenvalues of the matrix

$$R_u = A_{11} - A_{12}C_2^{-1}C_1. \tag{3.17}$$

In view of (3.16) it is clear that (3.3) will be satisfied and the corresponding closed-loop poles will approach the edge of the unit disc from the inside as $f \to \infty$.

The closed-loop tracking systems developed in section (2.4) will always exhibit high accuracy in the face of plant parameter variations since as $f \to \infty$ it is clear from (2.74) and (2.75) that $G(\lambda)$ is increasingly independent of the plant matrix. The same is true of the closed-loop tracking systems developed in section (2.3) if the steady-state conditions expressed by (2.17) correspond to kinematic relationships which hold between the state variables as a consequence of the dynamical structure of the plant (see Porter and Bradshaw [25]).

3.3 Structures of Fast-Sampling Error-Actuated Controllers with Extra-Measurements

It is assumed , in this section, that there are no transmission zeros in the right half plane, but that

$$\text{rank } (C_2B) < \ell \qquad (3.18)$$

and therefore extra-measurements are required in order to implement fast-sampling output feedback controllers. It follows from (3.7) and (3.8) that the extra-measurements cause the previously linearly dependent rows of (C_2B) to become independent so that

$$\text{rank } (F_2B) = \ell \qquad (3.19)$$

and therefore allows a design to be accomplished. Hence it follows from (2.49) and (2.73) that extra-measurements should only be used to change the dependent rows of (C_2B) since this allows the outputs having independent rows to retain their fast responses and to produce the best design for a given system. This means that the minimum number of extra measurements should be used, otherwise slow modes will be introduced into the output responses that may have been dominated by fast modes. It follows that the structuring of the controller falls into two parts, firstly the outputs that have extra-measurements added to them are considered and secondly the remaining outputs that have no extra-measurements added to them are considered. In the remainder of this section only the first of the above two parts is considered since the second is effectively considered in the next section.

It was shown in section (2.3) that as $f \to \infty$ the slow part of the transfer function matrix of fast-sampling controllers utilizing extra measurements is non-zero and hence the response of the outputs will be slow. However it follows from (2.50) and (2.52) that it may be possible to structure M and K_o so that the outputs will be increasingly non-interacting as $f \to \infty$, if M can be chosen so that $\bar{\Gamma}_y(\lambda)$ is diagonal and if $C_2F_2^{-1}$ is such that K_o can be chosen so that $\hat{\Gamma}_y(\lambda)$ is diagonal. It is clear from (2.52) and (3.7) that $\hat{\Gamma}_y(\lambda)$ will only be diagonal if $C_2F_2^{-1}$ and Σ are diagonal.

These 'centralized' controllers have the greatest structure necessary since further structuring would not improve the response of the system and would probably cause some deterioration in performance as well as incurring additional capital costs. It is clear that the cost of the extra hardware to implement these 'centralized' controllers is repaid by the responses being least interactive.

However it follows from (2.48) that the response of the outputs is dominated by the slow modes that are increasingly independent of K_o as $f \to \infty$, and hence it could be argued that K_o should be designed so that it is diagonal . This would usually result in initially interacting 'fast' responses followed by increasingly non-interacting 'slow' responses as $f\to\infty$, where it has again been assumed that M is such that $\bar{\Gamma}_y(\lambda)$ is diagonal.

3.4 Structures of Fast-Sampling Error-Actuated Controllers

It is assumed , in this section, that conditions (2.56) and (2.57) are satisfied and hence fast-sampling error-actuated control is possible. It is clear from (2.74) to (2.76) that the response of such systems is increasingly dominated by the 'fast' modes as $f\to\infty$. Furthermore it follows from (2.75) and (3.6) that when Σ is a diagonal matrix the response of the closed-loop systems will be fast and non-interacting as $f\to\infty$. The resulting K_o from (3.8), to produce these responses would have the greatest structure necessary, since increasing the structure would not improve the response of the system and would probably cause some deterioration in performance as well as incurring extra capital costs. It is clear that the cost of the extra-hardware to implement these ideal 'centralized' controllers results in the responses of the systems being least interacting. Moving away from these controllers reduces the capital cost by reducing the size of the communications system until, finally, it may be possible to have each output controlled by a corresponding input namely 'single-loop' control. These ideal 'decentralized' controllers have diagonal controller matrices, thus minimizing the capital cost although the interaction, indicated by the asymptotic transfer function matrix, may have substantially increased. Fast control is still maintained though since the 'slow' transfer function matrix is null.

However if C_2B is a diagonal matrix then both Σ and the controller matrices K_o, K_1 will be diagonal and the 'range' of controllers from centralized to decentralized will be a single controller. This is a special situation where a decentralized controller will produce increasingly non-interacting responses as $f \to \infty$.

3.5 Transmission Zeros

Transmission and decoupling zeros of linear multivariable continuous-time systems, governed by state and ouptut equations of the respective forms

$$\dot{x}(t) = A\,x(t) + B\,u(t) \tag{3.20}$$

and

$$y(t) = C\,x(t) \tag{3.21}$$

will now be considered . It is known (see, for instance, Porter and D'Azzo [26]) that the open loop transfer function matrix

$$G(\lambda) = C\,(\lambda I_n - A)^{-1}\,B \tag{3.22}$$

can be expressed in the form

$$G(\lambda) = U(\lambda)\,S^{-1}(\lambda) \tag{3.23}$$

where, in (3.20) to (3.23), $x(t) \varepsilon R^n$, $u(t) \varepsilon R^m$, $y(t) \varepsilon R^p$, $A \varepsilon R^{nxn}$, $B \varepsilon R^{nxm}$, $C \varepsilon R^{pxn}$, $G(\lambda) \varepsilon R^{pxm}$, $U(\lambda) \varepsilon R^{pxm}$ and $S(\lambda) \varepsilon R^{mxm}$. Popov [24] utilized the fact that the transfer function can be brought into the irreducible form

$$G_o(\lambda) = U_o(\lambda)\,S_o^{-1}(\lambda) \tag{3.24}$$

where

$$U(\lambda) = U_o(\lambda)\,R(\lambda), \tag{3.25}$$

$$S(\lambda) = S_o(\lambda)\,R(\lambda), \tag{3.26}$$

$R(\lambda)\varepsilon R^{mxm}$, $U_o(\lambda)\varepsilon R^{pxm}$, $S_o(\lambda)\varepsilon R^{mxm}$, and $U_o(\lambda)$, $S_o(\lambda)$ are relatively right prime polynomial matrices. The set of λ that causes the numerator matrix $U_o(\lambda)$ to lose rank were identified by Popov [24] as a 'system of invariants', and by Rosenbrock [27] as the 'zeros of $G(\lambda)$' and were finally called 'transmission zeros' (see , for instance, Pugh [28]). In addition Rosenbrock [27] identified the set of λ that causes $R(\lambda)$ to lose rank as 'decoupling zeros' and went on to explain in detail the relevance of the different types of decoupling zeros. Since the vehicle systems considered in this thesis are both controllable and observable then $R(\lambda)$ will be a constant matrix and there will be no decoupling zeros.

If the triple (A,B,C) of controllable and observable systems governed by the state and output equations given by (3.20) and (3.21) has a transmission zero, ν, then there exists an initial state, x(o), and inputs $u(t)=u(o)e^{\nu t}$ so that only the mode corresponding to the transmission zero is excited in the plant. When this occurs the outputs will be unaffected by the motions of the plant since modes corresponding to transmission zeros lie in the kernel of the output matrix and as a result are unobservable. The fast-sampling control theory presented in section (2.4) causes the relevant closed-loop poles to approach transmission zeros as $f\rightarrow\infty$, and hence leads to the automatic exploitation of the unobservability of the corresponding modes.

It can be shown that $U_o(\lambda)$ is a constant matrix (I_w) for the vehicle cascades considered in chapter four and so these systems have no transmission zeros. However transmission zeros play an important role in the fast-sampling control of trains considered in chapters six and seven, and are calculated by finding the eigenvalues of R_u, given by (3.17).

CHAPTER 4

CASCADES OF VEHICLES

4.1 Introduction

The two main considerations in the design of an automatic controller for vehicle cascades are passenger comfort and controller reliability. It is shown in this chapter that the application of the techniques developed in section (2.3) allows individual mathematical treatment of the above criteria. Both centralized and decentralized fast-sampling controllers are developed in section (4.4) for the linearized mathematical model developed in section (4.2) and the properties of the resulting closed-loop systems related to the work of other authors, summarized in section (4.3). Since both the centralized and decentralized fast-sampling controllers cause the outputs to closely track the command inputs it is clear that the designer has the problem of choosing sensible command inputs in order to guarantee passenger comfort. Accordingly in section (4.5) the properties of the closed-loop systems are investigated with regard to the command inputs and the results are both utilized and illustrated by the results of digital computer simulations presented in sections (4.6) and (4.7). Finally in section (4.8) a discussion on the chapter is presented.

4.2 Mathematical Model of a Vehicle Cascade

The vehicle cascade to be controlled is illustrated by figure (4.1) and consists of 'w' vehicles of masses $m_1, m_2, \ldots, m_w$ moving in a rectilinear cascade with absolute velocities $c_1(t)$, $c_2(t), \ldots, c_w(t)$ and absolute displacements $d_1(t)$, $d_2(t), \ldots, d_w(t)$. The driving force applied to the j^{th} vehicle of the cascade is $F_j(t)$ and the corresponding linearized drag force is $\alpha_j c_j(t)$. The absolute acceleration of each vehicle can be expressed in the form

$$\dot{c}_j(t) = \left[F_j(t) - \alpha_j c_j(t) \right] / m_j . \quad (j=1,\ldots,w) \qquad (4.1)$$

and the w-1 relative accelerations are

$$\delta\dot{c}_j(t) = \dot{c}_j(t) - \dot{c}_{j+1}(t) \quad (j=1,..,w-1) \qquad (4.2)$$

where

$$\delta c_j(t) = \delta\dot{d}_j(t) \qquad (j=1,..,w-1) \qquad (4.3)$$

and $\delta d_j(t)$ $(j=1,..,w-1)$ are the separations between the vehicles and can be expressed in the form

$$\delta d_j(t) = d_j(t) - d_{j+1}(t) - L_j \quad (j=1,..,w-1) \qquad (4.4)$$

where $L_j (j=1,..,w)$ are the vehicle lengths.

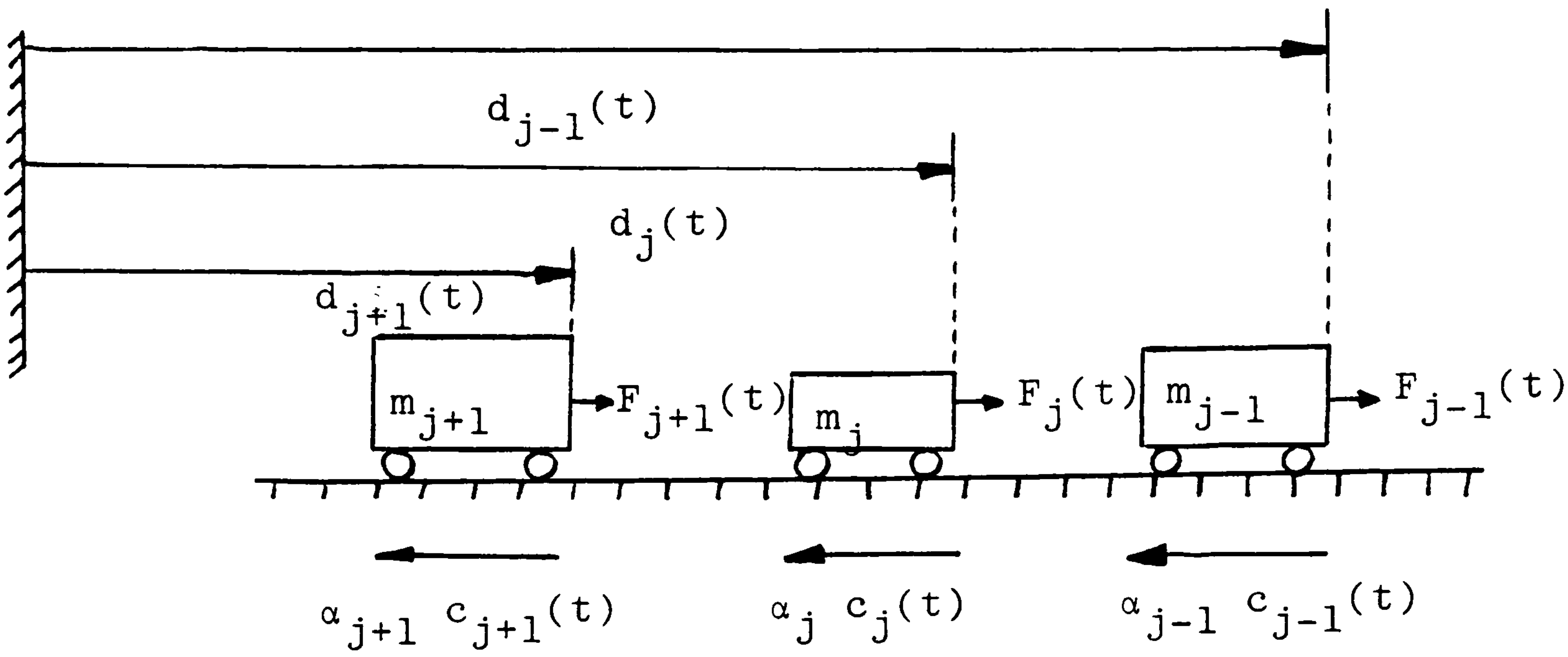

A Vehicle Cascade

Figure 4.1

Equations (4.1) to (4.3) can be combined to describe the motion of a vehicle cascade and one such combination takes the form

$$\begin{bmatrix} \dot{x}_1(t) \\ \dot{x}_2(t) \end{bmatrix} = \begin{bmatrix} A_{11} & A_{12} \\ A_{21} & A_{22} \end{bmatrix} \begin{bmatrix} x_1(t) \\ x_2(t) \end{bmatrix} + \begin{bmatrix} 0 \\ B \end{bmatrix} u(t) \qquad (4.5)$$

where

$$x_1(t) = \left[\delta d_1(t),\ \delta d_2(t), \ldots, \delta d_{w-1}(t)\right]', \tag{4.6}$$

$$x_2(t) = \left[c_1(t),\ \delta c_1(t), \ldots,\ \delta c_{w-1}(t)\right]' \quad , \tag{4.7}$$

$$A_{11} = 0, \tag{4.8}$$

$$A_{21} = 0, \tag{4.9}$$

$$A_{12} = \left[\begin{matrix} 0 & I_{w-1} \end{matrix}\right] \quad , \tag{4.10}$$

$$A_{22} = \begin{bmatrix} -\alpha_1/m_1 & 0 & 0 & \cdots & \cdots & 0 \\ \frac{\alpha_2}{m_2} - \frac{\alpha_1}{m_1} & -\alpha_2/m_2 & 0 & & & \vdots \\ \frac{\alpha_3}{m_3} - \frac{\alpha_2}{m_2} & \frac{\alpha_2}{m_2} - \frac{\alpha_3}{m_3} & -\frac{\alpha_3}{m_3} & & & \vdots \\ \frac{\alpha_4}{m_4} - \frac{\alpha_3}{m_3} & \frac{\alpha_3}{m_3} - \frac{\alpha_4}{m_4} & \frac{\alpha_3}{m_3} - \frac{\alpha_4}{m_4} & & & \vdots \\ \vdots & \vdots & \vdots & & & 0 \\ \overline{\frac{\alpha_w}{m_w} - \frac{\alpha_{w-1}}{m_{w-1}}} & \overline{\frac{\alpha_{w-1}}{m_{w-1}} - \frac{\alpha_w}{m_w}} & \overline{\frac{\alpha_{w-1}}{m_{w-1}} - \frac{\alpha_w}{m_w}} & \cdots\cdots & \overline{\frac{\alpha_w}{m_w} - \frac{\alpha_{w-1}}{m_{w-1}}} & -\frac{\alpha_w}{m_w} \end{bmatrix}$$

$$\tag{4.11}$$

$$B=\begin{bmatrix} 1 & 0 & 0 & 0 \dots & 0 \\ 1 & -1 & 0 & 0 \dots & 0 \\ 0 & 1 & -1 & 0 \dots & 0 \\ 0 & 0 & 1 & -1 & \vdots \\ \vdots & \vdots & & \ddots & \ddots \\ 0 & 0 & 0 & 1 & -1 & 0 \\ 0 & 0 & 0 \dots 0 & 1 & -1 \end{bmatrix} \tag{4.12}$$

and

$$u(t) = \left[\frac{F_1(t)}{m_1}, \frac{F_2(t)}{m_2}, \dots, \frac{F_w(t)}{m_w} \right]' \tag{4.13}$$

where $x_1(t) \, \varepsilon R^{w-1}$, $x_2(t) \, \varepsilon R^{w}$, $u(t) \, \varepsilon R^{w}$,

$A_{11} \, \varepsilon R^{(w-1)x(w-1)}$, $A_{12} \, \varepsilon R^{(w-1)xw}$, $A_{21} \, \varepsilon R^{wx(w-1)}$

$A_{22} \, \varepsilon R^{wxw}$ and $B \, \varepsilon R^{wxw}$.

If the outputs of the system are taken as the absolute velocity of the first vehicle and the vehicle separation distances then it follows from (4.6) and (4.7) that

$$C_1 = \begin{bmatrix} 0- \\ I_{w-1} \end{bmatrix} \varepsilon R^{wx(w-1)} \tag{4.14}$$

and

$$C_2 = \begin{bmatrix} 1 & 0- \\ 0_| & 0 \end{bmatrix} \varepsilon R^{wxw} \tag{4.15}$$

in the output equation

$$y(t) = \begin{bmatrix} C_1 & C_2 \end{bmatrix} \begin{bmatrix} x_1(t) \\ x_2(t) \end{bmatrix} . \tag{4.16}$$

It can be shown that the triple

$\begin{bmatrix} A_{11} & A_{12} \\ A_{21} & A_{22} \end{bmatrix}, \begin{bmatrix} 0 \\ B \end{bmatrix}, \begin{bmatrix} C_1 & C_2 \end{bmatrix}$ given by (4.8) to (4.12), (4.14) and (4.15) is both controllable and observable.

4.3 Review of the Literature on Vehicle Cascades

Fenton [3] attempted to assess the progress of automatic vehicle guidance and control and suggested the need for automatic vehicle systems stems from the large numbers of accidents and fatalities resulting from the steady growth in the use of automobiles. Fenton [3] explained the need for radical changes in order to prevent the chaos which would result from the unplanned growth of present vehicle systems and claimed the most frequently proposed solution for achieving automation consists of fully automated major roads and non-automated minor roads.

Some system for the automatic longitudinal control is required in every type of automated vehicle system incorporating unconnected vehicles. Levine and Athans [1] used Optimal Control Theory to control the corrective accelerations of each vehicle in a string. The resulting controller required full state feedback for each vehicle which, they admitted, would impose serious limits on their systems. Peppard and Gourishankar [29] also used Optimal Control Theory and found that the choice of the cost function greatly affected the behaviour of the resulting closed-loop system.

In marked contrast to the limitations of the size of system imposed by Optimal Control Theory is the way a Modal Controller greatly reduces the size of the communications system which was highlighted by Porter and Crossley [2] . These modal control laws are simple to compute and require only three state variables per vehicle.

Stefanek and Wilkie [30] claim the control strategy of several vehicles following a lead car may become unstable if the motion of the lead car is perturbed. Referring to the work done by Levine and Athans [1] , they proposed moving cell control in order to overcome the problems with the high number of feedback paths encountered with Optimal Control Theory.

Bender, Fenton and Olson [31] examine the practical application of a vehicle born system, whose performance had previously been examined by computer simulations. They described their multimode control system and the control of a 'string' of vehicles with respect to the lead vehicle. In their tests they equipped a saloon car and controlled it with respect to a phantom lead car, and claimed the entire system gave the effect of additive reaction times and hence increased the system capacity.

Whitney and Tomizuka [32] considered the sampled-data control of a string of vehicles. This took the form of a fixed reference system along the highway in the form of 'information posts'. They claimed this overcame the communications problem and also prevented the 'shock-wave' phenonomon present in moving reference systems when the motion is controlled with respect to a lead vehicle.

Rouse and Hoberock [33] considered the emergency control of vehicle platoons by utilizing a control law equation of the form

$$U_K(t) = P_1 \{\delta c_K(t)\} + P_2 \{\delta d_K(t)\} - h_K \}$$
$$+ P_3 \{ v - c_K(t) \}$$

where h_K is the steady state distance between the vehicles and v is the required velocity of the cascade. Rouse and Hoberock [33] stated that a cascade is 'string stable' when the amplitudes of the relative velocities and displacements are non-growing.

Schladover [34] utilized a non-linear controller in order to allow vehicles to entrain and extrain vehicle platoons. Schladover [34] stated that linear controllers cannot achieve entrainment or extrainment since high gains are necessary for accuracy at the final stages of the entrainment manoeuvre whilst the same controller would produce excessive control actions at the start of an entrainment manoeuvre. Both the analogue and sampled-data controllers presented were developed through computer simulations.

4.4 Fast-Sampling Control of Vehicle Cascades

For the linear model of vehicle cascades presented in section (4.2) it follows from (4.12) and (4.15) that

$$\text{rank } (C_2 B) = 1 \tag{4.17}$$

and hence extra-measurements will be necessary in order to utilize a fast-sampling controller. Accordingly if

$$M = \begin{bmatrix} 0- \\ \\ \text{diag}\left\{\frac{1}{\eta_1}, \ldots, \frac{1}{\eta_{w-1}}\right\} \end{bmatrix} \tag{4.18}$$

it follows from (2.18) , (4.6) to (4.8) and (4.10) that the extra-measurements vector assumes the form

$$r(t) = \left[0, \frac{\delta c_1(t0}{\eta_1}, \frac{\delta c_2(t)}{\eta_2}, \ldots, \frac{\delta c_{w-1}(t)}{\eta_{w-1}} \right]', \tag{4.19}$$

where no extra-measurement is added to the first output in order to preserve the one fast response that a fast-sampling controller would produce as $f \to \infty$. Hence it follows from (2.12), (2.28) (2.29), (4.14), (4.15) and (4.19) that

$$F_1 = C_1 \tag{4.20}$$

$$F_2 = \text{diag}\,\{1, \frac{1}{\eta_1}, \frac{1}{\eta_2}, \ldots, \frac{1}{\eta_{w-1}}\} \tag{4.21}$$

and from (2.50) and (2.51) that the 'slow' output and extra-measurement asymptotic transfer function matrices assume the respective forms

$$\bar{\Gamma}_y(\lambda) = \begin{bmatrix} 0 & 0 \\ 0 & \text{diag}\left\{\dfrac{\eta_i T}{\lambda - 1 + \eta_i T}\right\}_{i=1,\ldots,w-1} \end{bmatrix} \tag{4.22}$$

and

$$\bar{\Gamma}_r(\lambda) = \begin{bmatrix} 0 & 0 \\ 0 & \text{diag}\left\{\dfrac{-\eta_i T}{\lambda - 1 + \eta_i T}\right\}_{i=1,\ldots,w-1} \end{bmatrix} \tag{4.23}$$

as $f \rightarrow \infty$.

It further follows from (2.53), (4.10), (4.12), (4.18) and (4.21) that the 'fast' extra-measurement asymptotic transfer function matrix assumes the form

$$\hat{\Gamma}_r(\lambda) = \begin{bmatrix} 0 & 0 \\ 0 & \text{diag}\ \dfrac{1}{\lambda} \end{bmatrix} \tag{4.24}$$

as $f \rightarrow \infty$

when

$$\Sigma = I \tag{4.25}$$

in (3.7) and the corresponding 'centralized' controller matrices assume the form

$$K_o = \begin{bmatrix} 1 & 0 & 0 & \cdots & 0 \\ 1 & -\eta_1 & 0 & & \vdots \\ 1 & -\eta_1 & -\eta_2 & \ddots & \vdots \\ \vdots & & & \ddots & \vdots \\ 1 & -\eta_1 & -\eta_2 & & 0 \\ 1 & -\eta_1 & -\eta_2 & \cdots & -\eta_{w-1} \end{bmatrix} \tag{4.26}$$

and

$$K_1 = \begin{bmatrix} \rho_1 & 0 & 0 & \cdots & 0 \\ \rho_2 & -\rho_2\eta_1 & 0 & & \vdots \\ \rho_3 & -\rho_3\eta_1 & -\rho_3\eta_2 & \ddots & \vdots \\ \vdots & & & \ddots & 0 \\ \rho_w & -\rho_w\eta_1 & -\rho_w\eta_2 & \cdots & -\rho_w\eta_{w-1} \end{bmatrix} \tag{4.27}$$

from (3.7) (3.11), (3.12), (4.12) and (4.21). It can further be shown that the 'fast' extra-measurements asymptotic transfer function matrix assumes the form given by (4.31) as $f \to \infty$ when a decentralized fast-sampling controller, whose controller matrices are of the form

$$\hat{\Gamma}_r(\lambda) = \begin{bmatrix} 0 & 0 & 0 & \cdots & & 0 \\ \frac{\lambda-1}{\eta_1\lambda^2} & \frac{1}{\lambda} & & & & \vdots \\ \frac{\lambda-1}{\eta_2\lambda^3} & -\frac{\eta_1}{\eta_2}\left(\frac{\lambda-1}{\lambda^2}\right) & \frac{1}{\lambda} & & & \\ \vdots & \vdots & -\frac{\eta_2}{\eta_3}\left(\frac{\lambda-1}{\lambda^2}\right) & \ddots & & \\ \frac{\lambda-1}{\eta_{w-2}\lambda^{w-1}} & \frac{-\eta_1}{\eta_{w-2}}\left(\frac{\lambda-1}{\lambda^{w-2}}\right) & \frac{-\eta_2}{\eta_{w-2}}\left(\frac{\lambda-1}{\lambda^{w-3}}\right) & & & 0 \\ \frac{\lambda-1}{\eta_{w-1}\lambda^{w}} & \frac{-\eta_1}{\eta_{w-1}}\left(\frac{\lambda-1}{\lambda^{w-1}}\right) & \frac{-\eta_2}{\eta_{w-1}}\left(\frac{\lambda-1}{\lambda^{w-2}}\right) & \cdots & \frac{-\eta_{w-2}}{\eta_{w-1}}\left(\frac{\lambda-1}{\lambda^2}\right) & \frac{1}{\lambda} \end{bmatrix} \tag{4.31}$$

$$K_0 = \text{diag} \{1, -\eta_1, \ldots, -\eta_{w-1}\} \tag{4.28}$$

and

$$K_1 = \text{diag} \{\rho_1, -\rho_2\eta_1, \ldots, -\rho_w\eta_{w-1} \} \tag{4.29}$$

is employed. For both the centralized and decentralized controllers it can readily be shown from (2.52), (4.12), (4.15), (4.21), (4.25) and (4.27) that the 'fast' asymptotic output transfer function matrix assumes the form

$$\hat{\Gamma}_y(\lambda) = \begin{bmatrix} \frac{1}{\lambda} & 0- \\ & \\ 0_{|} & 0_{(w-1)x(w-1)} \end{bmatrix} \text{ as } f \to \infty. \tag{4.30}$$

It is clear from (4.22) and (4.30) that as $f\to\infty$ the responses of the outputs will be increasingly non-interacting following step command changes when either centralized or decentralized controllers are employed. Furthermore (4.22) and (4.30) indicate that the response of the first output is dominated by a 'fast' mode as $f\to\infty$, and the responses of the remaining outputs are dominated purely by 'slow' modes as $f\to\infty$.

It follows from (4.23) and (4.24) that as $f\to\infty$ the centralized fast-sampling controller, whose controller matrices are given by (4.26) and (4.27), produces increasingly non-interacting relative velocities following command changes since both the 'fast' and 'slow' transfer function matrices are diagonal. Hence if the centralized controller is employed any command changes only causes local changes as $f \to \infty$.

It is clear that the 'shock-wave' phenonomon noted, but not explained, by Whitney and Tomizuka [32] can be identified using the asymptotic transfer function matrices. If the decentralized controller, whose controller matrices are given by (4.28) and (4.29) is employed then a command change will cause changes in the relative velocities further down the string since (4.31) is not diagonal. Furthermore since (4.31) is the 'fast' transfer function matrix it is clear that a command change will cause an impulse (for a step command change) to travel rapidly down the cascade. It is this impulse or 'shock-wave' that carries the information about the command change down the cascade, that is transmitted by the controller structure if the centralized controller is employed. It immediately follows that utilizing the decentralized controller produces the 'shock-wave' phenonomon and that utilizing the centralized controller avoids the presence of 'shock-waves'. It must be emphasized that the above 'shock-waves' are purely a fast phenonomon since the 'slow' extra-measurements transfer function matrix is diagonal.

Finally it is clear from the structures of both the centralized and decentralized controllers and the nature of the feedback information that the controllers are of high integrity. This is a direct result of the fact that information is only taken from the forward direction and in the centralized controller is only passed back down the cascade. If an input fails and the vehicle decelerates non-catastrophically then it is clear that the leading vehicles will continue normally whilst the trailing vehicles will come to a halt by treating the 'failed' vehicle as a new lead vehicle. The above comments are not true for the Optimal Controller developed by Levine and Athans [1] that used full state feedback and full controller matrices. Similarly the Modal Controller developed by Porter and Crossley [2] used information from behind each vehicle which also indicates problems with integrity.

4.5 Entrainment of Vehicle Cascades

The fast-sampling controllers developed in section (4.4) can be used to decrease or to increase the separations between the vehicles in a cascade. When the separations between the vehicles are decreased the manoeuvre is known as 'entrainment'. Similarly when the separations are increased the manoeuvre is known as 'extrainment'. Schladover [34] claimed entrainment and extrainment manoeuvres are not possible when linear controllers are employed. However if sensible use is made of the command inputs then fast-sampling controllers will readily entrain or extrain vehicle cascades. Accordingly, in this section, the use of command inputs will be considered.

Assuming that step command changes of the form

$$v_i(KT) = v_i(o) \qquad (i=1,..,w:K=0,..,\infty) \tag{4.32}$$

are made and that the $\eta_j = \eta$ $(j=1,..,w-1)$, then it follows from (4.22), (4.23), (4.30) and (4.31) that as $f\rightarrow\infty$ the absolute velocity of the first vehicle and the relative velocities approach the forms

$$c_1\{(K+1)T\} = v_1(O) \tag{4.33}$$

and

$$\delta c_p \{(K+1)T\} = (1-\eta T)^K \eta v_{p+1}(0) \qquad (p=1,..,w-1) \tag{4.34}$$

when the centralized controller, whose controller matrices are given by (4.26) and (4.27) is employed, and approach (4.33) and

$$\delta c_p \{(K+1)T\} = (1-\eta T)^K \eta v_{p+1}(0) + v_1(0)\delta\{(K-p)T\} - \sum_{i=2}^{p} \delta\{(K-p+i-1)T\} \eta v_i(0) \qquad (p=1,..,w-1) \tag{4.35}$$

when the decentralized controller, whose controller matrices are given by (4.28) and (4.29), is employed and where

$$\delta\{(K-p)T\} = \begin{cases} 1 & K=p \\ 0 & K\neq p \end{cases} .$$

It is clear from (4.2) that

$$c_{j+1}(t) = c_j(t) - \delta c_j(t)$$

and therefore it follows from (4.32) to (4.35) that as $f\to\infty$ the absolute velocities approach (4.33) and

$$c_{p+1}\{(K+1)T\} = v_1(O) - (1-\eta T)^K \sum_{i=2}^{p+1} \eta v_i(O) \qquad (4.36)$$

$$(p=1,..,w-1)$$

when the centralized controller is employed, and approach (4.33) and

$$c_{p+1}\{(K+1)T\} = v_1(O) - (1-\eta T)^K \sum_{i=2}^{p+1} \eta v_i(O)$$

$$- v_1(O) \sum_{i=1}^{p} \delta\{(K-i)T\}$$

$$+ \sum_{j=2}^{p} \eta v_j(O) \sum_{i=1}^{p-j+1} \delta\{(K-i)T\} \qquad (4.37)$$

$$(p=1,..,w-1)$$

when the decentralized controller is employed. It follows directly from (4.36) and (4.37) that the use of simultaneous command changes to entrain or extrain a cascade of vehicles will rapidly cause velocity 'build-up' along the cascade and so result in the need for increasingly unrealistic driving force amplitudes. It is clear that the only sensible procedure is to apply the command changes sequentially so that velocity 'build up' does not occur. It further follows from (4.36) and (4.37) that a single change of command input will cause all the absolute velocities down the cascade to change in a similar manner. Also since the driving forces,

$$F_p(t) = m_p \dot{c}_p(t) + \alpha_p c_p(t),$$

$$(p=1,..,w)$$

are a function of the absolute velocity and absolute acceleration of the vehicles it is clear that a single command change will cause changes in the driving forces of all the following vehicles in the cascade.

It is apparent from the above analysis that some form of hierarchical command input control is desirable in order to prevent velocity 'build up' in the general situation. However no attempt will be made to present an hierarchical command input control scheme, although it is clear that the structure of such a scheme should maintain the integrity of the fast-sampling controllers by only allowing command changes further up a cascade to affect the implementation of a command change.

It is now clear that the fast-sampling control theory presented in section (2.3) not only allows a high integrity digital controller to be designed for a cascade of vehicles, but is easily extended to indicate how command changes should be implemented in order to produce a sensible and complete closed-loop system.

4.6 Entrainment of a Ten Vehicle Cascade Using a Decentralized Fast-Sampling Controller

A digital computer simulation of a ten vehicle cascade undergoing entrainment will be presented in this section. The entrainment is achieved by employing a decentralized fast-sampling controller and command inputs that are changed in sequence in order to avoid the velocity 'build-up' discussed in section (4.5).

If it is assumed that

$$\frac{\alpha_1}{m_1} = 0.4 , \tag{4.38}$$

$$\frac{\alpha_2}{m_2} = 0.25, \tag{4.39}$$

$$\frac{\alpha_3}{m_3} = 0.3, \tag{4.40}$$

$$\frac{\alpha_4}{m_4} = 0.35, \tag{4.41}$$

$$\frac{\alpha_5}{m_5} = 0.15, \tag{4.42}$$

$$\frac{\alpha_6}{m_6} = 0.20, \tag{4.43}$$

$$\frac{\alpha_7}{m_7} = 0.22, \tag{4.44}$$

$$\frac{\alpha_8}{m_8} = 0.18, \tag{4.45}$$

$$\frac{\alpha_9}{m_9} = 0.32 \qquad (4.46)$$

and

$$\frac{\alpha_{10}}{m_{10}} = 0.38 \qquad (4.47)$$

then it follows from (4.5) to (4.12), (4.14), (4.15), (4.20) and (4.21) that the plant, input, output and extra-measurement matrices assume the respective forms

$$A_{11} = 0 \quad \varepsilon \; R^{9x9}, \qquad (4.48)$$

$$A_{12} = \begin{bmatrix} 0_1 & I_9 \end{bmatrix}, \qquad (4.50)$$

$$A_{21} = 0 \quad \varepsilon \; R^{10x9}, \qquad (4.50)$$

$$A_{22} = \begin{bmatrix} -0.4 & 0 & 0 & 0 & 0 & 0 & 0 & 0 & 0 & 0 \\ -0.15 & -0.25 & 0 & 0 & 0 & 0 & 0 & 0 & 0 & 0 \\ 0.05 & -0.05 & -0.3 & 0 & 0 & 0 & 0 & 0 & 0 & 0 \\ 0.05 & -0.05 & -0.05 & -0.35 & 0 & 0 & 0 & 0 & 0 & 0 \\ -0.2 & 0.2 & 0.2 & 0.2 & 0.15 & 0 & 0 & 0 & 0 & 0 \\ 0.05 & -0.05 & -0.05 & -0.05 & -0.05 & -0.2 & 0 & 0 & 0 & 0 \\ 0.02 & -0.02 & -0.02 & -0.02 & -0.02 & -0.02 & -0.22 & 0 & 0 & 0 \\ -0.04 & 0.04 & 0.04 & 0.04 & 0.04 & 0.04 & 0.04 & -0.18 & 0 & 0 \\ 0.14 & -0.14 & -0.14 & -0.14 & -0.14 & -0.14 & -0.14 & -0.14 & -0.32 & 0 \\ 0.06 & -0.06 & -0.06 & -0.06 & -0.06 & -0.06 & -0.06 & -0.06 & -0.06 & -0.38 \end{bmatrix}$$

(4.51)

$$B = \begin{bmatrix} 1 & 0 & 0 & 0 & 0 & 0 & 0 & 0 & 0 & 0 \\ 1 & -1 & 0 & 0 & 0 & 0 & 0 & 0 & 0 & 0 \\ 0 & 1 & -1 & 0 & 0 & 0 & 0 & 0 & 0 & 0 \\ 0 & 0 & 1 & -1 & 0 & 0 & 0 & 0 & 0 & 0 \\ 0 & 0 & 0 & 1 & -1 & 0 & 0 & 0 & 0 & 0 \\ 0 & 0 & 0 & 0 & 1 & -1 & 0 & 0 & 0 & 0 \\ 0 & 0 & 0 & 0 & 0 & 1 & -1 & 0 & 0 & 0 \\ 0 & 0 & 0 & 0 & 0 & 0 & 1 & -1 & 0 & 0 \\ 0 & 0 & 0 & 0 & 0 & 0 & 0 & 1 & -1 & 0 \\ 0 & 0 & 0 & 0 & 0 & 0 & 0 & 0 & 1 & -1 \end{bmatrix}, \quad (4.52)$$

$$C_1 = \begin{bmatrix} 0- \\ I_9 \end{bmatrix} \quad (4.53)$$

$$C_2 = \begin{bmatrix} 1 & 0- \\ 0 & 0 \end{bmatrix} \varepsilon R^{10x10} \quad (4.54)$$

$$R_1 = 0 \ \varepsilon R^{10x9} \quad (4.55)$$

and

$$R_2 = \text{diag}\ \{0, \frac{10}{3}, \frac{10}{3}, \frac{10}{3}, \frac{10}{3}, \frac{10}{3}, \frac{10}{3}, \frac{10}{3}, \frac{10}{3}, \frac{10}{3}\} \quad (4.56)$$

when

$$\eta_i = 0.3, \quad (i=1,..,9). \quad (4.57)$$

A fast-sampling decentralized controller is readily synthesized for the ten vehicle cascade from the theory developed in section (4.4). Setting

$$\rho_i = 2 \quad (i=1,..,10) \tag{4.58}$$

together with (2.13), (4.28), (4.29) and (4.57) produces

$$u_1(KT) = f\,\{e_1(KT) + 2z_1(KT)\} \tag{4.59}$$

and

$$u_j(KT) = f\,\{-0.3e_j(KT) - 0.6\,z_j(KT)\} \quad (j=2,..,10) \tag{4.60}$$

where

$$e_1(KT) = v_1(KT) - c_1(KT) \tag{4.61}$$

$$e_j(KT) = v_j(KT) - \delta d_j(KT) - \delta c_j(KT)/0.3 \quad (j=2,..,10) \tag{4.62}$$

$$z_i\,\{(K+1)T\} = z_i(KT) + Te_i(KT) \quad (i=1,..,10) \tag{4.63}$$

and

$$f = 10 \text{ samples/second} \tag{4.64}$$

giving

$$T = 0.1 \text{ s} . \tag{4.65}$$

Since all the closed-loop poles for the sampling period given by (4.65) not only lie inside the unit disc but are approaching the asymptotic closed-loop poles (see table 4.1) it follows that the control law equations given by (4.59) and (4.60) will not only produce a stable closed-loop system but also be approaching non-interactive control of the outputs.

Simulation of the ten vehicle cascade, when controlled in accordance with (4.59) to (4.64) and subjected to the changes in command inputs illustrated by figures (4.2) and (4.3), produced the results given by figures (4.4) to (4.15) when the initial steady-state conditions were assumed to be

$$v_1(0) = 10 \text{ m/s} , \tag{4.66}$$

$$v_i(0) = 7\text{m}, \tag{4.67}$$

$$c_1(0) = 10 \text{ m/s}, \tag{4.68}$$

$$\delta c_i(0) = 0 \text{ m/s}, \ (i=1,..,9) \tag{4.69}$$

$$\delta d_i(0) = 7\text{m}, \quad (i=1,..,9) \tag{4.70}$$

$$u_1(0) = 4 \text{ m/s}^2 , \tag{4.71}$$

$$u_2(0) = 2.5 \text{ m/s}^2, \tag{4.72}$$

$$u_3(0) = 3 \text{ m/s}^2, \tag{4.73}$$

$$u_4(0) = 3.5 \text{ m/s}^2 , \tag{4.74}$$

$$u_5(0) = 1.5 \text{ m/s}^2 , \tag{4.75}$$

$u_6(0) = 2\ m/s^2$,

$u_7(0) = 2.2\ m/s^2$

$u_8(0) = 1.8\ m/s^2$,

$u_9(0) = 3.2\ m/s^2$,

$u_{10}(0) = 3.8\ m/s^2$,

$e_i(0) = 0, (i=1,..,10)$,

$z_1(0) = u_1(0)/20.0$,

and

$z_i(0) = -u_i(0)/6.0 \ (i=2,..,10)$

where the $u_i(0)$ (i=1,..,10) are non-zero because of the resistance to motion, and it is assumed that the cascade travels over level terrain. The controller will cause the outputs to track the command inputs so that the separations between the vehicles are reduced sequentially from 7m to 4m (see figure (4.3)) and the cascade maintains a velocity of 10 m/s throughout the whole manoeuvre (see figure (4.2)).

DECENTRALIZED CONTROLLER	
ASYMPTOTIC CLOSED-LOOP POLES T=0.1S	CLOSED-LOOP POLES T=0.1S
0.0, 0.0	0.2118±i 0.0192
0.0, 0.0	0.2365±i 0.0511
0.0, 0.0	0.2758±i 0.0644
0.0, 0.0	0.3159±i 0.0526
0.0, 0.0	0.3400±i 0.0198
0.97	0.97041
0.97	0.97042
0.97	0.97044
0.97	0.97045
0.97	0.97047
0.97	0.97048
0.97	0.97049
0.97	0.97050
0.97	0.97050
0.8, 0.8	0.7092±i 0.0044
0.8, 0.8	0.7161±i 0.0102
0.8, 0.8	0.7245±i 0.0098
0.8, 0.8	0.7304±i 0.0056
0.8	0.7325
0.8	0.7428

TABLE 4.1

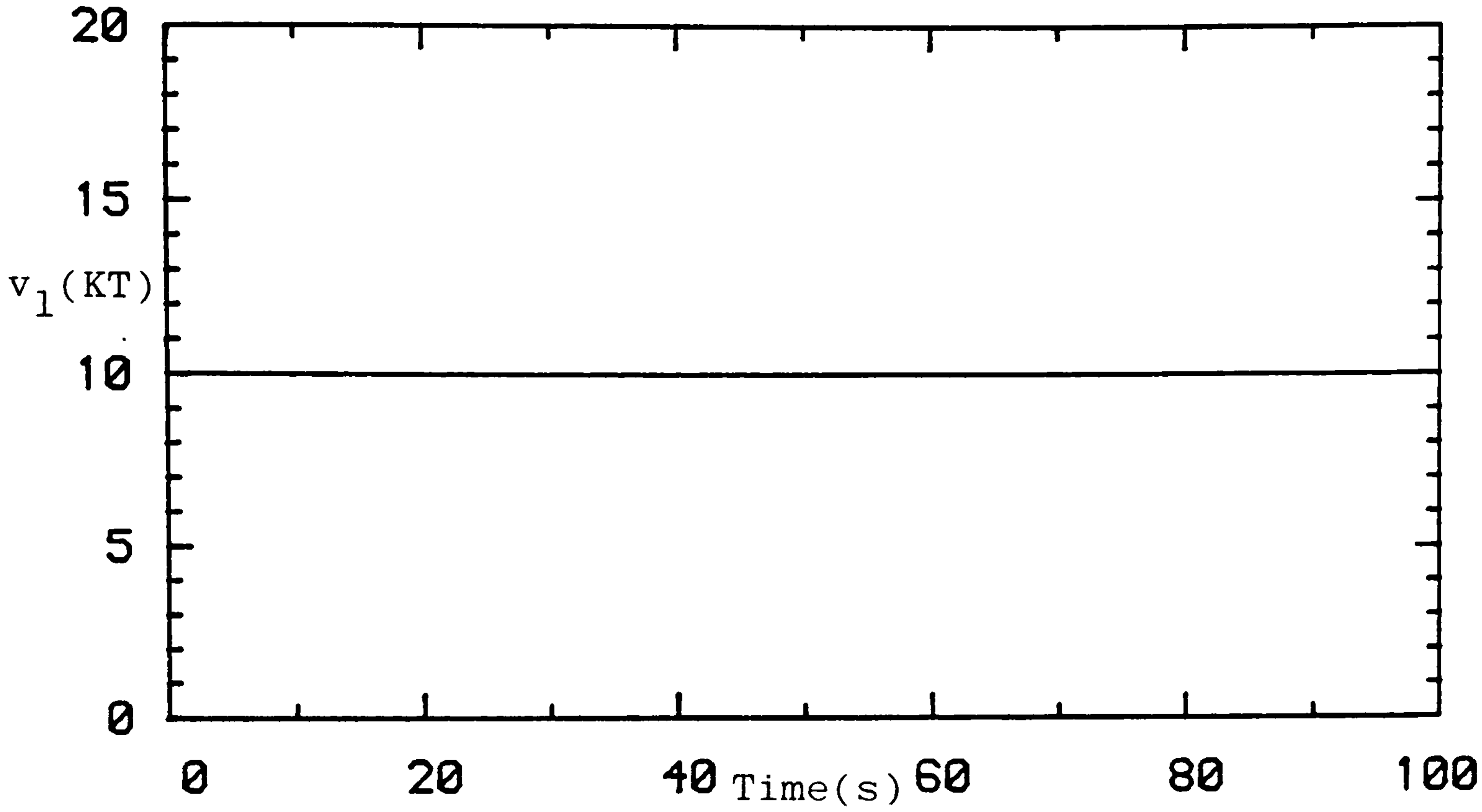

Figure 4.2

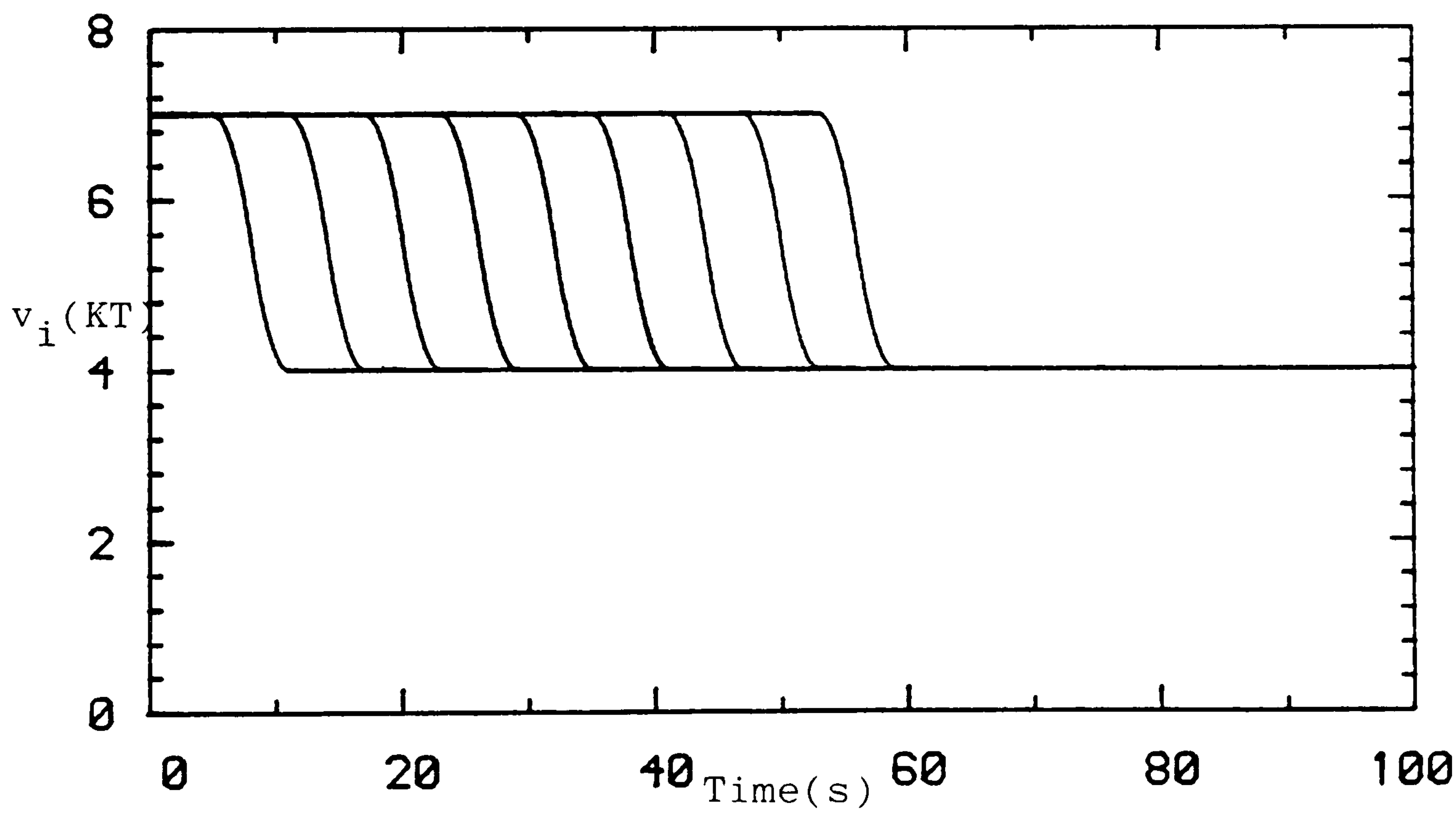

Figure 4.3

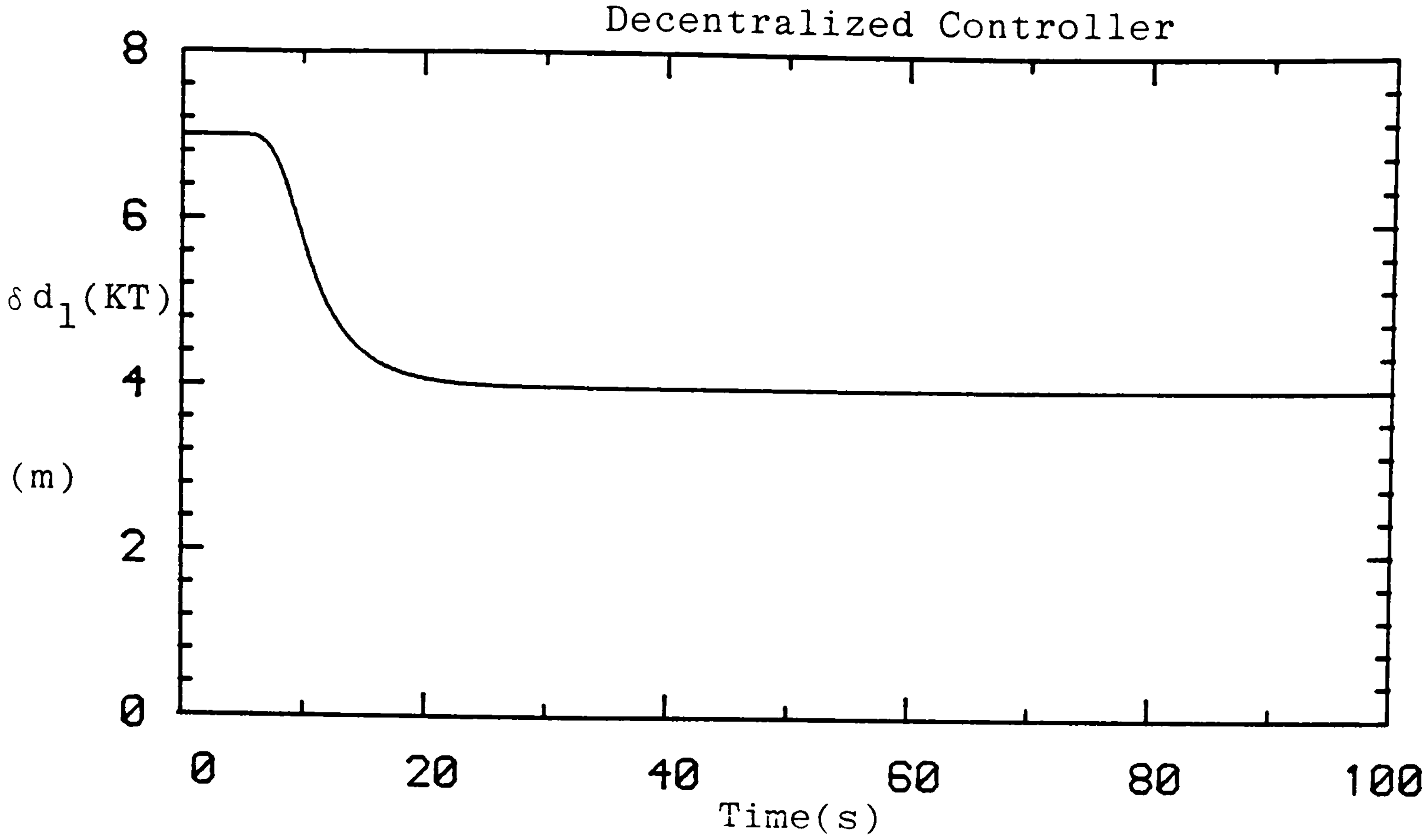

Figure 4.4

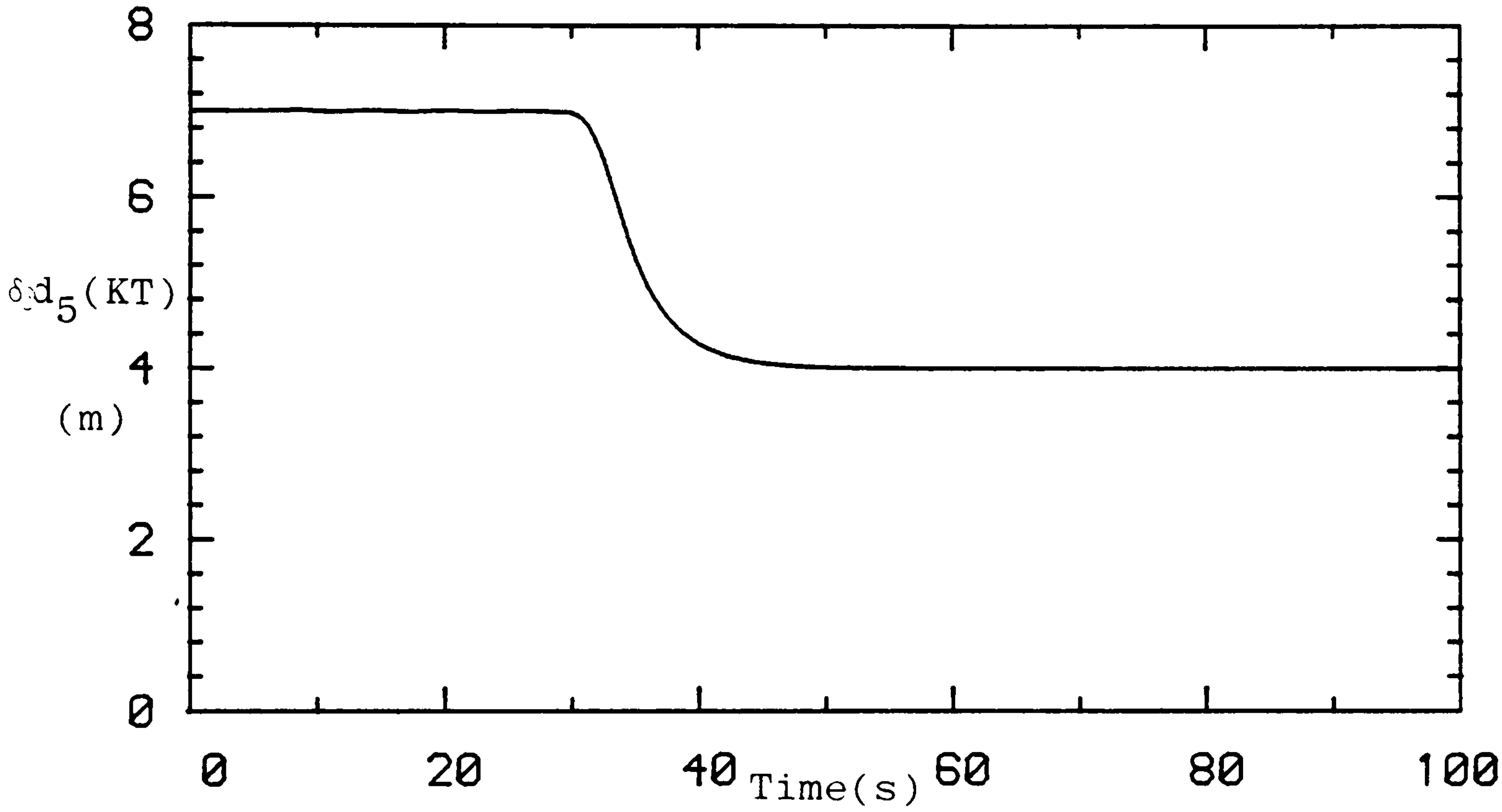

Figure 4.5

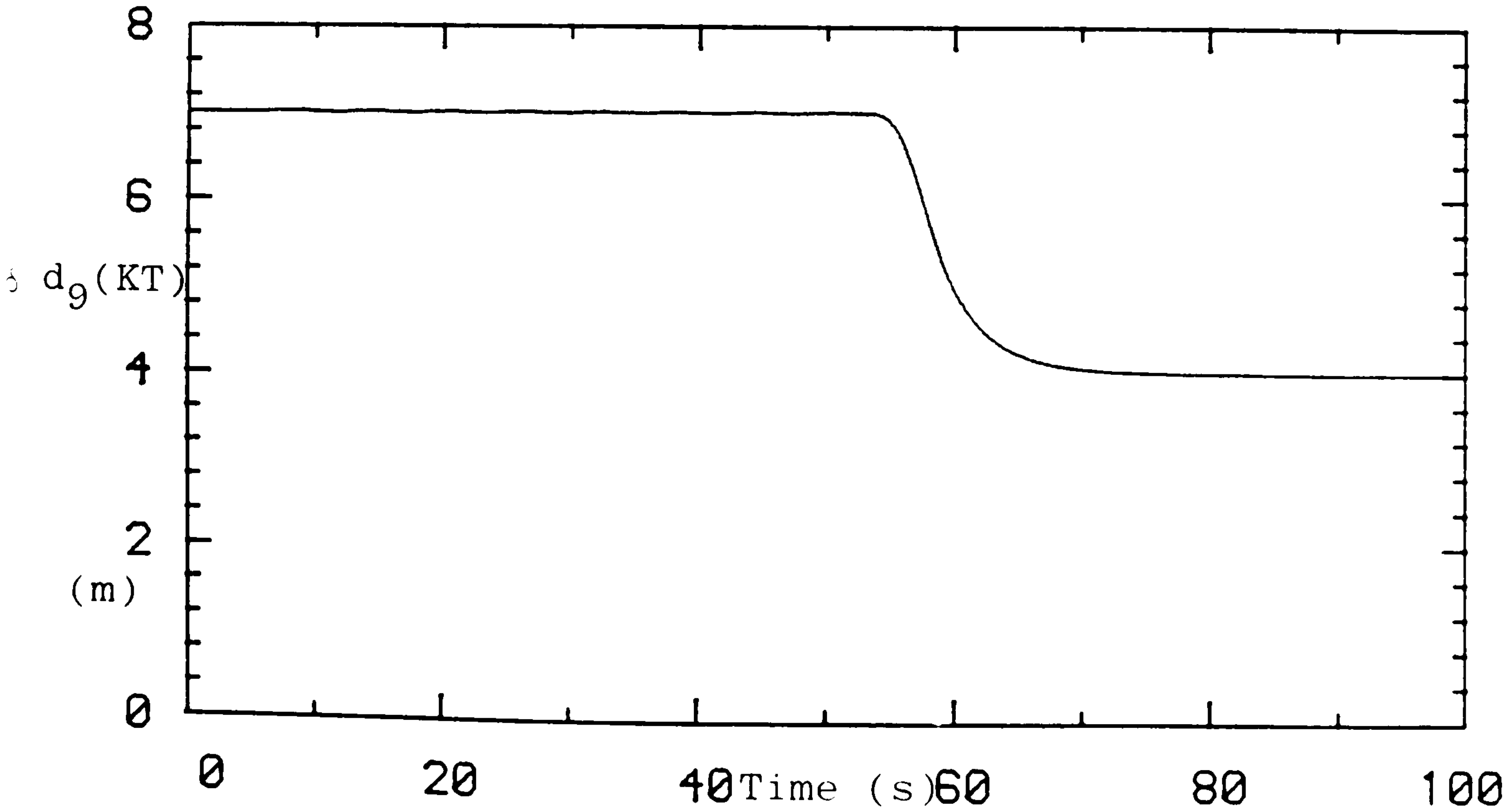

Figure 4.6

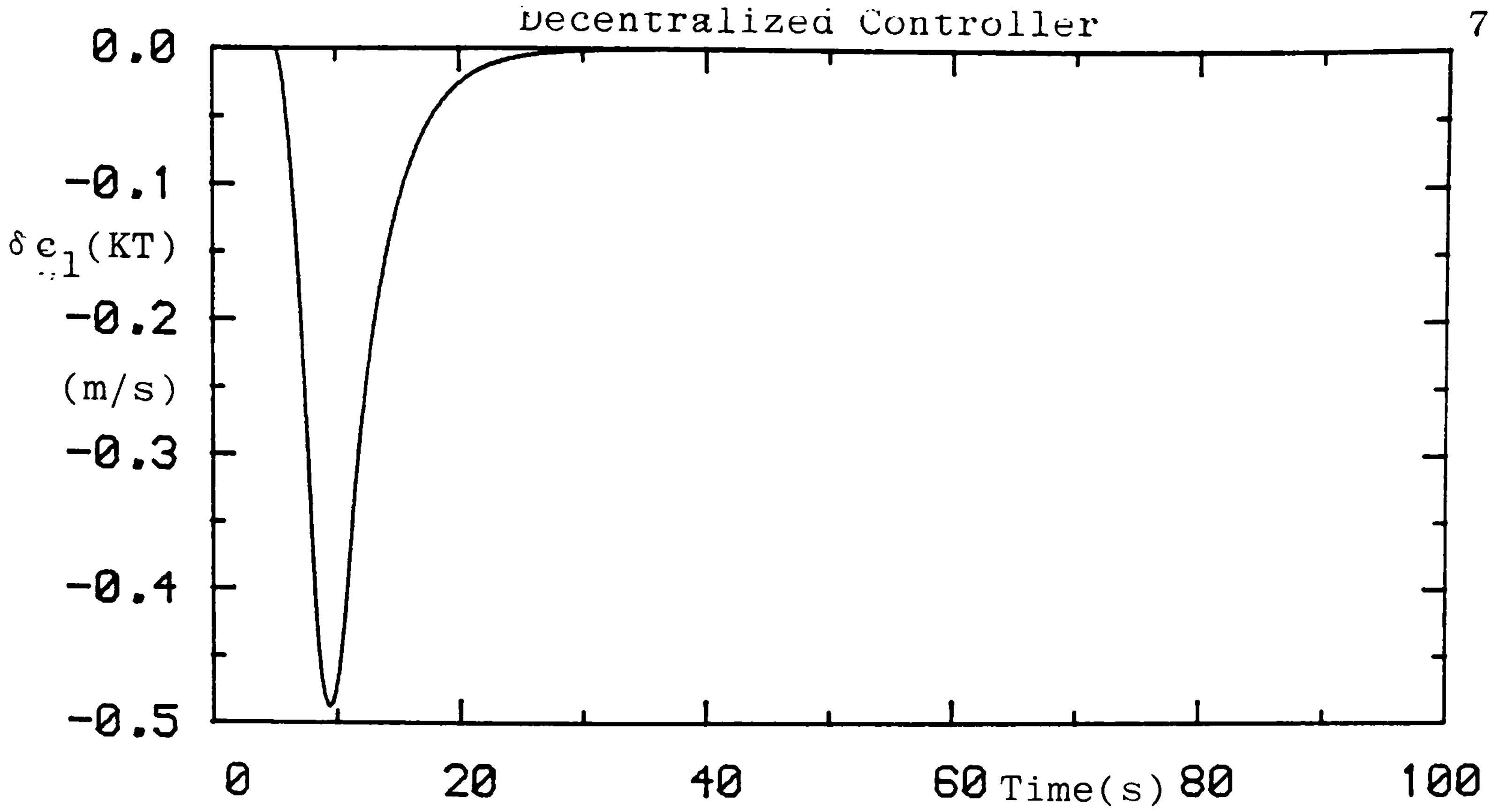

Figure 4.7

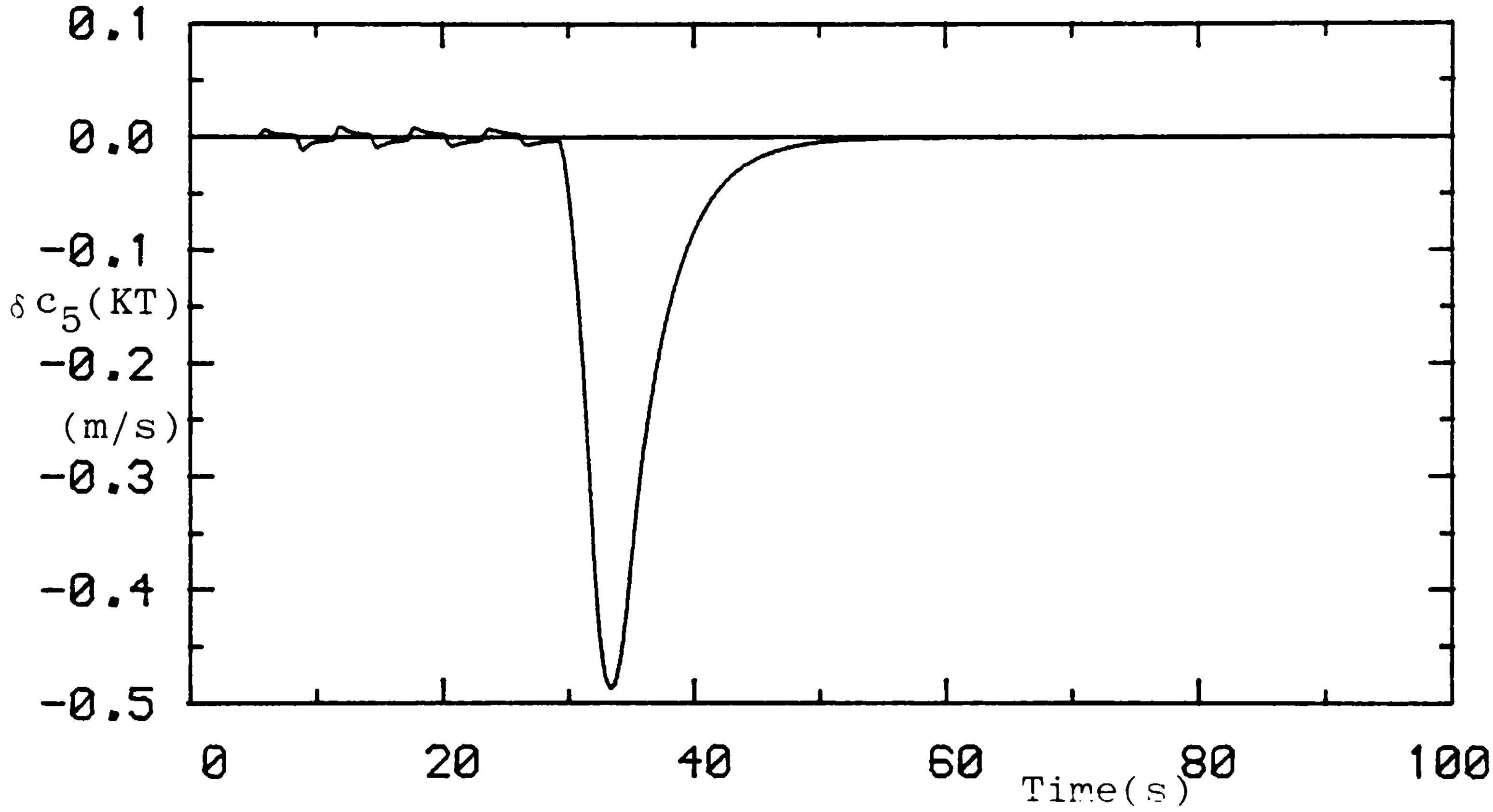

Figure 4.8

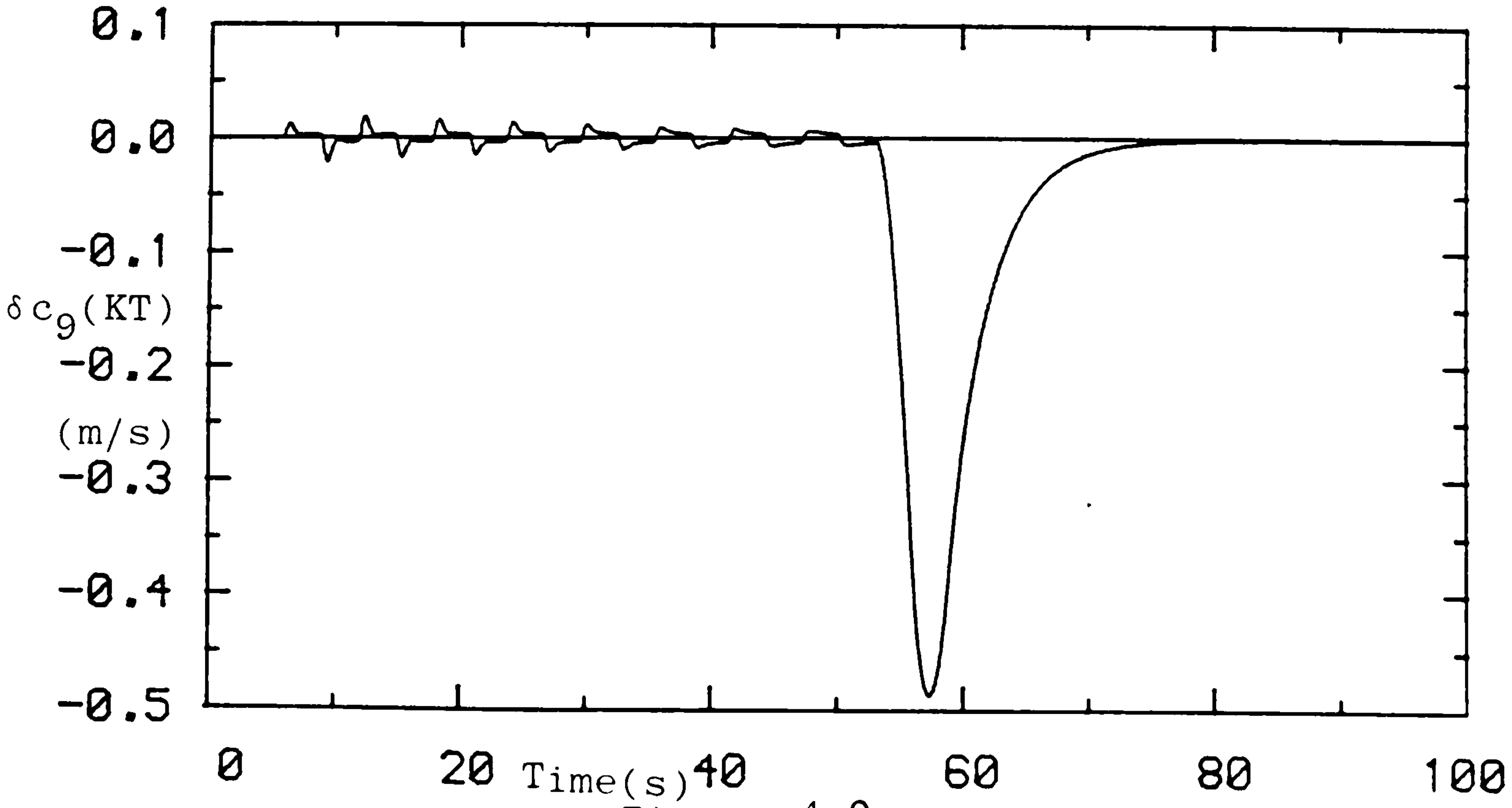

Figure 4.9

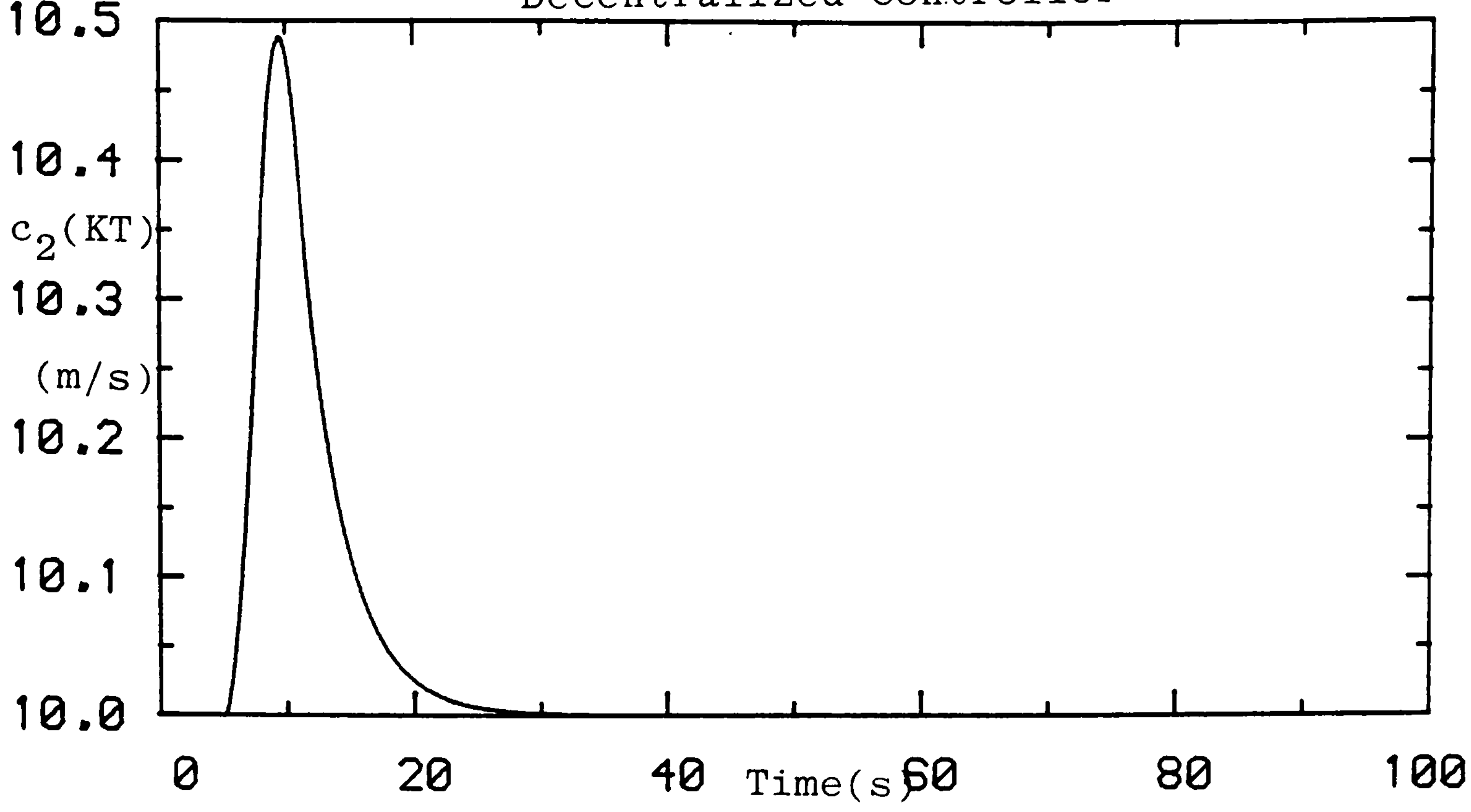

Figure 4.10

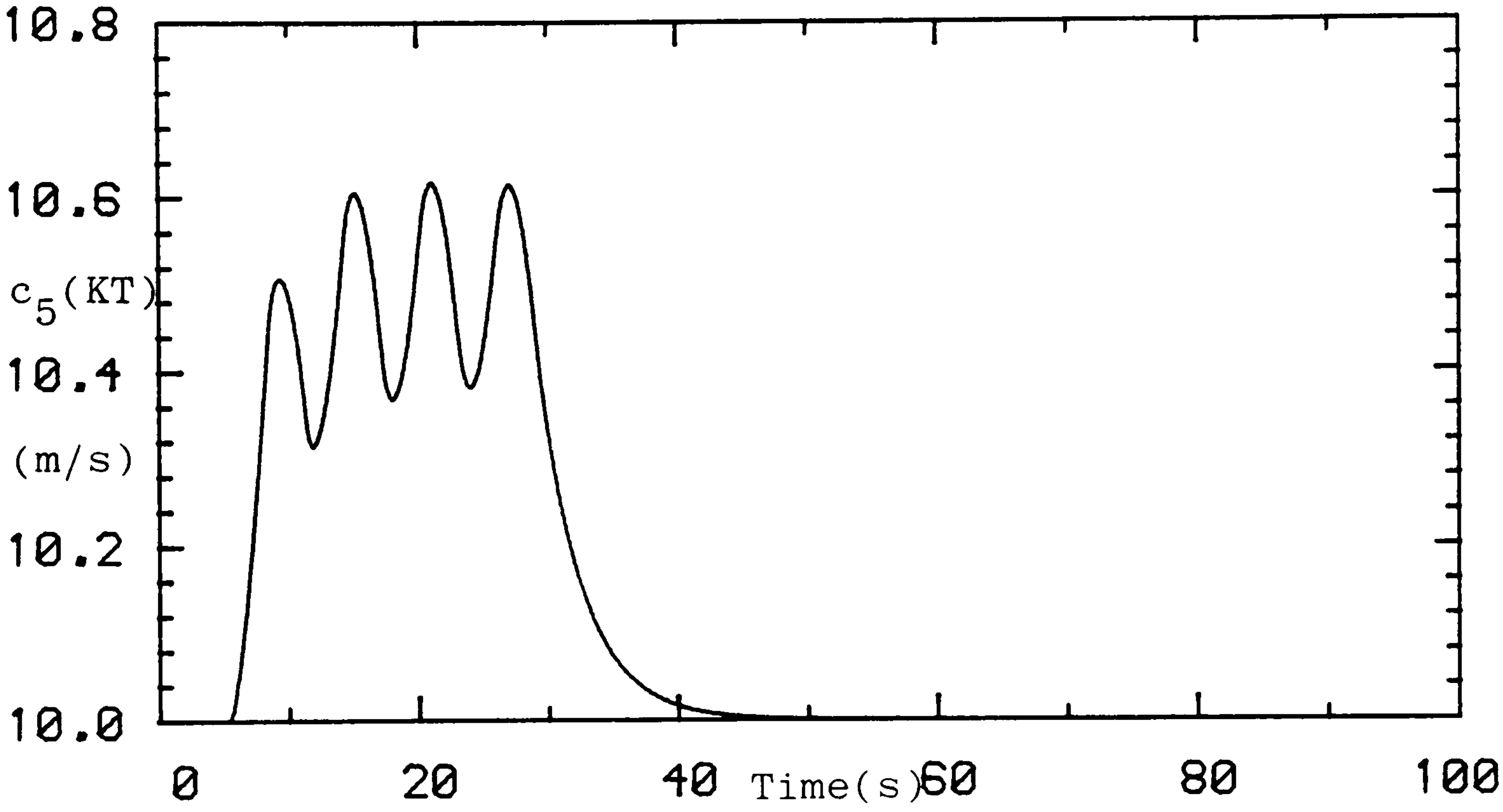

Figure 4.11

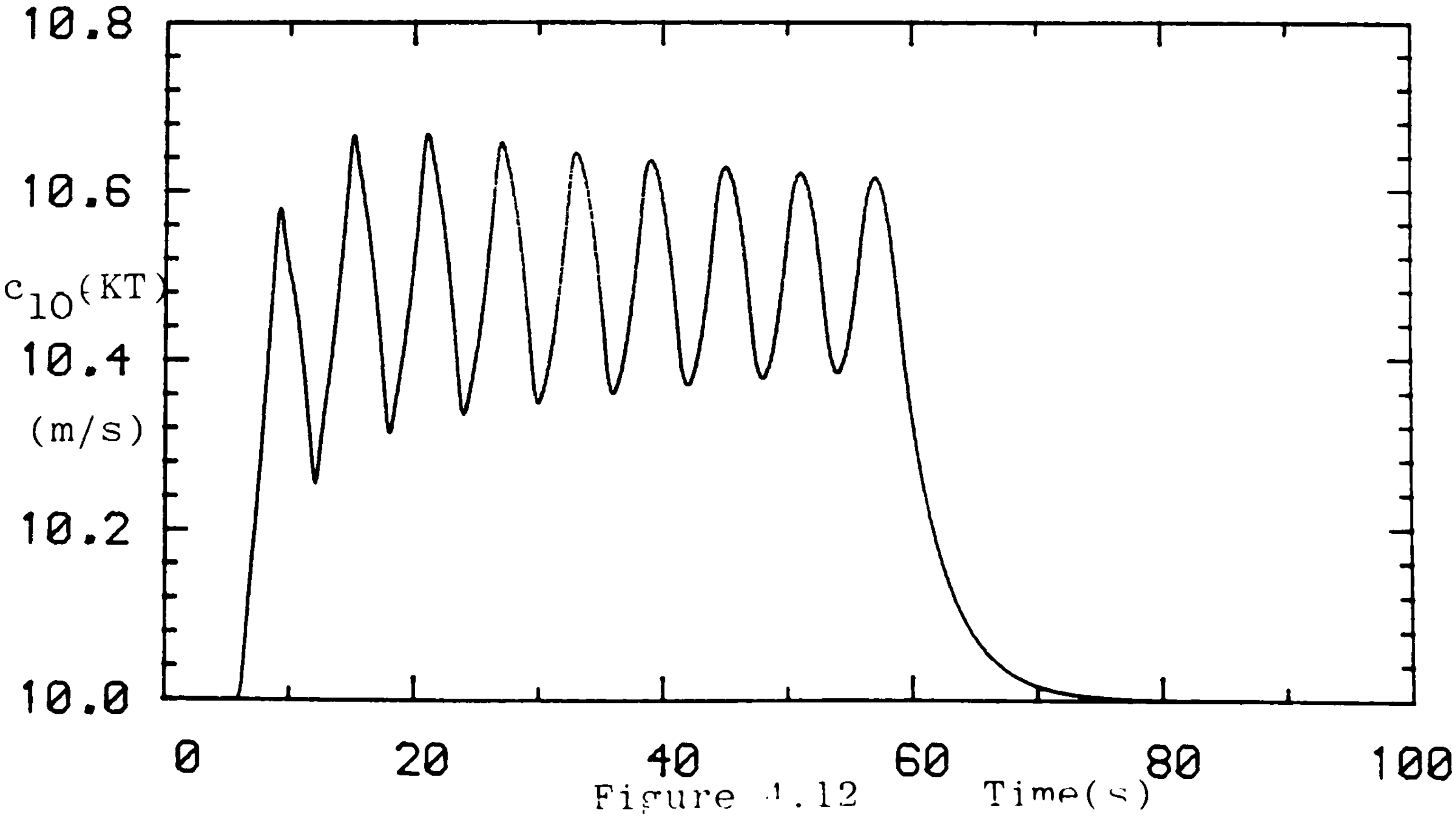

Figure 4.12

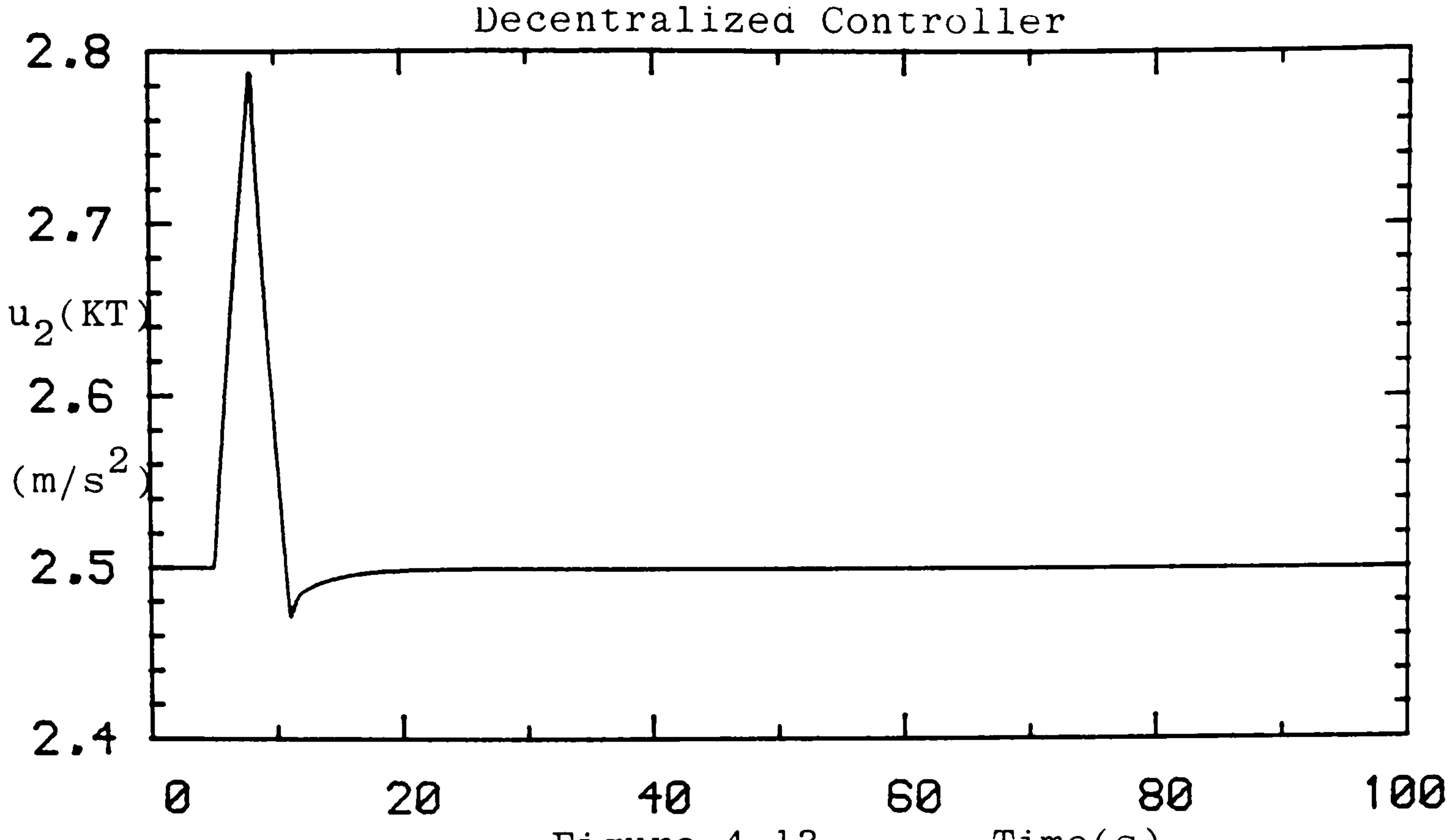

Figure 4.13

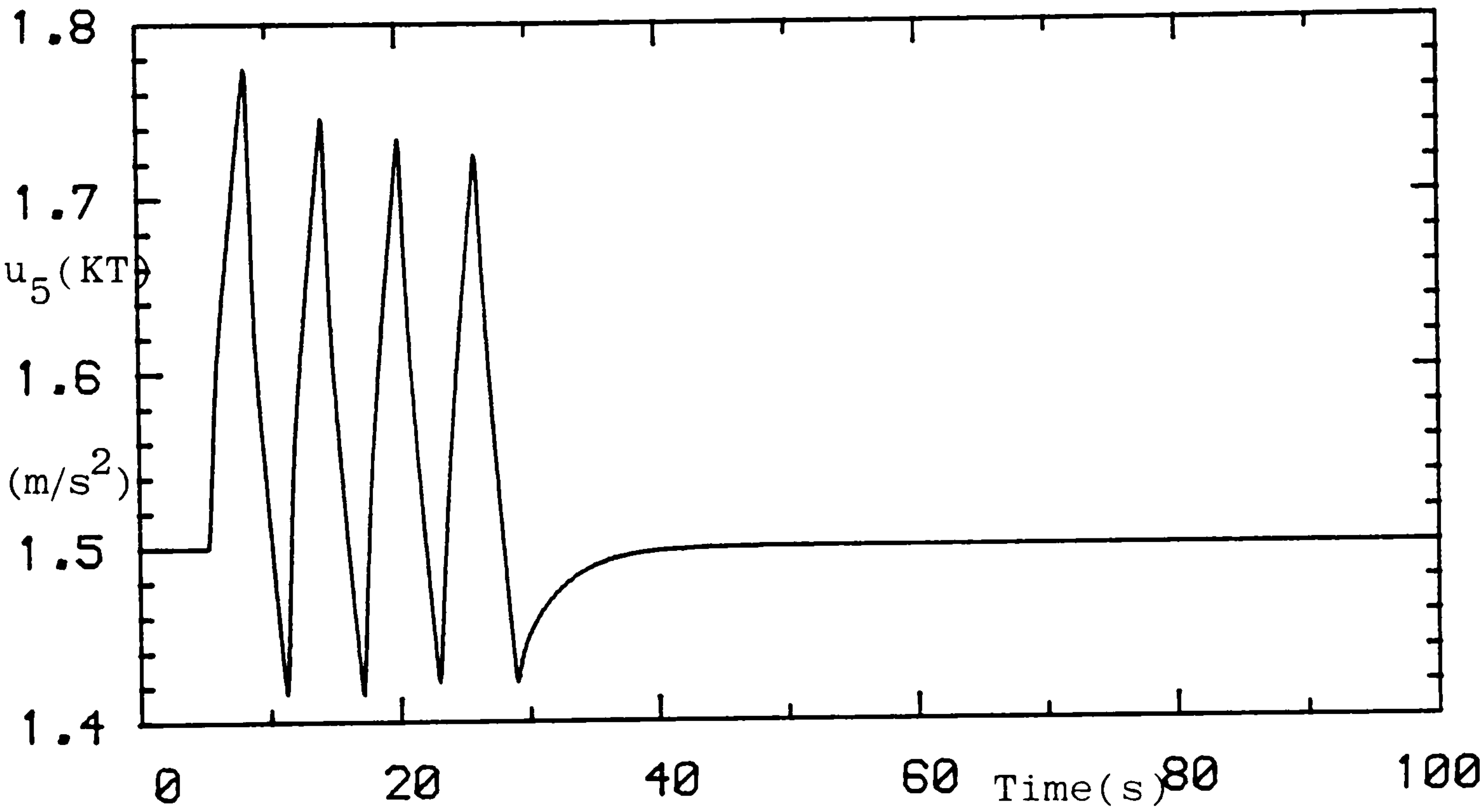

Figure 4.14

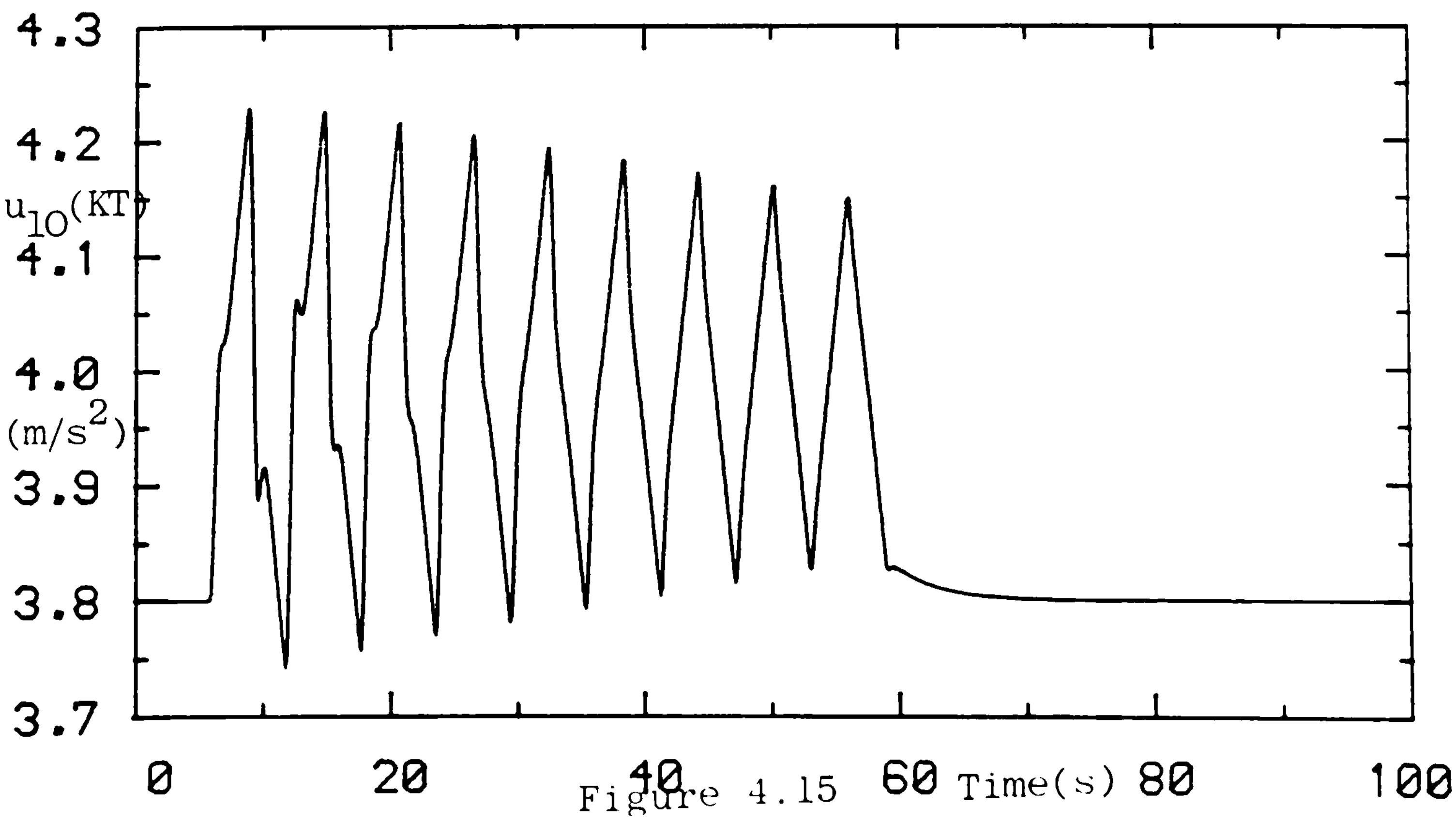

Figure 4.15

4.7 Entrainment of a Ten Vehicle Cascade Using a Centralized Fast-Sampling Controller

A further digital computer simulation of the ten vehicle cascade considered in section (4.6) will be presented in this section. The entrainment will be achieved by employing a centralized controller and the same command inputs as utilized in section (4.6).

The fast-sampling controller is again synthesized from the theory developed in section (4.4) and it follows directly from (2.14), (4.26), (4.27), (4.57) and (4.58) that

$$u_1(KT) = f \{ e_1(KT) + 2 z_1(KT) \} \quad (4.84)$$

and

$$u_j(KT) = f \{-0.3e_j(KT)-0.6 z_j(KT)\} + u_{j-1}(KT) \quad (4.85)$$

$$(j=2,..,w)$$

where $e_i(KT)$, $z_i(KT)$ $(i=1,..,10)$, f and T are again given by (4.61) to (4.65). Again since all the closed-loop poles for the sampling period given by (4.61) not only lie inside the unit disc but are approaching the asymptotic closed-loop poles (see table 4.2), it follows that the control law equations given by (4.61) to (4.65), (4.84) and (4.85) will not only produce a stable closed-loop system but also be approaching non-interactive control of the outputs and also approaching non-interacting relative velocities.

Simulation of the ten vehicle cascade, when controlled in accordance with (4.61) to (4.65), (4.84) and (4.85) and subjected to the changes in command inputs illustrated by figures (4.2) and (4.3), produced the results given by figures (4.16) to (4.27) when the initial steady-state conditions were assumed to be given by (4.66) to (4.82) and

$$z_j = \{u_{j-1}(0) - u_j(0)\} / 6.0 \quad (j=2,..,10) \tag{4.86}$$

CENTRALIZED CONTROLLER	
ASYMPTOTIC CLOSED-LOOP POLES T=0.1S	CLOSED-LOOP POLES T=0.1S
0.0	0.2681
0.0	0.2712
0.0	0.2817
0.0	0.2764
0.0	0.2850
0.0	0.2743
0.0	0.2872
0.0	0.2377
0.0, 0.0	0.2894±i (0.43E-10)
0.97	0.97041
0.97	0.97042
0.97	0.97044
0.97	0.97045
0.97	0.97047
0.97	0.97048
0.97	0.97049
0.97	0.97050
0.97	0.97050
0.8	0.7282
0.8	0.7265
0.8	0.7248
0.8	0.7236
0.8	0.7188
0.8	0.7206
0.8	0.7176
0.8	0.7163
0.8	0.7428
0.8	0.7163

TABLE 4.2

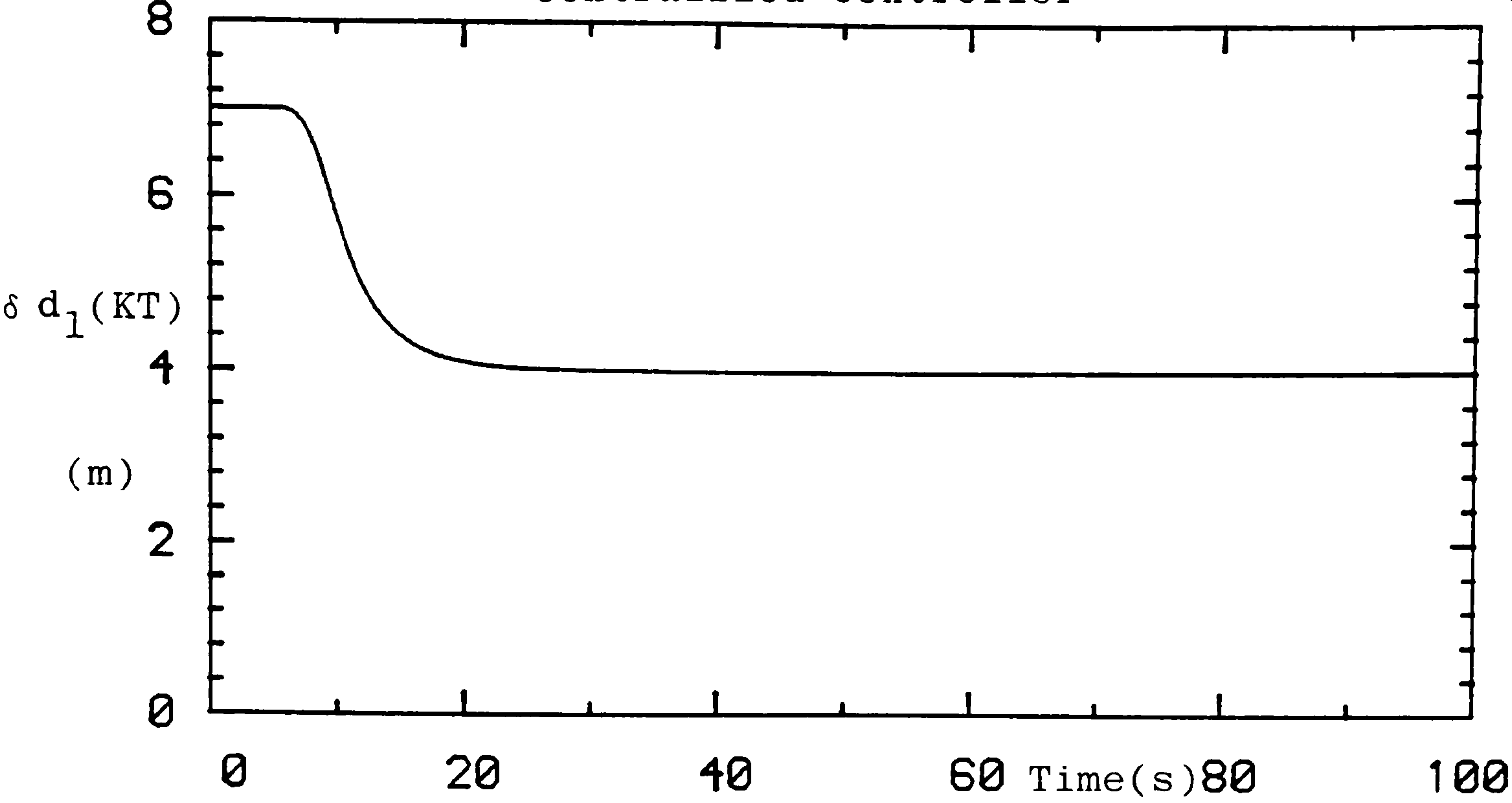

Figure 4.16

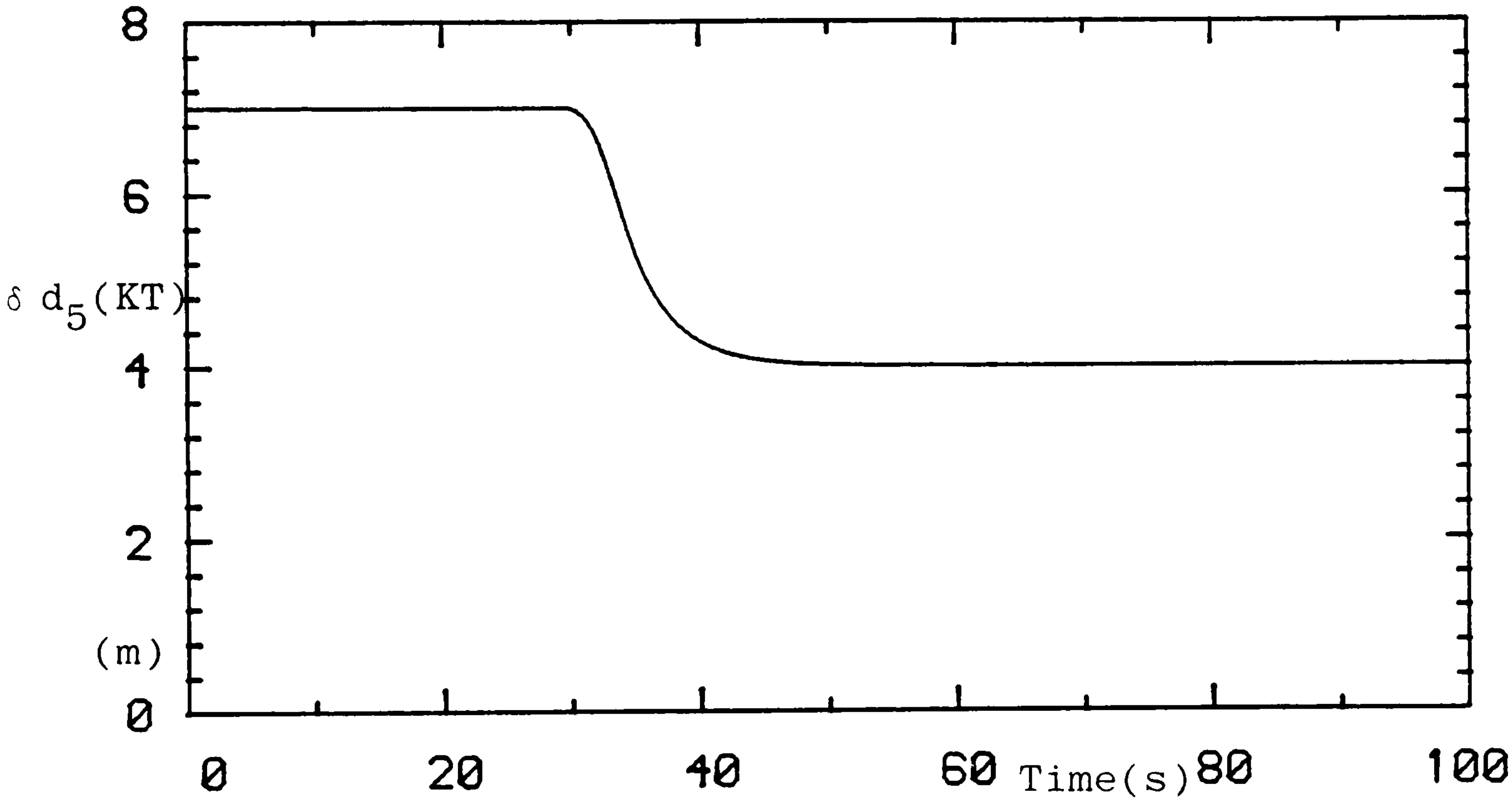

Figure 4.17

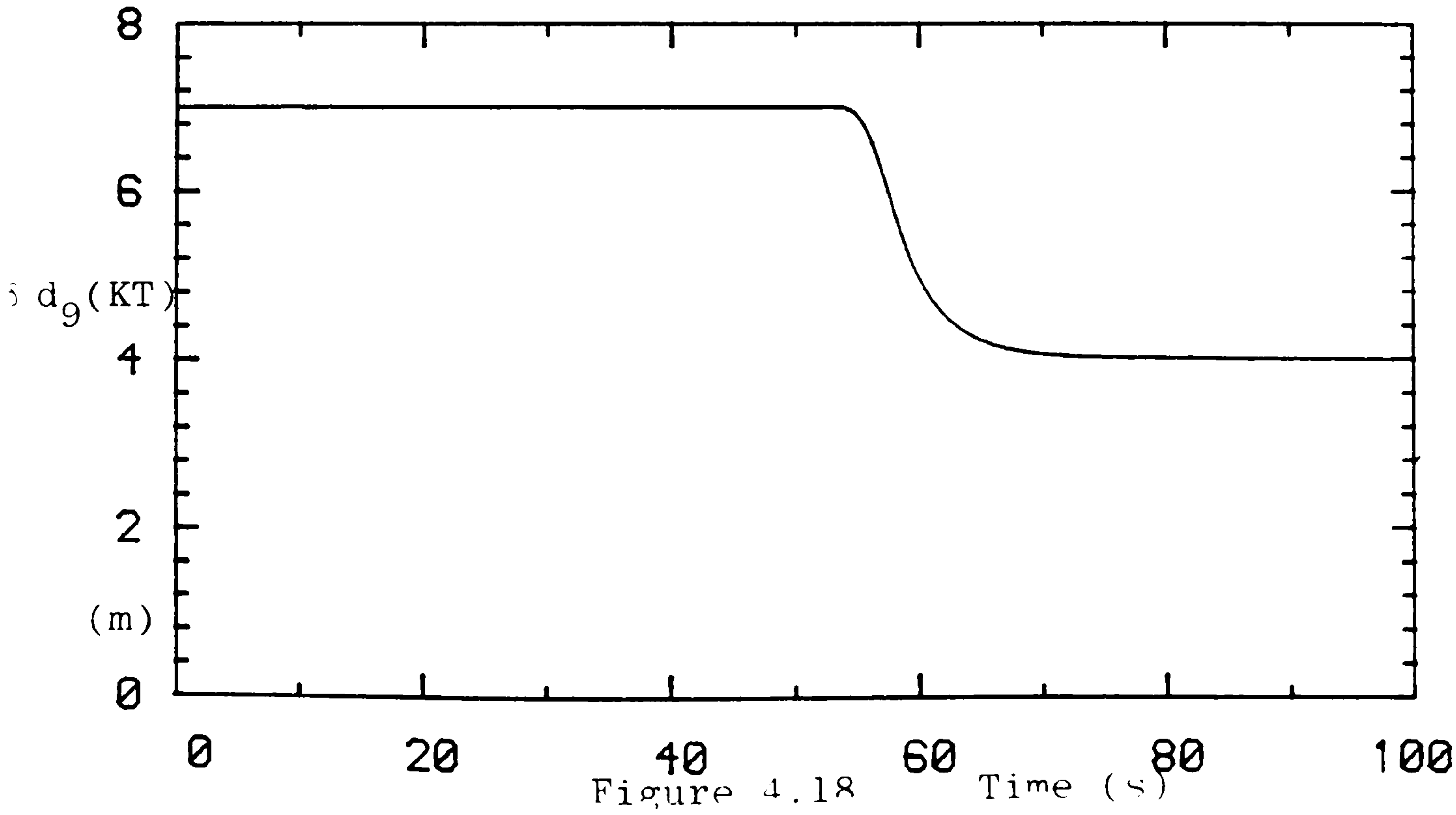

Figure 4.18

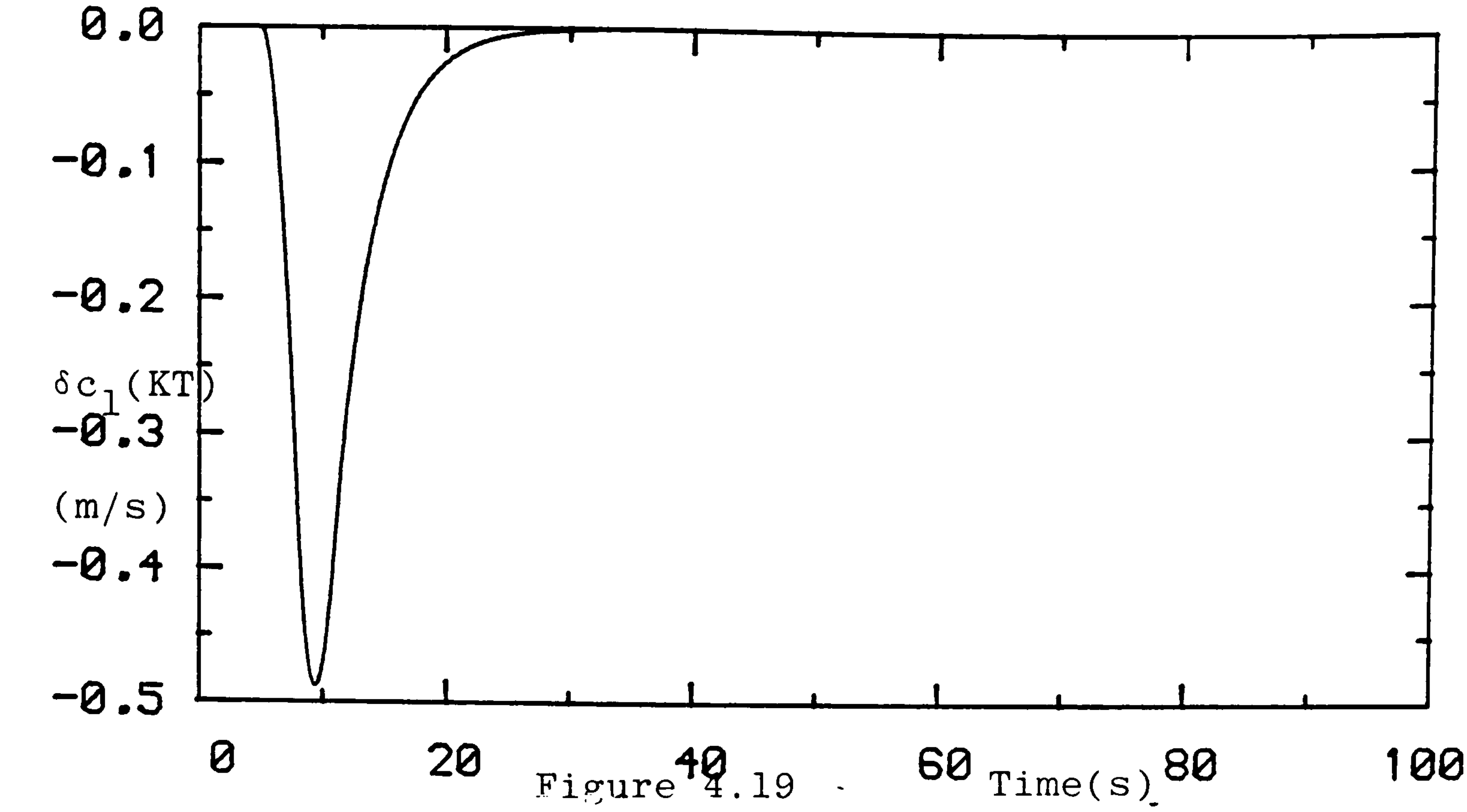

Figure 4.19

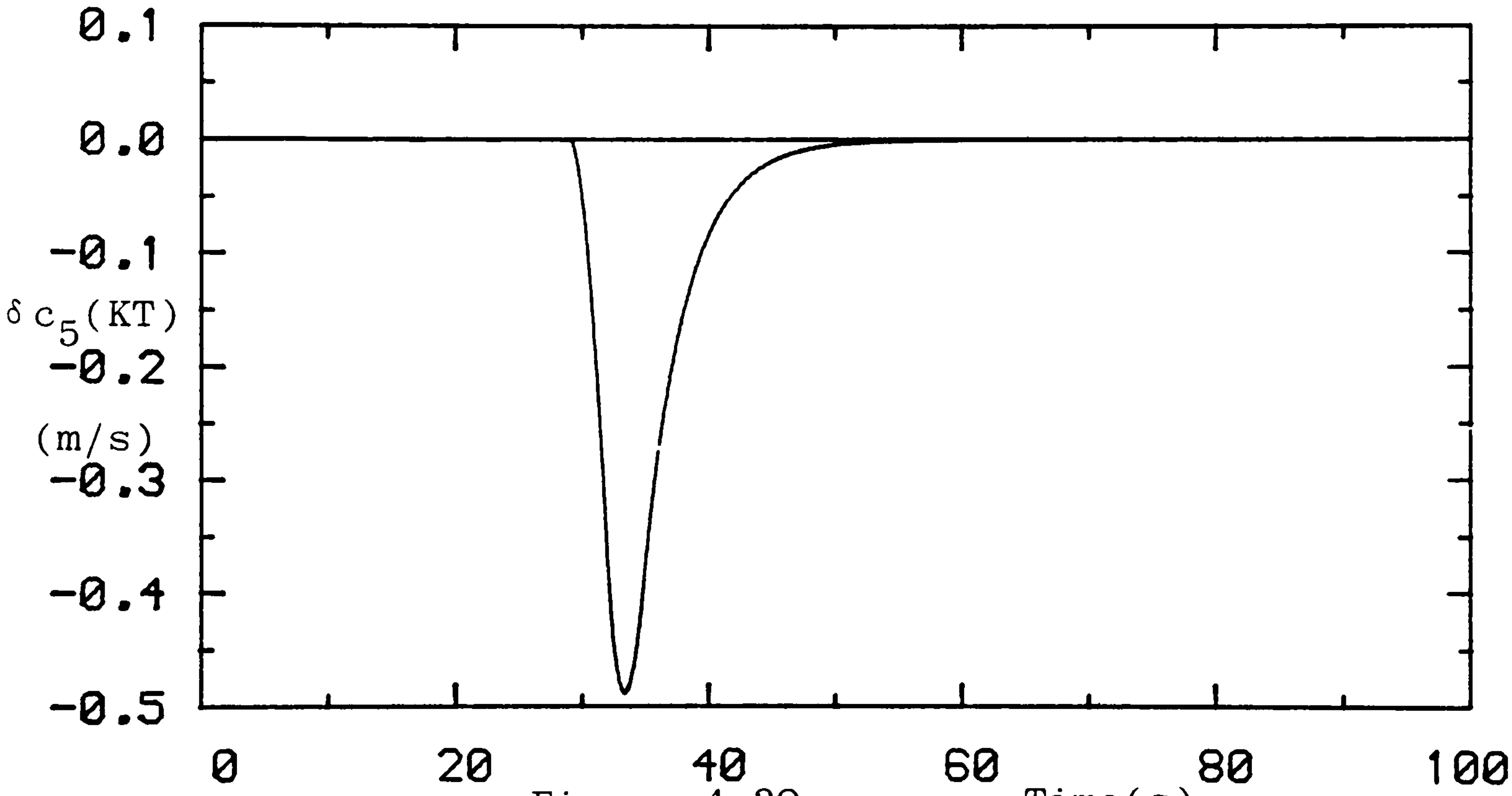

Figure 4.20

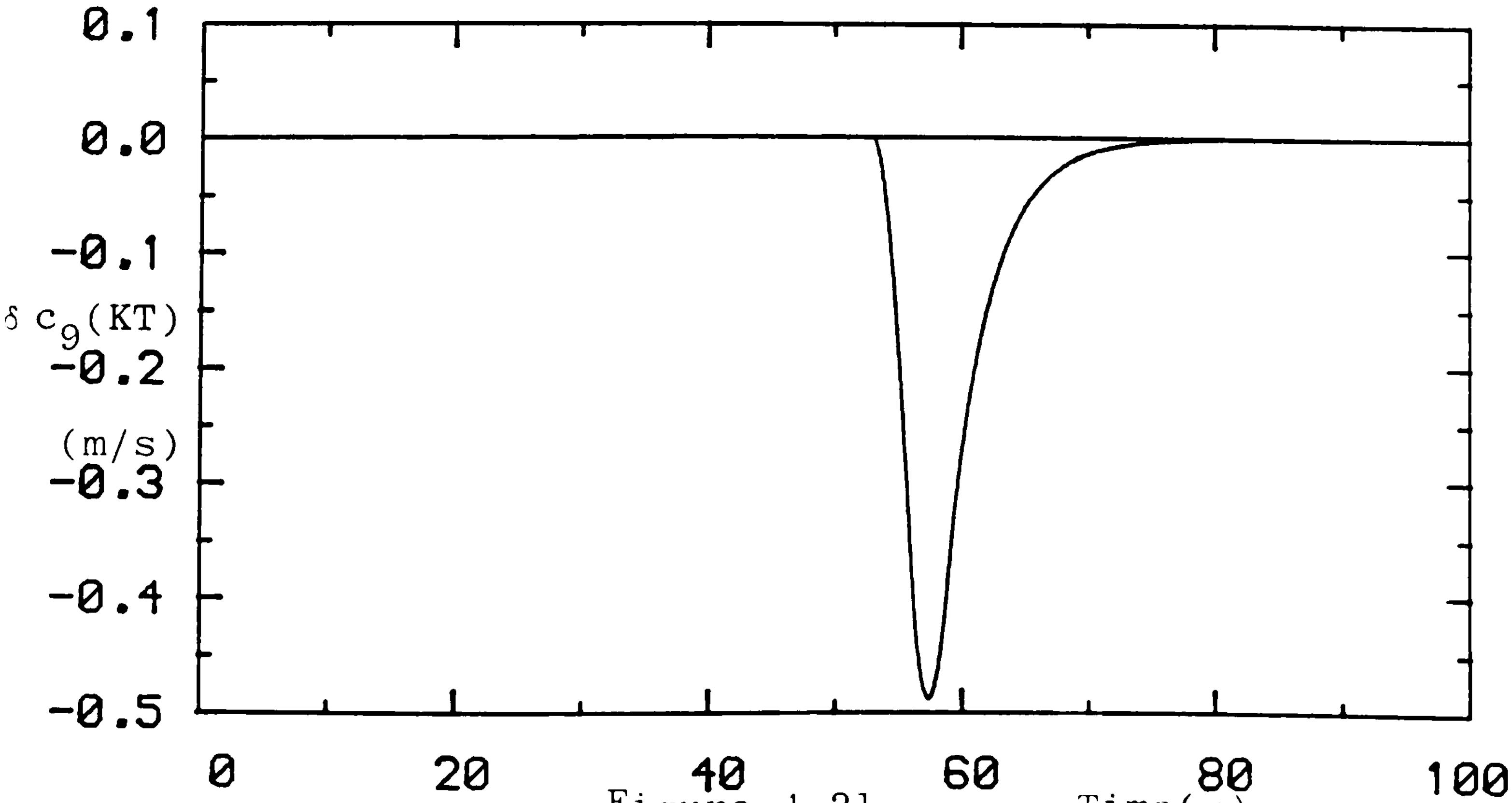

Figure 4.21

Centralized Controller

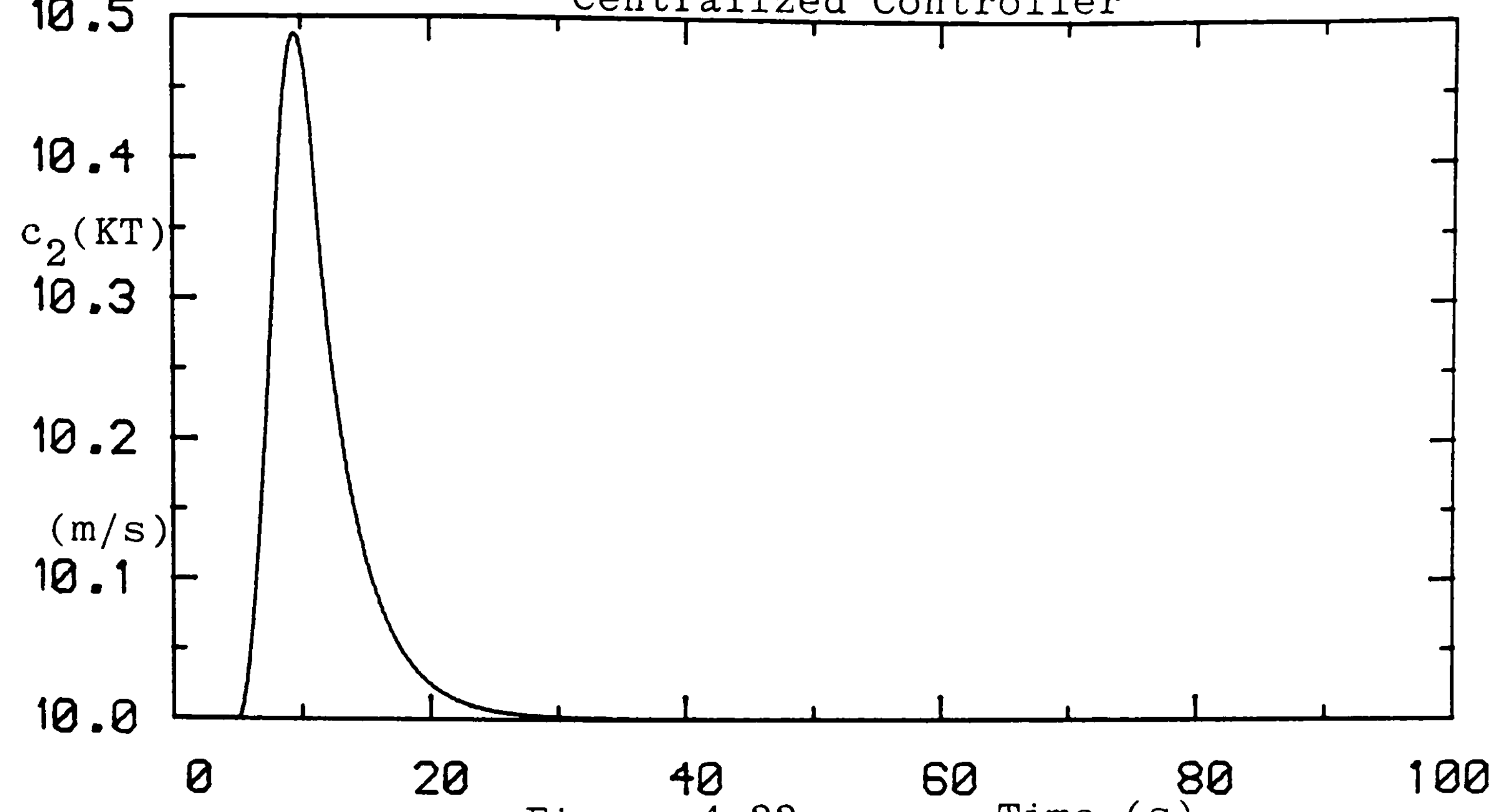

Figure 4.22

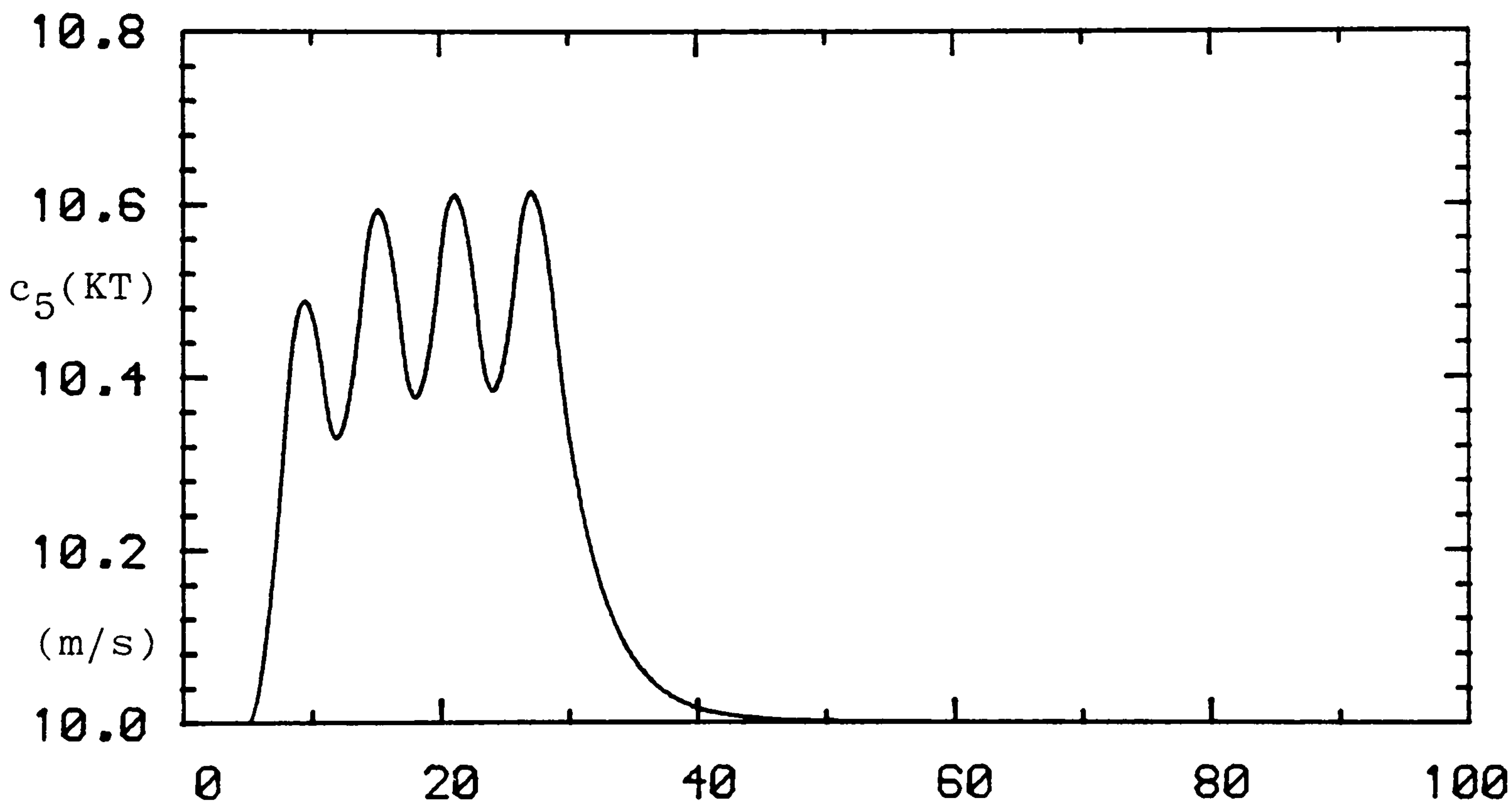

Figure 4.23

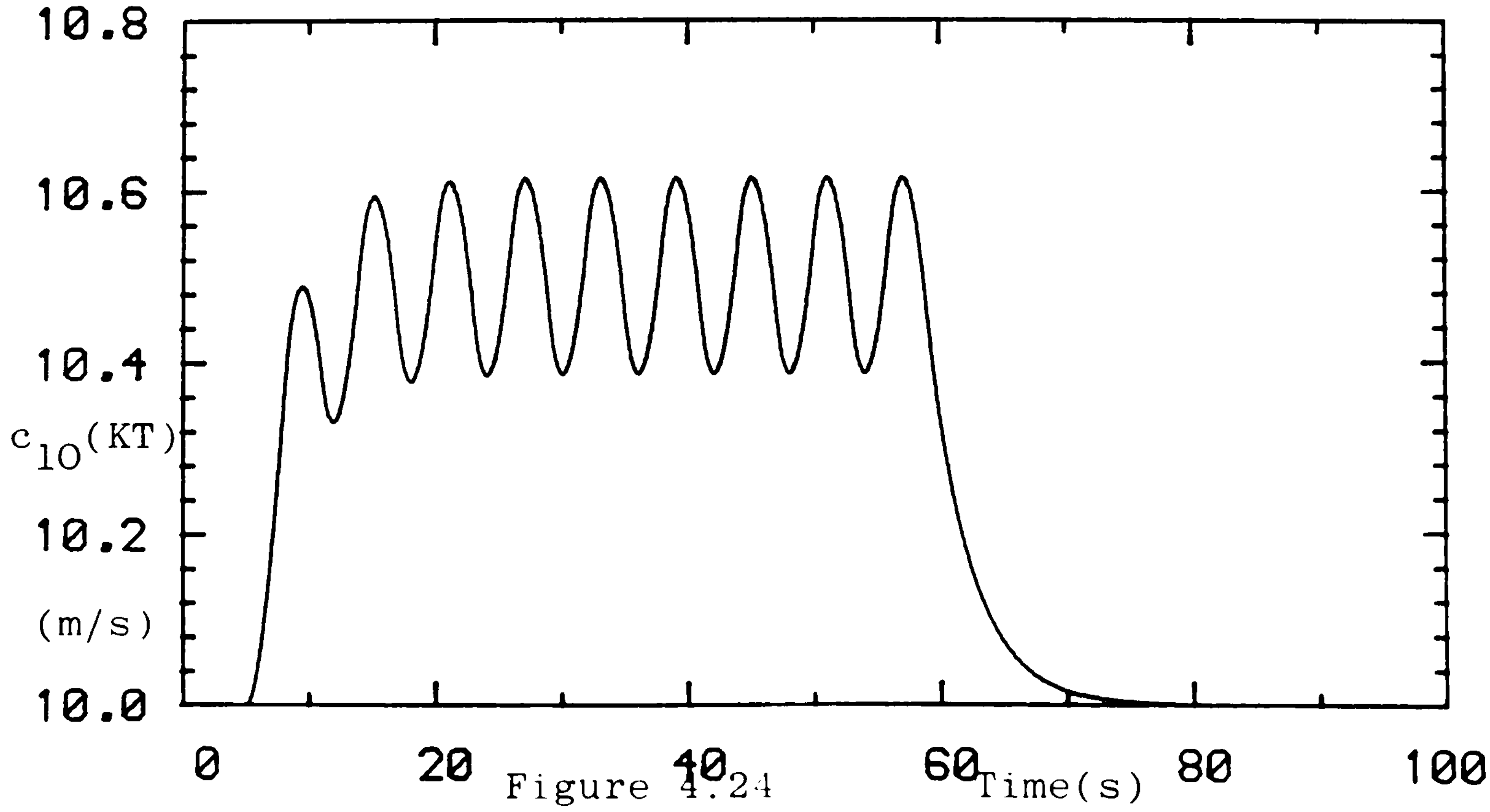

Figure 4.24

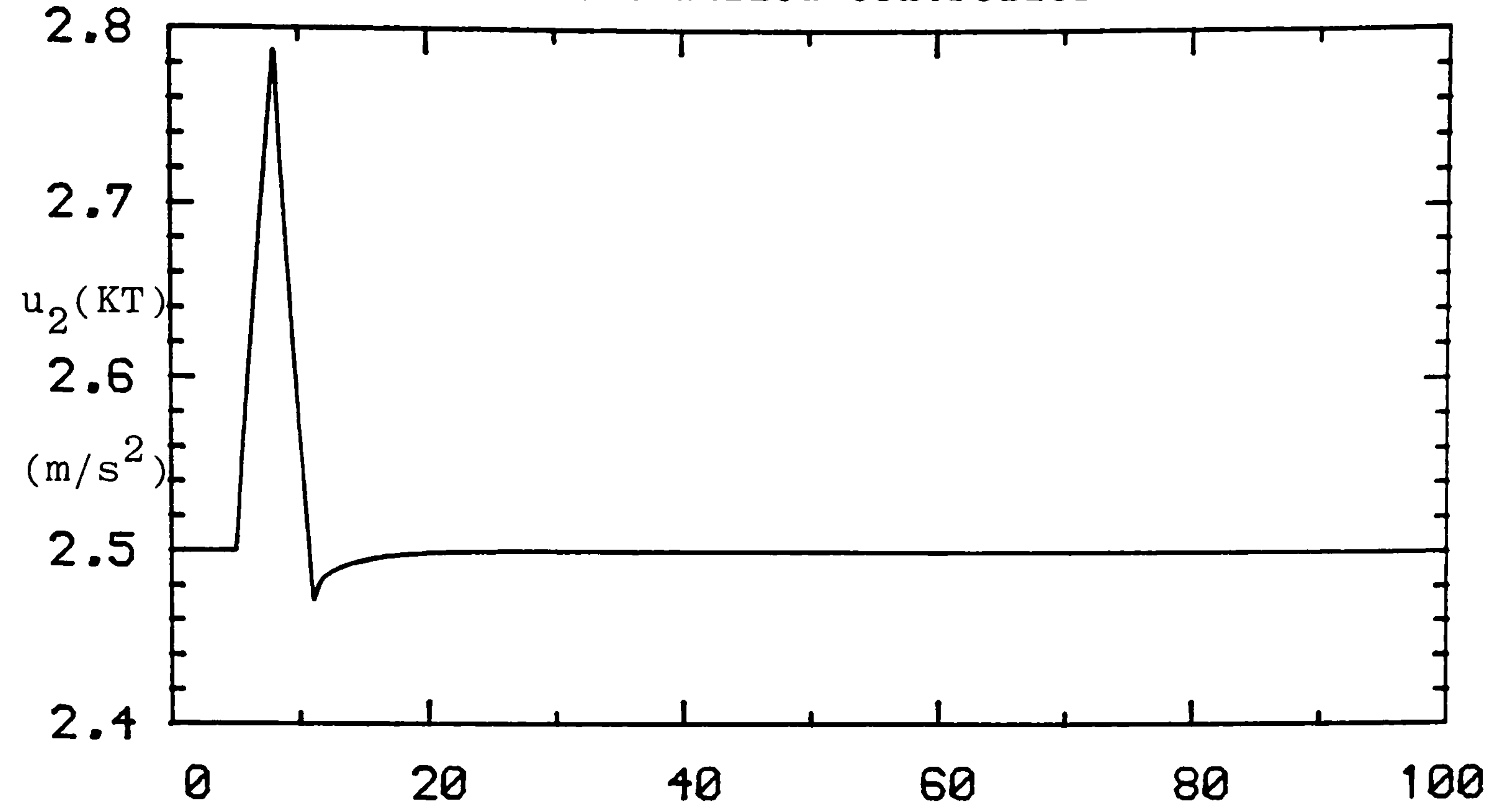

Figure 4.25 Time(s)

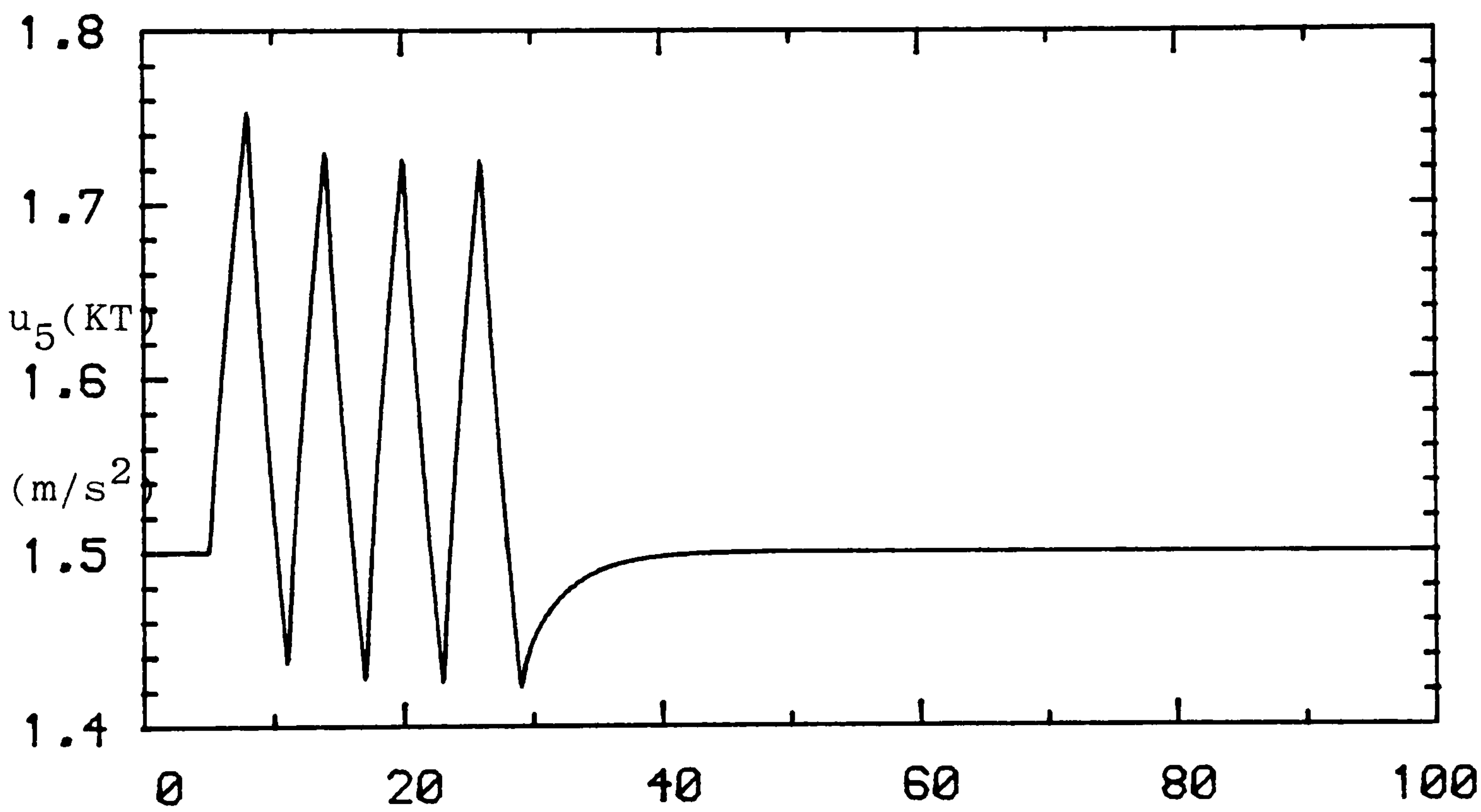

Figure 4.26 Time (s)

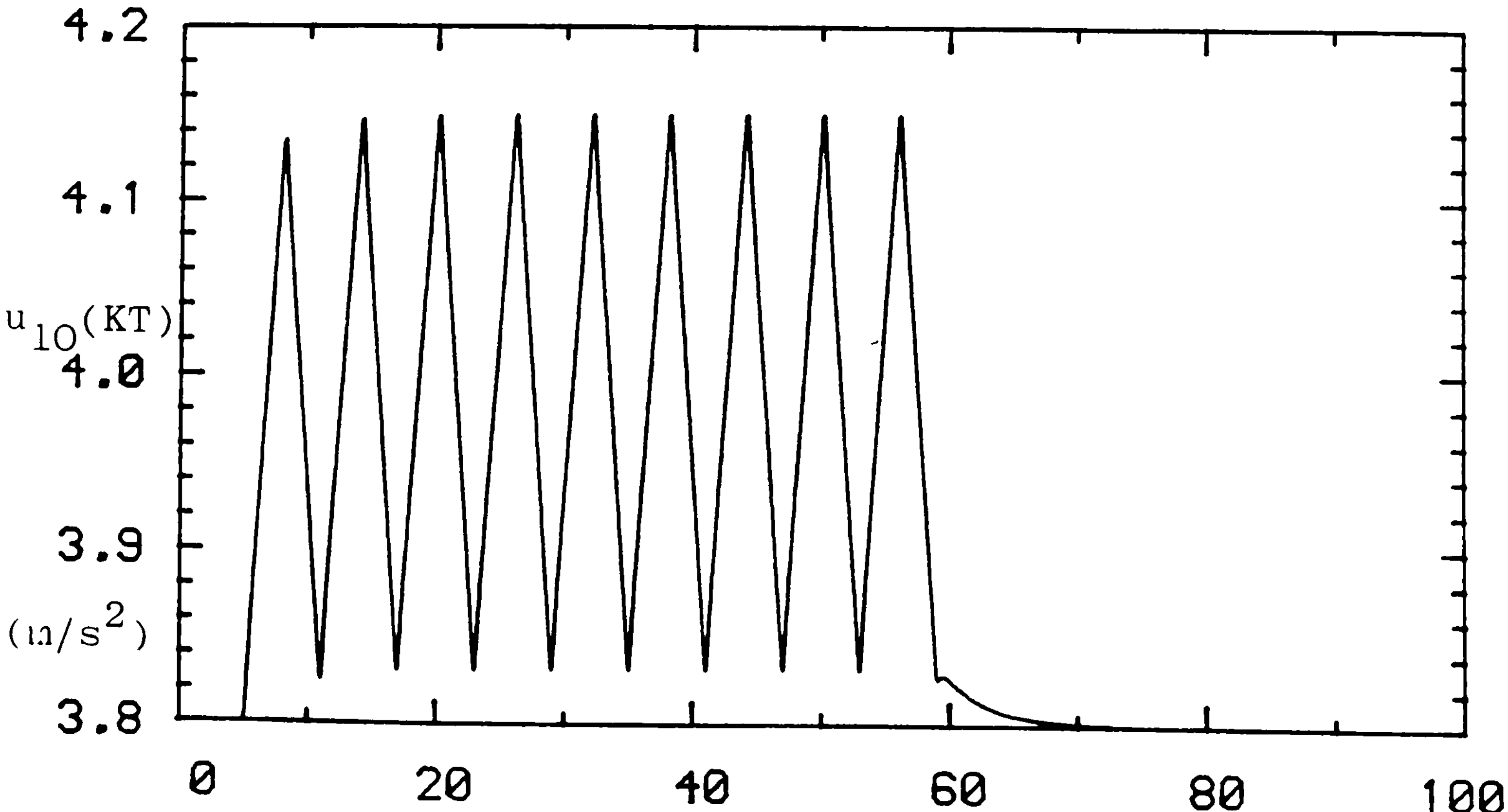

Figure 4.27 Time (s)

4.8 Discussion

It is clear from figures (4.4) to (4.6) and (4.16) to (4.18) that the decentralized and centralized fast-sampling controllers entrain the ten vehicle cascade considered whilst producing no overshoots in the outputs and also little interaction between them. Furthermore the centralized controller produces little interaction between the relative velocities (see figures (4.19) to (4.21)) whilst the decentralized controller does produce some interaction (see figures (4.7) to (4.9)) between the relative velocities which has been referred to as the 'shock wave' affect in sections (4.3) and (4.4). It is also evident from figures (4.10) to (4.12) and (4.22) to (4.24) that there is no absolute velocity 'build up' when either of the controllers is utilized because of the sequentially implemented command inputs. Hence it is clear that utilizing sequentially implemented command inputs effectively entrains a vehicle cascade whilst not requiring excessive control input amplitudes (see figures (4.13) to (4.15) and (4.25) to (4.27)), and utilizing the centralized controller eliminates the 'shock wave' affects.

Finally it must be emphasized that the singular perturbation analysis of the closed-loop transfer function matrices has not only predicted all of the above phenonema but also indicated how to utilize the command inputs in a sensible manner.

CHAPTER 5

LONGITUDINAL DYNAMICS OF TRAINS OF VEHICLES

5.1 Introduction

A review of the early work on the problems of train control is made in this chapter. Dudley [35] assumed trains to be simple vibratory systems and presented important results concerning their natural frequencies and the propagation of waves. Wikander [36] considered the draft gear action of long trains by assuming trains could be represented by bars, from which the fundamental properties of waves travelling along trains can be understood. Expressions for the damped natural frequencies are presented in section (5.4) together with the expression for the exponentionally decreasing amplitude envelope.

5.2 A Mathematical Model of Trains of Vehicles

The trains to be studied are illustrated by figure 5.1 and are assumed to consist of w vehicles of masses m_i (i=1,..,w) with couplings that are represented by linear springs of stiffnesses K_i (i=1,..,w-1). The trains are assumed to be moving over level terrain that has negligible resistance to motion. One set of equations that completely describes the motion of trains can be expressed in the form

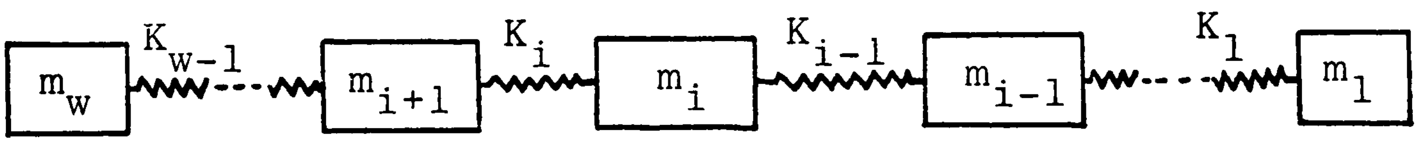

Figure 5.1

$$m_1\ddot{x}_1 = -K_1(x_1-x_2)$$

$$m_2\ddot{x}_2 = -K_2(x_2-x_3)+K_1(x_1-x_2)$$

$$m_3\ddot{x}_3 = -K_3(x_3-x_4) + K_2(x_2-x_3) \qquad (5.1)$$

- - - - - - - - - - - - - - - - - - -

- - - - - - - - - - - - - - - - - - -

$$m_{w-1}\ddot{x}_{w-1} = -K_{w-1}(x_{w-1}-x_w) + K_{w-2}(x_{w-2}-x_{w-1})$$

$$m_w\ddot{x}_w = K_{w-1}(x_{w-1}-x_w)$$

where the x_i (i=1,..,w) are the displacements of the vehicles about their equilibrium positions. Since these equations represent a simple vibratory system, putting

$$x_i = \bar{x}_i \sin(\omega_n t) \quad (i=1,..,w) \qquad (5.2)$$

leads directly to an eigenvalue problem of the form

$$m_1 \omega_{nj}^2 \bar{x}_1 = K_1(\bar{x}_1-\bar{x}_2)$$

$$K_1(\bar{x}_1-\bar{x}_2) + m_2\omega_{nj}^2 \bar{x}_2 = K_2(\bar{x}_2-\bar{x}_3)$$

$$K_2(\bar{x}_2-\bar{x}_3) + m_3\omega_{nj}^2 \bar{x}_3 = K_3(\bar{x}_3-\bar{x}_4)$$

--------------------------------------- (5.3)

$$K_{w-2}(\bar{x}_{w-2}-\bar{x}_{w-1}) + m_{w-1}\omega_{nj}^2 \bar{x}_{w-1} = K_{w-1}(\bar{x}_{w-1}-\bar{x}_w)$$

$$K_{w-1}(\bar{x}_{w-1}-\bar{x}_w) + m_w \omega_{nj}^2 \bar{x}_w = 0$$

where the ω_{nj} (j=1,..,w-1) are the natural frequencies and x_i (i=1,..,w) are the amplitudes of the vibrations of the vehicles about their equilibrium points.

5.3 Review of the Literature on the Dynamics of Trains of Vehicles

Dudley [35] used the analogous recti-linear case to the analysis of the torsional vibrations of identical discs equally spaced on a uniform shaft (see, for instance, Karman and Biot [37]), to show that the natural frequencies of a uniform train of w vehicles, each of mass m and coupled by linear springs of stiffnesses K, could be expressed in the form

$$\omega_{nj} = 2\sqrt{\frac{K}{m}} \sin\left\{ \frac{\pi}{2} \cdot \frac{j}{w} \right\} \qquad (5.4)$$

$$(j=1,..,w-1)$$

Furthermore Dudley [35] showed that the corresponding mode shape for each ω_{nj} (j=1,..,w-1) could be found from

$$\bar{x}_i = \cos\left\{ \frac{\pi}{2} \cdot \frac{j(2i-1)}{w} \right\} \qquad (5.5)$$

$$(i=1,--,w)$$

where x_i is the amplitude of the vibrations of the i^{th} vehicle about its equilibrium position. Dudley [35] further showed that the velocity of a wave in a uniform train could be expressed in the form

$$v_\omega = \omega L/\mu \qquad (5.6)$$

where

L = length of each vehicle,

$$\mu = 2 \sin^{-1} \{ \frac{\omega}{2} \sqrt{\frac{m}{K}} \} \qquad (5.7)$$

and ω is the angular velocity disturbing the system. Substituting ω_{nj} from (5.4) for ω in (5.6) and (5.7) gives

$$v_{\omega_{nj}} = L \sqrt{\frac{K}{m}} \sin\{ \frac{\pi}{2} (\frac{j}{w})\} \cdot \frac{2w}{\pi j} \qquad (5.8)$$

$$(j=1,..,w-1)$$

and figure 5.2 illustrates the variation of wavespeed at the highest and lowest natural frequencies for increasing numbers of vehicles in uniform trains. Dudley [35] also considered specific examples of non-uniform trains by utilizing Holzer's method (see, for instance, Tong [38]) to solve the resulting form of equations (5.3).

Finally it is interesting to note the properties of waves reflected from free and fixed ends of elastic bars. It has been shown (see, for instance, Tong [38]) that the displacement u a distance x from a reference satisfies

$$-u_{incident} = u_{reflected} \qquad (5.9)$$

at the fixed ends, and

$$-(\frac{\partial u}{\partial x})_{incident} = (\frac{\partial u}{\partial x})_{reflected} \qquad (5.10)$$

at the free ends. These properties are illustrated by figure (5.3).

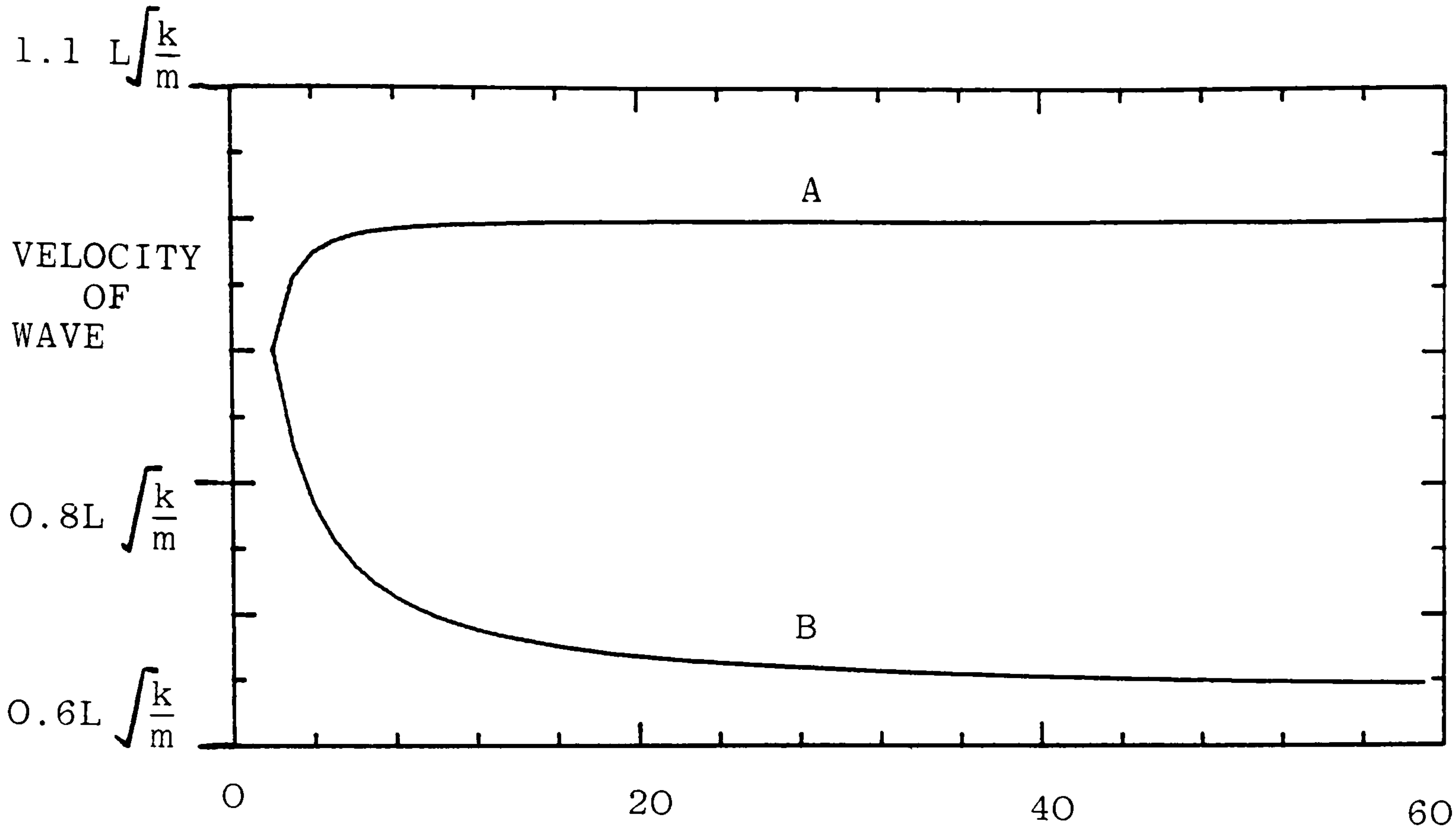

A, Lowest Natural Frequency

B, Highest Natural Frequency

Figure 5.2.

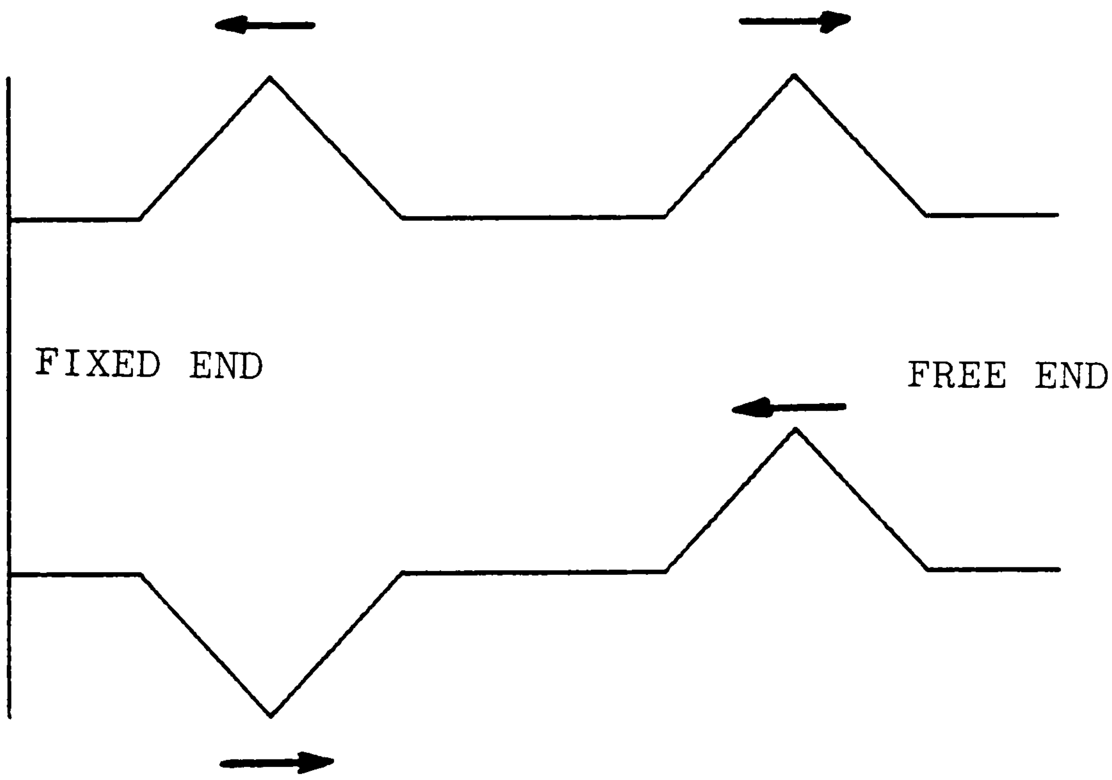

Figure 5.3.

5.4 The Open-Loop Poles of a Uniform Train of Vehicles

The open-loop poles of a uniform train of w vehicles, of masses m connected by couplings represented by linear springs of stiffnesses K and linear dashpots of damping coefficients δ, can be found by utilizing difference equations. It can be shown that an equation describing the motion of the j^{th} vehicle assumes the form

$$m\ddot{x}_j(t) = K(x_{j-1}(t) - 2x_j(t) + x_{j+1}(t)) + \delta\,(\dot{x}_{j-1}(t) - 2\dot{x}_j(t) + \dot{x}_{j+1}(t)) \quad (5.11)$$

where $x_{j-1}(t)$, $x_j(t)$ and $x_{j+1}(t)$ are the displacements of the $(j-1)^{th}$, j^{th} and $(j+1)^{th}$ vehicles from their equilibrium positions.

Assuming the motions of the vehicles are of the form

$$x_j(t) = \bar{x}_j\, e^{at} \quad (j=1,..,w) \quad (5.12)$$

produces the set of difference equations

$$0 = \bar{x}_{j-1} - (2-\alpha^2)\bar{x}_j + \bar{x}_{j+1} \quad (j=2,..,w-1) \quad (5.13)$$

where

$$a = \mu \pm i\,\omega_d\,, \tag{5.14}$$

$$\alpha^2 = \frac{-ma^2}{K+\delta a} \tag{5.15}$$

and the $\bar{x}_j$ (j=1,..,w) are the amplitudes. It is known (see, for instance, Karman and Biot [37]) that one solution to (5.13) assumes the form

$$\bar{x}_j = A\cos(qj) + B\sin(qj) \tag{5.16}$$

where

$$\cos q = 1 - \frac{\alpha^2}{2}\,. \tag{5.17}$$

In order to include the first and last vehicles in (5.13) it is necessary to assume that one extra vehicle is added to each end of the train, as illustrated by figure (5.5). It can be

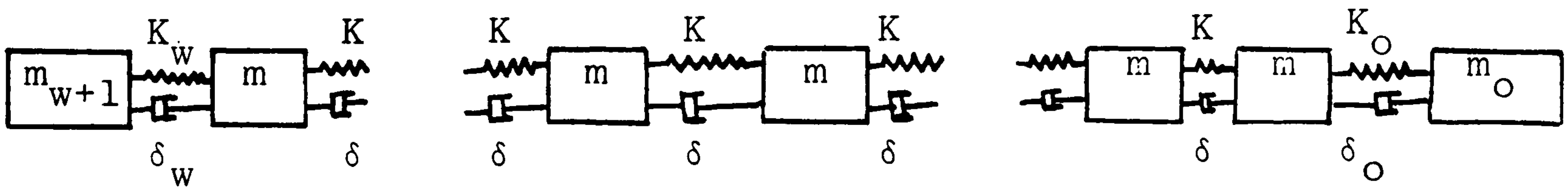

Figure (5.5)

shown from (5.12) and the equations of motion of the first and last vehicles in figure (5.5) that

$$0 = \bar{x}_2 - (1-\alpha^2)\bar{x}_1 - \frac{\bar{K}_o}{K+\delta a}\bar{x}_1 \tag{5.18}$$

and

$$0 = \bar{x}_{n-1} - (1-\alpha^2)\bar{x}_n - \frac{\bar{K}_w}{K+\delta a}\bar{x}_n \tag{5.19}$$

where

$$\bar{K}_o = \frac{K_o+\delta_o a}{1+\left(\frac{K_o+\delta_o a}{m_o a^2}\right)} \tag{5.20}$$

and

$$\bar{K}_w = \frac{K_w+\delta_w a}{1+\left(\frac{K_w+\delta_w a}{m_{w+1} a^2}\right)} . \tag{5.21}$$

It is clear from (5.13) that

$$0 = \bar{x}_o-(2-\alpha^2)\bar{x}_1+\bar{x}_2 \tag{5.22}$$

and

$$0 = \bar{x}_{w-1}-(2-\alpha^2)\bar{x}_w+\bar{x}_{w+1} , \tag{5.23}$$

and comparing these with (5.18) and (5.19), which take account of the end conditions, it follows that

$$\bar{x}_o + \left(\frac{\bar{K}_o}{K+\delta a} - 1\right)\bar{x}_1 = 0 \tag{5.24}$$

and

$$\bar{x}_{w+1} + \left(\frac{\bar{K}_w}{K+\delta a} - 1\right) \bar{x}_w = 0 \tag{5.25}$$

which are the boundary conditions for j=0 and j=w+1. Substituting for $\bar{x}_o$, $\bar{x}_1$, $\bar{x}_w$ and $\bar{x}_{w+1}$ in (5.24) and (5.25), by putting j=0,1,w and w+1 in (5.17), leads to the two expressions of the form

$$A(1-\cos q) - B \sin q = 0 \tag{5.26}$$

and

$$A(\cos q(w+1) - \cos qw) + B(\sin q(w+1)-\sin qw) = 0 \tag{5.27}$$

when

$$\bar{K}_w = \bar{K}_o = 0 \tag{5.28}$$

and the train has its original free ends. Equation (5.26) and (5.27) have a non-trivial solution for A and B when

$$(\cos(q)-1)\sin qn = 0 \tag{5.29}$$

and it follows from (5.17) and (5.29) that either

$$\alpha = 0 \tag{5.30}$$

or

$$\alpha_j = 2 \sin \left(\frac{j}{w} \cdot \frac{\pi}{2} \right) . \tag{5.31}$$

$(j=1,..,w-1)$

Substituting (5.14) into (5.15) and squaring (5.31) and equating the two results produces an expression of the form

$$\frac{-4}{m} \sin^2\left(\frac{j}{w} \cdot \frac{\pi}{2}\right) (K + \delta\mu \pm i\delta\omega_d)$$

$$= \mu^2 - \omega_d^2 \pm 2i\omega_d\mu \quad . \tag{5.32}$$

$(j=1,..,w-1)$

Equating the real and imaginary parts of (5.32) produces the expressions of the form

$$\mu_j = -2 \left(\frac{\delta}{m}\right) \sin^2 \left(\frac{j}{w} \cdot \frac{\pi}{2}\right) \tag{5.33}$$

and

$$\omega_{dj} = \sqrt{(\omega_{nj}^2 - \mu_j^2)} \tag{5.34}$$

$(j=1,..,w-1)$

for the real and imaginary parts of the open-loop poles, where the ω_{nj} $(j=1,..,w-1)$ are given by (5.4). Finally it is clear that the open-loop poles, given by the

$\mu_j \pm i\omega_{dj}$ (j=1,..,w-1), will lie on the locus

$$\omega_d^2 + 2\,\mu\,(\frac{K}{\delta}) + \mu^2 = 0 \tag{5.35}$$

whose bounds are given by

$$-\frac{2c}{m} \pm i\sqrt{(\frac{4K}{m} - 4\,\frac{\delta^2}{m^2})} \tag{5.36}$$

as $w \to \infty$, and the origin since (5.30) produces the rigid body solution for all w.

5.5 Summary

As the number of vehicles in a 'uniform' train increases the following characteristics become evident The highest natural frequency approaches

$$2\sqrt{\frac{K}{m}}$$

and the fundamental (non-zero) natural frequency approaches zero. The highest 'shock wave' velocity approaches

$$L\sqrt{\frac{K}{m}}$$

and the lowest 'shock wave' velocity approaches

$$\frac{2}{\pi} \; L\sqrt{\frac{K}{m}}$$

respectively for the lowest (non-zero) and highest natural frequencies.

It follows from figure (5.3) that the reflection of a series of waves at the free end of a train could result in amplitude build up and , eventually, to excessive coupler forces. This is one reason for having locomotives at the rear of a train. Another reason was suggested by Wikander [36] who described a train reaching the bottom of a grade where the couplers successively go into tension. If at the same point the driver increases the tractive effort causing a positive wave to travel down the train, whose speed is equal to the speed of the train, then the tractive effort wave will be stationary and cause additive tension in the couplings and finally produce a 'crack-the-whip' effect as the last vehicle passes the grade change. Both these affects should be alleviated by a properly controlled rear locomotive which causes the rear half of the train to be compressed (neglecting resistance to motion).

5.6 Conclusions

The theory presented in this chapter represents a successful attempt to understand the motions of trains through their open loop properties. Dudley [35] and Wikander [36] explained how problems could arise in practice due to inexperienced or bad train control. It is clear that one solution to the problems outlined by Dudley [35] and Wikander [36] is to remove the cause by automatically controlling trains. In the next two chapters the fast-sampling control theory presented in section (2.4) is utilized to develop effective speed controllers for trains and so remove the cause of possible 'crack-the-whip' affects and hence the need for rear locomotives.

CHAPTER 6

SINGLE LOCOMOTIVE POWERED TRAINS

6.1 Introduction

Two important criteria when considering the automatic control of freight trains are those of cost and reliability. In this chapter it is found that these criteria can be readily satisfied since it is shown that trains having single leading locomotives and outputs as the speeds of the locomotives belong to the class of systems considered in sections (2.4) and (2.5). The fast-sampling controller developed in section (6.4) for the w-vehicle train model developed in section (6.2) is simple and copes with trains of different lengths. Three different lengths of train are considered in section (6.5) and the results of digital computer simulations of the trains travelling over a gradient change presented together with the respective closed-loop pole and asymptotic closed-loop pole positions. Finally in section (6.6) the results presented in section (6.5) are discussed.

6.2 Mathematical Model

In this section a linear mathematical model of the w vehicle trains illustrated by figure 6.1 is developed for the case where the first vehicles are the only locomotives. It is assumed that the vehicles move with velocities $c_i(t)$ $(i=1,..,w)$ and have masses $m_i(i=1,..,w)$ and are connected by couplings that can be represented by linear springs of stiffnesses K_j $(j=1,..,w-1)$ and linear dashpots of damping coefficients δ_j $(j=1,..,w-1)$ and where the extensions of the couplings from the free lengths are $q_j(t)$ $(j=1,..,w-1)$. It is further assumed that the trains have negligible resistance to motion and the disturbances

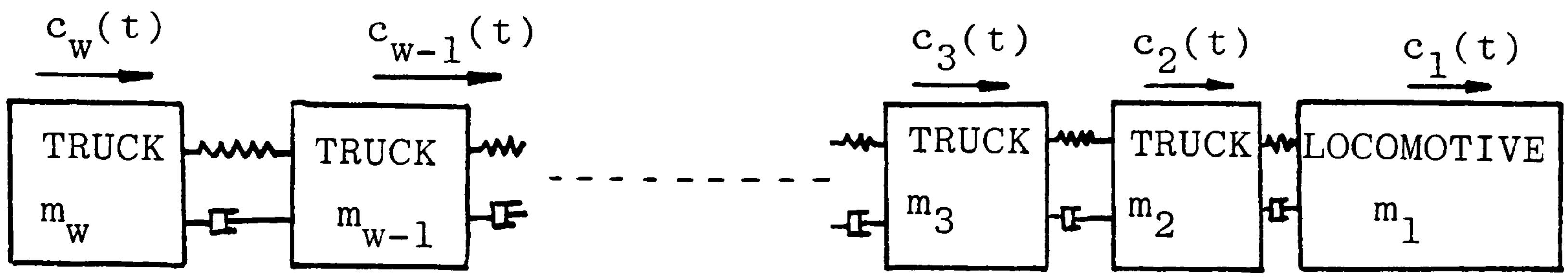

FIGURE 6.1

take the form of gradient changes and that the outputs are the absolute speeds of the locomotives. It follows that the state and output equations can be expressed in the matrix forms

$$\begin{bmatrix} \dot{x}_1(t) \\ \dot{x}_2(t) \end{bmatrix} = \begin{bmatrix} A_{11} & A_{12} \\ A_{21} & A_{22} \end{bmatrix} \begin{bmatrix} x_1(t) \\ x_2(t) \end{bmatrix} + \begin{bmatrix} 0 \\ B \end{bmatrix} u(t) \begin{bmatrix} D_1 \\ D_2 \end{bmatrix} d(t) \tag{6.1}$$

and

$$y(t) = \begin{bmatrix} C_1 & C_2 \end{bmatrix} \begin{bmatrix} x_1(t) \\ x_2(t) \end{bmatrix} \tag{6.2}$$

respectively where

$$x_1(t) = \Big[q_{w-1}(t),\ q_{w-2}(t), \ldots\ldots, q_3(t),\ q_2(t),\ q_1(t)\ , \\ c_w(t),\ c_{w-1}(t),\ c_{w-2}(t),\ \ldots\ldots, c_4(t), c_3(t), c_2(t) \Big]', \tag{6.3}$$

$$x_2(t) = \Big[c_1(t) \Big] \ , \tag{6.4}$$

$$A_{11} = \left[\begin{array}{l} 0,0,\ \ldots\ 0,0,0,-1,\ 1,\ 0\ ,\ldots\ldots\ldots\ldots\ 0,\ 0,\ 0 \\ 0,0,\ \ldots\ldots 0,0,0,0,-1,1,\ \ldots\ldots\ldots\ldots\ 0,\ 0,\ 0 \\ \text{- - - - - - - - - - - - - - - - - - - -} \\ 0,0,\ \ldots\ldots\ldots\ldots, 0,0,0,0,0,0,\ldots\ldots\ldots\ldots, -1,\ 1,\ 0 \\ 0,0,\ \ldots\ \ldots\ldots, 0,0,0,0,0,0,\ \ldots\ldots\ldots\ldots,\ 0, -1,\ 1 \\ 0,0,\ldots\ldots\ \ldots\ldots\ 0,0,0,0,0,0,\ \ldots\ldots\ldots\ldots,\ 0,\ 0\ ,\ 1 \\ \bar{\beta}_w, 0,\ \ldots\ldots\ldots, 0,0,0,-\bar{\gamma}_w, \gamma_w,\ 0,\ldots\ldots\ldots,\ 0,\ 0,\ 0 \\ -\beta_{w-1}, \bar{\beta}_{w-1}, \ldots\ldots 0,0,0,\gamma_{w-1},\ -(\gamma_{w-1}+\bar{\gamma}_{w-1}), \bar{\gamma}_{w-1}, \ldots\ldots, 0,0,0 \\ 0\ ,\ \ -\beta_{w-2}, \ldots, 0,0,0,0,\gamma_{w-2},\ -(\gamma_{w-2}+\bar{\gamma}_{w-2}), \ldots,\ 0,0,0 \\ \text{- - - - - - - - - - - - - - - - - - - -} \\ 0,\ 0,\ \ldots\ldots, \bar{\beta}_4,\ 0,\ 0,\ 0,\ 0,\ 0,\ \ldots\ldots, -(\gamma_4+\bar{\gamma}_4), \bar{\gamma}_4,\ 0 \\ 0,\ 0,\ \ldots\ldots, -\beta_3, \bar{\beta}_3,\ 0,\ 0,\ 0,\ 0, \ldots\ldots, \gamma_3 -(\gamma_3+\bar{\gamma}_3), \bar{\gamma}_3 \\ 0,\ 0,\ \ldots\ldots,\ 0, -\beta_2, \bar{\beta}_2,\ 0,\ 0,\ 0,\ \ldots, 0, \gamma_2, -(\gamma_2+\bar{\gamma}_2) \end{array} \right], \tag{6.5}$$

$$A_{12} = \left[0, 0, \ldots\ldots, 0, 0, 1, 0, 0, 0, \ldots\ldots, 0, 0, \gamma_2\right]', \quad (6.6)$$

$$A_{21} = \left[0, 0, \ldots\ldots, 0, 0, -\beta_1, 0, 0, 0, \ldots\ldots, 0, 0, \gamma_1\right], \quad (6.7)$$

$$A_{22} = \left[-\gamma_1\right], \quad (6.8)$$

$$\beta_i = K_i/m_i \quad , \quad (i=1,..,w-1) \quad (6.9)$$

$$\bar{\beta}_{i+1} = K_i/m_{i+1} \quad , \quad (i=1,..,w-1) \quad (6.10)$$

$$\gamma_i = \delta_i/m_i \quad , \quad (i=1,..,w-1) \quad (6.11)$$

$$\bar{\gamma}_{i+1} = \delta_i/m_{i+1} \quad , \quad (i=1,..,w-1) \quad (6.12)$$

$$B = \left[1\right] \quad , \quad (6.13)$$

$$C_1 = \left[0-\right], \quad (6.14)$$

$$C_2 = \left[1\right], \quad (6.15)$$

$$D_1 = \begin{bmatrix} 0 & 0 \\ I_{w-1} & 0 \end{bmatrix} \quad (6.16)$$

$$D_2 = \left[0- \quad 1\right] \quad , \quad (6.17)$$

$$u(t) = \left[F_1(t)/m_1\right] \quad , \quad (6.18)$$

$$d(t) = \left[-g \sin\theta_w(t) \; ,\ldots\ldots, -g \sin\theta_1(t)\right]', \quad (6.19)$$

$$n = 2w-1, \tag{6.20}$$

$x_1(t) \in R^{2w-2}$, $x_2(t) \in R^1$, $A_{11} \in R^{(2w-2)x(2w-2)}$,

$A_{12} \in R^{(2w-2)x1}$, $A_{21} \in R^{1x(2w-2)}$, $A_{22} \in R^{1x1}$.,

$C_1 \in R^{1x(2w-2)}$, $C_2 \in R^1$, $D_1 \in R^{(2w-2)xw}$,

$D_2 \in R^{1xw}$, $u(t) \in R^1$, $d(t) \in R^w$, $F_1(t)$ is the tractive force of the locomotive and $\theta_i(t)$ $(i=1,..,w)$ are the gradients of the terrain beneath the respective vehicles.

It can be shown that the trains are controllable, and only observable if the output is taken as a function of the absolute speed, as above.

6.3 Transmission Zeros of Trains with Single Leading Locomotives

It will be shown in this section that trains having single leading locomotives belong to the class of systems considered in section (2.4) when the outputs are taken as the speeds of the locomotives, as in section (6.2). The transmission zeros of these trains are considered, and general expressions developed for the transmission zeros of "uniform" trains.

It is clear that (2.56) is satisfied since it follows from (6.13) and (6.15) that

$$\text{rank}\ (C_2B) = 1 = \ell \quad , \tag{6.21}$$

and as a result (3.17) can be used to calculate the transmission zeros. It follows from (3.17) and (6.14) that the transmission zeros are the eigenvalues of the matrix A_{11}, given by (6.5). The matrix A_{11} is also equivalent to the plant matrix of the trains illustrated by figure (6.1) when the locomotives become fixed rigid bodies since $c_1(t)$ and therefore $x_2(t)$, given by (6.4), are null for such systems. It follows that the reduced system assumes the form

$$\dot{x}_1(t) = A_{11}\, x_1(t) \tag{6.22}$$

where $x_1(t)$ and A_{11} are given by (6.4) and (6.5).
For the case where

$$\delta_i > 0 \quad (i=1,..,w-1) \tag{6.23}$$

the systems described by (6.22) are always dissipative with the result that their open-loop poles will always lie in the left half of the complex plane. It therefore follows that the sets of transmission zeros of the original trains will also always lie in the left half of the complex plane. It is clear that (2.57) is satisfied and the methods developed in section (2.4) can be used to design a fast-sampling controller for trains having single leading locomotives since the resulting closed-loop systems will be stable under fast-sampling control.

It is known (see, for instance, Karman and Biot [37]) that when

$$K_i = K \quad , \tag{6.24}$$

$$\delta_i = \delta \quad , \tag{6.25}$$

$$m_i = m \tag{6.26}$$

and the locomotives in figure (6.1) are fixed, leaving w-1 vehicles free, then the undamped natural frequencies can be expressed in the form

$$\omega_r = 2\sqrt{\frac{K}{m}}\sin\left(\frac{2r-1}{2\omega-1}\cdot\frac{\pi}{2}\right) . \qquad (6.27)$$

$$(r=1,2,..,w-1)$$

It follows from (6.27), and a similar analysis to the one in section (5.4), that the transmission zeros of "uniform' trains can be expressed in the form

$$\nu_r = p_r \pm iq_r \quad (r=1,..,w-1) \qquad (6.28)$$

where

$$p_r = -2\left(\frac{\delta}{m}\right)\sin^2\left(\frac{2r-1}{2w-1}\cdot\frac{\pi}{2}\right) \qquad (6.29)$$

and

$$q_r = \sqrt{\left(\frac{4K}{m}\sin^2\left(\frac{2r-1}{2w-1}\cdot\frac{\pi}{2}\right) - p_r^2\right)} . \qquad (6.30)$$

Since the loci of the transmission zeros are of the form

$$q^2 + \frac{2K}{\delta}p + p^2 = 0 \qquad (6.31)$$

and are of identical form to that given by (5.35) for the open-loop poles and because both are also independent of w it is clear that the transmission zeros and the open-loop poles of any uniform train lie on the same curve for a given pair of damping and stiffness coefficients. It follows from (5.33), (5.34) and (6.28) to

(6.30) that the dampled-natural frequencies and the transmission zeros will be increasingly crowded away from the imaginary axis, and will also have the same bounds, namely

$$p_r = -2\ (\frac{\delta}{m}) \qquad (6.32)$$

and

$$q_r = 2\sqrt{(\frac{K}{m} - \frac{\delta^2}{m^2})} \qquad (6.33)$$

as $w \to \infty$.

6.4 Fast-Sampling Speed Control of Single Locomotive Trains

It is clear from section (6.3) that trains with single leading locomotives belong to the class of systems considered in sections (2.4) and (2.5).

As a result the theory from section (2.4) can be utilized to develop a suitable algorithm for the speed control of such trains by using the mathematical model developed in section (6.2).

It follows from (3.8), (3.9), (6.13) and (6.15) that the 'proportional' controller constant assumes the form

$$K_o = 1 \tag{6.34}$$

and from (3.11) and (3.12) that the 'integrator' controller constant assumes the form

$$K_1 = \rho . \tag{6.35}$$

Substituting (6.34) and (6.35) into (2.13) produces a speed control algorithm of the form

$$u(KT) = f \{ e(KT) + \rho z(KT) \} \tag{6.36}$$

where

$$e(KT) = v(KT) - c_1(KT) \tag{6.37}$$

and z(KT) is given by (2.15). It can further be shown from (2.75) , (2.76) , (2.87) , (6.13) and (6.15) that the asymptotic transfer function matrix that relates the output to changes in command and disturbances assumes the form

$$\begin{bmatrix} \Gamma(\lambda) & \Gamma_D(\lambda) \end{bmatrix} = \begin{bmatrix} \frac{1}{\lambda} & , & 0 \end{bmatrix} \qquad (6.38)$$

as $f \to \infty$.

Hence it is clear from (6.38) that as $f \to \infty$ the output will tightly track step command changes and be completely unaffected by step disturbances.

In the next section numerical examples are presented that utilize the theory developed in this section. These examples will underline the integrity of fast-sampling controllers since it will be shown that one control algorithm copes easily with trains of differing lengths.

6.5 Five, Ten and Twenty Vehicle Trains

In this section the fast-sampling speed control of five, ten and twenty vehicle trains is considered. It is assumed that the trains consist of equal masses connected by identical couplings, as illustrated by figure (6.2).

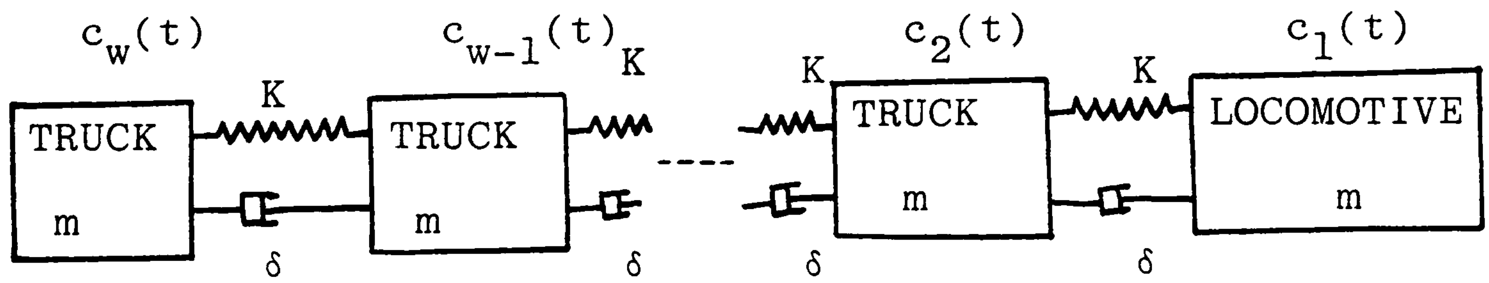

$w = 5,\ 10,\ 20$

Figure 6.2.

It follows from figure (6.2), equations (6.9) to (6.12),

$$m = 1.0 \times 10^5 \quad \text{kg} \qquad (6.39)$$

$$K = 2.0 \times 10^6 \quad \text{N/m} \qquad (6.40)$$

and

$$\delta = 1.0 \times 10^5 \quad \text{Ns/m} \qquad (6.41)$$

that

$$\beta_j = \bar{\beta}_{j+1} = 20 \qquad (j=1,..,w-1) \qquad (6.42)$$

and

$$\gamma_j = \bar{\gamma}_{j+1} = 1 \qquad (j=1,..,w-1) \qquad (6.43)$$

and from (6.5) to (6.15) that, for the five vehicle train, the plant, input and output matrices assume the respective forms

$$A=\begin{bmatrix} 0 & 0 & 0 & 0 & -1 & 1 & 0 & 0 & 0 \\ 0 & 0 & 0 & 0 & 0 & -1 & 1 & 0 & 0 \\ 0 & 0 & 0 & 0 & 0 & 0 & -1 & 1 & 0 \\ 0 & 0 & 0 & 0 & 0 & 0 & 0 & -1 & 1 \\ 20 & 0 & 0 & 0 & -1 & 1 & 0 & 0 & 0 \\ -20 & 20 & 0 & 0 & 1 & -2 & 1 & 0 & 0 \\ 0 & -20 & 20 & 0 & 0 & 1 & -2 & 1 & 0 \\ 0 & 0 & -20 & 20 & 0 & 0 & 1 & -2 & 1 \\ 0 & 0 & 0 & -20 & 0 & 0 & 0 & 1 & -1 \end{bmatrix}, \qquad (6.44)$$

$$B = \begin{bmatrix} 0 & 0 & 0 & 0 & 0 & 0 & 0 & 0 & 1 \end{bmatrix}^1 \qquad (6.45)$$

and

$$C = \begin{bmatrix} 0 & 0 & 0 & 0 & 0 & 0 & 0 & 0 & 1 \end{bmatrix} \qquad (6.46)$$

and correspondingly similar forms for the ten and twenty vehicle trains when the state vector is as given by (6.3) and (6.4). Hence the transmission zeros of the three triples (A, B, C) for the five, ten and twenty vehicle trains can be found using (3.17) and are presented in table (6.1). The discrete-time domain equivalents of the transmission zeros and the remaining asymptotic closed-loop poles are presented in tables (6.2), (6.3) and (6.4) together with the closed loop poles for the five, ten and twenty vehicle trains when the fast-sampling controller given by (6.36) and (6.37) is utilized with

$$T = 0.1s,\ 0.01s \tag{6.47}$$

and

$$\rho = 0.05 . \tag{6.48}$$

Since all the closed-loop poles, for the sampling periods given by (6.47) , not only lie inside the unit disc but are also approaching the asymptotic closed-loop poles it follows that the control law equation

$$u(KT) = f\ \{\ e(KT) + 0.05\ z\ (KT)\} \tag{6.49}$$

$$(T = \frac{1}{f} = 0.1,\ 0.01)$$

will not only produce a stable closed-loop system but also give tight speed control of the five, ten and twenty vehicle trains.

Simulations of the five, ten and twenty vehicle trains controlled in accordance with (6.37) using T=0.1s, over a gradient profile illustrated by figure (6.3), produced the results given by figures (6.4) to (6.15) when the initial steady state conditions were assumed to be

$$q_i(0) = 0 \quad (i=1,..,w-1) \quad , \tag{6.50}$$

$$c_j(0) = 10 \text{ m/s} \quad (j=1,..,w), \tag{6.51}$$

$$y(0) = 10 \text{ m/s} \quad , \tag{6.52}$$

$$v(0) = 10 \text{ m/s} \quad , \tag{6.53}$$

$$u(0) = 0 \tag{6.54}$$

and

$$\theta_j(0) = 0 \quad (j=1,..,w). \tag{6.55}$$

TRANSMISSION ZEROS		
FIVE VEHICLE TRAIN	TEN VEHICLE TRAIN	TWENTY VEHICLE TRAIN
-0.06±i 1.55	-0.0136±i 0.739	-0.0032±i 0.36
-0.50±i 4.45	-0.121±i 2.19	-0.029±i 1.08
-1.17±i 6.75	-0.323±i 3.58	-0.080±i 1.79
-1.77±i 8.22	-0.598±i 4.86	-0.155±i 2.48
	-0.917±i 5.99	-0.251±i 3.15
	-1.246±i 6.95	-0.368±i 3.82
	-1.547±i 7.71	-0.500±i 4.45
	-1.79±i 8.27	-0.645±i 5.04
	-1.95±i 8.61	-0.800±i 5.60
		-0.96±i 6.12
		-1.12±i 6.60
		-1.28±i 7.04
		-1.43±i 7.42
		-1.57±i 7.76
		-1.69±i 8.05
		-1.80±i 8.29
		-1.89±i 8.48
		-1.95±i 8.61
		-1.99±i 8.69

TABLE 6.1

FIVE VEHICLE TRAIN			
ASYMPTOTIC CLOSED-LOOP POLES T=0.1S	CLOSED-LOOP POLES T=0.1S	ASYMPTOTIC CLOSED-LOOP POLES T=0.01S	CLOSED-LOOP POLES T=0.01S
0.0	-0.0138	0.0	-0.00416
0.995	0.9949	0.9995	0.9995
0.994±i 0.155	0.939±i 0.141	0.9994±i 0.0155	0.9989±i 0.0154
0.950±i 0.444	0.834±i 0.387	0.9950±i 0.0444	0.9937±i 0.0441
0.883±i 0.675	0.686±i 0.540	0.9883±i 0.0675	0.9859±i 0.0666
0.823±i 0.822	0.570±i 0.609	0.9823±i 0.0822	0.9791±i 0.0806

TABLE 6.2

TEN VEHICLE TRAIN			
ASYMPTOTIC CLOSED-LOOP POLES T=0.1S	CLOSED-LOOP POLES T=0.1S	ASYMPTOTIC CLOSED-LOOP POLES T=0.01S	CLOSED-LOOP POLES T=0.01S
0.0	-0.0138	0.0	-0.00416
0.995	0.99472	0.9995	0.9995
0.9986±i 0.074	0.9737±i 0.069	0.99986±i 0.0074	0.99963±i 0.0074
0.988±i 0.219	0.945±i 0.207	0.9988±i 0.0219	0.9984±i 0.0219
0.968±i 0.358	0.892±i 0.329	0.9968±i 0.0358	0.9960±i 0.0356
0.940±i 0.486	0.823±i 0.429	0.9940±i 0.0486	0.9927±i 0.0482
0.908±i 0.599	0.748±i 0.505	0.9908±i 0.0599	0.9890±i 0.0592
0.875±i 0.695	0.675±i 0.558	0.9875±i 0.0695	0.9852±i 0.0685
0.845±i 0.771	0.613±i 0.593	0.9845±i 0.0771	0.9817±i 0.0758
0.821±i 0.827	0.566±i 0.613	0.9821±i 0.0827	0.9789±i 0.0811
0.805±i 0.861	0.537±i 0.623	0.9805±i 0.0861	0.9771±i 0.0843

TABLE 6.3

TWENTY VEHICLE TRAIN			
ASYMPTOTIC CLOSED-LOOP POLES T=0.1S	CLOSED-LOOP POLES T=0.1S	ASYMPTOTIC CLOSED-LOOP POLES T=0.01S	CLOSED-LOOP POLES T=0.01S
0.0	-0.0138	0.0	-0.00416
0.995	0.9944	0.9995	0.99949
0.9997±i 0.036	0.988±i 0.034	0.99997±i 0.0036	0.99986±i 0.00358
0.997±i 0.108	0.981±i 0.105	0.9997±i 0.0108	0.9996±i 0.0108
0.992±i 0.179	0.966±i 0.173	0.9992±i 0.0179	0.9989±i 0.0178
0.985±i 0.248	0.945±i 0.238	0.9985±i 0.0248	0.9981±i 0.0248
0.975±i 0.316	0.919±i 0.298	0.9975±i 0.0316	0.9969±i 0.0315
0.963±i 0.382	0.888±i 0.354	0.9963±i 0.0382	0.9955±i 0.0380
0.950±i 0.445	0.853±i 0.404	0.9950±i 0.0445	0.9939±i 0.0442
0.936±i 0.504	0.816±i 0.447	0.9936±i 0.0504	0.9922±i 0.0500
0.920±i 0.560	0.779±i 0.485	0.9920±i 0.0560	0.9904±i 0.0555
0.904±i 0.612	0.741±i 0.517	0.9904±i 0.0612	0.9886±i 0.0606
0.888±i 0.660	0.704±i 0.544	0.9888±i 0.0660	0.9867±i 0.0652
0.872±i 0.704	0.670±i 0.566	0.9872±i 0.0704	0.9848±i 0.0694
0.857±i 0.742	0.638±i 0.583	0.9857±i 0.0742	0.9831±i 0.0731
0.843±i 0.776	0.609±i 0.600	0.9843±i 0.0776	0.9815±i 0.0763
0.831±i 0.805	0.585±i 0.607	0.9831±i 0.0805	0.9800±i 0.0791
0.820±i 0.829	0.564±i 0.615	0.9820±i 0.0829	0.9788±i 0.0813
0.811±i 0.848	0.548±i 0.620	0.9811±i 0.0848	0.9780±i 0.0831
0.805±i 0.861	0.536±i 0.624	0.9805±i 0.0861	0.9771±i 0.0843
0.801±i 0.869	0.529±i 0.626	0.9801±i 0.0869	0.9766±i 0.0851

TABLE 6.4

GRADIENT PROFILE AND POSITION OF THE FIRST VEHICLE AT K = O

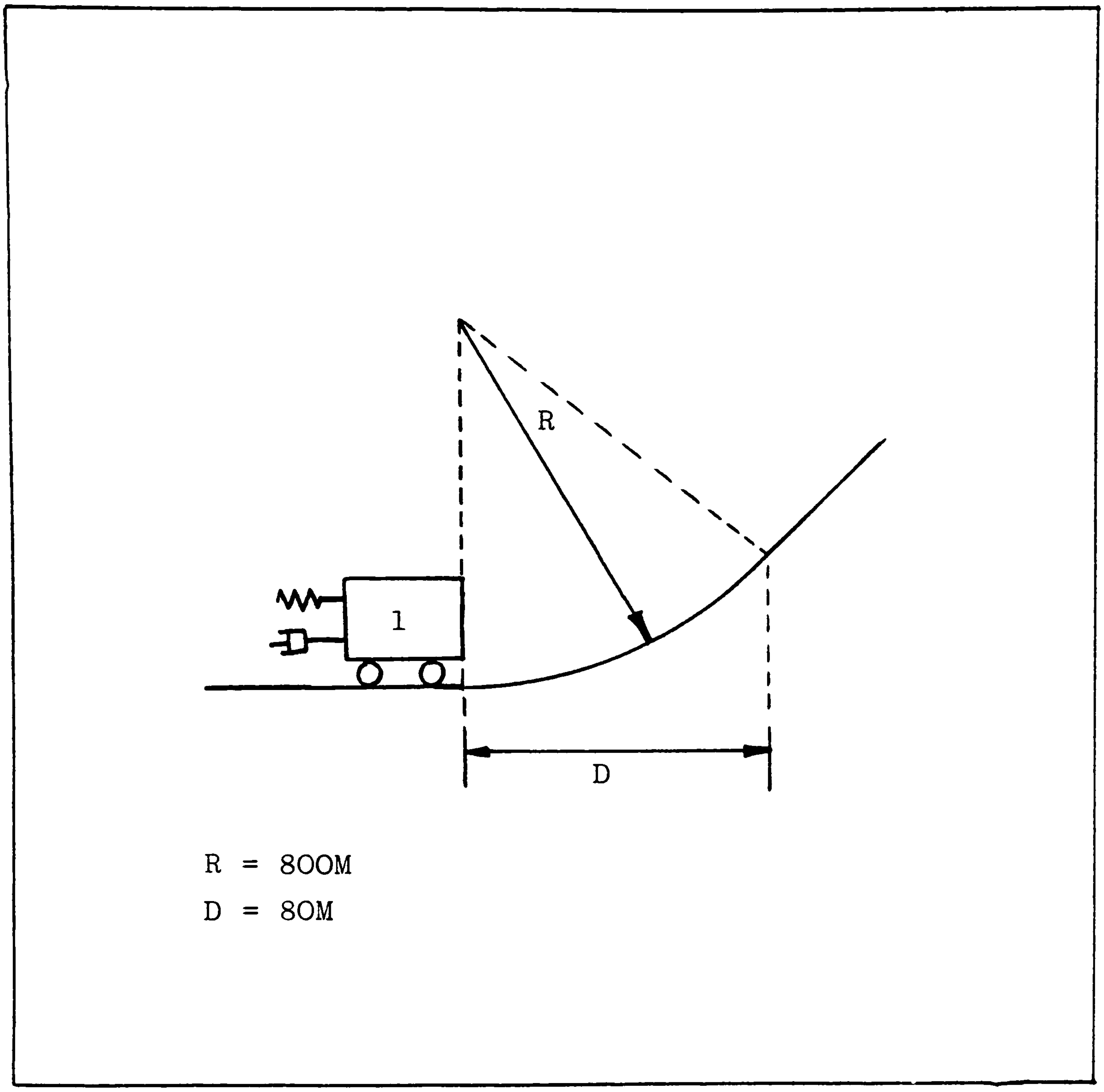

Figure 6.3.

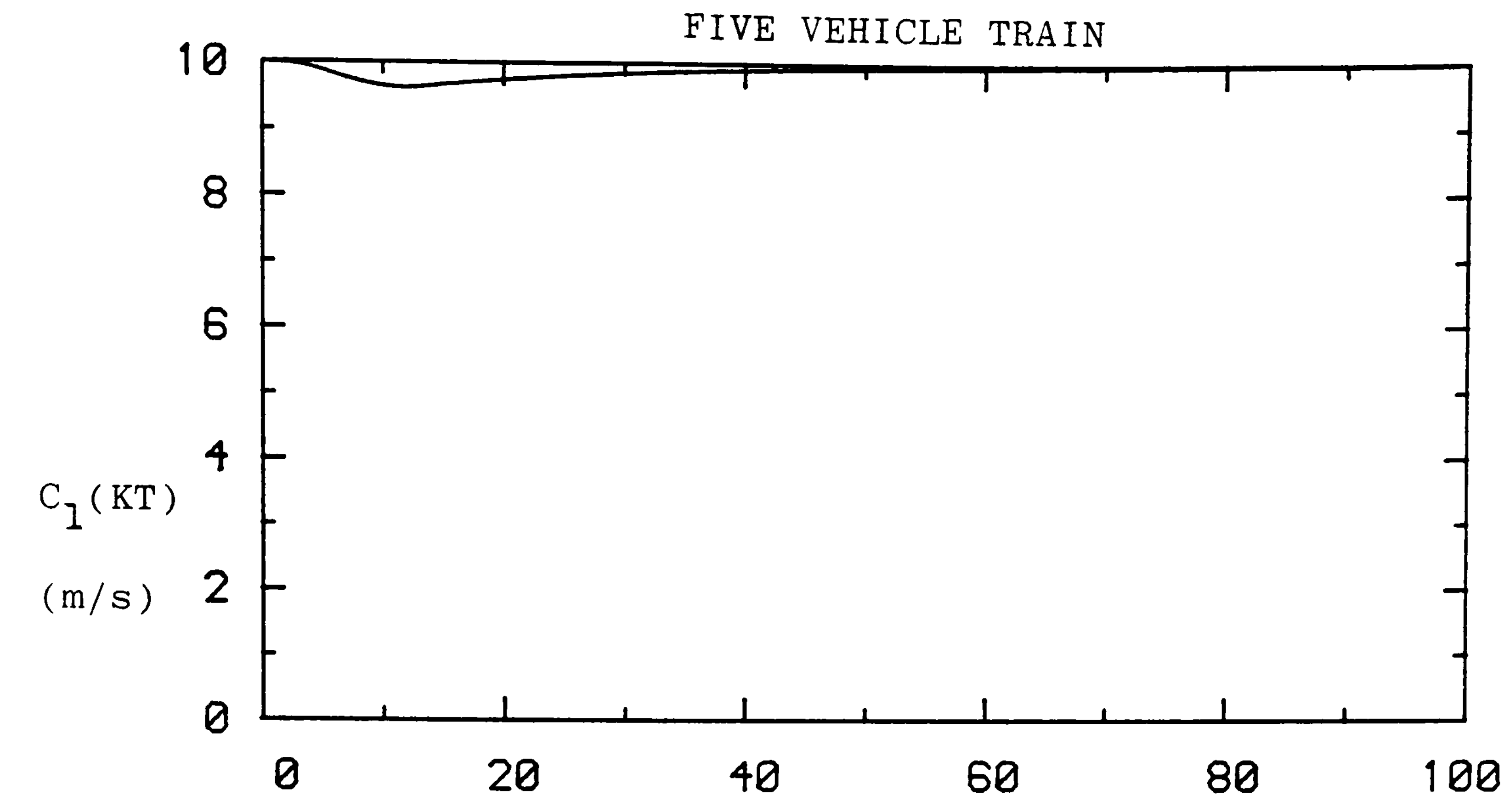

Figure 6.4

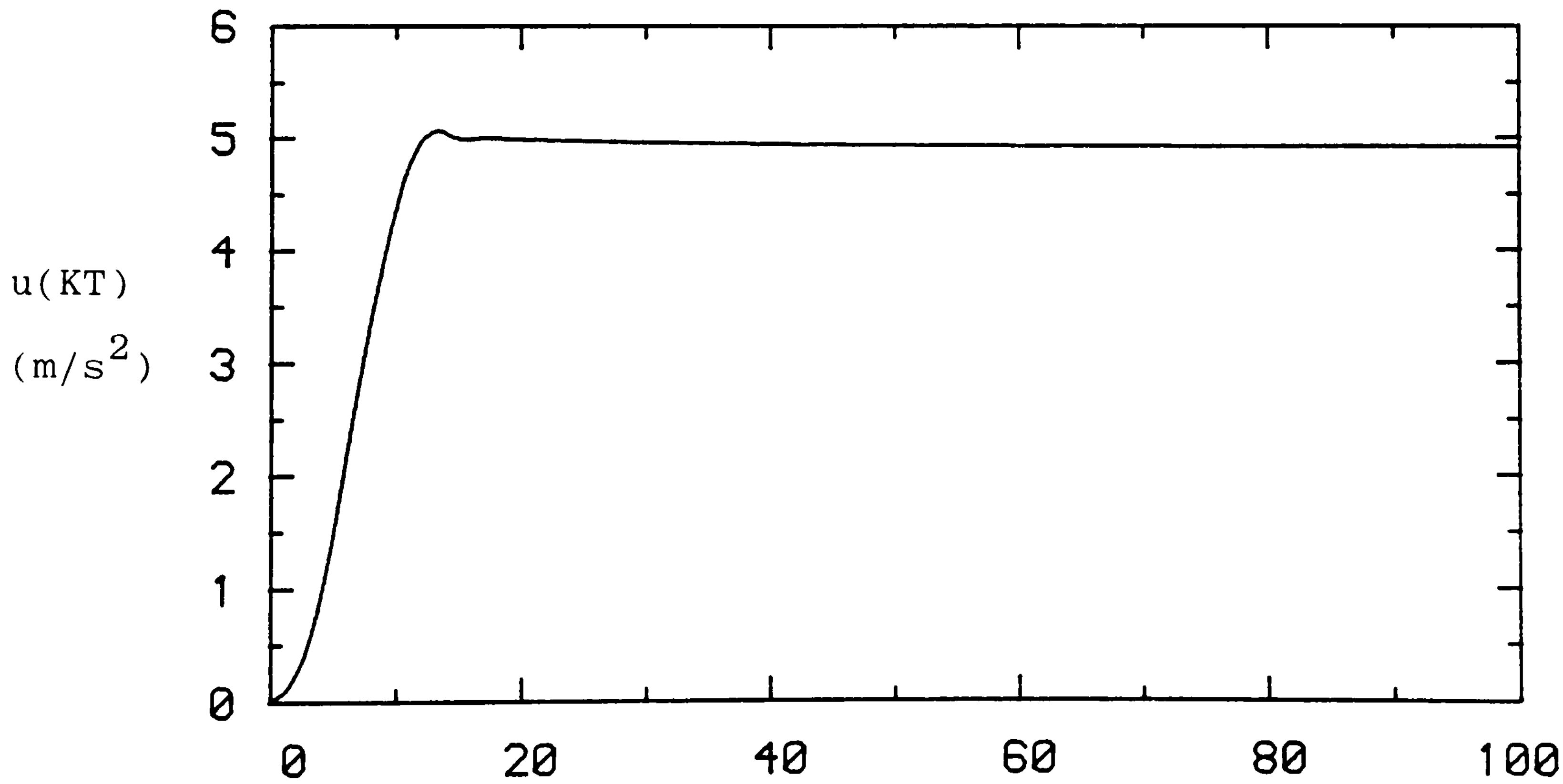

Figure 6.5

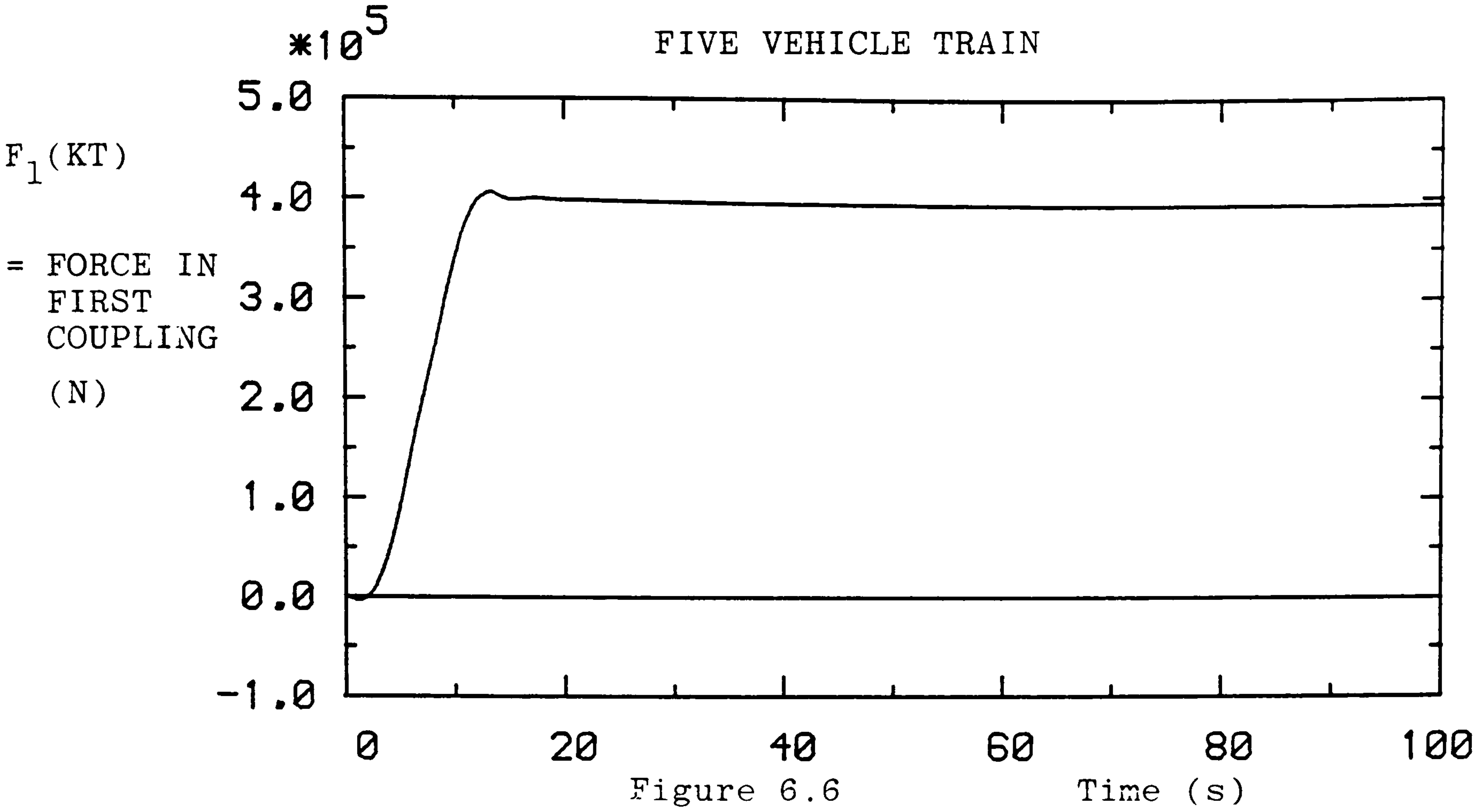

Figure 6.6

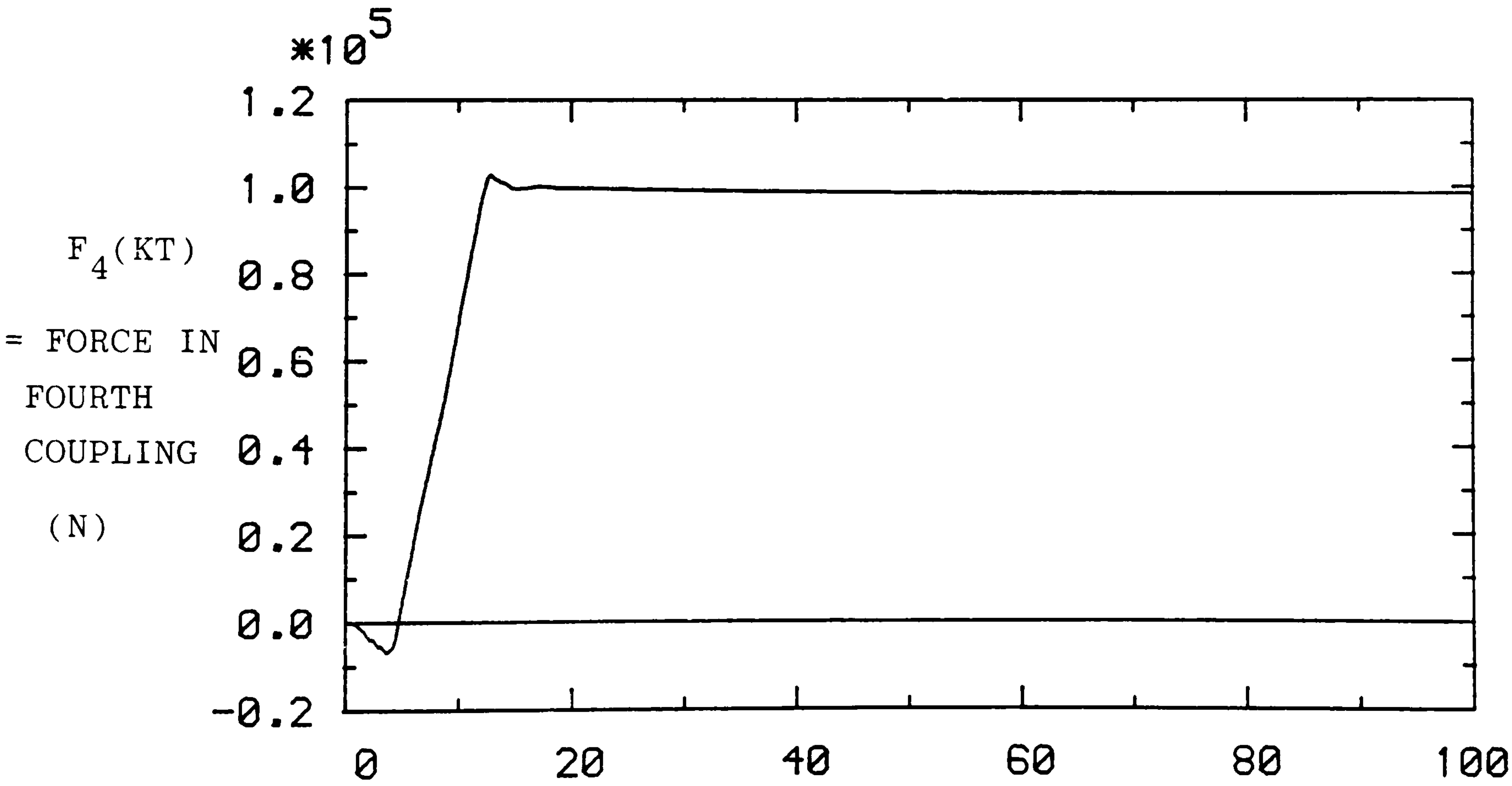

Figure 6.7

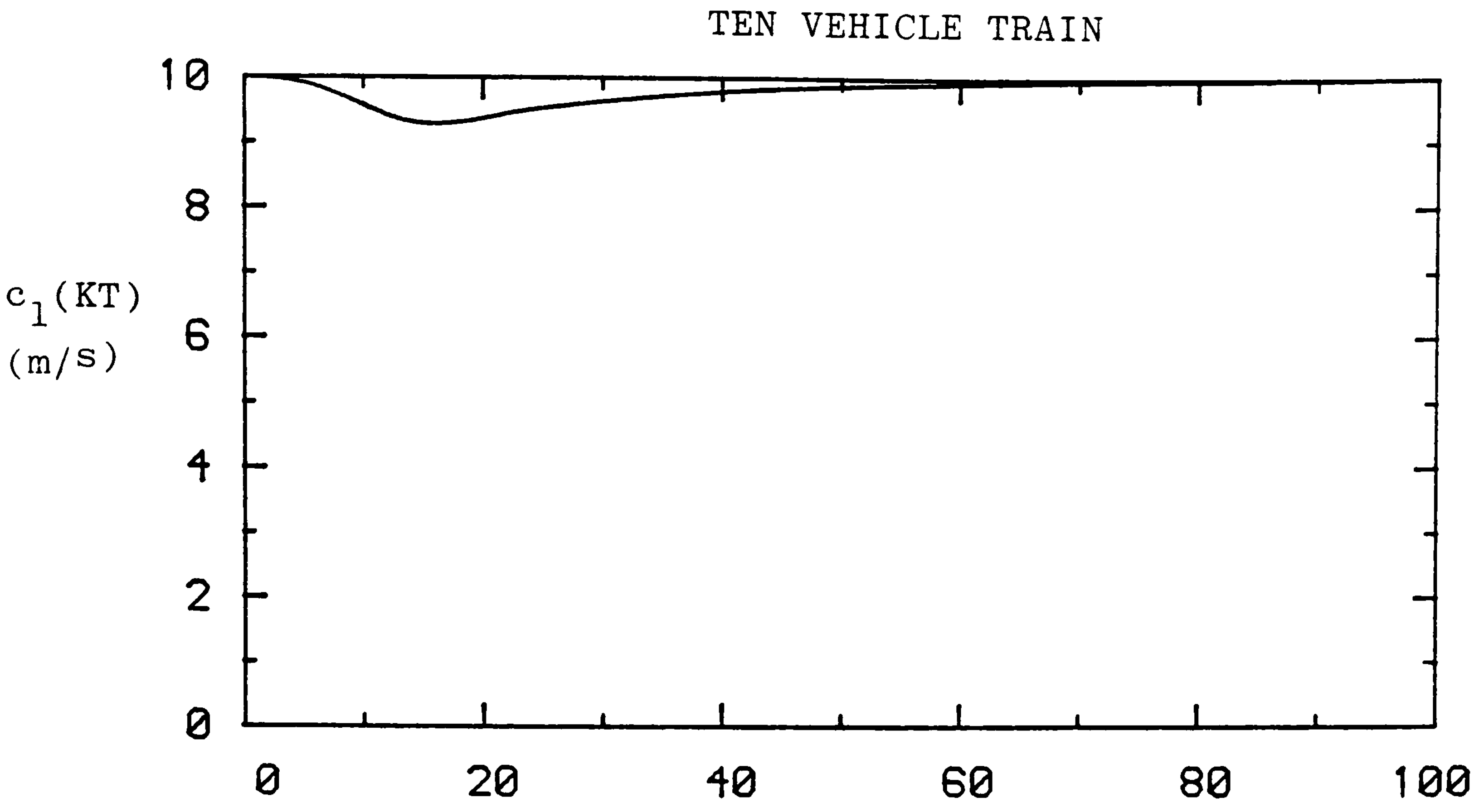

Figure 6.8

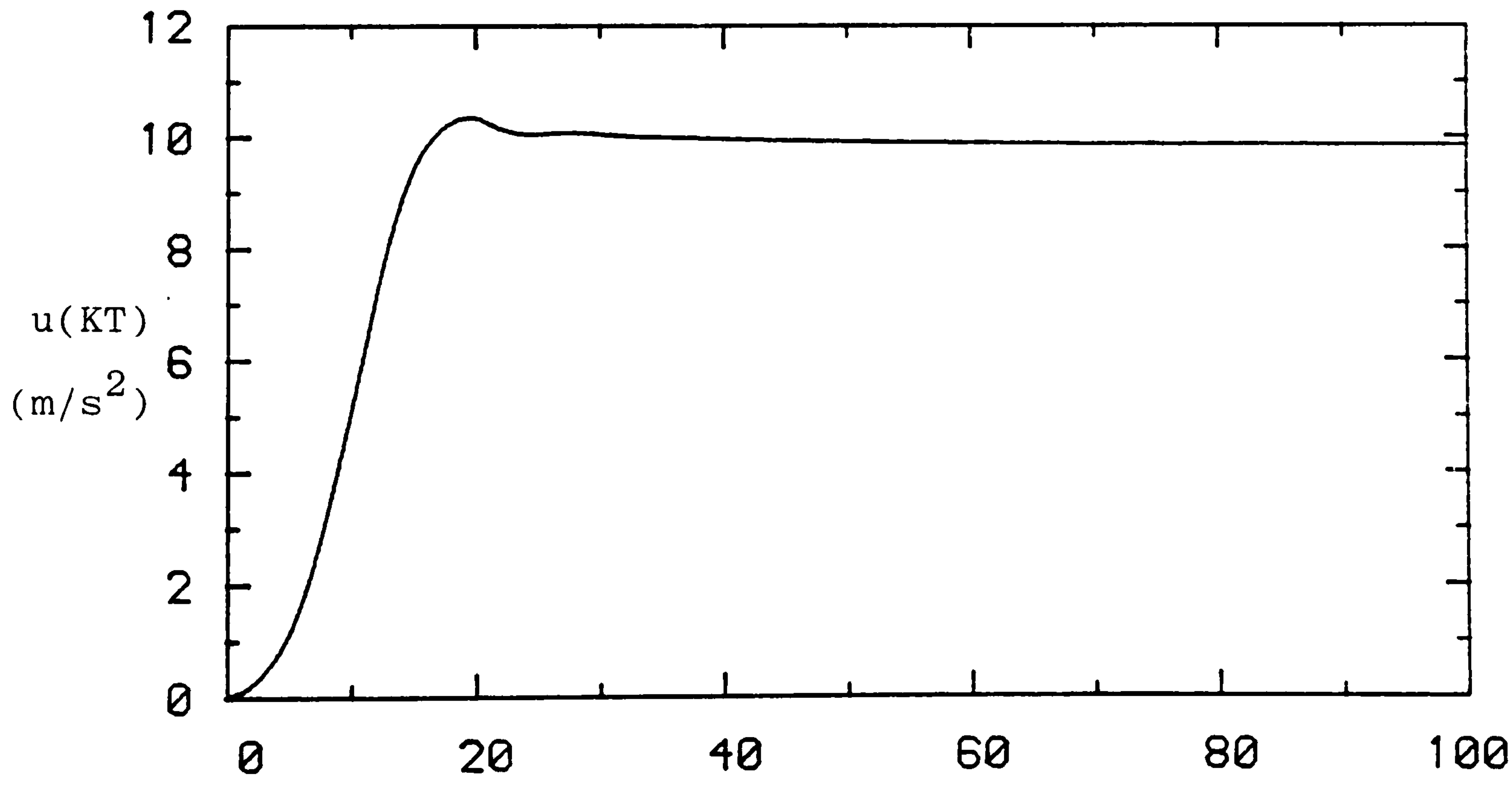

Figure 6.9

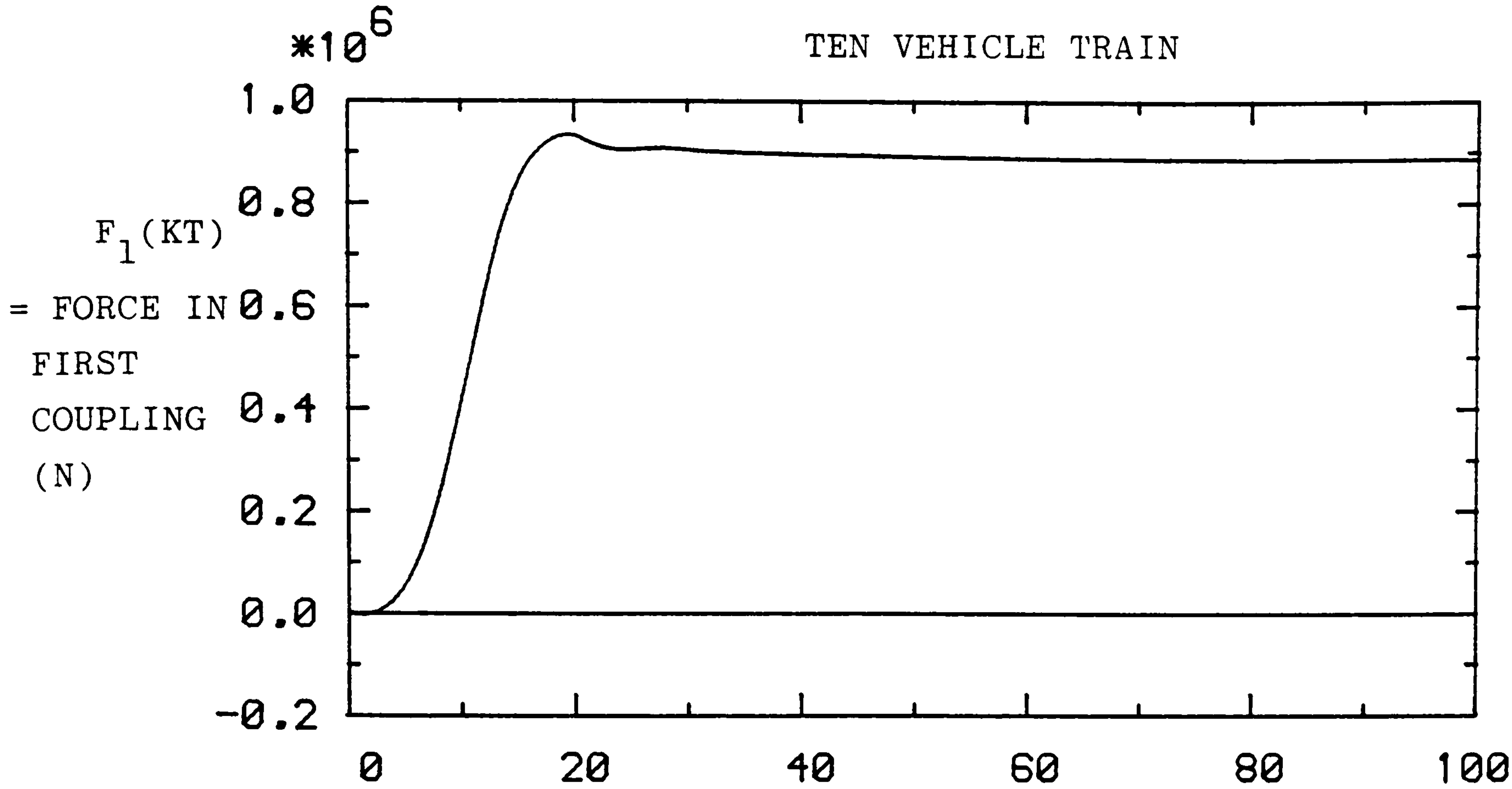

Figure 6.10

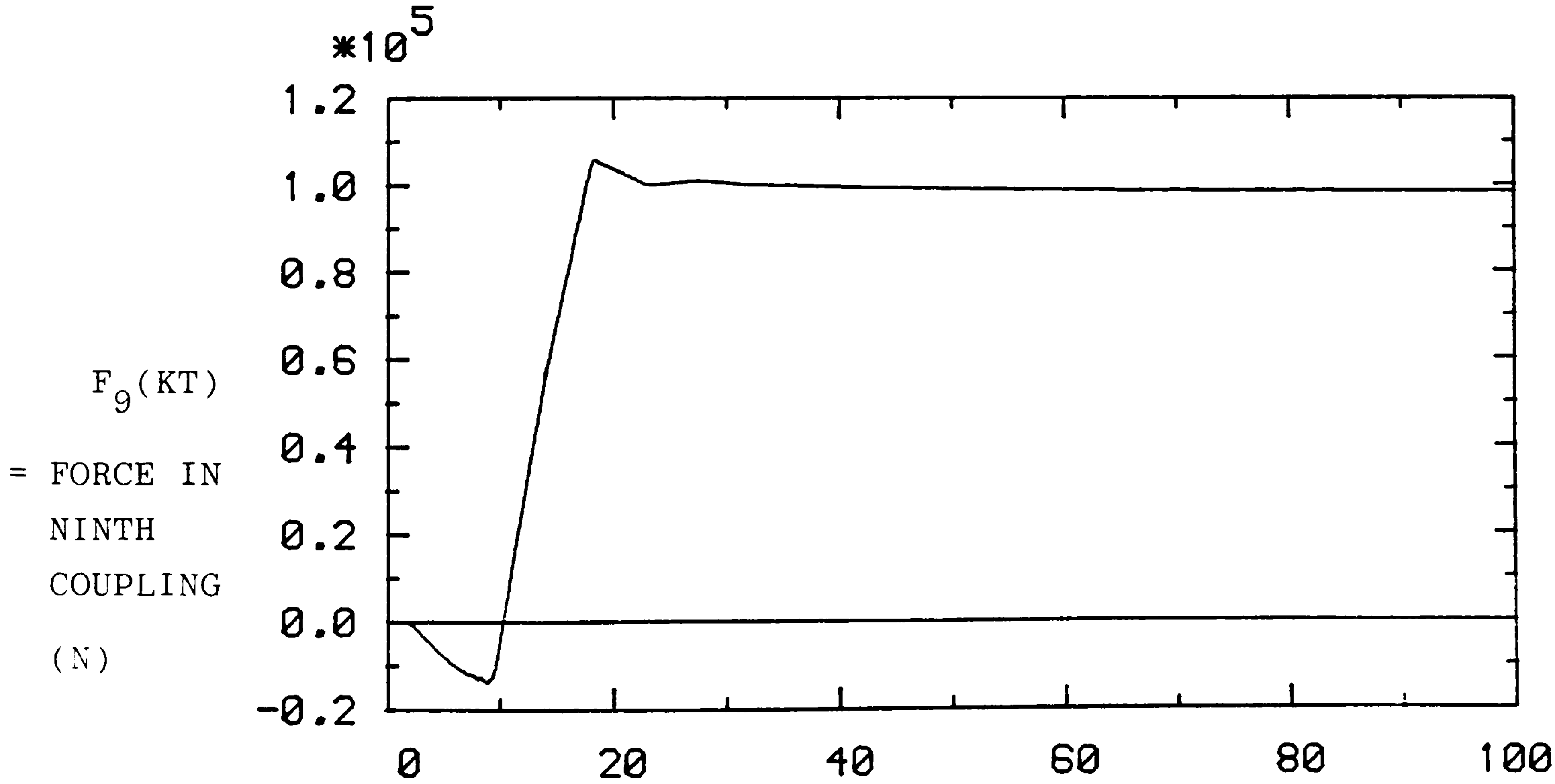

Figure 6.11

TWENTY VEHICLE TRAIN

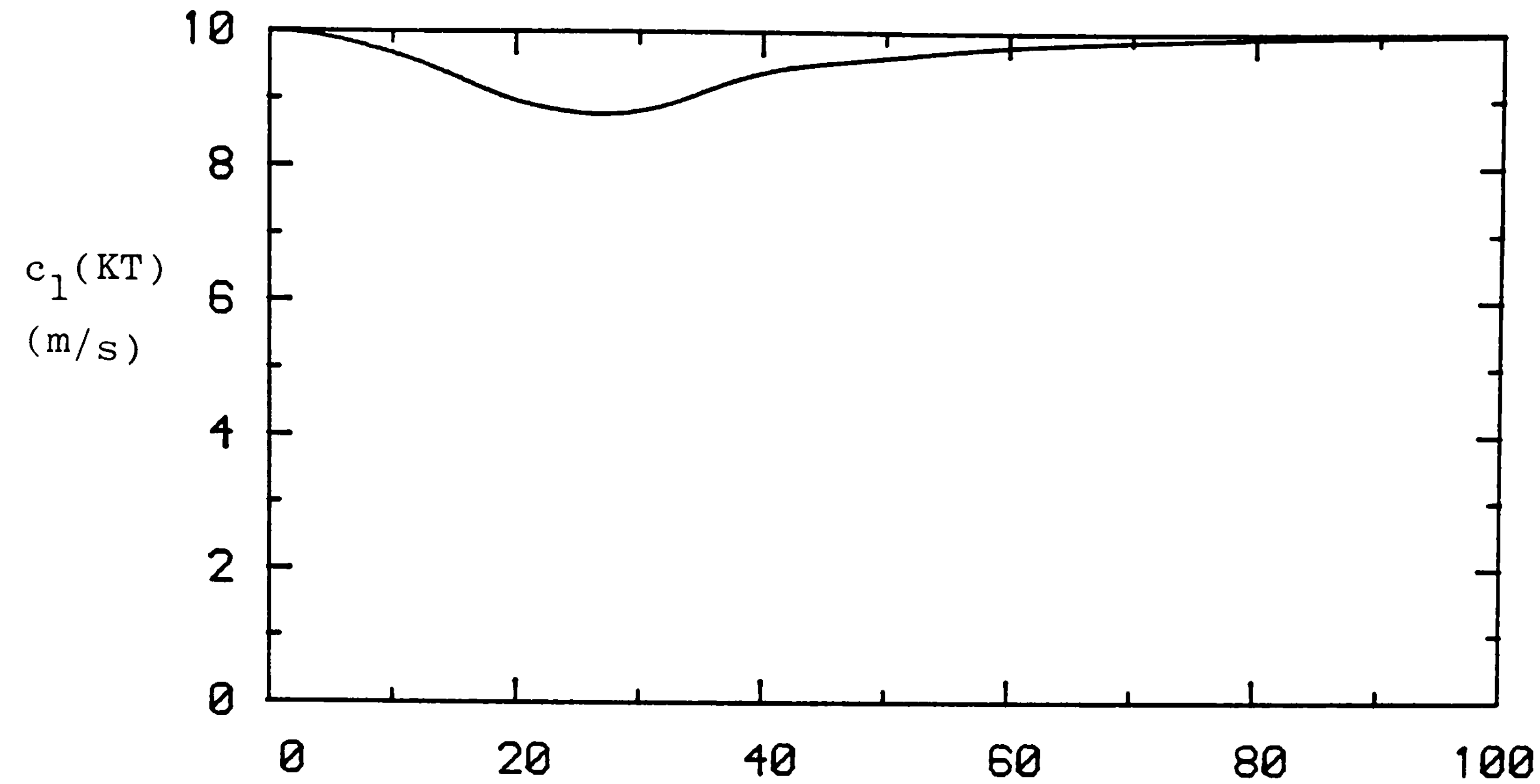

Figure 6.12

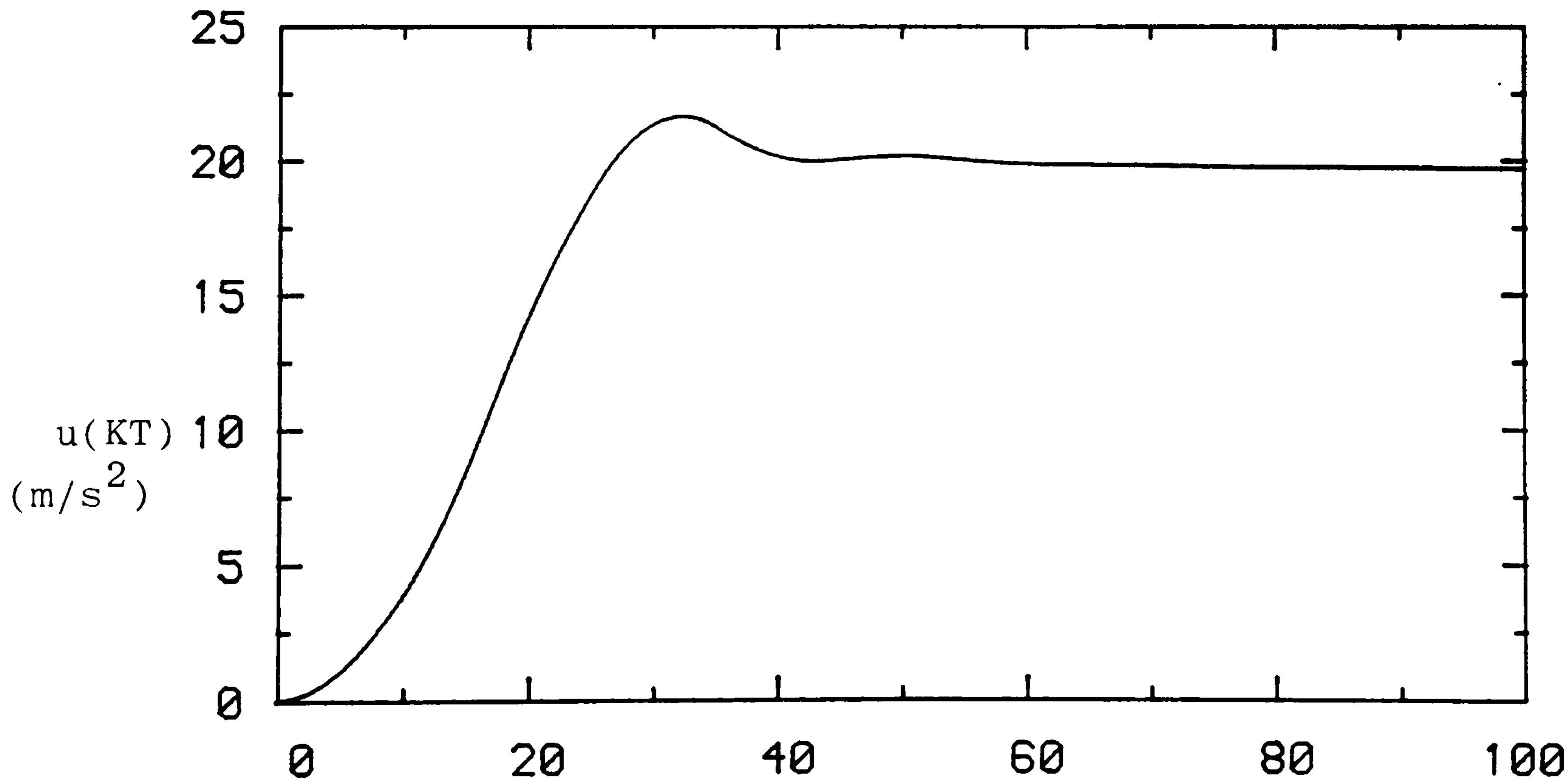

Figure 6.13

TWENTY VEHICLE TRAIN

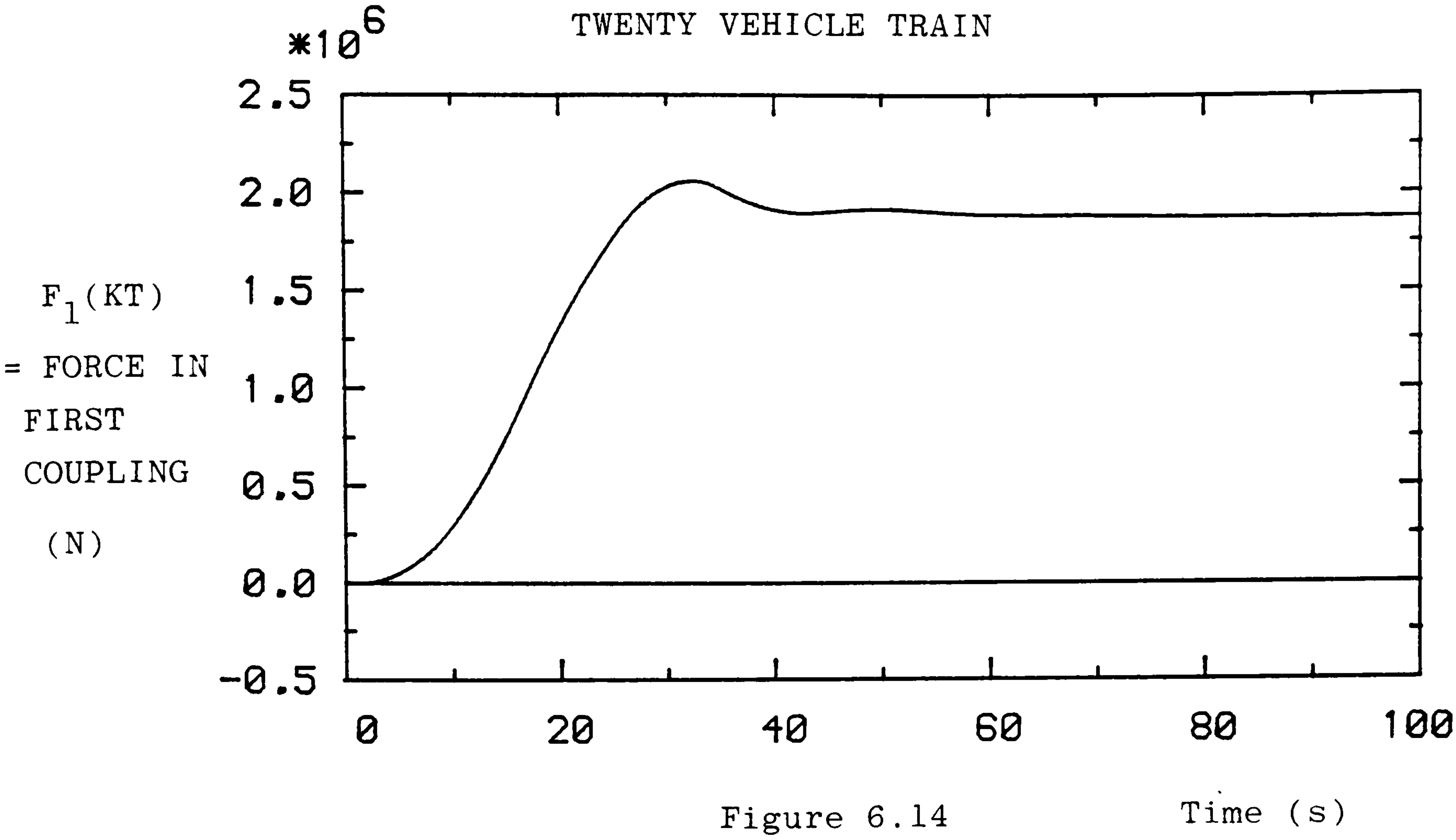

Figure 6.14

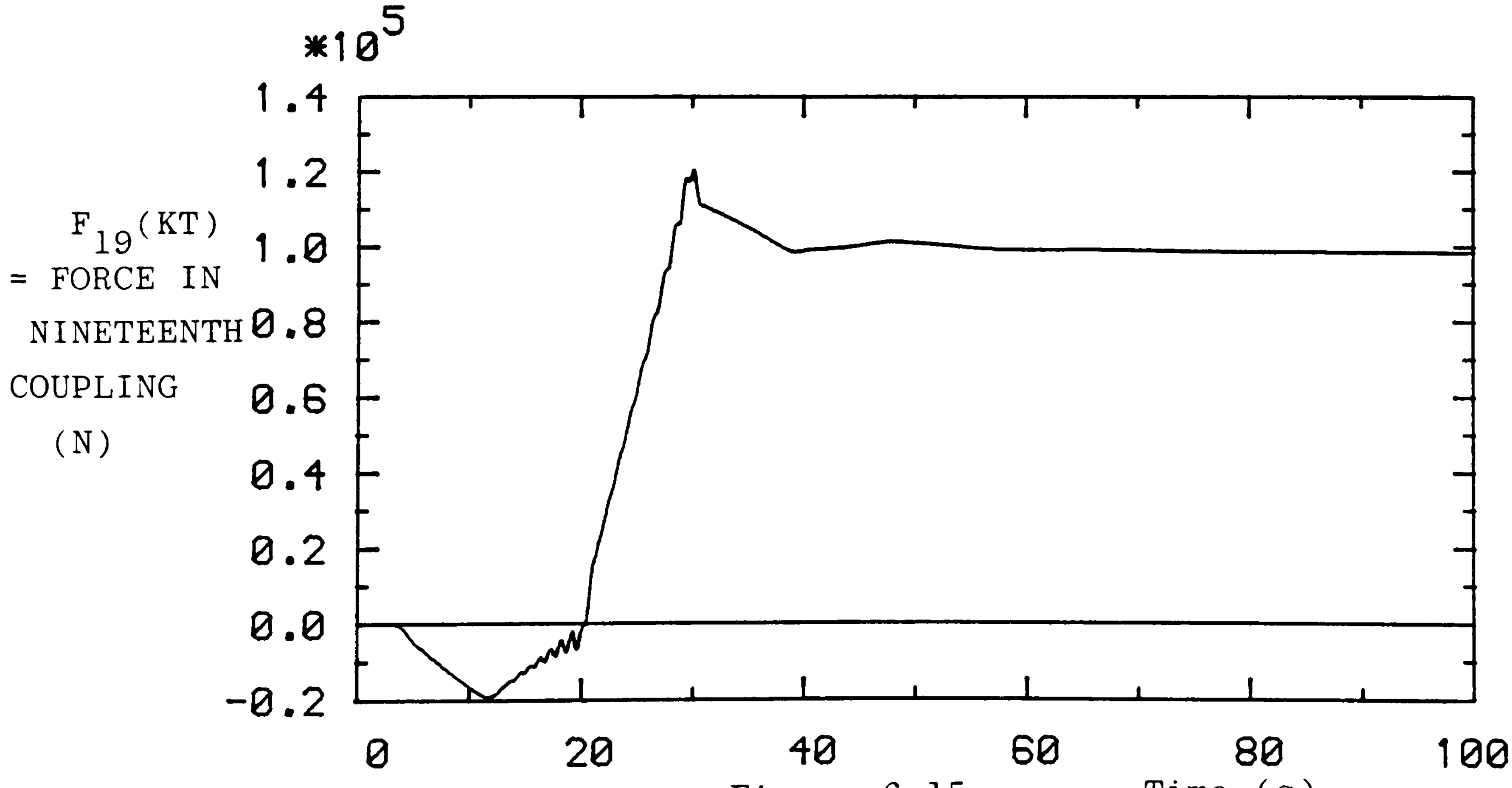

Figure 6.15

OPEN LOOP POLE (X) AND TRANSMISSION ZERO (O)
LOCATIONS FOR THE FIVE VEHICLE TRAIN

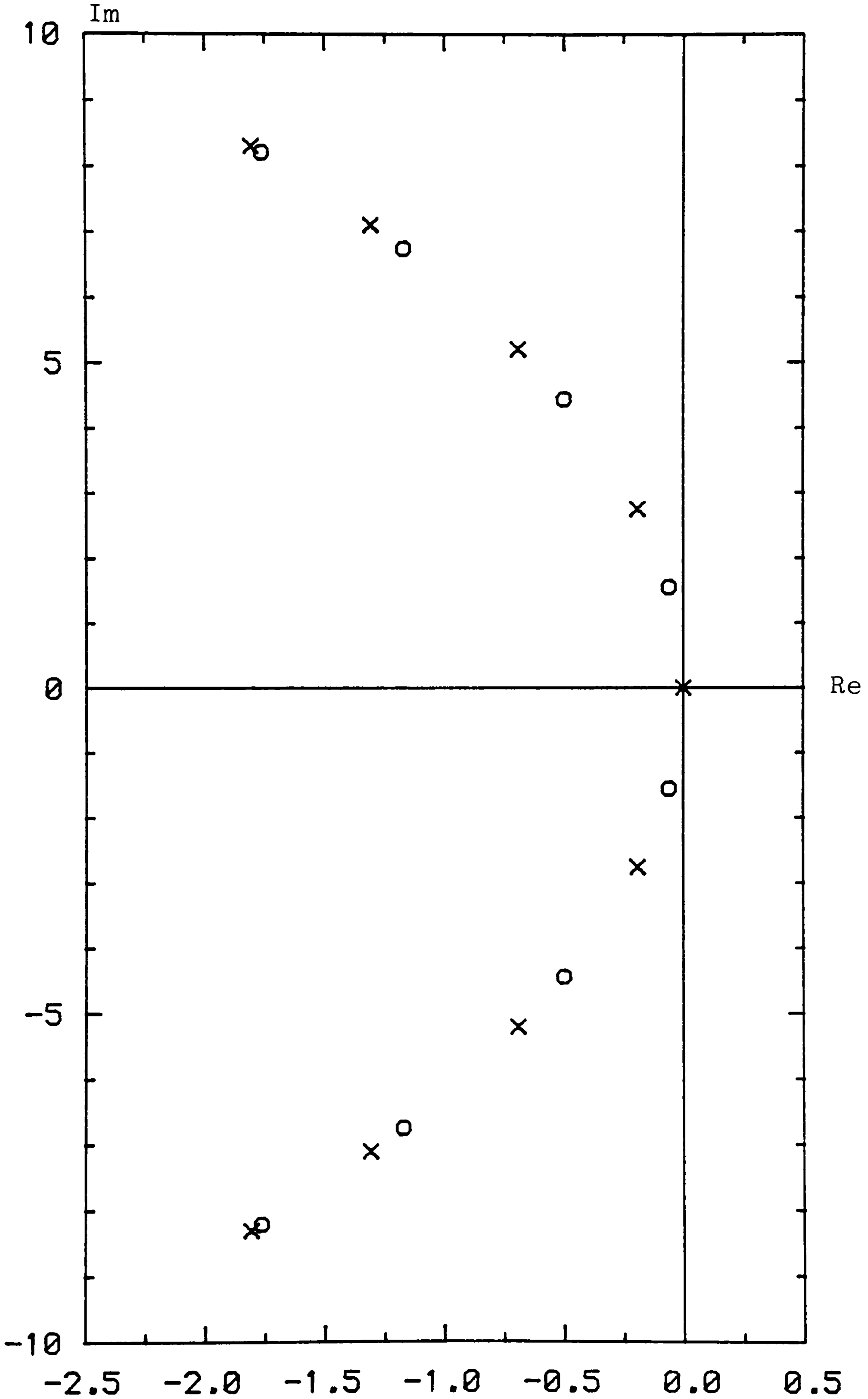

Figure 6.16

OPEN LOOP POLE (X) AND TRANSMISSION ZERO (O) LOCATIONS FOR THE TEN VEHICLE TRAIN

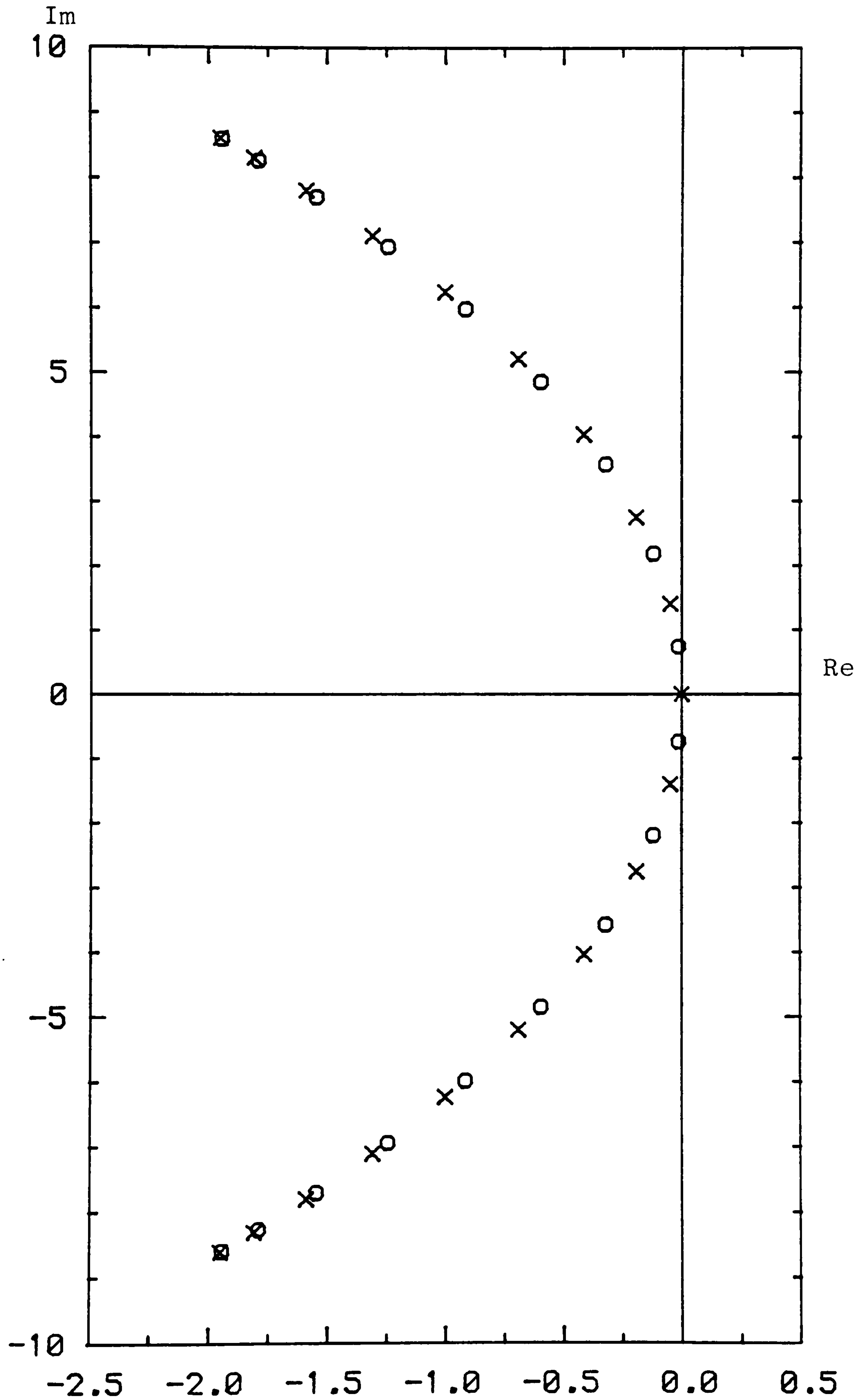

Figure 6.17

OPEN LOOP POLE (X) AND TRANSMISSION ZERO (O)
LOCATIONS FOR THE TWENTY VEHICLE TRAIN

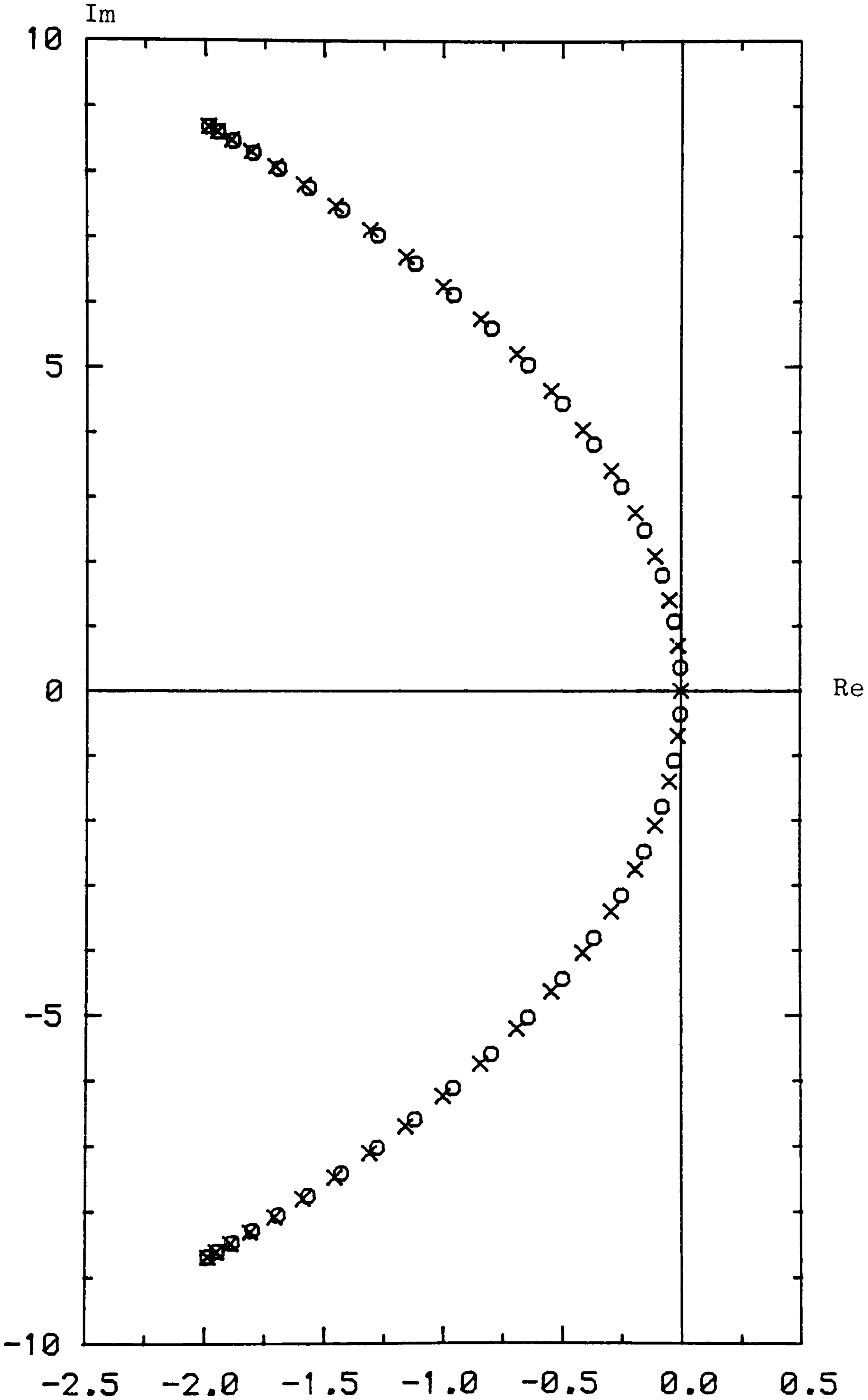

Figure 6.18

6.6 Discussion

The responses of the three trains given by (6.4) to (6.15) shows the same fast-sampling controller can successfully reject a disturbance due to a gradient change in each of the trains considered, whilst not producing excessive or oscillatory coupler forces. It is clear that stable fast-sampling controllers always exist since it was shown in section (6.3) that the sets of transmission zeros of trains having single leading locomotives always lie in the left half of the complex plane and are equivalent to the sets of open-loop poles of the same trains when the locomotives become fixed rigid bodies. It was also shown in section (6.3) for uniform trains with the same stiffness and damping coefficients that the sets of open-loop poles and the sets of transmission zeros lie on the same curve with the same bounds (as $w \to \infty$) and are increasingly closer together away from the imaginary axis, as illustrated by figures (6.16) to (6.18) for the three uniform trains considered in this chapter. Since as the sampling frequency increases the root loci move from the open-loop poles to the closest transmission zeros, and the 'rigid-body pole' approaches the 'fast closed-loop zero' it is clear how the same controller is able to cope with

all three trains and produce good performance.
This is a very important factor in the choice of automatic controllers because any automatic train controller must be insensitive to variations in train lengths to be useful for day to day operation. The fast-sampling controller presented in this chapter not only satisfies this important criterion but also has good disturbance rejection properties , good tracking properties and is also insensitive to variations of the plant parameters.

CHAPTER 7

MULTI-LOCOMOTIVE POWERED TRAINS

7.1 Introduction

In this chapter trains with a single leading locomotive and a second locomotive as the pth vehicle are considered. It is shown that such trains belong to the class of systems considered in sections (2.4) and (2.5) when the outputs are taken as the speeds of the leading locomotives and the forces in the (p-1)th couplings. A fast-sampling decentralized controller is developed in section (7.5) for the w-vehicle train model developed in section (7.2). This is an ideal decentralized controller since it produces increasingly non-interactive control of the outputs as the sampling frequency increases. Furthermore the control algorithm is simple and effectively controls trains of different lengths. The results of digital computer simulations of three trains (w=10,20 and 40) travelling over a gradient change are presented in section (7.6) together with the closed-loop poles and asymptotic closed-loop poles. The results presented in section (7.6) are discussed in section (7.7). A review of the literature on freight trains and the control of freight trains is made in section (7.4). The fast-sampling control of a one-hundred vehicle train is considered in section (7.8) and the results of digital computer simulations presented for the case where it travels over undulating terrain. Finally in section (7.9) the conclusions to the chapter are presented.

7.2 Mathematical Model

A linear mathematical model of the w-vehicle trains illustrated by figure (7.1) is developed in this section, for the case where the first and the pth vehicles are locomotives. It is assumed that the vehicles are moving with velocities $c_i(t)$ (i=1,..,w) and have masses m_i (i=1,..,w) and are connected by couplings that can be represented by linear springs of stiffnesses K_j (j=1,..,w-1) and linear dashpots of damping coefficients δ_j (j=1,..,w-1) and where the extensions of the couplings from the free lengths are $q_j(t)$ (j=1,..,w-1). It is further assumed

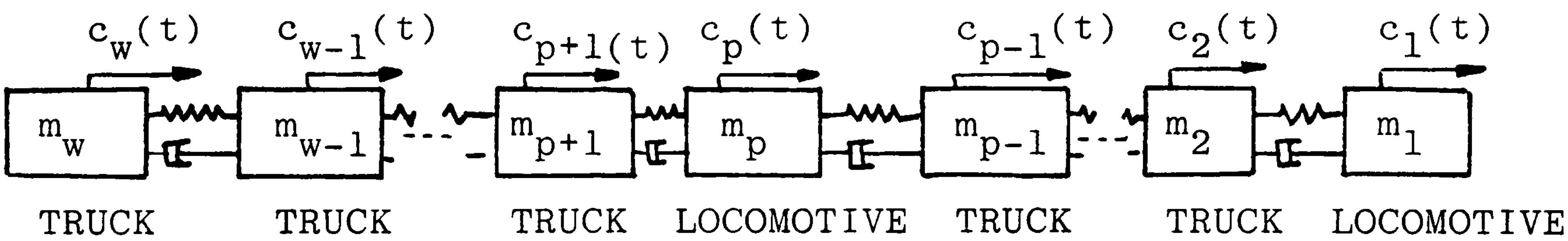

Figure 7.1

that the trains have negligible resistance to motion and the disturbances take the form of gradient changes and that the outputs are the absolute speed of the first locomotive and the force in the (p-1)th coupling. It follows that the state and output equations can be expressed in the matrix forms given by (6.1) and (6.2) respectively, where

$$x_1(t) = \Big[q_{w-1}(t), q_{w-2}(t), \ldots\ldots, q_{p+1}(t), q_p(t), q_{p-1}(t), q_{p-2}(t), \ldots\ldots, q_2(t), q_1(t), c_w(t), c_{w-1}(t), c_{w-2}(t), \ldots \ldots, c_{p+2}(t), c_{p+1}(t), c_{p-1}(t), c_{p-2}(t), \ldots, c_3(t), c_2(t)\Big]', \tag{7.1}$$

$$x_2(t) = \Big[c_1(t),\ c_p(t)\Big]' , \tag{7.2}$$

$$B = I_2 , \tag{7.3}$$

$$C_1 = \begin{bmatrix} 0 & 0 & \ldots & 0 & 0 & 0 & 0 & \ldots & 0 & 0 & 0 & 0 & 0 & \ldots & \ldots & 0 & 0 & 0 & 0 & \ldots & 0 & 0 \\ 0 & 0 & \ldots & 0 & 0 & K_{p-1} & 0 & \ldots & 0 & 0 & 0 & 0 & 0 & \ldots & \ldots & 0 & 0 & \delta_{p-1} & 0 & \ldots & 0 & 0 \end{bmatrix}, \tag{7.4}$$

$$C_2 = \begin{bmatrix} 1 & 0 \\ 0 & -\delta_{p-1} \end{bmatrix}, \tag{7.5}$$

$$A_{11} = \begin{bmatrix} A_1 & A_2 \\ A_3 & A_4 \end{bmatrix}, \tag{7.6}$$

$$A_1 = 0 \in R^{(w-1)x(w-1)} ,$$

$$A_2 = \begin{bmatrix} -1, & 1, & 0, & \ldots\ldots, & 0, & 0, & 0, & 0, & \ldots, & 0, & 0 \\ 0, & -1, & 1, & \ldots\ldots, & 0, & 0, & 0, & 0, & \ldots, & 0, & 0 \\ \hdashline 0, & 0, & 0, & \ldots\ldots, & -1, & 1, & 0, & 0, & \ldots\ldots, & 0, & 0 \\ 0, & 0, & 0, & \ldots\ldots, & 0, & -1, & 0, & 0, & \ldots\ldots, & 0, & 0 \\ 0, & 0, & 0, & \ldots\ldots, & 0, & 0, & 1, & 0, & \ldots\ldots, & 0, & 0 \\ 0, & 0, & 0, & \ldots\ldots, & 0, & 0, & -1, & 1, & \ldots\ldots, & 0, & 0 \\ \hdashline 0, & 0, & 0, & \ldots\ldots, & 0, & 0, & 0, & 0, & \ldots\ldots & -1, & 0 \\ 0, & 0, & 0, & \ldots\ldots, & 0, & 0, & 0, & 0, & \ldots\ldots & 0, & -1 \end{bmatrix} \in R^{(w-1)x(w-2)}$$

$$A_3 = \left[\begin{array}{l}
\beta_w\,,\ 0,\ \ldots\ldots,\ 0,\ 0,\ 0,\ 0,\ \ldots,\ 0,\ 0 \\
-\beta_{w-1}\cdot\beta_{w-1},\ \ldots\ldots,\ 0,\ 0,\ 0,\ 0,\ \ldots,\ 0,\ 0 \\
0,\ ,-\beta_{w-2}\cdot\ \ldots\ldots,\ 0,\ 0,\ 0,\ 0,\ \ldots,\ 0,\ 0 \\
\hline
0.\ 0,\ \ldots\ldots,\beta_{p+2},\ 0,\ 0,\ 0,\ \ldots\ldots\ 0,\ 0, \\
0,\ 0,\ \ldots\ldots,-\beta_{p+1},\beta_{p+1},\ 0.\ 0,\ \ldots\ldots\ 0,\ 0, \\
0,\ 0,\ \ldots\ldots,\ 0,\ 0\,,\ -\beta_{p-1},\beta_{p-1},\ldots\ 0,\ 0, \\
\hline
0,\ 0,\ \ldots\ldots,\ 0,\ 0,\ 0,\ 0\,,\ \ldots,\ \beta_3,\ 0 \\
0,\ 0,\ \ldots\ldots,0,\ 0,\ 0,\ 0,\ \ldots\ldots,\ \beta_2,\ \beta_2
\end{array}\right]$$

$\varepsilon\ R^{(w-2)x(w-1)}$,

$$A_4 = \left[\begin{array}{l}
-\gamma_w,\ \gamma_w,\ 0,\ \ldots\ldots\ 0,0,0,0,\ldots\ldots,\ 0,\ 0 \\
-\gamma_{w-1},-(\gamma_{w-1}+\gamma_{w-1}),\gamma_{w-1},\ldots,\ 0,0,0,0,\ldots\ldots,\ 0,\ 0 \\
0\ \ \gamma_{w-2},\ -(\gamma_{w-2}+\gamma_{w-2}),\ldots,0,0,0,0,\ldots\ldots,\ 0,\ 0 \\
\hline
0,\ 0\ ,0,\ldots,-(\gamma_{p+2}+\gamma_{p+2}),\gamma_{p+2},\ 0,\ 0,\ \ 0,\ 0 \\
0,\ 0,\ 0,\ldots,\ \gamma_{p+1},-(\gamma_{p+1}+\gamma_{p+1}),0,\ 0,\ \ 0,\ 0 \\
0,\ 0,\ 0,\ldots,\ 0,\ 0,\ -(\gamma_{p-1}+\gamma_{p-1}),\ 0,\ \ldots\ldots\ 0,\ 0 \\
0,\ 0,\ 0,\ldots,\ 0,\ 0,\ \gamma_{p-2},\ -(\gamma_{p-2}+\gamma_{p-2}),\ \ldots\ 0,\ 0 \\
\hline
0,\ 0,\ 0,\ \ldots\ldots\ 0,\ 0,\ 0,\ 0,\ \ldots-(\gamma_3+\gamma_3),\ \gamma_3 \\
0,\ 0,\ 0,\ \ldots\ldots\ 0,\ 0,\ 0,\ 0,\ \ldots\ \gamma_2,\ -(\gamma_2+\gamma_2)
\end{array}\right]$$

$\varepsilon\ R^{(w-2)x(w-2)}$

$$A_{12} = \begin{bmatrix} 0 & 0 & \ldots & 0 & 1 & -1 & 0 & \ldots & 0 & 0 & 0 & 0 & 0 & \ldots & 0 & \bar{\gamma}_{p+1} & \gamma_{p-1} & 0 & \ldots & 0 & 0 \\ 0 & 0 & \ldots & 0 & 0 & 0 & 0 & \ldots & 0 & 1 & 0 & 0 & 0 & \ldots & 0 & 0 & 0 & 0 & \ldots & 0 & \bar{\gamma}_2 \end{bmatrix}' , \qquad (7.7)$$

$$A_{21} = \begin{bmatrix} 0 \ldots & 0 & 0 & 0 & 0 & 0 & 0 \ldots 0 & -\beta_1 & 0 & 0 & 0 & \ldots & 0 & 0 & 0 & 0 & \ldots & 0 & \gamma_1 \\ 0 \ldots & 0 & 0 & -\beta_p & \bar{\beta}_p & 0 & 0 \ldots 0 & 0 & 0 & 0 & 0 & \ldots & 0 & \gamma_p & \bar{\gamma}_p & 0 & \ldots & 0 & 0 \end{bmatrix} \qquad (7.8)$$

$$A_{22} = \begin{bmatrix} -\gamma_1 & 0 \\ 0 & -(\gamma_p + \bar{\gamma}_p) \end{bmatrix} , \qquad (7.9)$$

$$D_1 = \begin{bmatrix} 0 & 0 \\ I_{w-2} & 0 \end{bmatrix} , \qquad (7.10)$$

$$D_2 = \begin{bmatrix} 0 & I_2 \end{bmatrix} , \qquad (7.11)$$

$$d(t) = \Big[-g\sin\theta_w(t), \ldots, -g\sin\theta_{p+1}(t), -g\sin\theta_{p-1}(t), \ldots \ldots -g\sin\theta_2(t), -g\sin\theta_1(t), -g\sin\theta_p(t) \Big]' , \qquad (7.12)$$

$$u(t) = \begin{bmatrix} F_1(t) / m_1 \\ F_p(t)/m_p \end{bmatrix} , \qquad (7.13)$$

$x_1(t) \in R^{2w-3}$, $x_2(t) \in R^2$, $A_{11} \in R^{(2w-3)x(2w-3)}$

$A_{12} \in R^{(2w-3)x2}$, $A_{21} \in R^{2x(2w-3)}$, $A_{22} \in R^{2x2}$,

$D_1 \in R^{(2w-3)xw}$, $D_2 \in R^{2xw}$, $d(t) \in R^w$, $u(t) \in R^2$,

$C_1 \in R^{2x(2w-3)}$, $C_2 \in R^{2x2}$. $B \in R^{2x2}$, β_j, $\bar{\beta}_{j+1}$,

γ_j and $\bar{\gamma}_{j+1}$ (j=1,..,w-1) are given by (6.9) to (6.12), n is given by (6.20), $F_1(t)$ and $F_p(t)$ are the tractive forces of the two locomotives and $\theta_i(t)$ (i=1,..,w) are the gradients of the terrain beneath the respective vehicles.

It can be shown that the two locomotive powered trains are controllable and observable when the outputs are the speed of the first vehicle and the force in the coupler in front of the second locomotive, as considered above.

7.3 Transmission Zeros of Trains with Two Locomotives

It will be shown in this section that trains having locomotives as the first and pth vehicles belong to the class of systems considered in section (2.4) when the outputs are taken as the speeds of the first locomotives and the forces in the (p-1)th couplings.

It is clear that (2.56) is satisfied, since it follows from (7.3) and (7.5) that

$$\text{rank } (C_2 B) = 2 = \ell \qquad (7.14)$$

and as a result (3.17) can be used to calculate the transmission zeros. It follows from (3.17) that the transmission zeros are the eigenvalues of the matrix $(A_{11}-A_{12}C_2^{-1}C_1)$. Using the transformation matrix

$$T_1 = \begin{bmatrix} I_{w-p} & 0 & 0 & 0 \\ 0 & 0 & I_{w-p} & 0 \\ 0 & I_{p-1} & 0 & 0 \\ 0 & 0 & 0 & I_{p-2} \end{bmatrix} \in R^{(2w-3)x(2w-3)} \qquad (7.15)$$

and (7.4) to (7.7) produces the new matrix

$$T_1(A_{11}-A_{12}\ C_2^{-1}C_1)T_1^{-1} = \begin{bmatrix} A_a & A_b & A_c \\ 0 & \frac{-K_{p-1}}{\delta_{p-1}} & 0 \\ 0 & 0 & A_d \end{bmatrix}$$

$$= A_T \;\varepsilon\; R^{(2w-3)x(2w-3)}, \qquad (7.15)$$

where

$$
A_a = \left[\begin{array}{ccccc|cccccc}
0 & \cdots & \cdots & \cdots & 0 & -1 & 1 & 0 & 0 & \cdots & 0 \quad 0 \\
\vdots & & & & \vdots & 0 & -1 & 1 & 0 & & \vdots \\
\vdots & & & & \vdots & \vdots & & \ddots & \ddots & & 0 \\
\vdots & & & & \vdots & \vdots & & & & -1 & 1 \\
0 & 0 & \cdots & \cdots & 0 & 0 & \cdots & \cdots & \cdots & 0 & -1 \\
\bar{\beta}_w & 0 & \cdots & \cdots & 0 & -\bar{\gamma}_w & \bar{\gamma}_w & & 0 & \cdots & 0 \\
-\beta_{w-1} & \bar{\beta}_{w-1} & & & \vdots & \gamma_{w-1} & -(\gamma_{w-1}+\bar{\gamma}_{w-1}) & \bar{\gamma}_{w-1} & & & \vdots \\
0 & -\beta_{w-2} & \ddots & & \vdots & 0 & \ddots & \ddots & \ddots & & 0 \\
\vdots & & \ddots & \ddots & 0 & \vdots & & \ddots & \ddots & & \bar{\gamma}_{p+2} \\
0 & \cdots & 0 & -\beta_{p+1} & \bar{\beta}_{p+1} & 0 & \cdots & \cdots & 0 & \gamma_{p+1} & -(\gamma_{p+1}+\bar{\gamma}_{p+1})
\end{array}\right]
$$

$$\varepsilon \quad R^{2(w-p)x2(w-p)} \quad , \qquad (7.17)$$

$$
A_b = \begin{bmatrix} 0 \ \varepsilon \ R^{w-p-1} \\ K_{p-1}/\delta_{p-1} \\ 0 \ \varepsilon \ R^{w-p-1} \\ \gamma_{p+1} K_{p-1}/\delta_{p-1} \end{bmatrix} \varepsilon \ R^{2(w-p)} \qquad (7.18)
$$

$$A_c = \begin{bmatrix} 0 \in R^{(w-p-1)\times(p-2)} & 0 \in R^{w-p-1} & 0 \in R^{(w-p-1)\times(p-3)} \\ 0 \in R^{p-2} & 1 & 0 \in R^{p-3} \\ 0 \in R^{(w-p-1)\times(p-2)} & 0 \in R^{w-p-1} & 0 \in R^{(w-p-1)\times(p-3)} \\ 0 \in R^{p-2} & \gamma_{p+1} & 0 \in R^{p-3} \end{bmatrix} \qquad (7.19)$$

$$\in \; R^{2(w-p)\times(2p-4)}$$

and

$$A_d = \left[\begin{array}{cccc|cccccccc} 0 & \cdots & \cdots & 0 & -1 & 1 & 0 & 0 & \cdots & \cdots & \cdots & 0 \\ 0 & & & \vdots & 0 & -1 & 1 & 0 & & & & \vdots \\ \vdots & & & \vdots & 0 & 0 & -1 & 1 & & & & \vdots \\ \vdots & & & \vdots & \vdots & & & & & & & 0 \\ 0 & \cdots & \cdots & 0 & 0 & \cdots & \cdots & \cdots & 0 & 0 & -1 & 1 \\ 0 & \cdots & \cdots & 0 & 0 & \cdots & \cdots & \cdots & 0 & 0 & 0 & -1 \\ \bar{\beta}_{p-1} & 0 & \cdots & 0 & -\bar{\gamma}_{p-1} & \bar{\gamma}_{p-1} & & 0 & 0 & \cdots & \cdots & 0 \\ -\beta_{p-2} & \bar{\beta}_{p-2} & & \vdots & \gamma_{p-2} & -(\gamma_{p-2}+\bar{\gamma}_{p-2}) & & \bar{\gamma}_{p-2} & 0 & \cdots & \cdots & 0 \\ 0 & -\beta_{p-3} & & \vdots & 0 & \gamma_{p-3} & & (\gamma_{p-3}+\bar{\gamma}_{p-3}) & & \bar{\gamma}_{p-3} & & \vdots \\ \vdots & & & 0 & \vdots & & \ddots & & \ddots & & \ddots & 0 \\ \vdots & & & & \vdots & & & & & & & \bar{\gamma}_3 \\ 0 & \cdots & 0 \; -\beta_2 & \bar{\beta}_2 & 0 & \cdots & \cdots & \cdots & 0 & & \gamma_2 & -(\gamma_2+\bar{\gamma}_2) \end{array}\right] \qquad (7.20)$$

$$\in \; R^{(2p-4)\times(2p-4)} \, .$$

It follows directly from (3.17) and (7.16) that the set of transmission zeros is comprised of $-K_{p-1}/\delta_{p-1}$, the eigenvalues of Aa given by (7.17) and the eigenvalues of Ad given by (7.20). Since the structures of Aa and Ad are identical to the structure of A_{11} given by (6.5), the set of transmission zeros can be pictured as comprising of the transmission zeros of two 'subtrains' with an additional transmission zero for the connecting coupling. Furthermore since it was shown in section (6.3) that the transmission zeros of single locomotive powered trains always lie in the left half of the complex plane it is clear that the transmission zeros of each 'subtrain' will also always lie in the left half of the complex plane. It follows directly that the sets of transmission zeros of two locomotive powered trains always lie in the left half of the complex plane when the outputs are the speeds of the locomotives and the forces in the (p-1)th couplings. It is clear that (2.57) is satisfied and a fast-sampling controller can be designed for the two locomotive trains of section (7.2) by employing the theory developed in section (2.4).

For any uniform trains it is clear that the sets of open-loop poles and the sets of transmission zeros of each 'subtrain' will lie on the same curve for any number of vehicles and given stiffness and damping coefficients since the open-loop poles assume the form given by (5.33) and (5.34) and the transmission zeros of each 'subtrain' can be expressed in the form given by (6.28) to (6.30) . Finally it is clear that when the second locomotive is the ($\frac{w}{2}$ + 1)th vehicle then the sets of transmission zeros for each subtrain are identical, since the train has been split into two identical trains.

7.4 Review of the Literature on Unit Trains

'Unit' trains, or extra-long freight trains, are used on long overland tracks in North and South America, South Africa and Australia for hauling bulk commodities. The increasing use of unit trains is a direct result of their economy of operation. Unit trains are more economic to use because they require fewer staff to operate them, less manoeuvering and only single as opposed to double tracks.

Taylor, Tausch, Whitney and Kelly [4] describe the concept of using unit trains by outlining examples used in the U.S.A.. The problems associated with coupler failure when operating trains over gradients is mentioned and one solution of limiting train sizes to suit particular routes is covered. The use of train and regenerative brakes is also detailed.

Ashman [5] describes the conventional methods of controlling locomotives in a train and goes on to describe a radio controlled system, 'Locotrol', that allows either independent control or duplication of the control applied to the leading locomotive(s) to be applied to other locomotives in the train. Parker [42] describes the growth in the use of 'Locotrol' in America, Brazil and Australia, and also gives details of the problems and solutions of using remote radio controlled locomotives in tunnels.

Peppard, McLane, Sundareswaran and Bayoumi [6] , [43] applied linear optimal control theory to two and three vehicle models, illustrated by figure (7.2), in order to design speed controllers for trains with multiple locomotives. The controllers for the two models were then assumed to be decentralized controllers for unit trains. It is clear, at the outset, that their 'decentralized' controllers were not derived on the basis

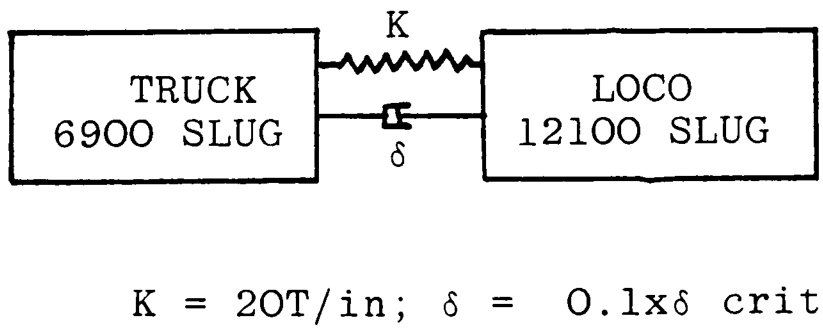

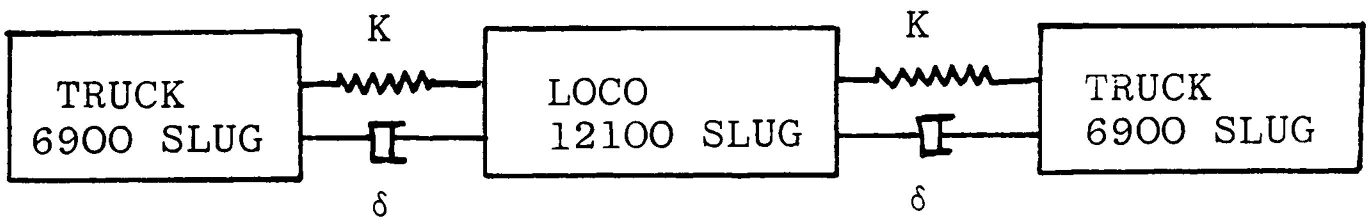

Figure 7.2

of decentralized control theory or even their own train model and as a result required extensive computer simulations to determine the cost function. Further computer analysis was required to assess the affects of their assumptions concerning some of the states used for feedback and finally further computer simulations were required to implement their analogue controller using digital equipment.

7.5 Fast-Sampling Controllers for Trains With Two Locomotives

It is clear that trains with locomotives as the first and pth vehicles belong to the class of systems considered in sections (2.4) and (2.5) since it was shown in section (7.3) that transmission zeros always lie on the left half of the complex plane and that

$$\text{rank } (C_2B) = \ell = 2 \text{ .} \qquad (7.21)$$

As a result the theory from section (2.4) is now utilized to develop a suitable algorithm for the control of two locomotive powered trains by using the mathematical model developed in section (7.2).

It follows from (7.3) to (7.5), (3.8) and (3.9) that the 'proportional' controller matrix assumes the form

$$K_o = \begin{bmatrix} 1 & 0 \\ 0 & -1/\delta_{p-1} \end{bmatrix} \qquad (7.22)$$

and from (3.11) and (3.12) that the 'integrator' controller matrix assumes the form

$$K_1 = \begin{bmatrix} \rho_1 & 0 \\ 0 & -\rho_2/\delta_{p-1} \end{bmatrix} \text{ .} \qquad (7.23)$$

Substituting (7.22) and (7.23) into (2.13) yields the control algorithm

$$u(KT) = f\begin{Bmatrix} e_1(KT) + \rho_1 z_1(KT) \\ -e_2(KT)/\delta_{p-1} - \rho_2 z_2(KT)/\delta_{p-1} \end{Bmatrix} \tag{7.24}$$

where

$$e_1(KT) = v_1(KT) - c_1(KT) \quad , \tag{7.25}$$

$$e_2(KT) = v_2(KT) - F_{p-1}(KT), \tag{7.26}$$

$F_{p-1}(KT)$ is the force in the $(p-1)^{th}$ coupling and $z_1(KT)$ and $z_2(KT)$ are given by (2.19). It can further be shown from (2.75), (2.76), (2.87) , (7.3) and (7.5) that the asymptotic transfer function matrix relating the outputs to the command inputs and the disturbances assumes the form

$$\begin{bmatrix}\Gamma(\lambda) \ , & \Gamma_D(\lambda)\end{bmatrix} = \left[\begin{array}{cc|cc} \frac{1}{\lambda} & 0 & 0 & 0 \\ 0 & \frac{1}{\lambda} & 0 & 0 \end{array}\right] \tag{7.27}$$

as $f \to \infty$, and hence as the sampling frequency increases the outputs will be increasingly non-interacting when the system is subjected to changes in command and be increasingly unaffected by disturbances.

In the next section numerical examples are presented that utilize the theory developed in this section. These examples will again underline the integrity of fast sampling controllers since it will be shown that one control algorithm copes easily with trains of different lengths.

7.6 Ten, Twenty and Forty Vehicle Trains

In this section the fast-sampling control of ten, twenty and forty vehicle trains with leading locomotives and a second locomotive as the sixth, eleventh and twenty-first vehicle respectively is considered. It is assumed that the trains consist of equal masses connected by identical couplings as illustrated by figure (7.3).

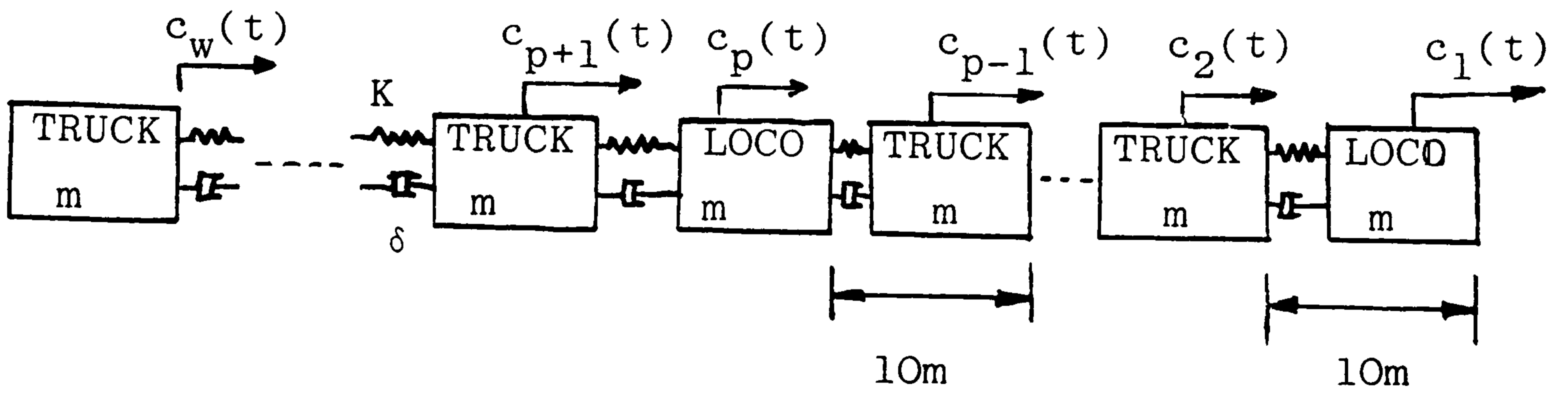

$w = 10, 20, 40$

$p = 6, 11, 21$

Figure 7.3

It follows from figure (7.2) and equations (6.9) to (6.12) that

$$\beta_j = \bar{\beta}_{j+1} = 20 \quad (j=1,..,w-1) \tag{7.28}$$

and

$$\gamma_j = \bar{\gamma}_{j+1} = 1 \quad (j=1,..,w-1) \tag{7.29}$$

and from (7.3) to (7.8) that, for the ten vehicle train, the plant, input and output matrices assume the respective forms

$$A = \begin{bmatrix} A_1 & A_2 \\ A_3 & A_4 \end{bmatrix} , \tag{7.30}$$

$$B = \begin{bmatrix} 0&0&0&0&0&0&0&0&0&0&0&0&0&0&0&0&0&1&0 \\ 0&0&0&0&0&0&0&0&0&0&0&0&0&0&0&0&0&0&1 \end{bmatrix}' , \tag{7.31}$$

and

$$C = \begin{bmatrix} 0&0&0&0&0&0&0&0&0&0&0&0&0&0&0&0&0&1&0 \\ 0&0&0&0&K&0&0&0&0&0&0&0&0&\delta&0&0&0&0&-\delta \end{bmatrix} \tag{7.32}$$

where

$$A_1 = 0 \in R^{9x9} , \tag{7.33}$$

$$A_2 = \begin{bmatrix} -1&1&0&0&0&0&0&0&0&0 \\ 0&-1&1&0&0&0&0&0&0&0 \\ 0&0&-1&1&0&0&0&0&0&0 \\ 0&0&0&-1&0&0&0&0&0&1 \\ 0&0&0&0&1&0&0&0&0&-1 \\ 0&0&0&0&-1&1&0&0&0&0 \\ 0&0&0&0&0&-1&1&0&0&0 \\ 0&0&0&0&0&0&-1&1&0&0 \\ 0&0&0&0&0&0&0&-1&1&0 \end{bmatrix} , \tag{7.34}$$

$$A_3 = \begin{bmatrix} 20 & 0 & 0 & 0 & 0 & 0 & 0 & 0 & 0 \\ -20 & 20 & 0 & 0 & 0 & 0 & 0 & 0 & 0 \\ 0 & -20 & 20 & 0 & 0 & 0 & 0 & 0 & 0 \\ 0 & 0 & -20 & 20 & 0 & 0 & 0 & 0 & 0 \\ 0 & 0 & 0 & 0 & -20 & 20 & 0 & 0 & 0 \\ 0 & 0 & 0 & 0 & 0 & -20 & 20 & 0 & 0 \\ 0 & 0 & 0 & 0 & 0 & 0 & -20 & 20 & 0 \\ 0 & 0 & 0 & 0 & 0 & 0 & 0 & -20 & 20 \\ 0 & 0 & 0 & 0 & 0 & 0 & 0 & 0 & -20 \\ 0 & 0 & 0 & -20 & 20 & 0 & 0 & 0 & 0 \end{bmatrix} \qquad (7.35)$$

and

$$A_4 = \begin{bmatrix} -1 & 1 & 0 & 0 & 0 & 0 & 0 & 0 & 0 & 0 \\ 1 & -2 & 1 & 0 & 0 & 0 & 0 & 0 & 0 & 0 \\ 0 & 1 & -2 & 1 & 0 & 0 & 0 & 0 & 0 & 0 \\ 0 & 0 & 1 & -2 & 0 & 0 & 0 & 0 & 0 & 1 \\ 0 & 0 & 0 & 0 & -2 & 1 & 0 & 0 & 0 & 1 \\ 0 & 0 & 0 & 0 & 1 & -2 & 1 & 0 & 0 & 0 \\ 0 & 0 & 0 & 0 & 0 & 1 & -2 & 1 & 0 & 0 \\ 0 & 0 & 0 & 0 & 0 & 0 & 1 & -2 & 1 & 0 \\ 0 & 0 & 0 & 0 & 0 & 0 & 0 & 1 & -1 & 0 \\ 0 & 0 & 0 & 1 & 1 & 0 & 0 & 0 & 0 & -2 \end{bmatrix} \qquad (7.36)$$

and corresponding similar forms for the twenty and forty vehicle trains and where the state vector is given by (7.1) and (7.2). Hence the transmission zeros of the three triples (A,B,C) of the ten, twenty and forty vehicle train can be found using (3.17) and are presented in table (7.1). The discrete-time domain equivalents of the three sets of transmission zeros and the remaining asymptotic closed-loop poles are presented in tables (7.2), (7.3) and (7.4) together with the closed -loop poles for the two sampling periods given by (6.47) and where

$$\rho_1 = \rho_2 = 0.05 \qquad (7.37)$$

in (7.23) to give K_1. Since all the closed-loop poles, for the periods given by (6.47) , lie inside the unit disc it follows that the control law equations formed from (6.47), (7.22) to (7.24) and (7.37), namely

$$u_1(KT) = f \{ e_1(KT) + 0.05\ z_1(KT) \} \qquad (7.38)$$

and

$$u_2(KT) = -f \{ e_2(KT) + 0.05\ z_2(KT)\} / \delta_{p-1} \qquad (7.39)$$

where $\delta_{p-1} = \delta$ given by (6.41), will produce stable closed-loop systems. Simulations of the ten, twenty and forty vehicle trains when controlled in accordance with (7.38) and (7.39), using $T = {}^1/f = 0.1$ s over a gradient profile illustrated by figure (6.3), produced the results given by figures (7.4) to (7.21) when the initial steady state conditions were assumed to be

$$q_i(0) = 0 \quad (i=1,..,w-1), \tag{7.40}$$

$$c_j(0) = 0 \quad (j=1,..,w), \tag{7.41}$$

$$y_1(0) = 10 \text{ m/s} , \tag{7.42}$$

$$y_2(0) = 0 , \tag{7.43}$$

$$v_1(0) = 10 \text{ m/s} , \tag{7.44}$$

$$v_2(0) = 0 , \tag{7.45}$$

$$u_i(0) = 0 \quad (i=1,2) \tag{7.46}$$

and

$$\theta_j(0) = 0 \quad (j=1,..,w). \tag{7.47}$$

TRANSMISSION ZEROS		
TEN VEHICLE TRAIN	TWENTY VEHICLE TRAIN	FORTY VEHICLE TRAIN
-0.06±i 1.55	-0.0136±i 0.739	-0.0032±i 0.36
-0.50±i 4.45	-0.121±i 2.19	-0.029±i 1.08
-1.17±i 6.75	-0.323±i 3.58	-0.080±i 1.79
-1.77±i 8.22	-0.600±i 4.86	-0.155±i 2.48
-20	-0.917±i 5.99	-0.251±i 3.16
	-1.250±i 6.95	-0.368±i 3.82
	-1.550±i 7.71	-0.500±i 4.45
-0.06±i 1.55	-1.79±i 8.27	-0.645±i 5.04
-0.50±i 4.45	-1.95±i 8.61	-0.800±i 5.60
-1.17±i 6.75	-20	-0.96±i 6.12
-1.77±i 8.22		-1.12±i 6.60
-20	-0.0136±i 0.739	-1.28±i 7.04
	-0.121±i 2.19	-1.43±i 7.42
	-0.323±i 3.58	-1.57±i 7.76
	-0.600±i 4.86	-1.69±i 8.05
	-0.917±i 5.99	-1.80±i 8.29
	-1.250±i 6.95	-1.89±i 8.48
	-1.550±i 7.71	-1.95±i 8.61
	-1.79±i 8.27	-1.99±i 8.69
	-1.95±i 8.61	-20
	-20	-0.0032±i 0.36
		-0.029±i 1.08
		-0.080±i 1.79
		-0.155±i 2.48
		-0.251±i 3.16
		-0.368±i 3.82
		-0.500±i 4.45
		-0.645±i 5.04
		-0.800±i 5.60
		-0.96±i 6.12
		-1.12±i 6.60
		-1.28±i 7.04
		-1.43±i 7.42
		-1.57±i 7.76
		-1.69±i 8.05
		-1.80±i 8.29
		-1.89±i 8.48
		-1.95±i 8.61
		-1.99±i 8.69
		-20

TABLE 7.1

TEN VEHICLE TRAIN			
ASYMPTOTIC CLOSED-LOOP POLES T=0.1S	CLOSED-LOOP POLES T=0.1S	ASYMPTOTIC CLOSED-LOOP POLES T=0.01S	CLOSED-LOOP POLES T=0.01S
0.0	-0.0138	0.0	-0.00416
0.9950	0.9948	0.9995	0.9995
0.994±i 0.155	0.957±i 0.162	0.9994±i 0.0155	0.9992±i 0.0145
0.950±i 0.444	0.840±i 0.405	0.9950±i 0.0444	0.9941±i 0.4340
0.883±i 0.675	0.686±i 0.550	0.9883±i 0.0675	0.9862±i 0.0662
0.823±i 0.822	0.573±i 0.611	0.9823±i 0.0822	0.9792±i 0.0805
0.0, -1.0	-.196±i 0.833	0.0, 0.8	0.1097, 0.772
0.9950	0.9955	0.99950	0.99951
0.994±i 0.155	0.964±i 0.129	0.9994±i 0.0155	0.9990±i 0.0164
0.950±i 0.444	0.857±i 0.385	0.9950±i 0.0444	0.9937±i 0.0448
0.883±i 0.675	0.699±i 0.543	0.9883±i 0.0675	0.9859±i 0.0670
0.823±i 0.822	0.569±i 0.612	0.9823±i 0.0822	0.9791±i 0.0807

TABLE 7.2

TWENTY VEHICLE TRAIN			
ASYMPTOTIC CLOSED-LOOP POLES T=0.1S	CLOSED-LOOP POLES T=0.1S	ASYMPTOTIC CLOSED-LOOP POLES T=0.01S	CLOSED-LOOP POLES T=0.01S
0.0	-0.0138	0.0	-0.00416
0.9950	0.99455	0.99950	0.99950
0.9986±i 0.074	0.984±i 0.080	0.99986±i 0.0074	0.99977±i 0.0069
0.988±i 0.219	0.952±i 0.217	0.9988±i 0.0219	0.9985±i 0.0214
0.968±i 0.358	0.896±i 0.339	0.9968±i 0.0358	0.9960±i 0.0360
0.940±i 0.486	0.825±i 0.437	0.9940±i 0.0486	0.9927±i 0.0485
0.908±i 0.599	0.748±i 0.511	0.9908±i 0.0600	0.9890±i 0.0595
0.875±i 0.695	0.675±i 0.562	0.9875±i 0.0695	0.9851±i 0.0687
0.845±i 0.771	0.613±i 0.595	0.9845±i 0.0771	0.9817±i 0.0759
0.821±i 0.827	0.565±i 0.614	0.9821±i 0.0827	0.9789±i 0.0812
0.805±i 0.861	0.537±i 0.624	0.9805±i 0.0861	0.9771±i 0.0843
0.0, -1.0	-.196±i 0.833	0.0, 0.8	0.1097, 0.772
0.9950	0.99556	0.99950	0.99951
0.9986±i 0.074	0.9855±i 0.063	0.99986±i 0.0074	0.9997±i 0.0078
0.988±i 0.219	0.958±i 0.202	0.9988±i 0.0219	0.9984±i 0.0223
0.968±i 0.358	0.904±i 0.327	0.9968±i 0.0358	0.9961±i 0.0352
0.940±i 0.486	0.833±i 0.429	0.9940±i 0.0486	0.9929±i 0.0479
0.908±i 0.599	0.755±i 0.506	0.9908±i 0.0600	0.9891±i 0.0590
0.875±i 0.695	0.681±i 0.560	0.9875±i 0.0695	0.9853±i 0.0684
0.845±i 0.771	0.616±i 0.594	0.9845±i 0.0771	0.9818±i 0.0758
0.821±i 0.827	0.567±i 0.614	0.9821±i 0.0827	0.9789±i 0.0811
0.805±i 0.861	0.537±i 0.624	0.9805±i 0.0861	0.9771±i 0.0843

TABLE 7.3

FORTY VEHICLE TRAIN			
ASYMPTOTIC CLOSED-LOOP POLES T=0.1S	CLOSED-LOOP POLES T=0.1S	ASYMPTOTIC CLOSED-LOOP POLES T=0.01S	CLOSED-LOOP POLES T=0.01S
0.0	-0.0138	0.0	-0.00416
0.995	0.99407	0.9995	0.99949
0.9997±i 0.036	0.9936±i 0.039	0.99997±i 0.0036	0.99993±i 0.0034
0.997±i 0.108	0.987±i 0.102	0.9997±i 0.0108	0.9996±i 0.0110
0.992±i 0.179	0.973±i 0.170	0.9992±i 0.0179	0.9990±i 0.0181
0.985±i 0.248	0.952±i 0.236	0.9985±i 0.0248	0.9981±i 0.0250
0.975±i 0.316	0.925±i 0.297	0.9975±i 0.0316	0.9969±i 0.0317
0.963±i 0.382	0.894±i 0.353	0.9963±i 0.0382	0.9955±i 0.0382
0.950±i 0.445	0.859±i 0.403	0.9950±i 0.0445	0.9940±i 0.0443
0.936±i 0.504	0.821±i 0.448	0.9936±i 0.0504	0.9922±i 0.0502
0.920±i 0.560	0.783±i 0.486	0.9920±i 0.0560	0.9904±i 0.0560
0.904±i 0.612	0.745±i 0.518	0.9904±i 0.0612	0.9988±i 0.0607
0.888±i 0.660	0.708±i 0.545	0.9888±i 0.0660	0.9867±i 0.0653
0.872±i 0.704	0.672±i 0.567	0.9872±i 0.0704	0.9848±i 0.0695
0.857±i 0.742	0.640±i 0.584	0.9857±i 0.0742	0.9831±i 0.0731
0.843±i 0.776	0.611±i 0.598	0.9843±i 0.0776	0.9815±i 0.0763
0.831±i 0.805	0.586±i 0.608	0.9831±i 0.0805	0.9800±i 0.0791
0.820±i 0.829	0.565±i 0.615	0.9820±i 0.0829	0.9788±i 0.0813
0.811±i 0.848	0.548±i 0.621	0.9811±i 0.0848	0.9778±i 0.0831
0.805±i 0.861	0.536±i 0.624	0.9805±i 0.0861	0.9771±i 0.0843
0.801±i 0.869	0.529±i 0.626	0.9801±i 0.0869	0.9766±i 0.0851
0.0, -1.0	-.196±i 0.833	0.0, 0.8	0.1097, 0.7722
0.995	0.99562	0.9995	0.99951
0.9997±i 0.036	0.9935±i 0.030	0.99997±i 0.0036	0.99989±i 0.0038
0.997±i 0.108	0.985±i 0.110	0.9997±i 0.0108	0.9996±i 0.0106
0.992±i 0.179	0.970±i 0.178	0.9992±i 0.0179	0.9990±i 0.0176
0.985±i 0.248	0.949±i 0.243	0.9985±i 0.0248	0.9981±i 0.0246
0.975±i 0.316	0.921±i 0.303	0.9975±i 0.0316	0.9970±i 0.0313
0.963±i 0.382	0.890±i 0.359	0.9963±i 0.0382	0.9956±i 0.0378
0.950±i 0.445	0.854±i 0.408	0.9950±i 0.0445	0.9940±i 0.0440
0.936±i 0.504	0.817±i 0.451	0.9936±i 0.0504	0.9923±i 0.0499
0.920±i 0.560	0.779±i 0.488	0.9920±i 0.0560	0.9905±i 0.0554
0.904±i 0.612	0.741±i 0.521	0.9904±i 0.0612	0.9886±i 0.0605
0.888±i 0.660	0.704±i 0.547	0.9888±i 0.0660	0.9867±i 0.0651
0.872±i 0.704	0.670±i 0.568	0.9872±i 0.0704	0.9849±i 0.0693
0.857±i 0.742	0.638±i 0.585	0.9857±i 0.0742	0.9831±i 0.0730
0.843±i 0.776	0.609±i 0.598	0.9843±i 0.0776	0.9815±i 0.0764
0.831±i 0.805	0.585±i 0.608	0.9831±i 0.0805	0.9800±i 0.0791
0.820±i 0.829	0.564±i 0.615	0.9820±i 0.0829	0.9788±i 0.0813
0.811±i 0.848	0.548±i 0.621	0.9811±i 0.0848	0.9778±i 0.0831
0.805±i 0.861	0.536±i 0.624	0.9805±i 0.0861	0.9771±i 0.0844
0.801±i 0.869	0.529±i 0.626	0.9801±i 0.0869	0.9766±i 0.0851

TABLE 7.4

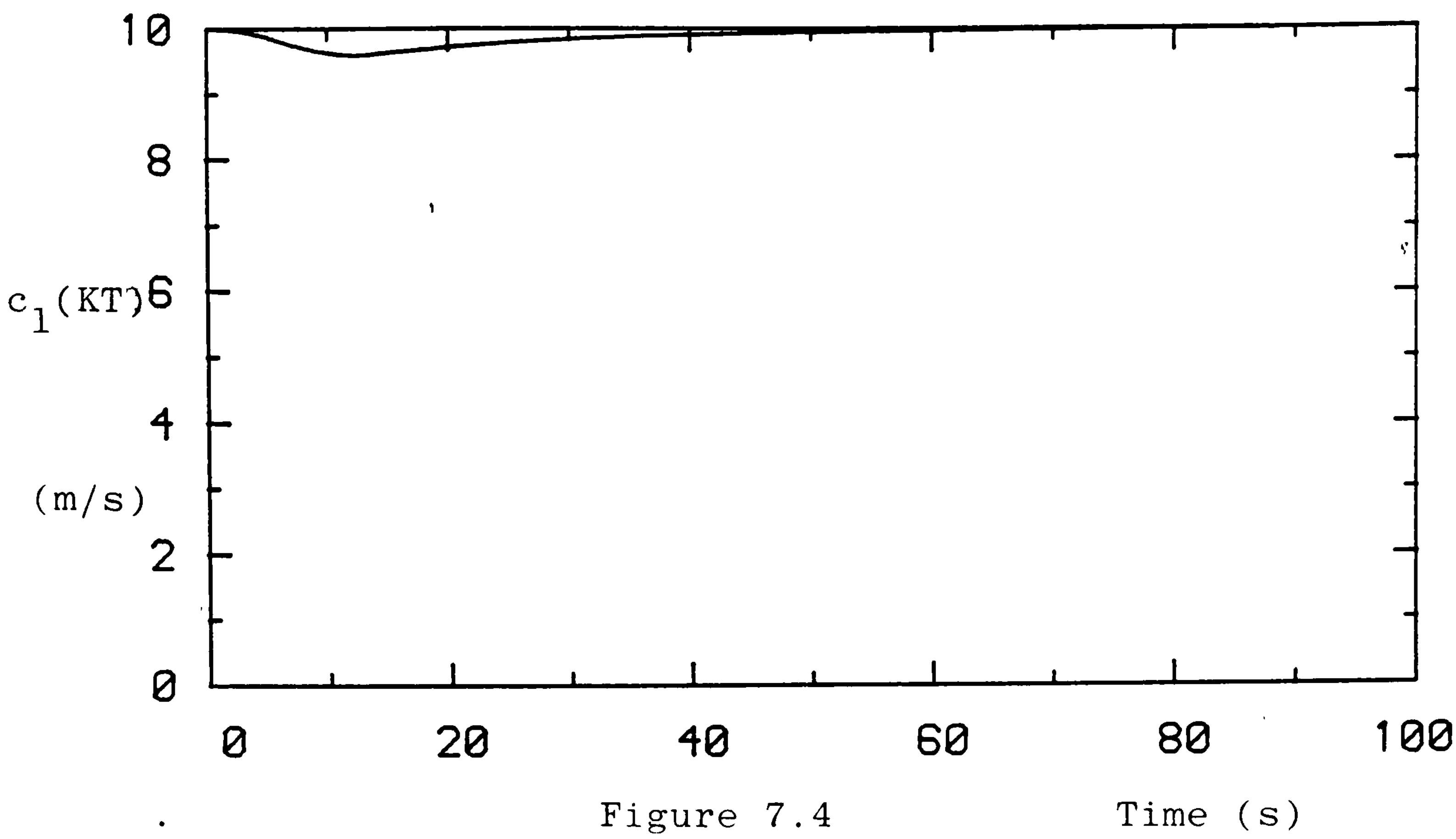

Figure 7.4

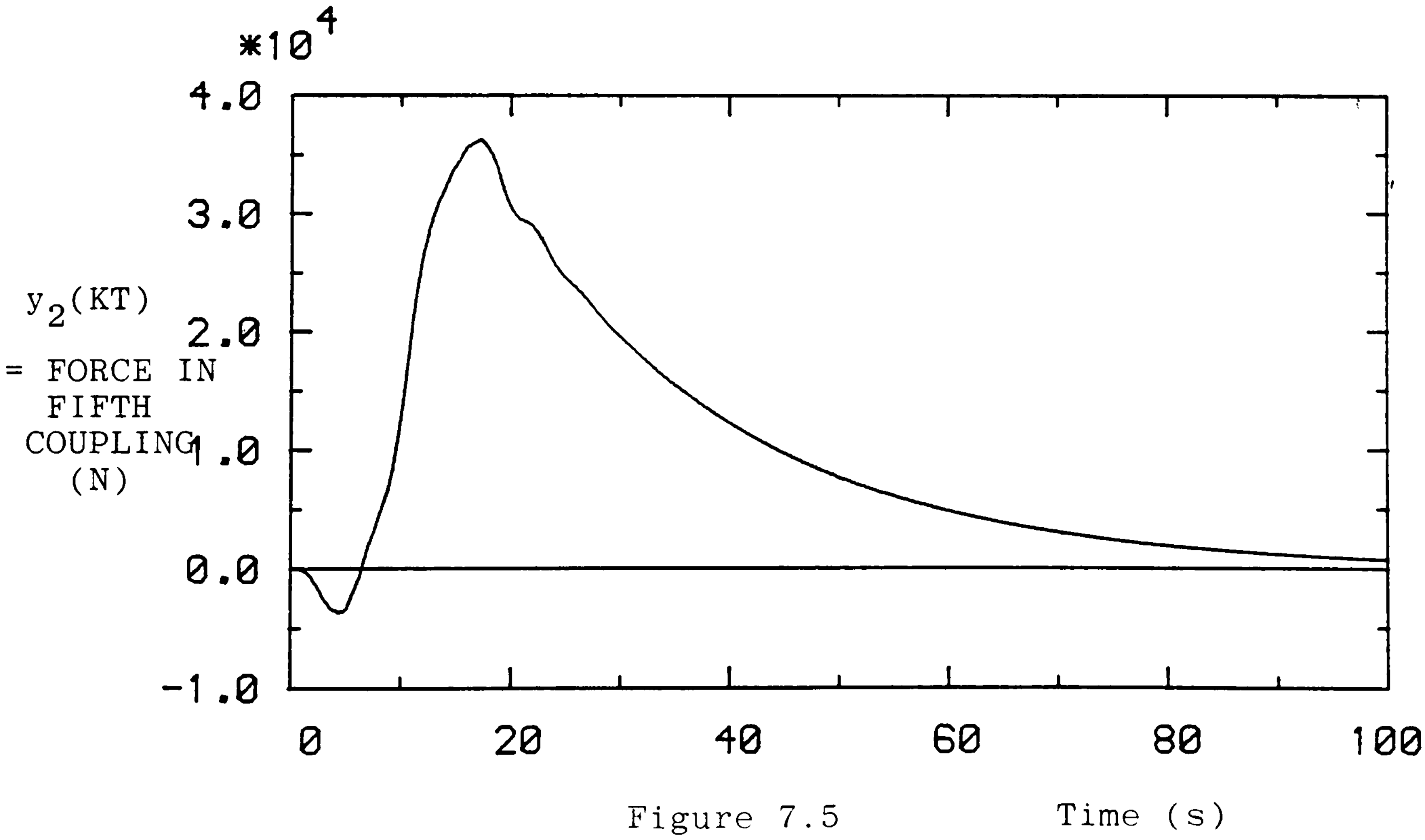

Figure 7.5

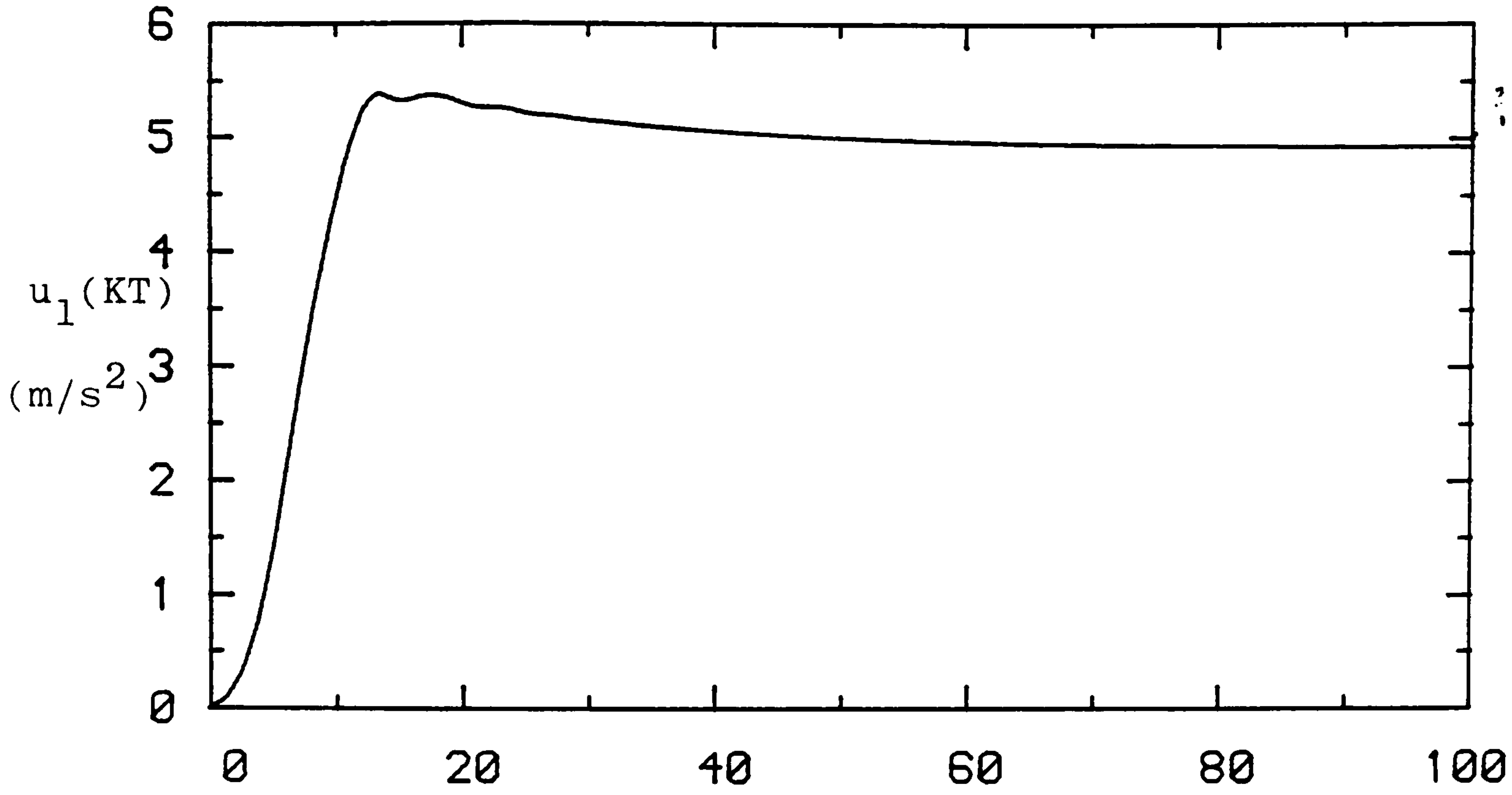

Figure 7.6 Time (s)

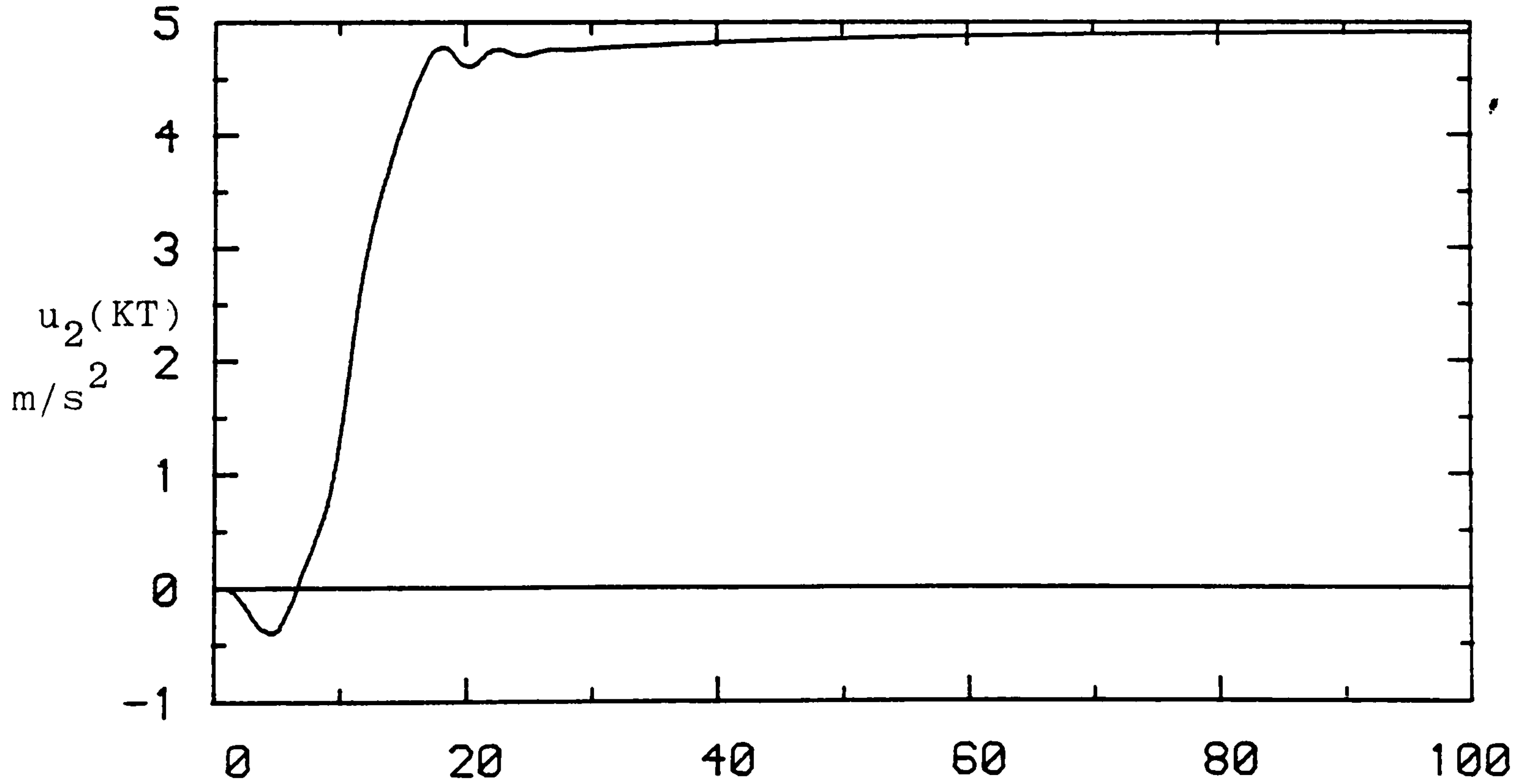

Figure 7.7 Time (s)

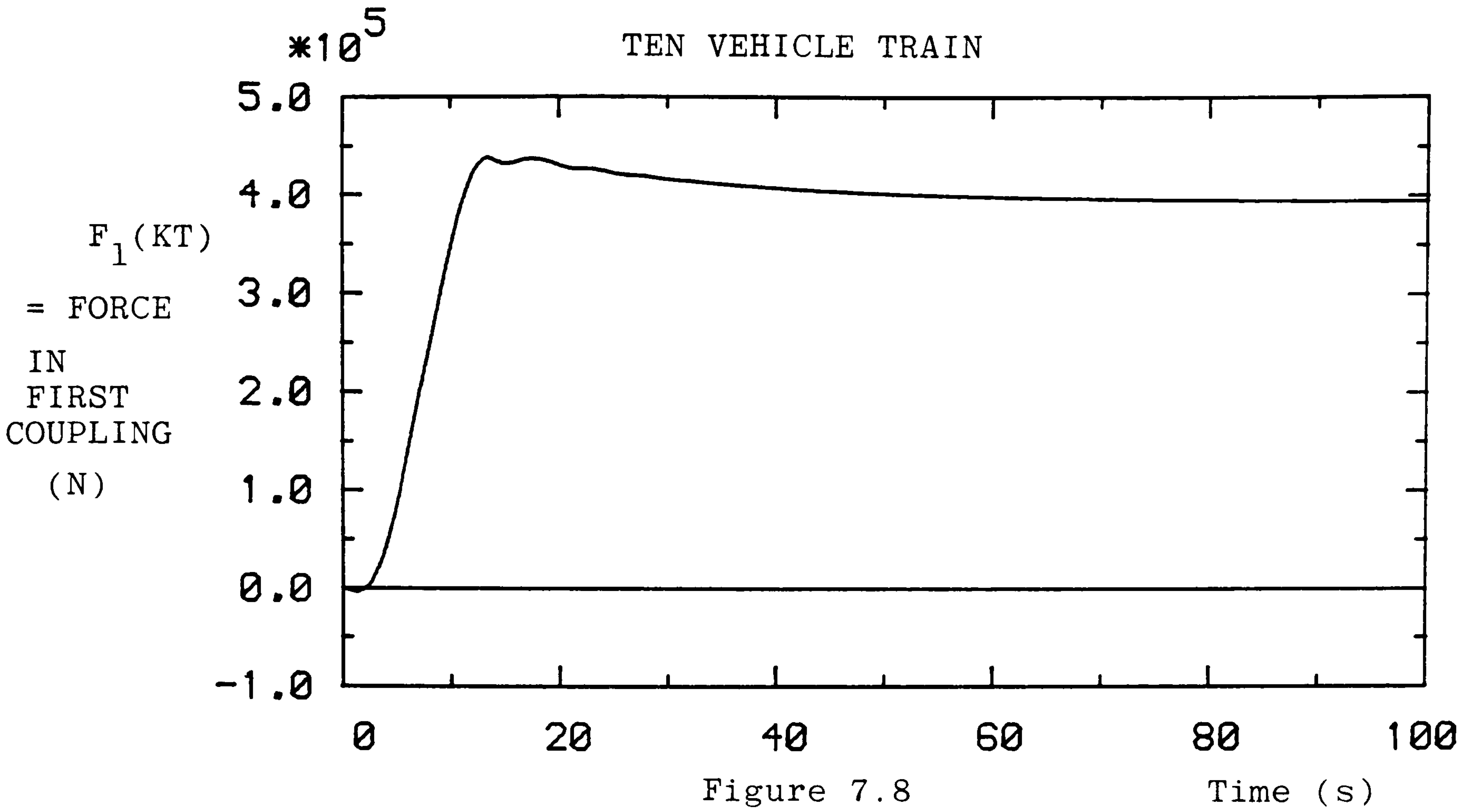

Figure 7.8

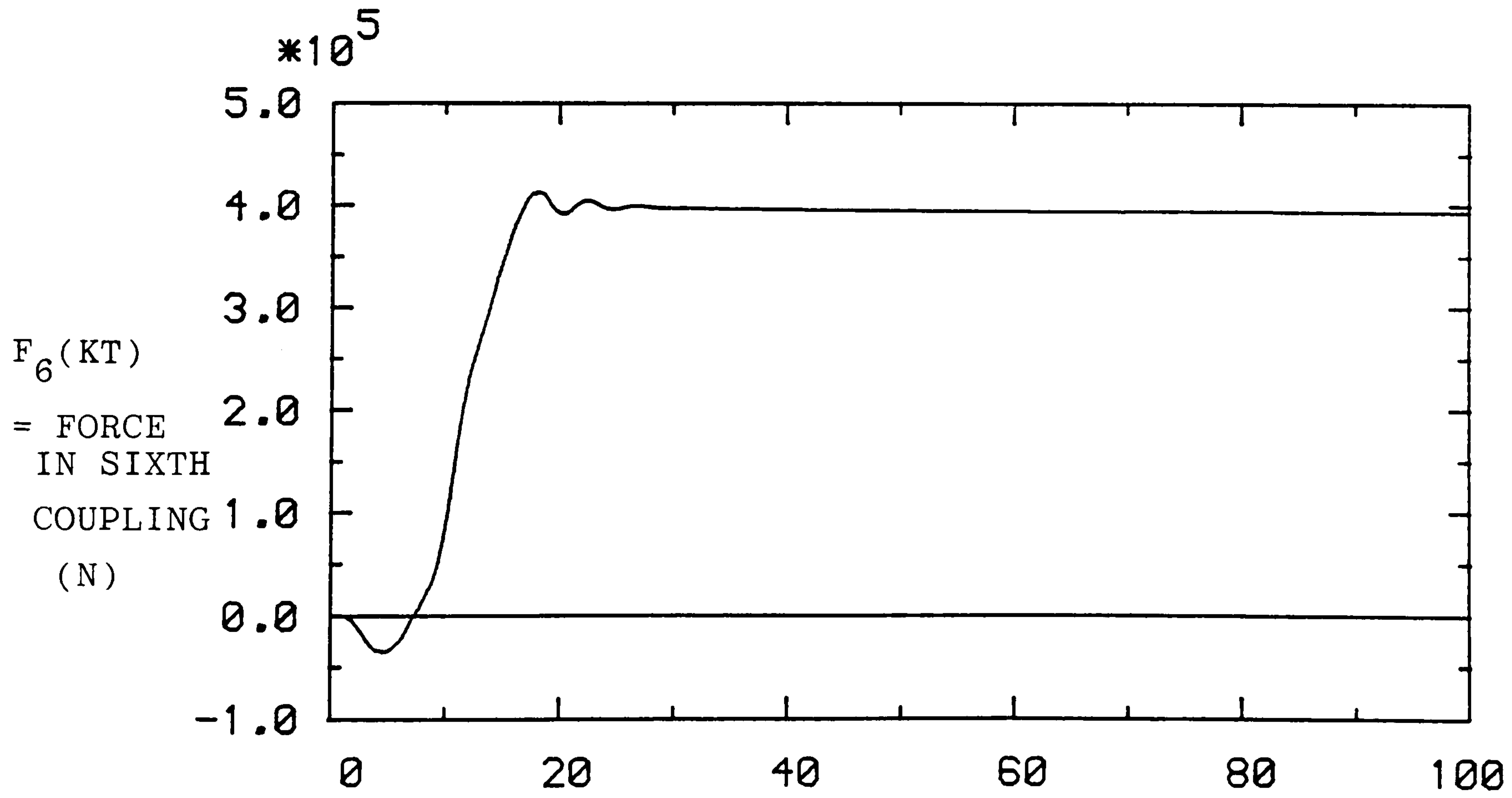

Figure 7.9

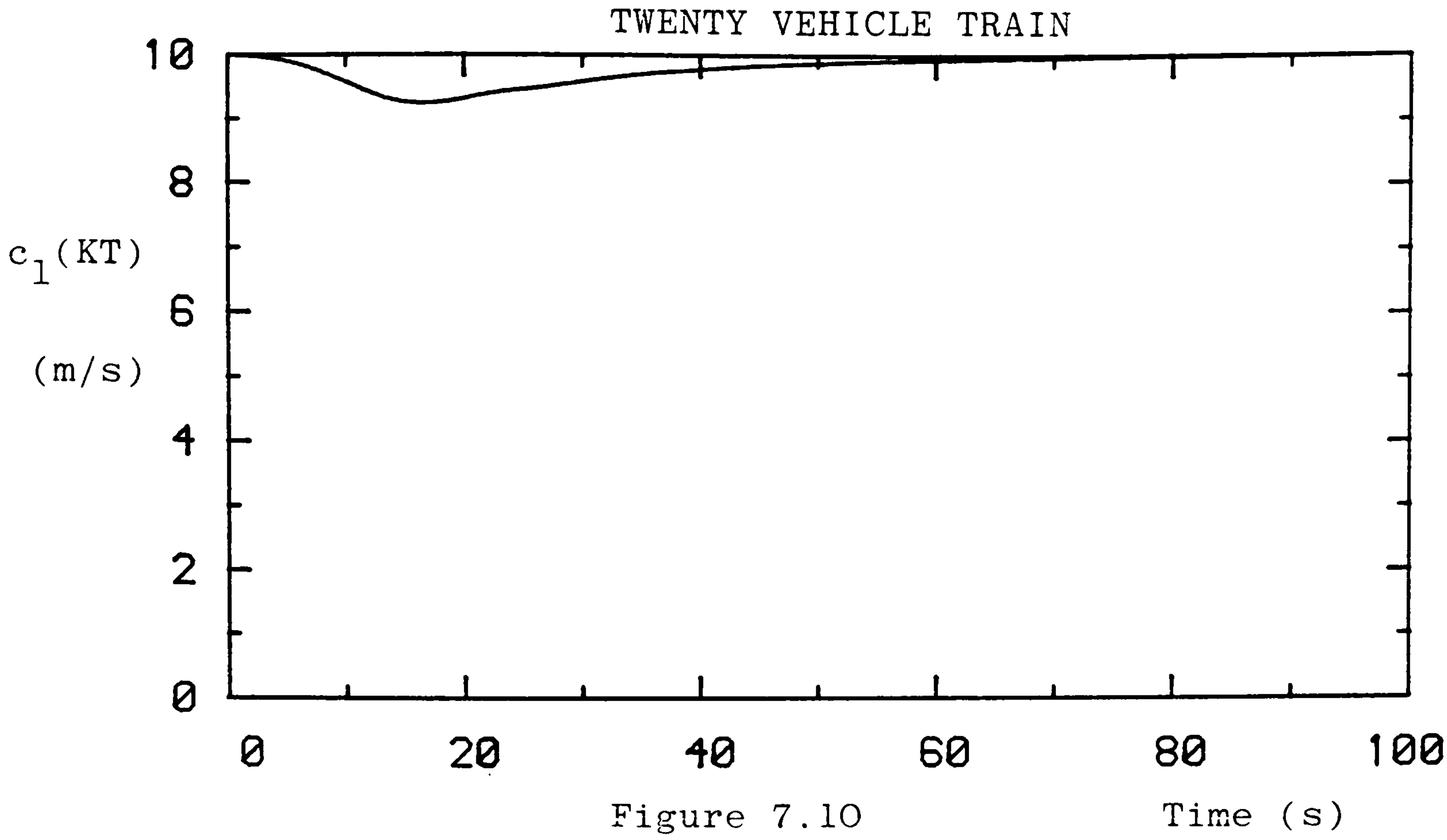

Figure 7.10

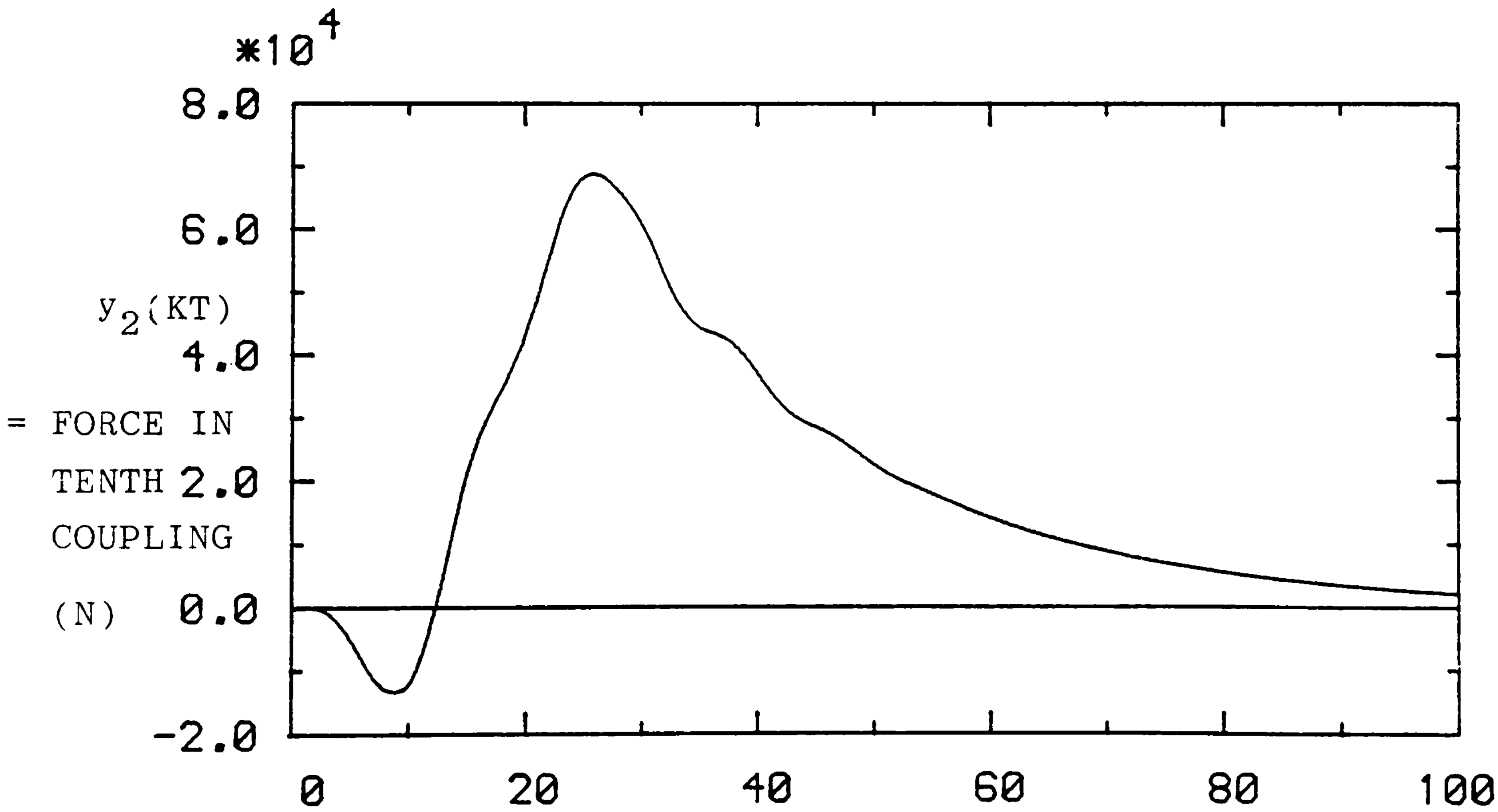

Figure 7.11

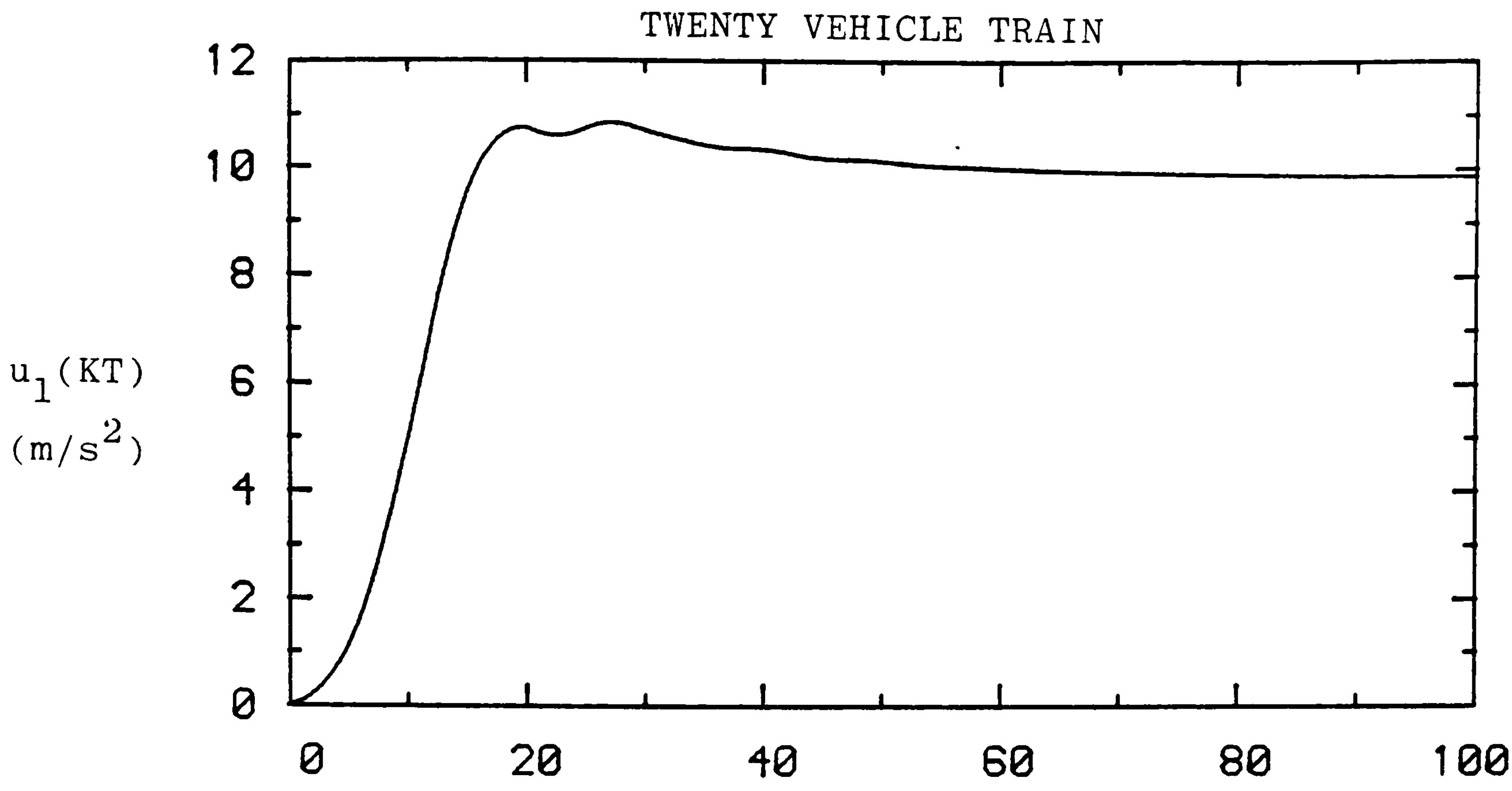

Figure 7.12

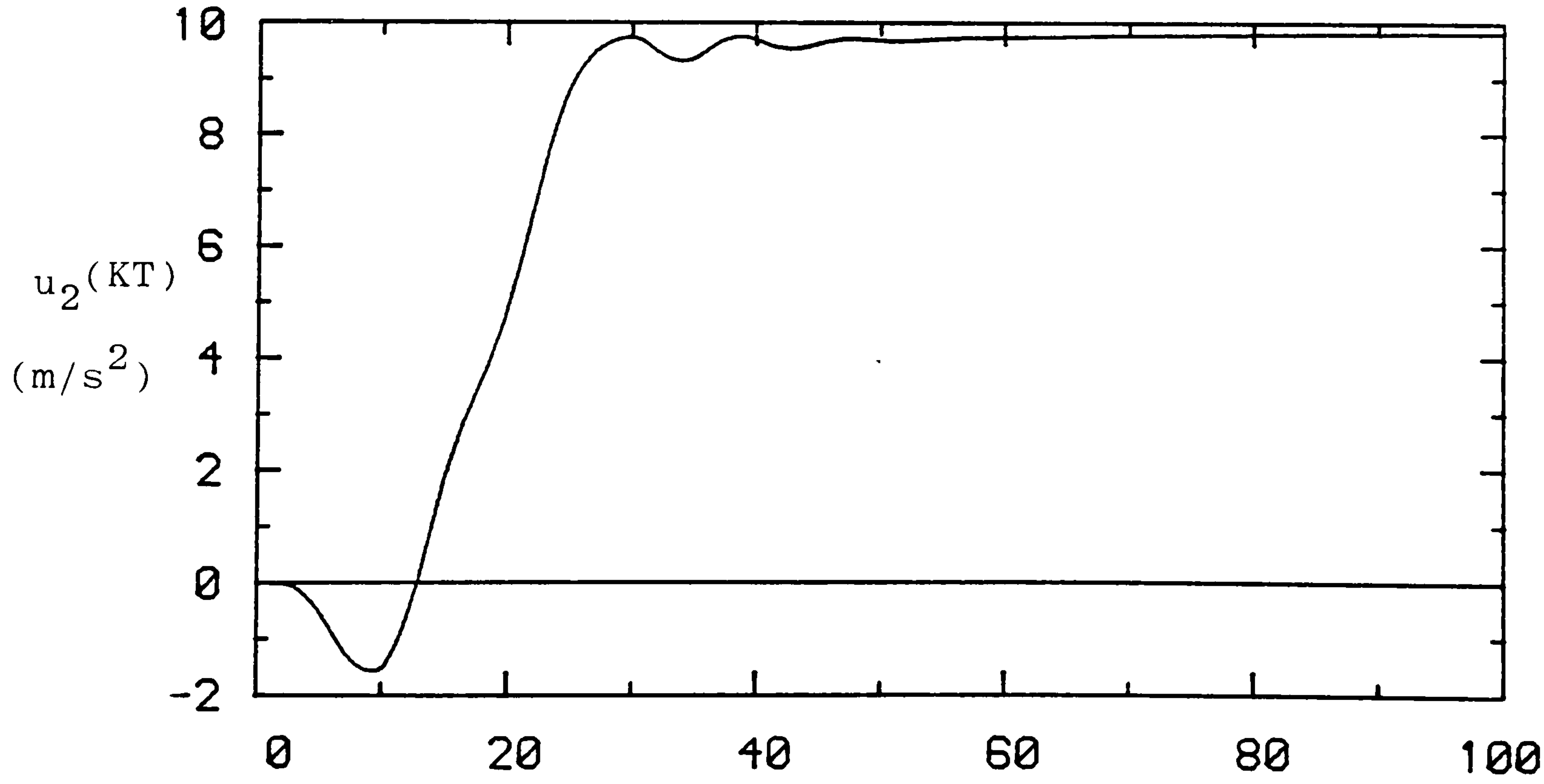

Figure 7.13

TWENTY VEHICLE TRAIN

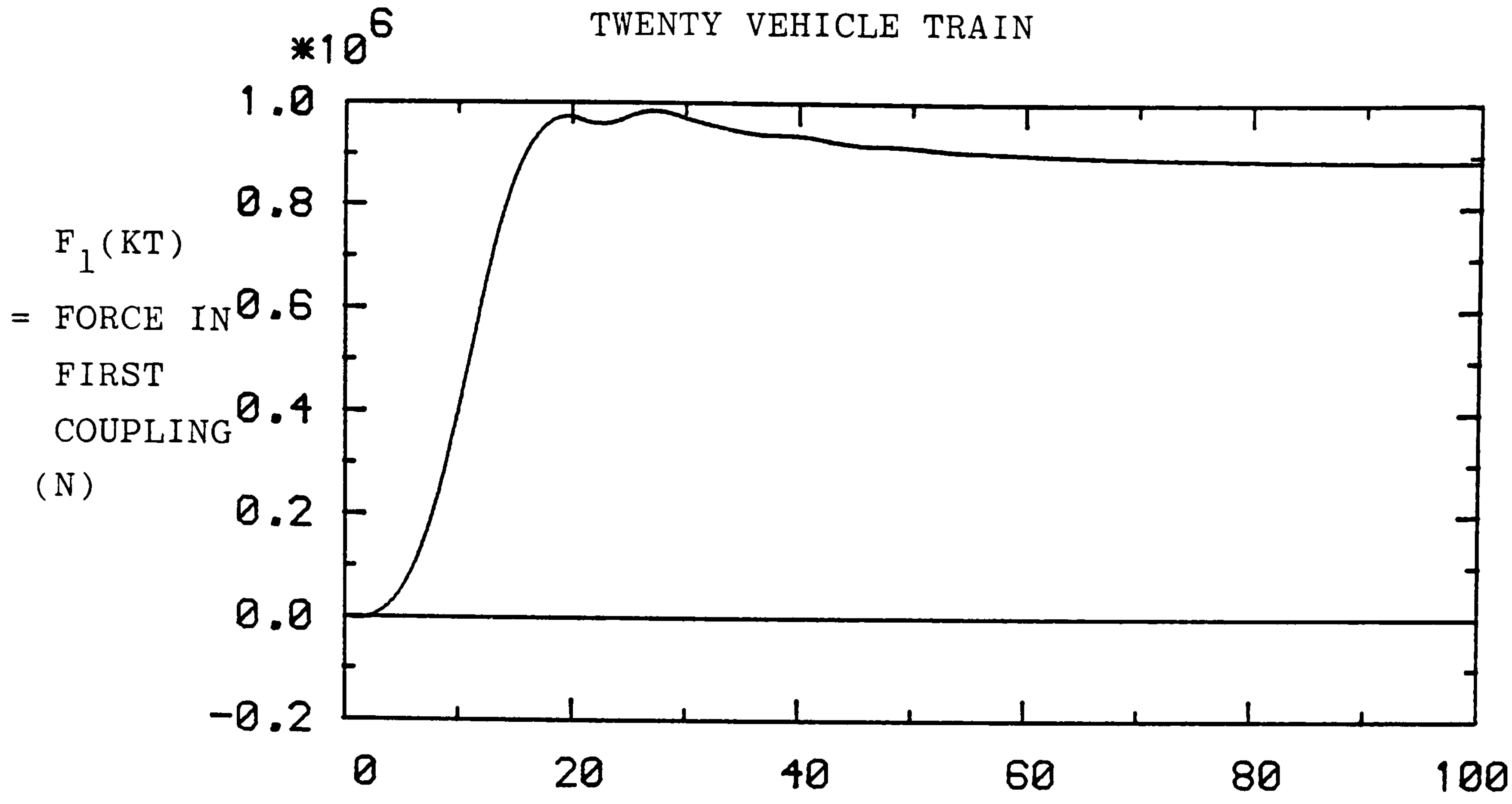

Figure 7.14

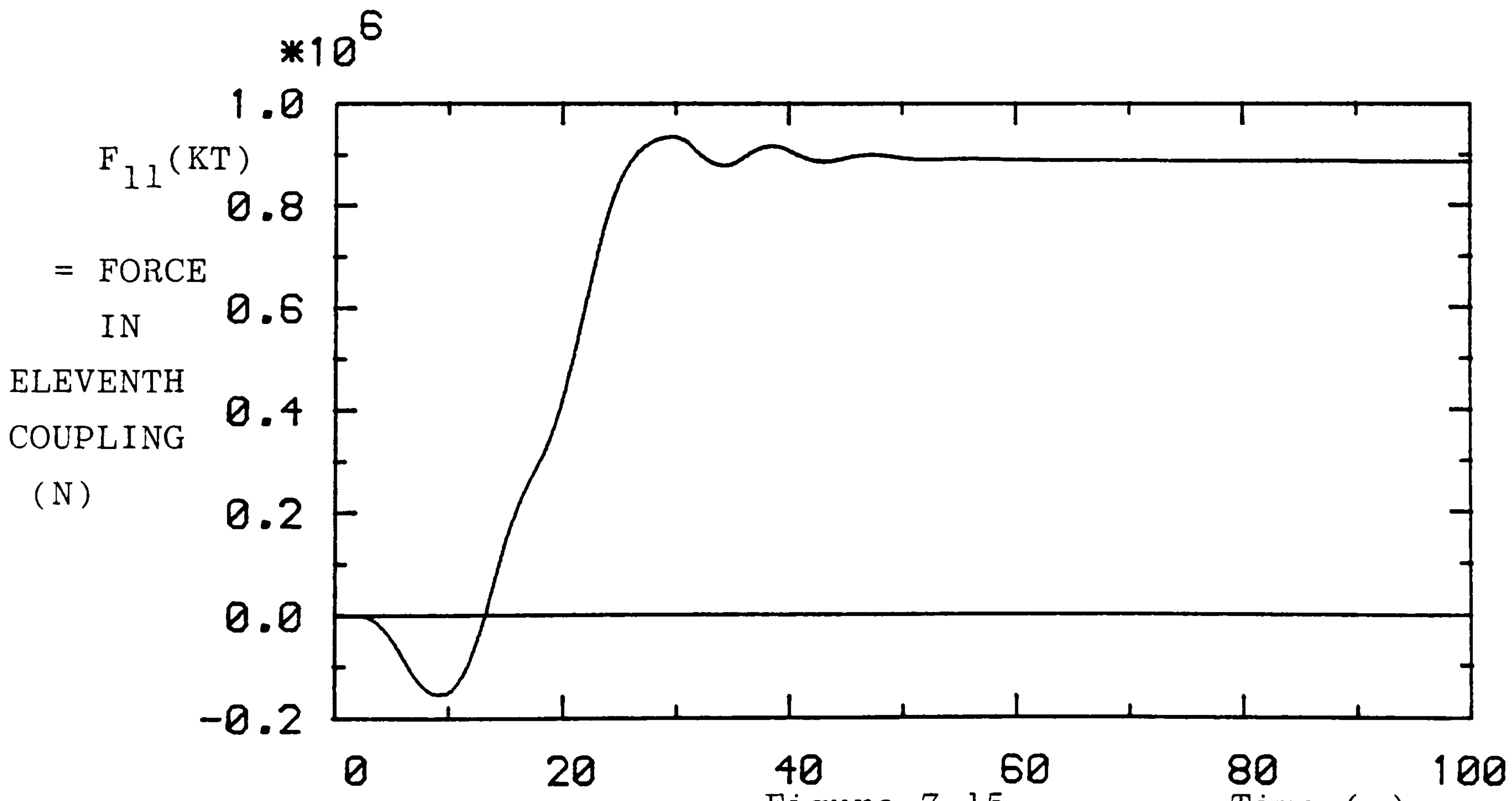

Figure 7.15

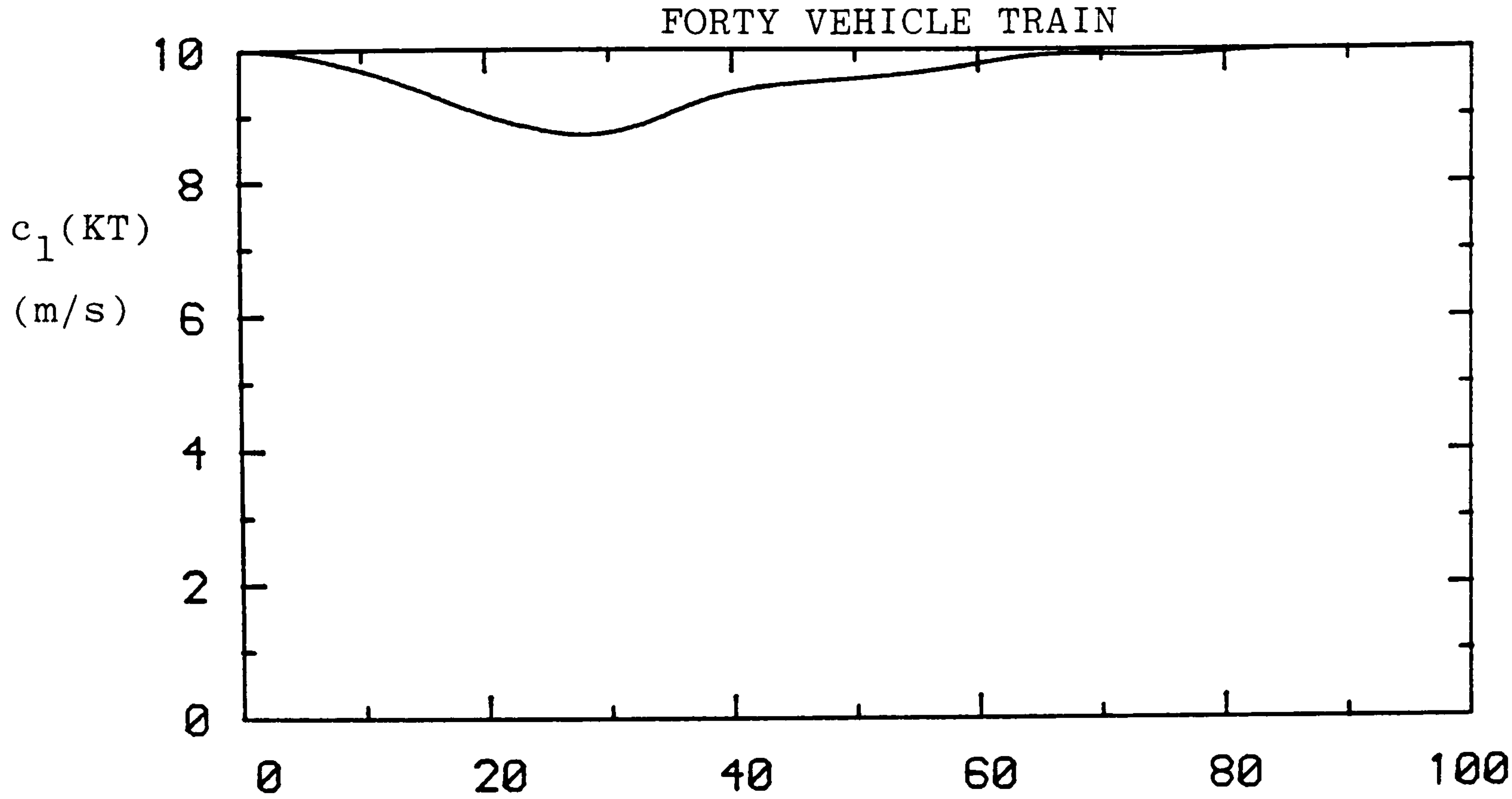

Figure 7.16

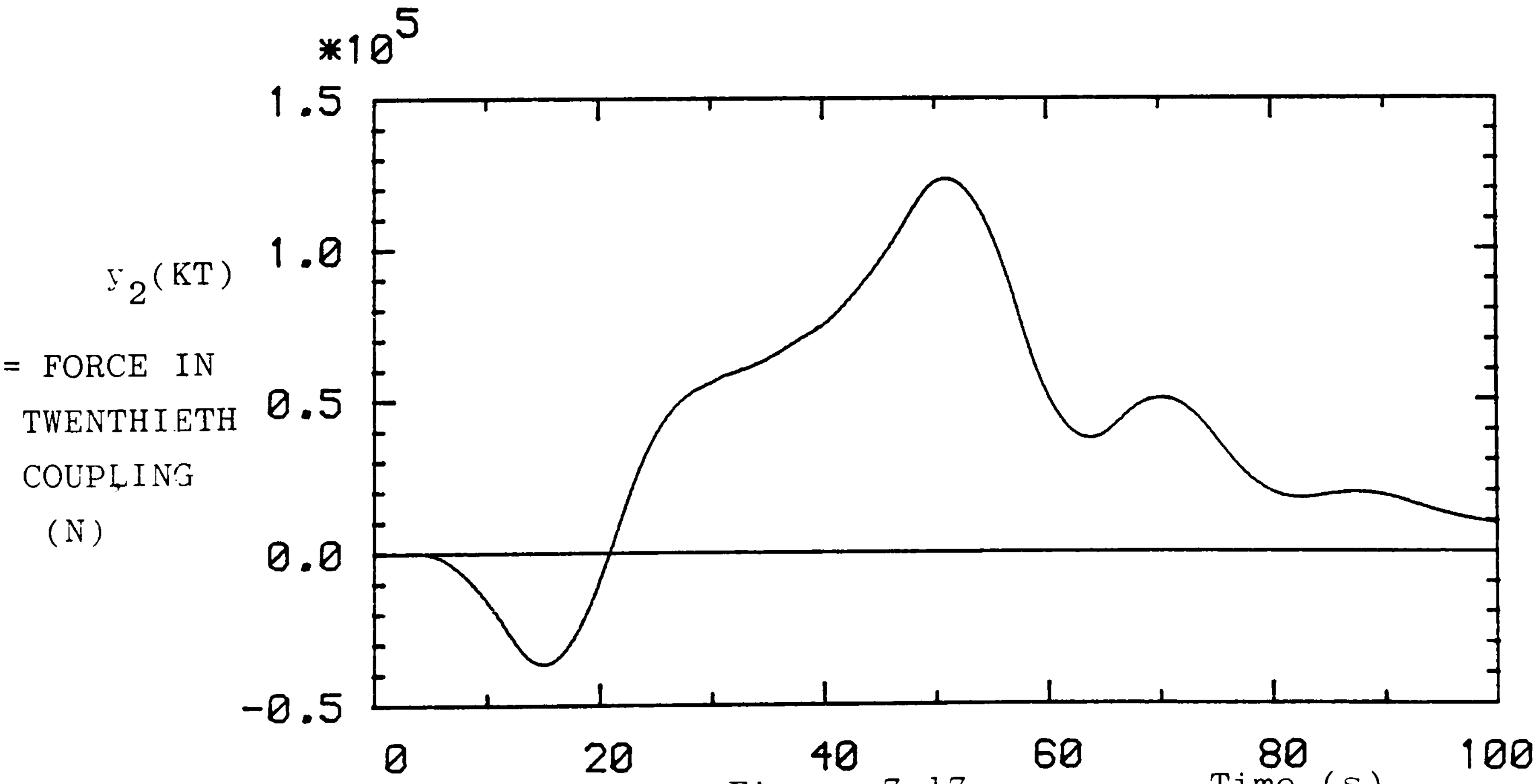

Figure 7.17

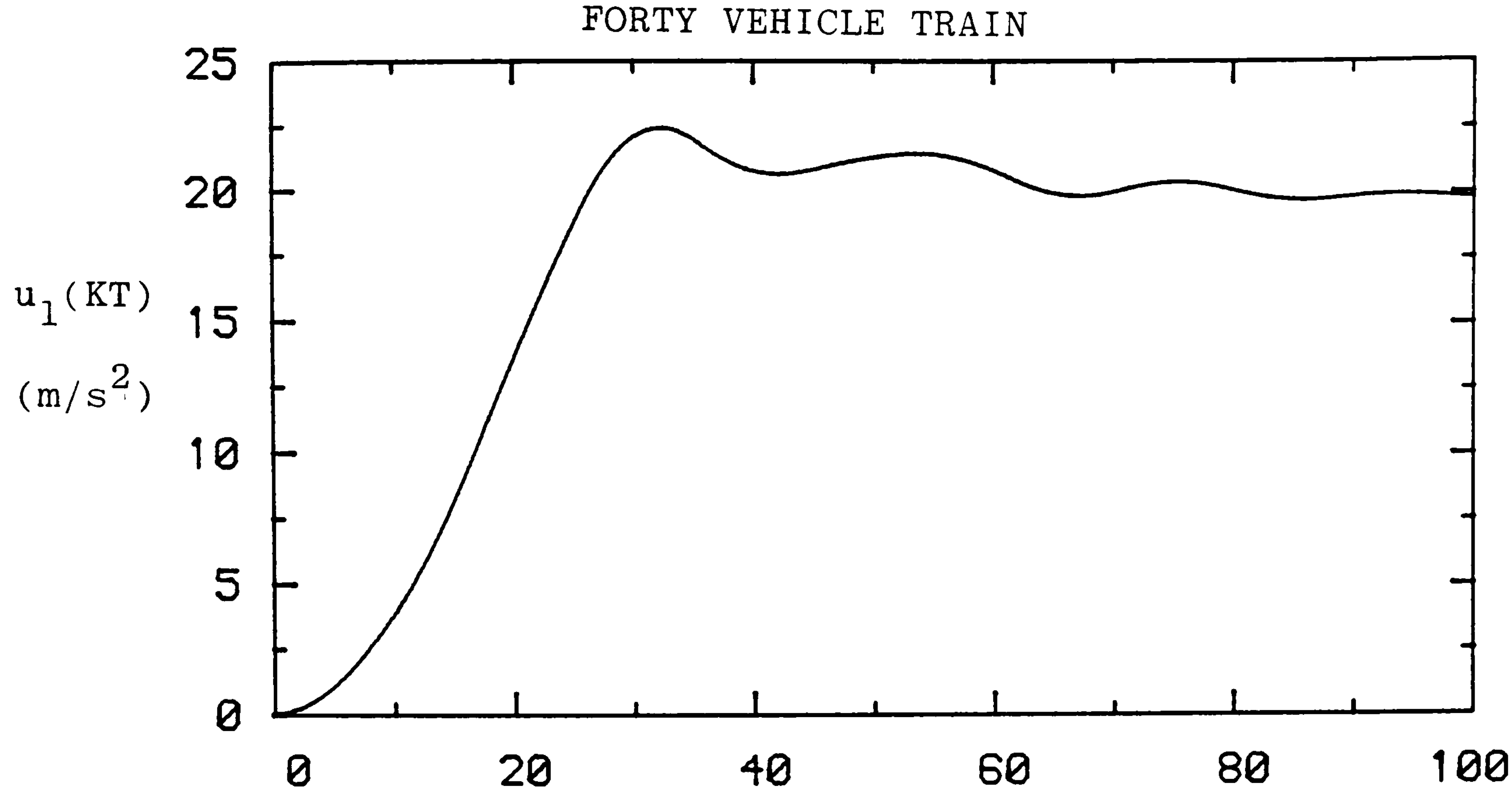

Figure 7.18

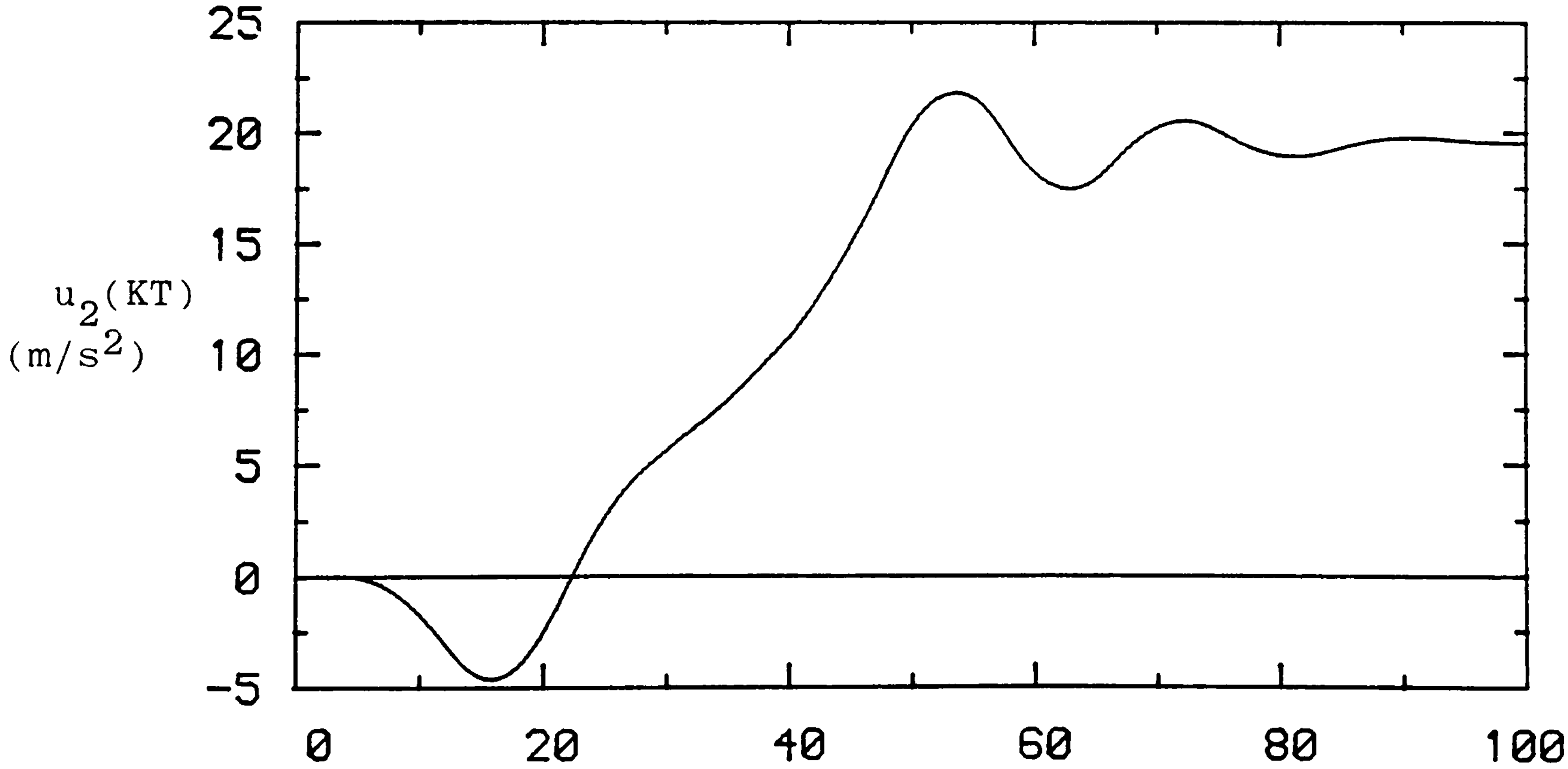

Figure 7.19

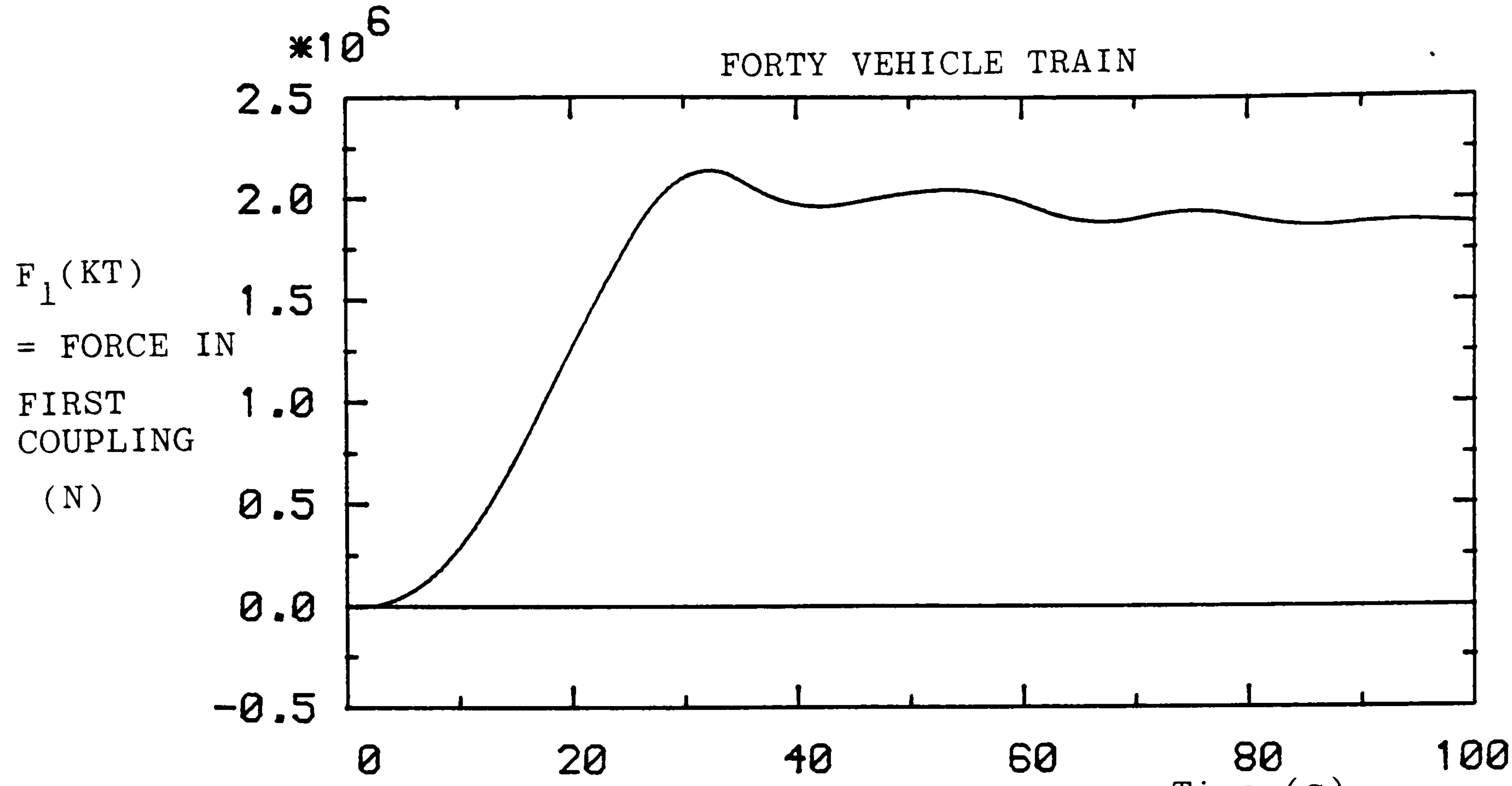

Figure 7.20

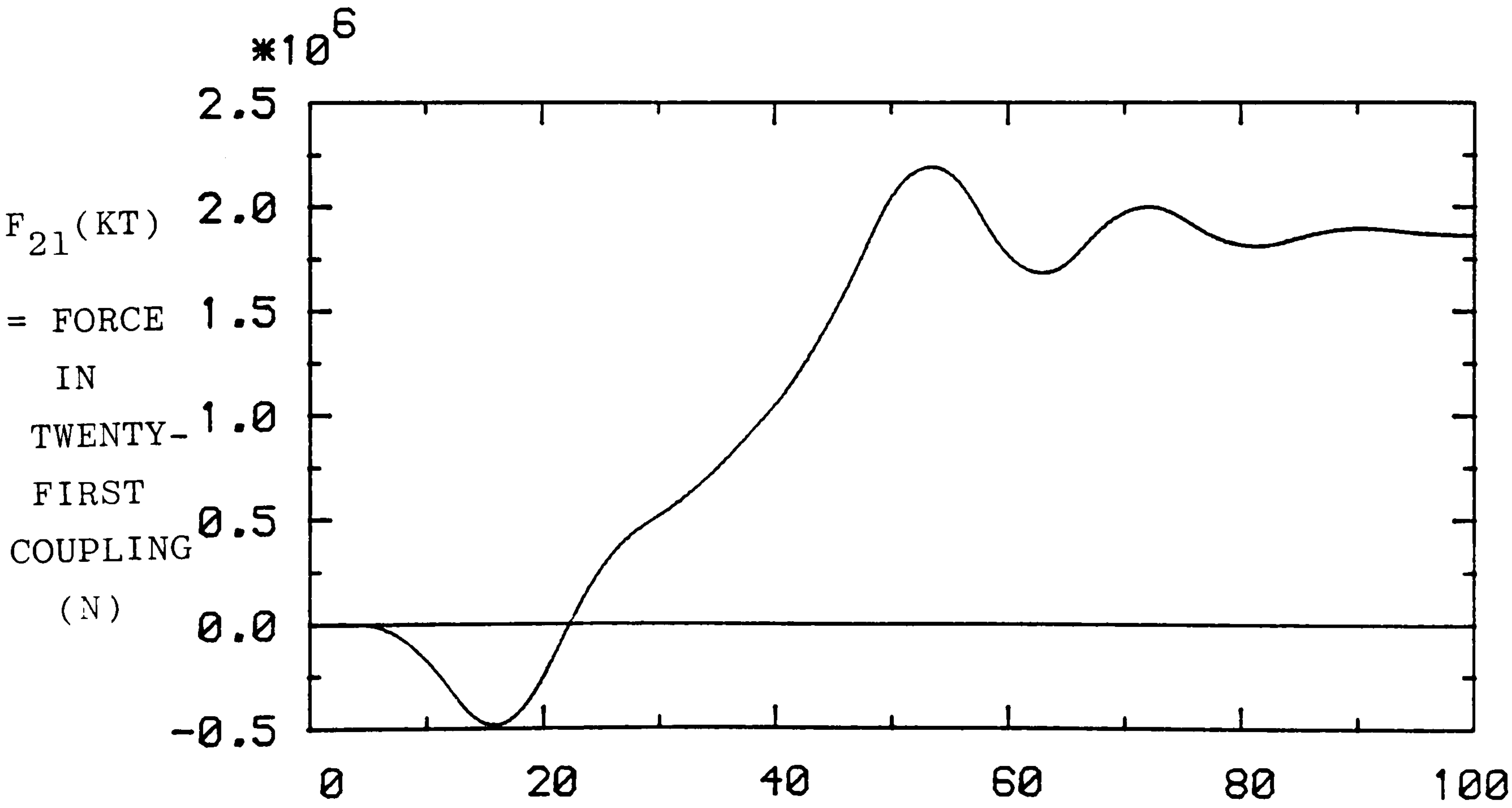

Figure 7.21

OPEN LOOP POLE (X) AND TRANSMISSION ZERO (O) LOCATIONS FOR THE TEN VEHICLE TRAIN

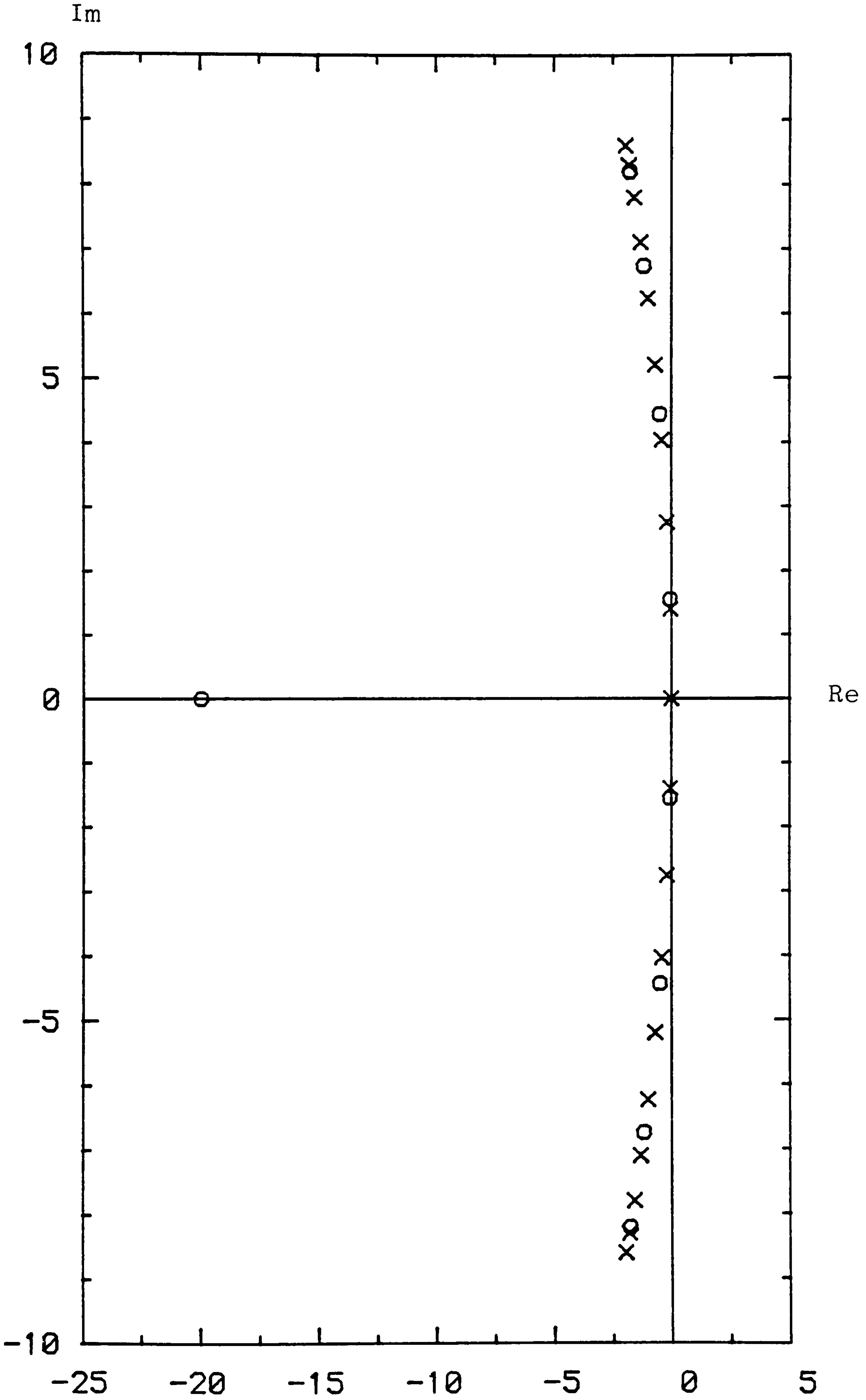

Figure 7.22

OPEN LOOP POLE (X) AND TRANSMISSION ZERO (O)
LOCATIONS FOR THE TWENTY VEHICLE TRAIN

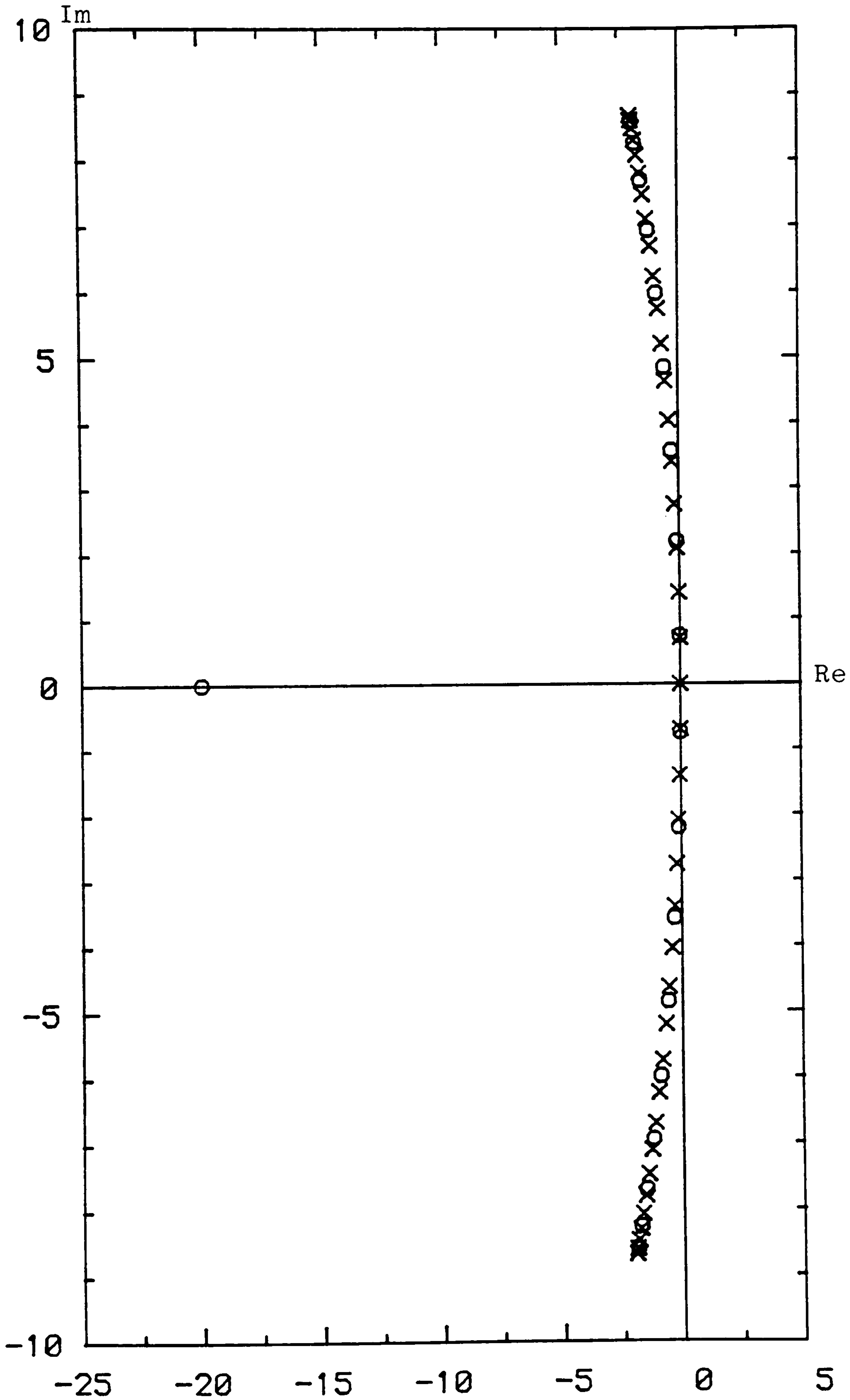

Figure 7.23

OPEN LOOP POLE (X) AND TRANSMISSION ZERO (O) LOCATIONS FOR THE FORTY VEHICLE TRAIN

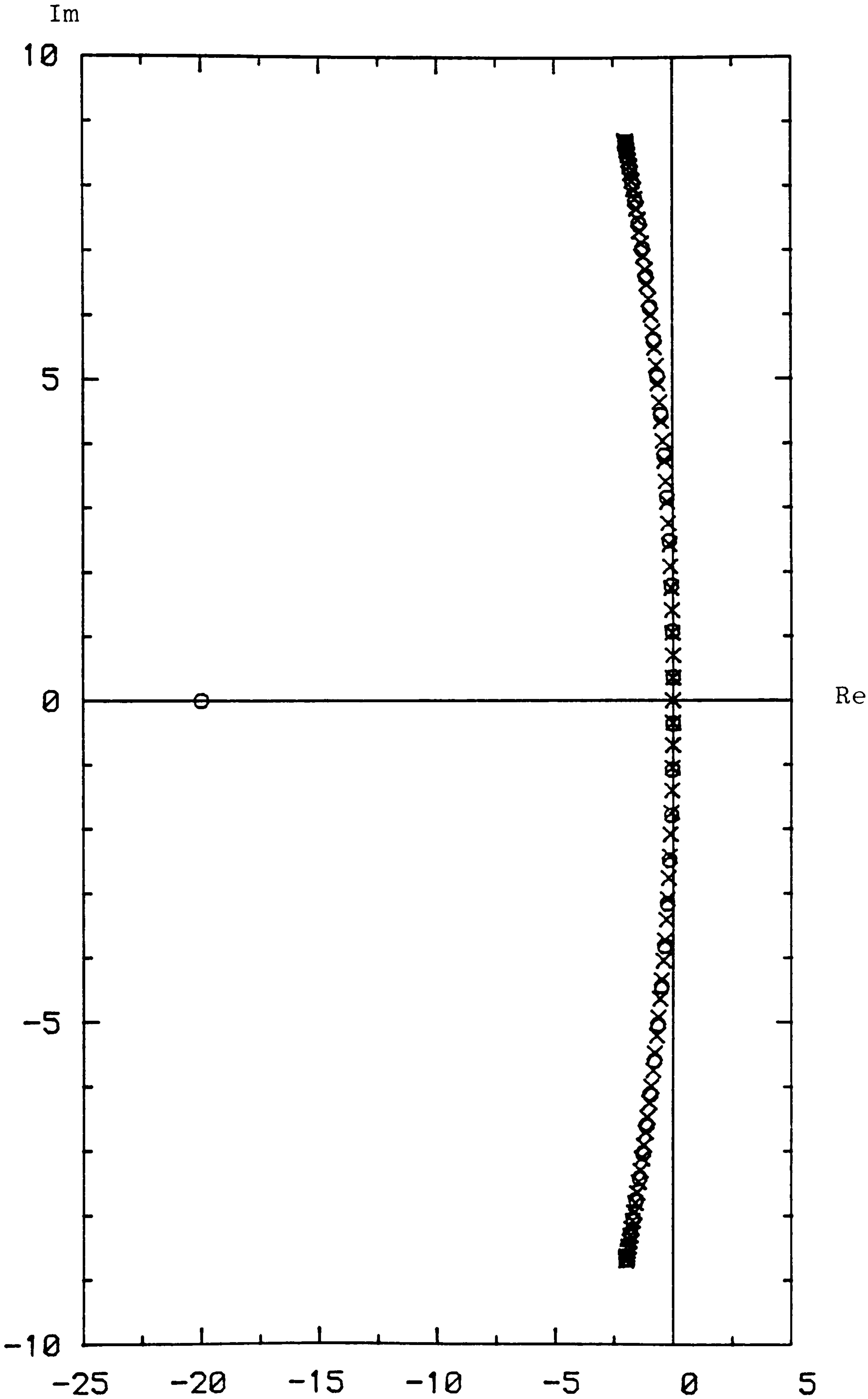

Figure 7.24

7.7 Discussion on the Fast-Sampling Control of Trains with Two Locomotives

It is clear, from figures (7.4) to (7.21) that the fast-sampling controllers effectively split the trains into two halves in the steady-state. Furthermore the responses corresponding to the speeds of the first locomotives, namely figures (7.4) , (7.10) and (7.16), are clearly very similar to the speeds of the single locomotive powered trains given by figures (6.4), (6.8) and (6.12) which illustrates that even in the transient stages each train is behaving as a pair of coupled trains. This is further underlined by the inputs to the trains being almost identical save for an expected time delay and is illustrated by figures (7.6), (7.7), (7.12), (7.13), (7.18) and (7.19). The time delay between the input responses is dependent on the vehicle lengths, the number of vehicles between the locomotives and the train speed. It is clear from this that identical control of locomotives in a unit train at severe gradient changes would not be satisfactory, and a simple improvement to the 'Locotrol' system could be the inclusion of a time delay, although it must be emphasized that 'sensible' handling of the leading locomotive is still required.

The open-loop pole and transmission zero diagrams (see figures (7.22), (7.23) and (7.24) have coincident pairs of transmission zeros separated by non-coincident pairs of open-loop poles. This underlines the results from section (7.3) where it was shown that the set of transmission zeros consists of a set for each 'subtrain' with an additional transmission zero for the coupling 'linking' the two 'subtrains' . It is also clear from figures (7.22) to (7.24) that the open-loop pole and the relevant transmission zero locations lie on the same curve with the same bounds (as $w \rightarrow \infty$) as those presented in chapter six (see figures (6.16), (6.17) and (6.18). It is therefore not surprising that the same fast-sampling controller can cope with trains of different lengths and also produces responses (see figures (7.4) to (7.21)) similar to those presented in chapter six (see figures (6.4) to (6.15)).

7.8 Fast-Sampling Control of a 100 Vehicle Train Travelling over Undulating Terrain

It has been suggested (see, for instance, Taylor et al. [4]) that handling problems can occur when long trains encounter vertical reverse curves. Hence in this section the results from a simulation of a one hundred vehicle train travelling over the vertical reverse curve given by figure (7.25) are presented. The train is again assumed to consist of equal masses, given by (6.39), and identical couplings whose stiffness and damping coefficients are given by (6.40) and (6.41), and is illustrated by figure (7.3) in which

$$w = 100$$

and

$$p = 51.$$

It is further assumed that the train is controlled in accordance with (7.38) and (7.39) with T = 0.1 s, and has initial steady-state conditions given by (7.40) to (7.47). The results of the digital computer simulation are presented as figures (7.26) to (7.31).

GRADIENT PROFILE OF THE UNDULATING TERRAIN AND THE POSITION OF THE FIRST VEHICLE AT K = O

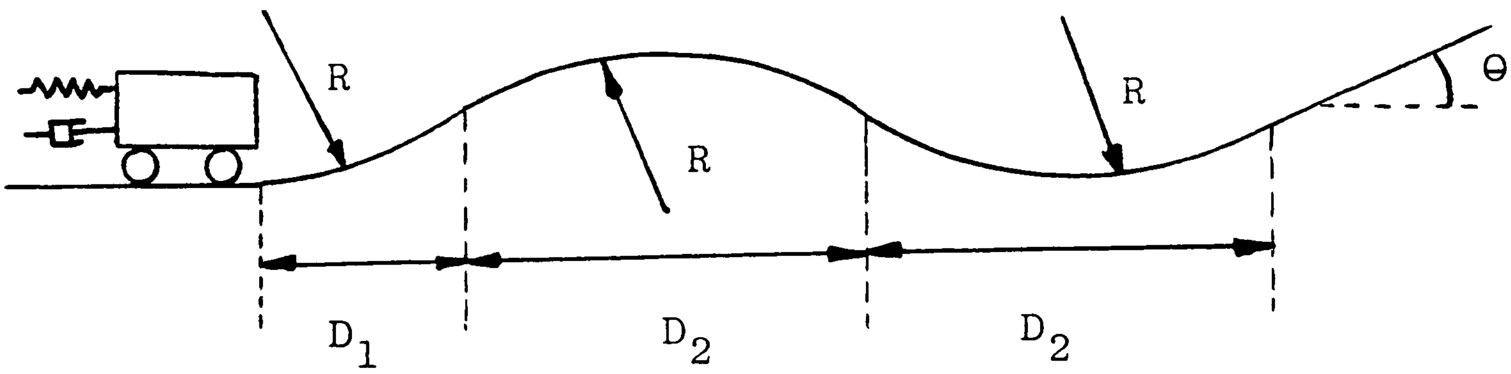

R = 800m

D_1 = 80m

D_2 = 160m

$\theta = 5.7^{o}$

Figure 7.25

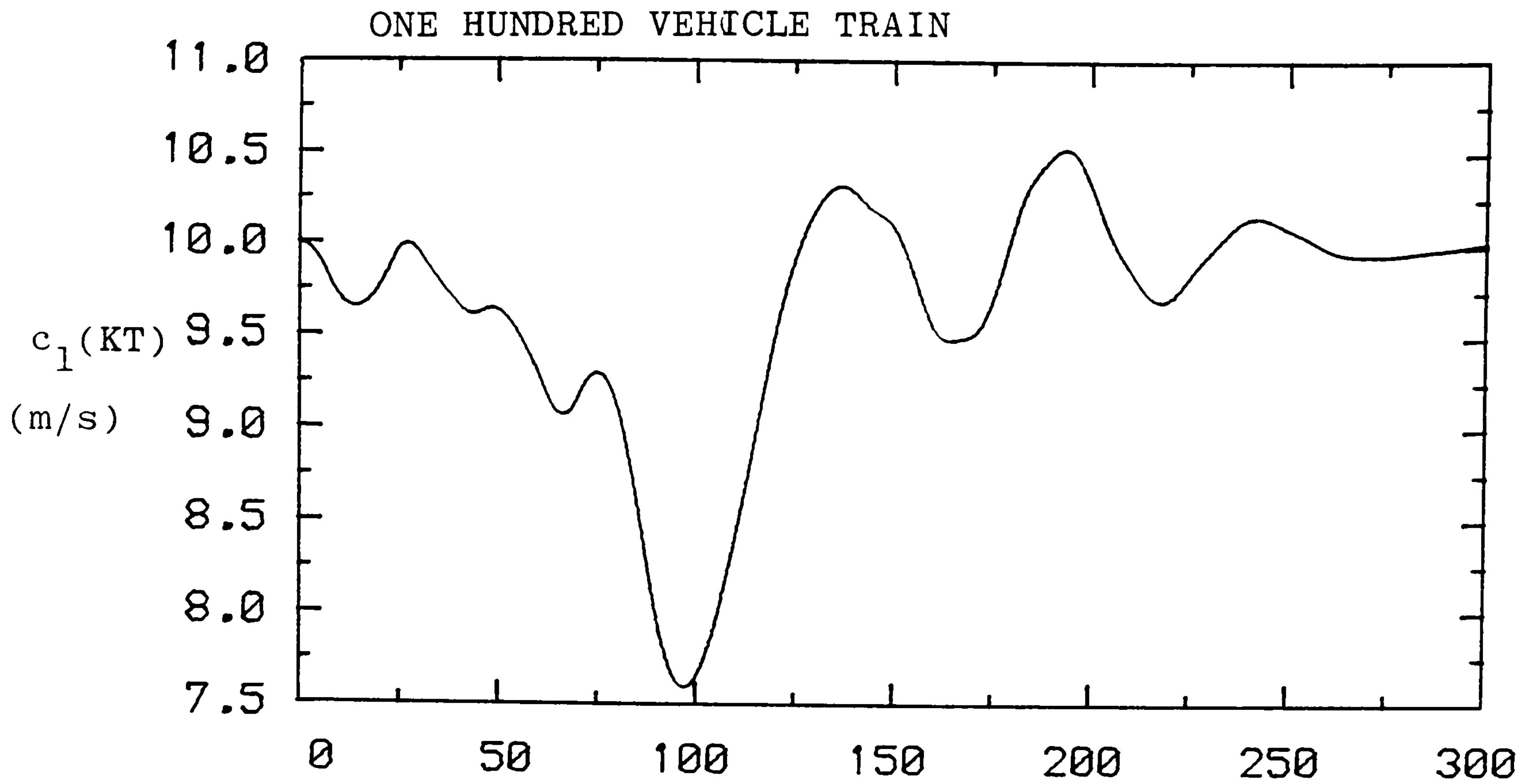

Figure 7.26

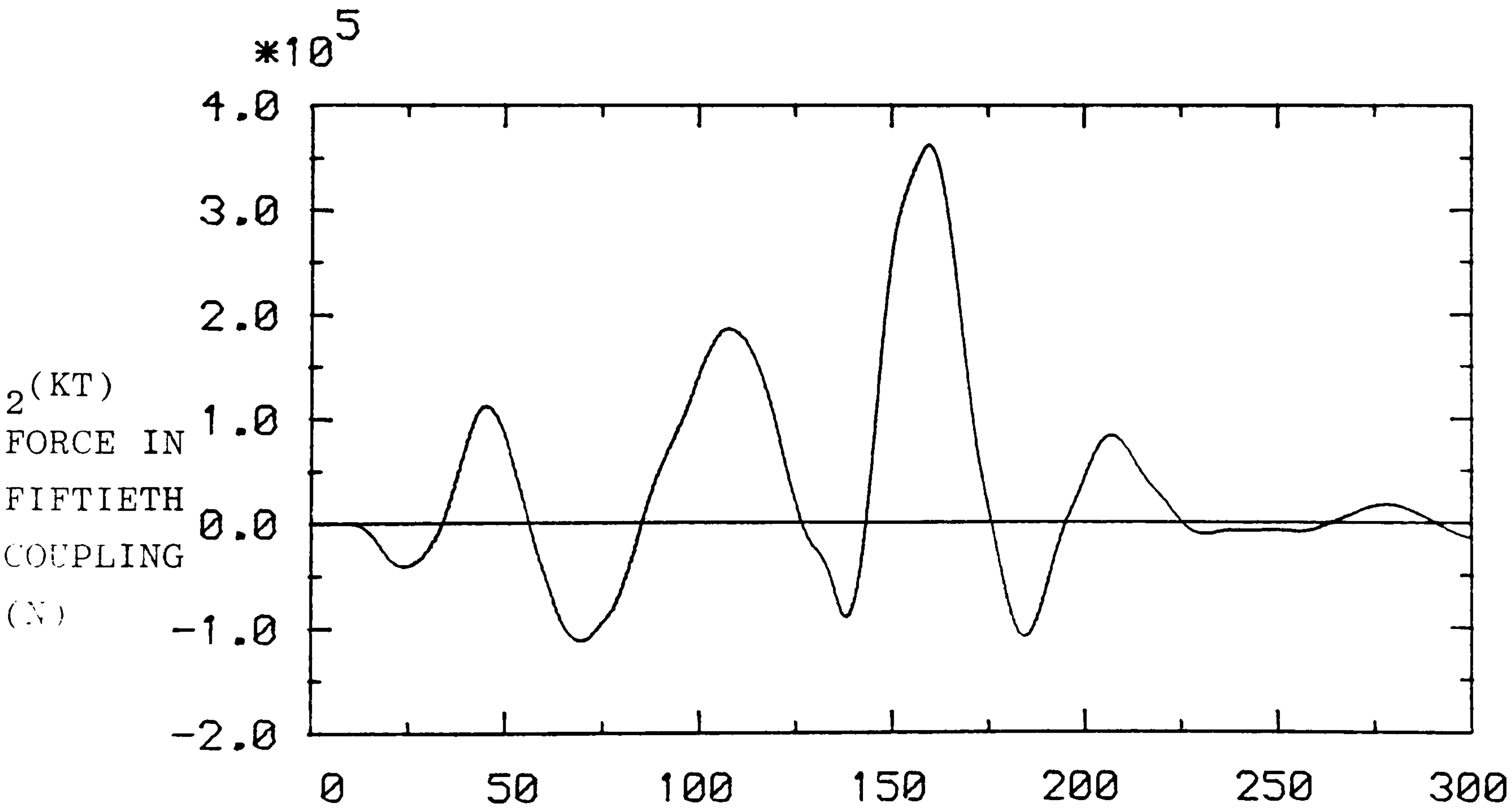

Figure 7.27

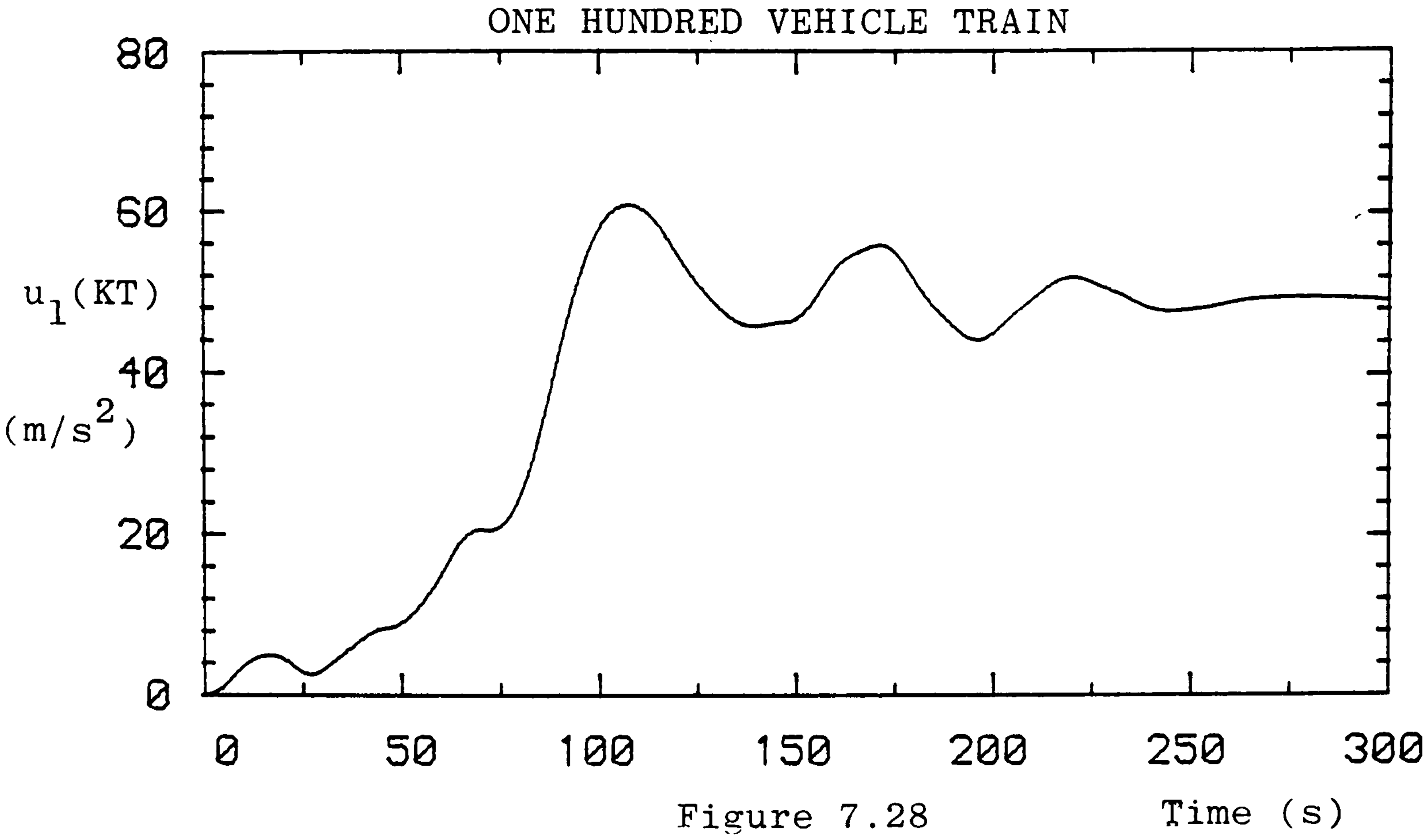

Figure 7.28

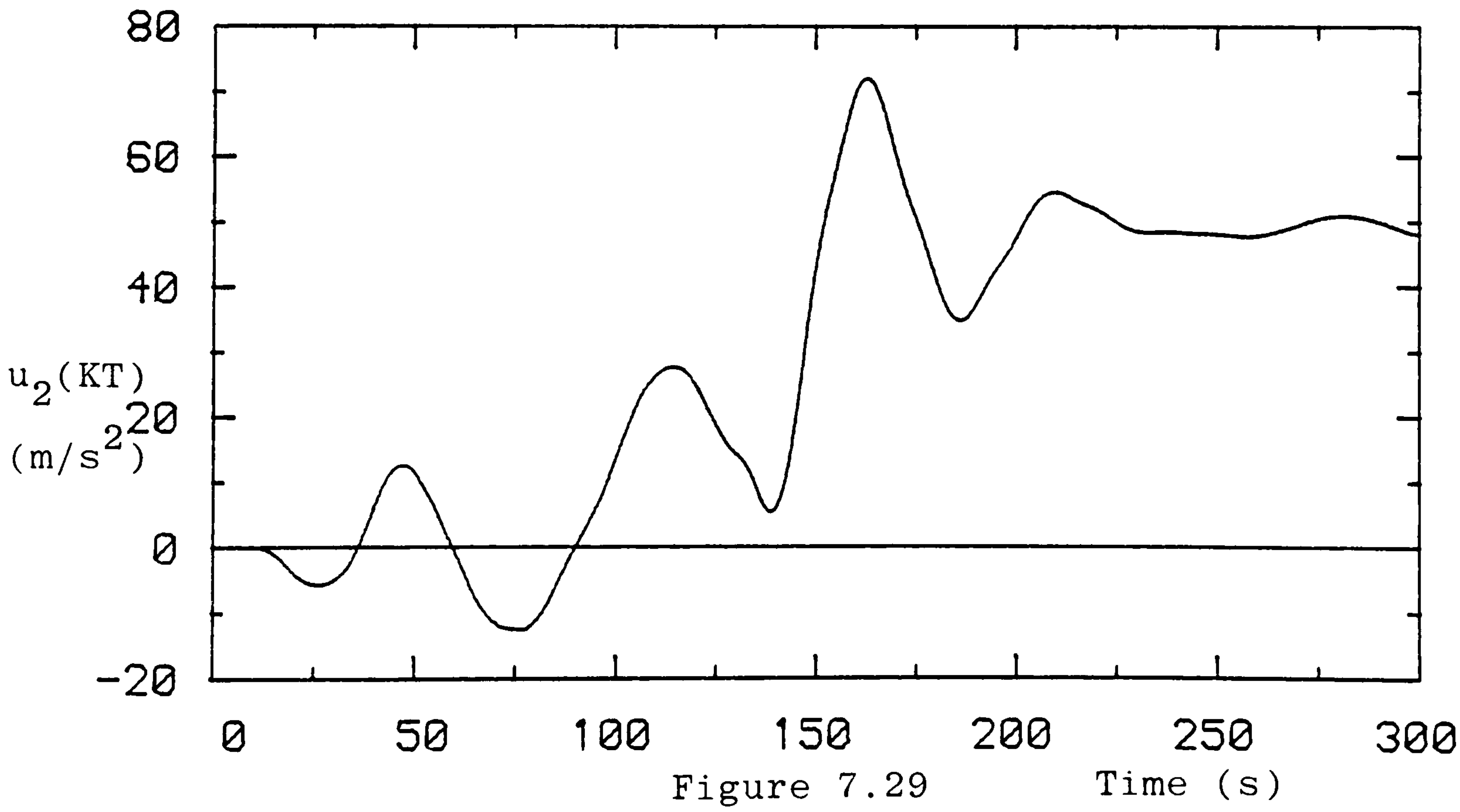

Figure 7.29

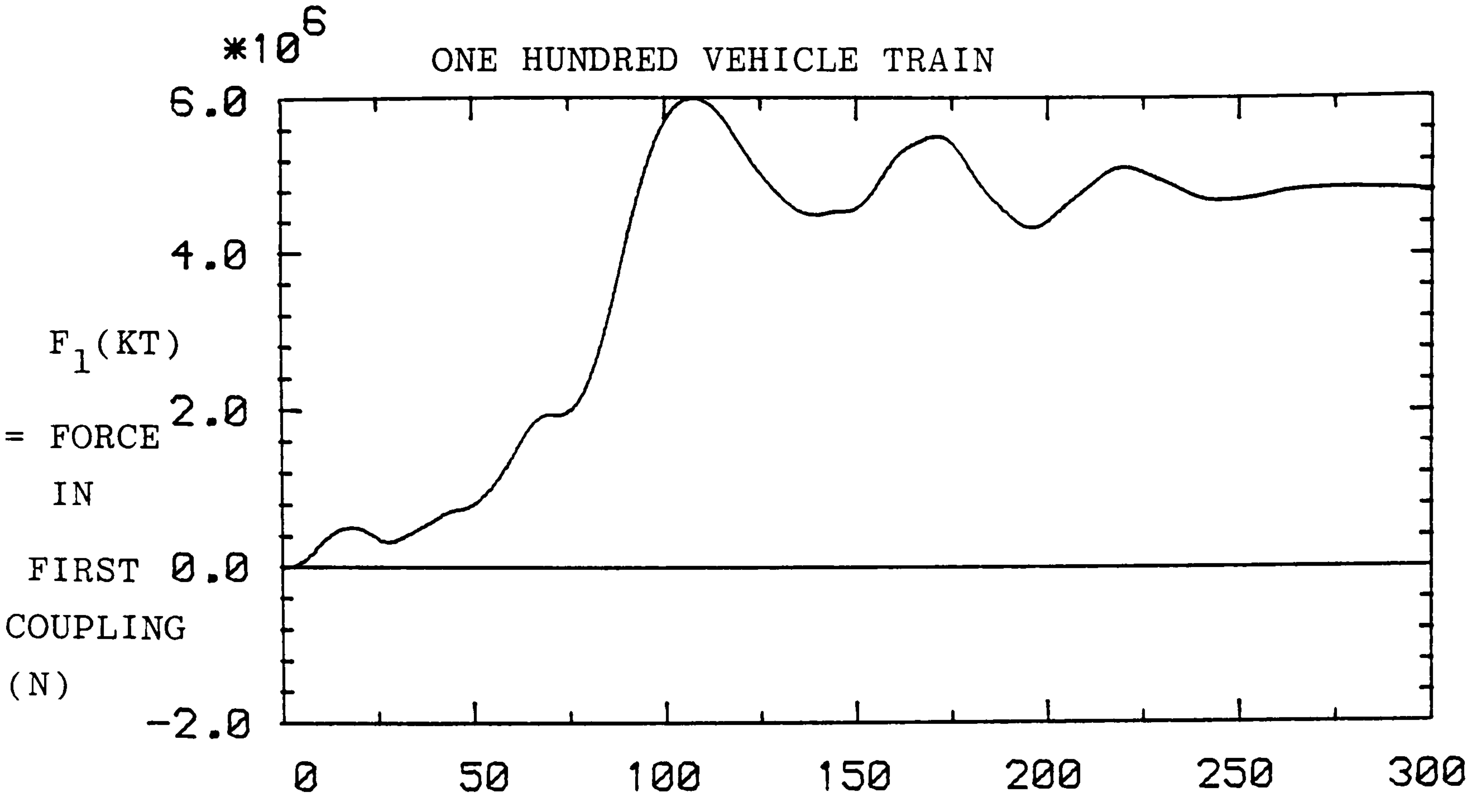

Figure 7.30

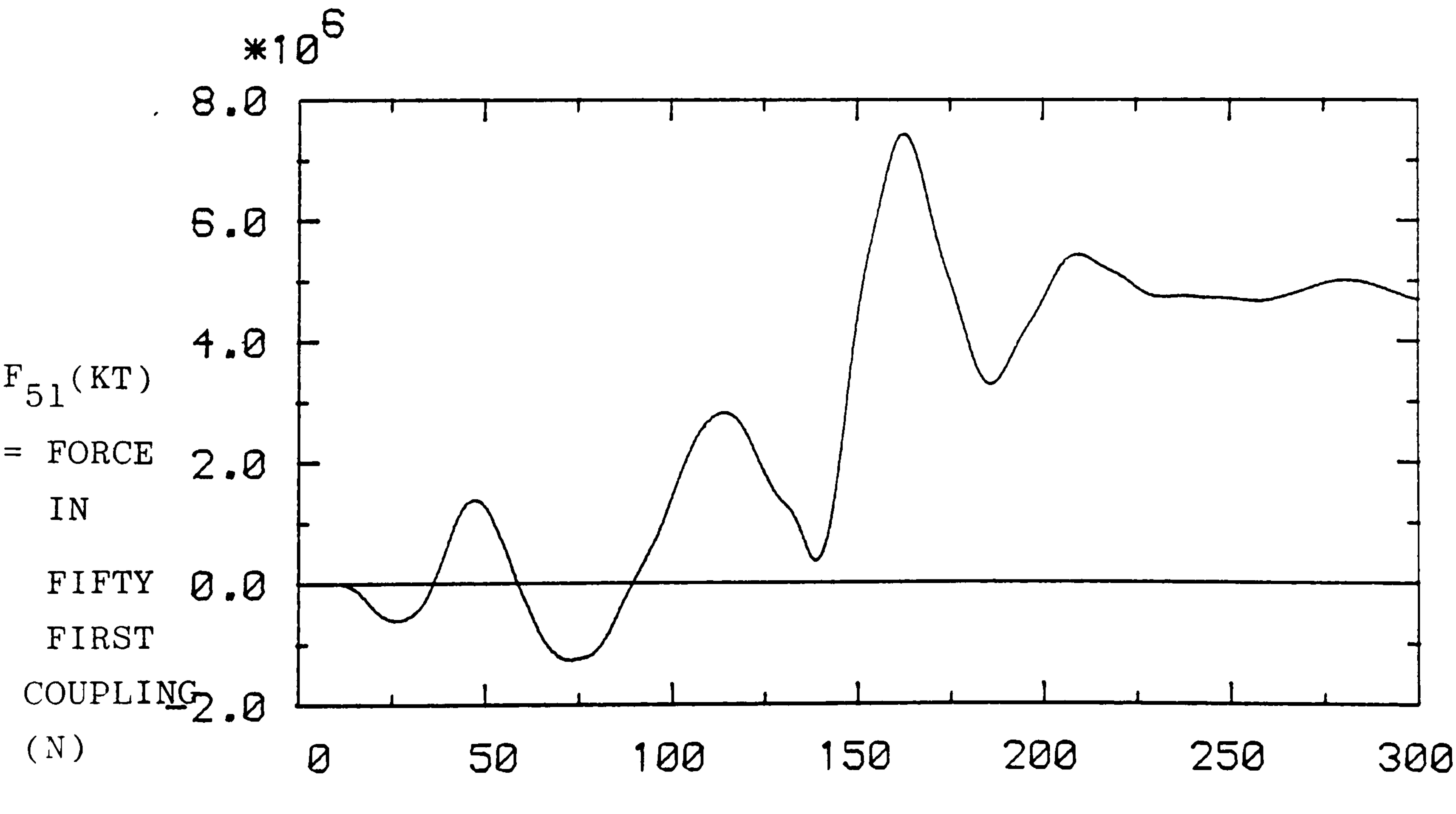

Figure 7.31

7.9 Conclusions

It follows from figures (7.4) to (7.20) and (7.25) to (7.31) that not only does the fast-sampling controller given by (7.30) and (7.31) with T = 0.1 s provide tight control of the four trains considered, but is clearly stable for trains of greatly different lengths. Furthermore it is clear from figures (7.4), (7.10), (7.16) and (7.26) that the maximum loss of speed does not increase linearly with increasing numbers of vehicles. It also follows from figures (7.26) to (7.31) that the only totally successful solution to train handling must be an automatic controller since the inclusion of a simple time delay (as suggested in section (7.7)) in the 'Locotrol' system does not hold on undulating terrain and also requires 'sensible' train handling. Such an automatic controller would have to be insensitive to variations in train length in order to be available for general use. It is clear that the fast-sampling controller developed in this chapter satisfies this criterion. Furthermore it produces good disturbance rejection and tracking properties, requires the minimum amount of information and could be extended to incorporate many 'sub-trains' into a train since no change in the fundamental properties would occur.

CHAPTER 8

CONCLUSIONS AND RECOMMENDATIONS FOR FURTHER WORK

8.1 General Conclusions

In this thesis the fast-sampling control theory presented in section (2.3) has been extended to include cases where the matrix equal to the product to the output and input matrices is not of full rank. The theory developed in sections (2.3), (2.4) and (2.5) has been successfully applied to the design of fast-sampling controllers for vehicle cascades and trains respectively. It is clear that the theory presented in chapter two is both readily applied and produces high performance controllers with the minimum amount of information.

8.2 Vehicles Cascades (Conclusion)

It is clear that both the fast-sampling controllers developed in chapter four produce non-interactive control of the outputs and good performance. No apparent benefit is gained from using the centralized controller, save that of eliminating the relative velocity interactions or 'shock-waves' which were small for the example considered. It has been shown that a linear controller can entrain (and therefore extrain) a cascade of vehicles by sensible use of the command inputs. Furthermore the controllers produce closed-loop systems that are both robust and of high integrity making them ideal bases for any further research and development. Finally it must be emphasized that the work in chapter five represents the first time the kinematics of a vehicle cascade have been deliberately exploited to produce effective centralized and decentralized control algorithms.

8.3 Trains (Conclusions)

It is clear from chapters six and seven that when a train is controlled using the relevant fast-sampling controller then the ouptuts of the closed-loop system are tightly controlled. Furthermore since the transmission zeros of trains with single and multiple locomotives always lie in the left half of the complex plane it follows that such fast-sampling controllers will always exist for trains of different configurations. It was shown that single controllers can control trains of greatly differing lengths both with and without locomotives in the train. It is clear from chapter seven that when locomotives are used in trains then a fast-sampling controller can effectively divide a whole train into two or more (if more locomotives are used) subtrains. It must be emphasized that fast-sampling train controllers produce good performance and cope easily with trains of different lengths and as a result are ideal for general use on most railways. This represents the first time that fundamental properties of trains have been deliberately exploited in the design of train controllers to propose an effective solution to train handling problems.

8.4 Recommendations for Further Work on the Theory in Chapter Two

The control theory presented in chapter two assumed the sensors and actuators had negligible dynamics; that is the relevant transfer functions are assumed to be unity. Incorporation of controllers designed using these assumptions will always lead to some deterioration in performance because of the additional phase lags introduced by sensors and actuators. Porter [44] has considered the design of fast-sampling error-actuated controllers for linear multivariable plants with explicit actuator dynamics. In order to ensure that no instability occurs due to the sensor and actuator dynamics further analysis of the systems considered in sections (2.3) and (2.4) is necessary.

It was assumed in chapter two that the calculations to determine the necessary inputs took a negligible amount of time. It is clear this assumption may not hold in practice and so requires further consideration. One solution is to delay the implementation of the required input for one or more time periods. A solution along these lines clearly requires an investigation of the effects of introducing further time delays into the closed-loop systems.

8.5 Recommendations for Further Work on Vehicle Systems

Since the theory presented in chapter two was used to design the fast-sampling controllers for the vehicle systems it is clear that all the recommendations in section (8.4) have to be considered. It is clear that introducing time delays in the sensors and actuators would require reassessment of the analyses in this thesis. In particular it should prove interesting to investigate the advantages of centralized, as opposed to decentralized, control of a vehicle cascade when time delays are introduced into the cascaded vehicle model in chapter four.

The inherent non-linearities of the two systems considered in this thesis will also require further analysis of the closed-loop system. For vehicle cascades the only non-linearities are the drag coefficients which will vary considerably, although not unpredictably, at different speeds. An analysis of given systems should produce stable controllers for the worst conditions encountered. The trains have two main non-linearities. First the coupler parameters which as for the vehicle cascades could be assumed to take their worst operating values to calculate a stable controller. However the couplers also contain dead zones and the resulting effects may be more difficult to analyse without simply resorting to simulations.

REFERENCES

1. W.S. Levine and M. Athans, "On the optimal error regulation of a string of moving vehicles", I.E.E.E. Trans. on Automatic Control, Vol. AC-11, pp355-361, 1966.

2. B. Porter and T.R. Crossley, "Modal control of cascaded vehicle systems", Int. J. Sys. Sci., Vol. 1, pp111-122, 1970.

3. R.E. Fenton, "Automatic vehicle guidance and control - A state of the art survey", I.E.E.E. Trans. on Vehicular Technology, Vol. VT-19, pp153-161, 1970.

4. R.E. Taylor, R.G. Tausch, D.E. Whitney and J.J. Kelly, "Hauling of heavy trains by U.S. railroads", Rail International, Vol. 2, No. 8, pp685-693, 1971.

5. W. Ashman, "Remote control of locomotives", Telecommunications, Vol. 2, No. 9, pp17-19, 1968.

6. P.J. McLane, L.E. Peppard and K.K. Sundareswaran, "Decentralized feedback controls for the brakeless operation of multi-locomotive powered trains", I.E.E.E. Trans. on Automatic Control, Vol. 21, pp358-362, 1976.

7. B. Porter and A. Bradshaw, "Design of linear multivariable discrete-time tracking systems incorporating fast-sampling error-actuated controllers", Int. J. Sys. Sci. Vol. 11, pp817-826.1980.

8. B. Porter and A. Bradshaw, "Asymptotic properties of linear multivariable discrete-time tracking systems incorporating fast-sampling error-actuated controllers", Int. J. Sys. Sci., Vol. 11, pp1279-1293, 1980.

9. B. Porter and A.T. Shenton, "Singular Perturbation analysis of transfer function matrices of a class of multivariable linear systems", Int. J. Control, Vol.21, pp655-660, 1975.

10. W.M. Dudley, "Analysis of the longitudinal motions in trains of several cars", A.S.M.E. Journal of Applied Mechanics, Vol. 63, ppA-145 to A-151, 1946.

11. O.R. Wikander, "Draft gear action in long trains", Trans. A.S.M.E., Vol.57, pp317-334, 1935.

12. A. Tihonov, "On the dependence of solutions of differential equations on a small parameter", (Russian), Mat Sb, Vol. 22, pp193-204, 1948.

13. A. Tihonov, "On a system of differential equations containing small parameters", (Russian), Mat Sb, Vol. 27, pp147-156, 1950.

14. A. Tihonov, "Systems of differential equations containing small parameters in the derivatives", (Russian), Mat. Sb, Vol. 31, pp575-586, 1952.

15. A. I. Klimushev and N.N. Krasovsky, "Classical methods of the theory of stability applied to singularly perturbed system", P.M.M. Journal of App. Math. and Mech., Vol 25, pp1011-1025,1961.

16. P. Sannuti and P.V. Kokotovic, "Near optimum design of linear systems by a singular perturbation method", I.E.E.E. Trans. Auto Control Vol. AC-14, pp15-22, 1969.

17. B. Porter, "Singular perturbation methods in the design of stabilization feedback controllers for linear multivariable system". Int. Control, Vol 20, pp 689-692, 1974.

18. A. T. Shenton "Asymptotic modal control of singularly perturbed dynamical systems", Ph.D Thesis, University of Salford, 1977.

19. B. A. Sangolola "Singular perturbation methods of asyptotic closed-loop eisenstructure assignment in the design of feedback control systems",Ph.D.Thesis, University of Salford, 1980.

20. C. W. Gear, "The automatic integration of stiff ordinary differential eqations", I.F.I.P. Congress, 1968.

21. L. Lapidus and R. C. Aitken, "Numerical integration of stiff dynamic system", Trans A.S.M.E., Series (G), J. of Dynamic Systems, Measurement and Control Vol. 96, pp5-6, 1974.

22. A. J. M. Spencer at al., "Engineering Mathematics" Vol. 2, Von Nostrand Reinhold, 1977.

23. B. Porter and A. Bradshaw, "Design of linear multivariable continuous-time high-gain error actuated output-feedback regulators", Int. J. Sys. Sci.,Vol.10. pp113-121, 1979.

24. V. M. Popov, "some properties of control systems with irreducible matrix transfer functions", Lecture Notes in Mathematics, Springer, Vol. 144,pp169-180,1969.

25. B. Porter and A. Bradshaw, "Design of direct digital flight-mode control systems for high-performance aircraft". Proceedings of the I.E.E.E. 1981 National Aerospace and Electronics Conference, Dayton, Ohio, U.S.A., pp 1292-1298, 1981.

26. B. Porter and J.J. D'Azzo, "Transmission zeros of linear multivariable continuous-time system", Electronics letters, Vol. 13, pp 753-755,1977.

27. H.H. Rosenbrock, "State space and multivariable theory", Nelson, 1970.

28. A. C. Pugh, "Transmission and system zeros", Int. J. Control, , Vol 26, pp 315-324,1977.

29. L.E. Peppard and V. Gourishankar, "An optimal car-following system", I.E.E.E. Trans on Vehicular Technology, Vol. VT-21, pp 67-73, 1972.

30. R. G. Stefanek and D. F. Wilkie, "Control aspects of a dual mode transportation system", I.E.E.E. Trans. on vehicular Technology, Vol. VT-22, pp7-13, 1973.

31. J. G. Bender, R. E. Fenton and K. W. Olson, "An experimental study of vehicle automatic longitudinal control", I.E.E.E. Trans. on Vehicular Technology, Vol. VT-20, pp 114-123, 1971.

32. D. E. Whitney and M. Tomizuka, "Normal and emergency control of a string of vehicles by fixed reference sampled-data control", I.E.E.E. Trans, on Vehicular Technology, Vol. VT-21,pp128-138, 1972.

33. R. J. Rouse and L.L. Hoberock, "Emergency control of vehicle platoons: Control of following law vehicles", Trans A.S.M.E. Series (G) J. of Dynamic Systems, Measurement and Control Vol.98,pp239-244,1976.

34. S.E. Schladover, "Vehicle - Follower control for dynamic entrainment of automated guideway transit vehicles", Trans. A.S.M.E. Series (G) J. of Dynamic systems, Measurement and Control, Vol.101,pp314-320,1979.

35. W. M. Dudley, "Analysis of the longitudinal motions in trains of several cars", A.S.M.E. Journal of applied Mechanics, Vol. 63,pp A-145 to A-151, 1946.

36. O.R. Wikander, "Draft gear action in long trains", Trans. A.S.M.E., Vol. 57,pp 317-334, 1935.

37 T. Von Karman and M.A.Biot, "Mathematical methods in engineering" Chapter 11, McGraw-Hill, 1940.

38. Kin N. Tong, "Theory of mechanical vibrations", Wiley, pp 304-309, 1960.

39. P. Lancaster, "Lambda-matrices and vibrationg systems" Pergamon Press, 1966.

40. B. Porter and A. Bradshaw, "Asymptotic properties of linear multivariable continuous-time tracking systems incorporating high-gain error-actuated controllers", Int. J. Sys. Sci., Vol.10,pp1433-1444, 1979.

41. A. J. M. Spencer et al.," Engineering Mathematics", Vol.1, Van Nostrand Reinhold, 1977.

42. Parker et.al., "Railway Mechanical Engineering Car and Locomotive Design, A Century of Progress", A.S.M.E. Rail Transportation Division, 1979.

43. K.K. Sundareswaran, P. J. McLane and M.M. Bayoumi, "Observers for linear systems with arbitrary plant disturbances", I.E.E.E. Trans. on Automatic Control. Vol. AC-22, pp870-871,1977.

44. B. Porter, "Fast-sampling error-actuated controllers for linear and multivariable plants with explicit actuator dynamics", University of Salford Report Number USAME/DC/105/79.